CONTOUR RIDGE MODELLING USING FUZZY LOGIC AND PROCESS BASED APPROACHES FOR IMPROVED RAINWATER HARVESTING

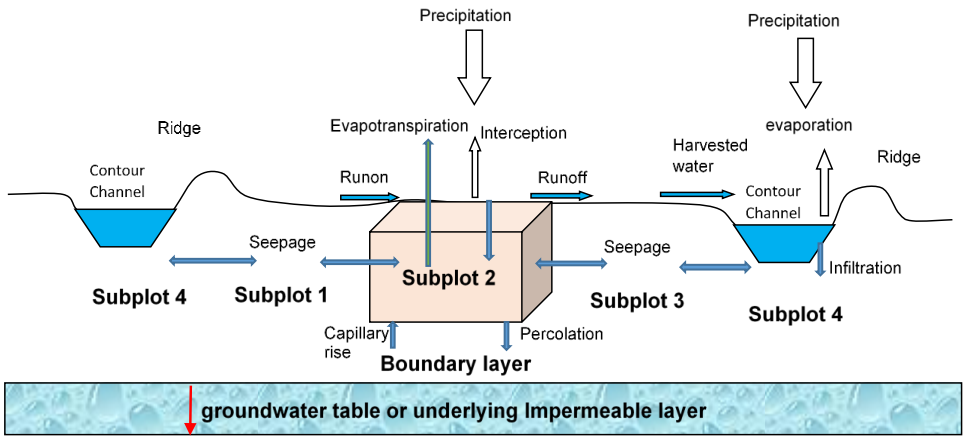

Alexander Mhizha

A thesis submitted to the Faculty of Engineering and the Built Environment, University of the Witwatersrand, Johannesburg, in fulfilment of the requirements of the degree of Doctor of Philosophy.

Johannesburg, February 2017

DECLARATION

I declare that this thesis is a product of my own unaided work. It has not been submitted to any other University before for any degree or examination. It is hereby being submitted to the University of Witwatersrand, Johannesburg for the Degree of Doctor of Philosophy.

13th day of February in the year of 2017

DEDICATIONS

To my late father for the wisdom he displayed despite his lack of formal education and my late mother for sacrificing her comfort so that I could get secondary education that opened opportunities for University education.

To my late daughter Tendai who died while on her first step of acquiring education in that tragic road accident when I was about to embark on this study and to my son Munashe who was born with disability and died during the course of this study.

To my family, my wife Junior, daughter Nyaradzo and sons Tashinga and Ngonidzashe, you endured the hardships when I was away in the field in Zhulube Catchment, Filabusi and in Johannesburg for this study.

ABSTRACT

Rainwater harvesting is used as a way of improving crop yields in rain fed agriculture by capturing excess rainfall and storing it in-situ or in reservoirs for use during dry spells. Contour ridges are one of the many rainwater harvesting technologies that are used although little is known about their effectiveness. Contour ridges harvest runoff generated in the cropped field upstream of the ridges.

The traditional contour ridge type in Zimbabwe was introduced by the government in the 1950s to control soil erosion through safely draining away runoff from cropped fields and is commonly referred to as graded contour (GC) ridges. In the 1990s the country experienced severe and more frequent droughts leading stakeholders to experiment on contour ridges that retain the runoff instead of draining it away which are known as dead level contour (DLC) ridges. There was therefore the need to find out if there are benefits derived from this change and assess conditions under which benefits would be experienced. Previous studies have shown that rainwater harvested by contour ridges can improve water availability in downstream fields. However these studies did not investigate the conditions under which such benefits are realised. In addition no attempt to model water harvesting by contour ridges have been made in Zimbabwe while the contour ridges are widely being used for soil and water conservation. This research investigated the effect of contour ridges by comparing soil moisture between plots with DLC and GC ridges using plots with no contours as a control.

Experimental work was carried out in Zhulube, in Matebeleland South Province of Zimbabwe. Matebeleland South Province falls within the semi-arid area in which rainfall is characterised by mid-season dry spells leading to frequent crop failure. In addition, the area often receives high rainfall intensities leading to soil erosion and sedimentation of rivers. DLC and GC ridges were constructed in farmers' fields where maize crops were planted. Soil moisture measurements were done using a micro gopher soil moisture profiler while runoff plots were used to measure runoff generation. A fuzzy model was developed using data from this experiment and a previous study in Masvingo Province of Zimbabwe to simulate runoff generation at field scale while a process based water balance model was also developed to simulate soil moisture changes within the root zone of the cropped area.

The results from this study indicate that DLC are effective in clay and loamy soils where runoff generation is significant and not in sandy soils due to insignificant generation of runoff under the rainfall regimes of semi-arid areas. Fuzzy logic was found to be a useful method of incorporating uncertainty in modelling runoff at field scale. A mass water balance model developed on process based principles was able to model soil moisture in the root zone reasonably well (NSE =0.55 to 0.66 and PBIAS=-1.3% to 6.1%) and could help to predict the water dynamics in contour ridged areas as would be required in determining the suitable dimensions and spacing of contour ridges. Further research is required to improve the fuzzy component of the model for estimation of runoff when more data becomes available. In addition experiments to validate methods of estimating macro pore fluxes and lateral transfer of water from the contour ridge channel to the downslope field are also recommended. The model structure can be improved by adopting the representative elementary watershed approaches to include momentum and energy balances in addition to mass balance that was used in this study.

ACKNOWLEDGEMENTS

This research would not have been possible without various people and organisations that helped in many different ways towards the attainment of the research goal.

My most sincere thanks go to my supervisor Prof. J. G. Ndiritu for his patience, encouragement and endurance in guiding me throughout the study. I would not have done it without your support. I also wish to thank all the staff in The School of Civil and Environmental Engineering at the University of Witwatersrand, Johannesburg, for the support throughout the course of the study. Dr. Nyagumbo, previously with The University of Zimbabwe Department of Soil Science and Agricultural Engineering, thank you so much for input and guidance during the early stages of the research work.

I am very grateful to the Challenge Programme for Water and Food PN17 and The University of Witwatersrand for sponsoring this research. I also wish to thank senior researchers in the Challenge programme namely Prof. A. Taigbenu, Prof P. van der Zaag, Prof S. Walker, Prof S. Ulrlenbrook, Dr. A. Senzanje and Dr. S. Twomlow for the guidance and criticism offered during workshops. To WaterNet secretariat teams lead by Dr. T. Gumbo, Prof. I. Nhapi, Dr. D. Love and Dr. J. M.Onema thank you so much for the support. Dr. W. Nyabeze thank you so much for creating the initiative that led into the initiation of this study.

To my colleagues in the Department of Civil Engineering at the University of Zimbabwe (Dr. Makurira, Dr. Misi, Eng. Hoko, Dr. Tumbare, Mr. Gumindoga and many others who left the Department) thanks for supporting and encouraging me. I wish to specifically thank Prof. Vassileva for your motherly encouragement and Dr. Salahuddin for shouldering the load while most of us were on leave.

I would not be honest if I do not thank the people who played a central role in the research. The participating farmers (Mrs Nkala, Ms Ncube, Ms Mpofu, Mr. Ndlovu and Mr. Nkomo) were very encouraging to work with and thank you for making your fields available for my experiments. To the leadership of Zhulube, Mr. Mpofu and your team I thank you so much for accepting me in your community. To Tshazi Secondary School; Mr. Ndlovu and your staff thank you so much for the accommodation.

All the field data collection in Zhulube were achieved through the assistance of the reliable Mr. Lewis Ndlovu and Miss Sithabile Ndlovu. Thank you very much for your wonderful work.

The special last gratitude is reserved for many fellow PhD students I shared thoughts, ideas and encouragement with; thank you guys. Particular mention is made of Paulo Kagoda who in addition taught me how to program in python.

.

TABLE OF CONTENTS

LIST OF APPENDICES

LIST OF FIGURES

LIST OF TABLES

LIST OF SYMBOLS

Symbol	Description
R, Q	Runoff or discharge
R_{in}	Run-on
P	Precipitation
ET	Evapotranspiration
$\frac{\partial\theta}{\partial x}$	Soil moisture gradient being change in soil moisture over distance x.
F	Infiltration
I	Interception
θ	Soil moisture
T	Transpiration
Y	Yield
Φ	Soil moisture flow (flux)
Δ	change
t	time

ACRONYMS AND ABBREVIATIONS

Acronyms or Abbreviations	Meaning
DLC	dead level contours
GC	Standard graded contours
NC	Non contour
kg	Kilogram
ha	hectare
mm	millimeter
NGO	non-governmental organization
SSI	Smallholder Systems Innovation
CPWF	Challenge Programme for Water and Food
USA	United States of America
FIS	fuzzy inference system
SWI	Soil water index

1 INTRODUCTION

1.1 General background to the study

Small holder farmers in semi-arid regions of developing countries experience frequent crop failure mainly due to low and unreliable rainfall in addition to other factors such as soil nutrient deficiency and poor farming practices (Hatibu et al., 2003; Barron, 2004). A study carried out on farmer fields in Insiza District of Zimbabwe by Mupangwa (2007) shows that grain yield per hectare changed from 1173kg for the 2005/06 growing season with rainfall of 538mm to 304kg for the 2006/07 growing season with rainfall of 375mm. Most of the small holder farmers in Zimbabwe and many parts of Southern Africa practice rain fed crop farming due to lack of infrastructure for irrigation. Although the rainfall in semi- arid areas of Southern Africa is low the average annual total is above the amount needed for supporting crop growth. However total crop failure is still experienced in these semi-arid areas due to occurrence of dry spells despite rainfall being higher than the 300mm/a threshold below which water rather than soil nutrients becomes the main limiting factor for crop growth. The water stress caused by dry spells can occur as many as up to 4 times in one rainy season (Chibulu, 2007). The uneven temporal distribution of rainfall, results in losses due to unproductive processes such as runoff.

Rockström (2000) showed that nonproductive water loses in rain fed smallholder farming practices can be as high as between 70 – 80% with runoff accounting for 10 to 25%. Rockström (2000) further suggested that if such loses can be reduced the yield gap in rain fed farming systems can be reduced. Among the methods that can be used to reduce runoff loses is rainwater harvesting technologies such as pot holing (basin planting), infiltration pits, fanya juus and contour ridges (sometimes referred to as contour bunds). Rainwater harvesting was developed and adopted in different parts of the world (e.g. India, Yemen, North and East Africa) to retain runoff water within the agricultural plot and improve water availability to crops (Prinz and Malik, 2002). Apart from runoff being harvested from within the field, it can also be harvested off field from adjacent catchment areas such as grazing land, forested area, rock catchments, build up areas, roads drainage systems and channeled to the field (Makurira et al, 2009; Laker, 2004). Such runoff quantities could be higher than that from the field due to the higher runoff coefficient

in off field areas. In some cases the off field catchment area can also be larger than the infield catchment area.

Despite rainwater harvesting having the capacity to reduce risk there is a low level of adoption of rainwater harvesting technologies due to high labour requirements and inappropriateness of the technologies in certain conditions where they are sometimes applied (Laker, 2004). As indicated by Prinz and Malik (2002) successes of runoff harvesting have often been based on experience and trial and error rather than scientifically based techniques. Among runoff harvesting technologies that are used with little scientifically based knowledge is the contour ridges techniques. Several literature cite contour ridges as one of the methods for rainwater harvesting but provide no explanation nor evidence of how contour ridges contribute to moisture improvement (Al Ali et al, 2008; Nasri et al, 2004; Falkenmark et al, 2001). In particular, no guideline has been found on how contour ridges could be designed for rainwater harvesting. Existing design in Zimbabwe has been done with some parameters being adopted from the United States due to lack of local data (Elwell, 1981) and the design is basically aimed at safely draining away the water from the field (Hagman, 1999). Munamati and Nyagumbo (2010) in a study of socio-economic factors on performance and effectiveness of dead level contours in Zimbabwe noted that the conditions under which rainwater harvesting technologies perform well have not been fully explored and suggested that this has led to indiscriminate recommendations of the rainwater harvesting technologies.

1.2 Problem statement

There has been a realization that in areas of low rainfall, instead of draining water away from the field through contour ridges, the ridges should be used to retain the water. A new design of contour ridges called dead level contours (DLC) was developed and implemented in Mzingwane Catchment in Matebeleland South Province of Zimbabwe (Mupangwa et al, 2006) through the help of Practical Action, a nongovernmental organization. The adoption of this practice was done without the effectiveness of the practice in terms of soil moisture retention and crop yield being known and this triggered an interest in establishing the effectiveness of the practice among researchers in Zimbabwe.

Among the first to study the effect of contour ridges on soil moisture was Mugabe (2004) who carried out a study in Chivi District located in South East Zimbabwe and found out that standard graded contour ridges, designed to drain away water from the field, incorporated with infiltration pits improved water availability in the field. Mupangwa et al (2011) carried out a similar study in Gwanda District located in South West Zimbabwe and observed that improvement in moisture conditions in a field with dead level contour ridges were realized after heavy rains exceeding 40mm/d. Elsewhere Makurira (2010) found there is moisture improvement due to fanya juus (a form of contour ridges in which the soil is thrown upslope instead of down slope) in a biannual climate of Makanya Catchment in Tanzania.

The results obtained by these researchers suggest that use of contour ridges improves water availability to crops. Despite these promising results on the use of contour ridges for rainwater harvesting, the conditions under which the contour ridges are effective were not investigated. There was no investigation on the influence of soil type on the effectiveness of contour ridges. Except for the study by Makurira (2010) the performance of the contour ridge treatment was not compared to other treatments including a control. In addition no attempt was made on developing a model for estimating runoff generated in the contoured field that take into account the uncertainties associated with the physical and climatic conditions that prevail in areas where contour ridges are required for water conservation. However Makurira (2010) developed a water balance - based model for estimating soil moisture in the root zone of a field with fanya juus. Makurira's (2010) model used input data observed from the site which limits its use only to the experimental sites. In addition the model did not handle moisture redistribution; an important aspect in transferring harvested runoff from the contour ridge.

This research investigated conditions under which contour ridges could perform well and also developed a model that estimates both the runoff generated from rainfall that is harvested by the contour ridges and the soil moisture change in the root zone of the field where contour ridges are incorporated. Several factors affect runoff generation and soil moisture changes at field scale both of which could affect effectiveness of contour ridges as a rainwater harvesting technology. Among these factors are slope of the land, soil type, rainfall characteristics (rainfall intensity and duration) and antecedent soil moisture. This study was restricted to the effect of soil type, antecedent soil moisture and rainfall

characteristics. Land slope was not considered since the data that was used for the study was obtained from fields with comparable slopes. Determination of effectiveness of contour ridges in particular field conditions focused on collecting empirical evidence from the field and developing a model for estimating runoff generation at field scale with limited data given the uncertainty associated with the estimation of key parameters in conventional methods. In addition a conceptual framework that allows incorporation of improvements as they become available was developed to estimate soil moisture changes in the root zone of the growing crops.

1.3 Justification

A number of factors in combination need to be met for effectiveness of contour ridges. Runoff needs to be generated, and the harvested water needs to be retained in the contour ridge and infiltrated into the soil. The soil moisture then needs to be transferred within the soil at a rate that will allow availability to the crops. Knowledge of the conditions in which runoff is generated such as effect of soil type on the effectiveness of contour ridges used as rainwater harvesting would assist implementation agencies in identifying target fields for implementing contour ridges. Runoff generation capacity of a target field is the basic criterion upon which the field's suitability for rainwater harvesting could be based. However it is not possible to obtain runoff data for all fields where contour ridges may need to be implemented necessitating the need to have a model for estimating runoff at field scale given the uncertainty in soil type, soil moisture and rainfall. Such a model cannot be calibrated for every individual site hence the need to consider an approach that enables use of a model calibrated using data obtained from a limited number of sites at various other sites while reducing uncertainity arising from the absence of calibration. The model that was developed can be used to estimate the components (interception, infiltration and runoff) in which rainfall can be partitioned into in the cropped area and how the runoff harvested by the contour ridges can be partitioned into evaporation and infiltration. The model can also be used to estimate the soil moisture partitioning into groundwater recharge and evapotranspiration.

1.4 Study objectives

This study was aimed at establishing the effects of dead level contours and graded contours under different soil types on rainwater harvesting and crop yield and to formulate a modelling framework that could be used for guiding their design.

Main Objective

To investigate the rainwater harvesting potential of contour ridges in semi-arid agricultural fields and develop a model for simulating runoff generation and soil moisture improvements in a contoured field.

Specific objectives

Objective 1

To assess water conservation by dead level contours and compare with standard graded contour ridges and hence determine effectiveness of dead level contour ridges as a rainwater harvesting technology in two soil types namely sandy soil and loam soil.

Objective 2

To evaluate crop yield benefit of employing dead level contour ridges for water conservation in different soil types by comparing yields from field plots with dead level contours with yields in field plots using standard graded contour ridges.

Objective 3

To formulate a model for estimating soil moisture in a field with contour ridges and test its performance using field data.

Objective 4

To investigate the potential of using fuzzy logic in handling uncertainties in input data when modelling runoff at field scale.

1.5 Thesis outline

This thesis is presented in eight chapters including this introduction chapter. Chapter 2 presents a review of available literature on rainwater harvesting in general with particular emphasis on field observations for contour ridged fields and modelling field responses to rainwater harvesting techniques. This study was carried out in two parts. The first part was to investigate water conservation by contour ridges while the second part was to develop a model for assessing water conservation by contour ridge. Chapter 3 discusses possible methods that could be used to develop a model for estimation of soil moisture in a contour ridged field. Chapter 4 describes the details of the study site and the methodology that was followed in carrying out the field experimental work and the data analysis methods to draw conclusions on field observations. The field work was carried out in Zhulube area that falls in Mzingwane catchment of Matebeleland South in Zimbabwe. A framework for modelling a contoured field is presented in Chapter 5. This includes the methods that were used in developing and testing a model for contour ridges and the development of a fuzzy model for estimating runoff at field scale. In Chapter 6, an assessment of the effectiveness of dead level contours in terms of the improvement in soil moisture based on field observations is carried out. An evaluation of whether the improvement in soil moisture could be translated into crop yield benefit based on field observations is also presented in this chapter. The results of the developed contour ridge model that integrates surface and sub-surface processes at field scale are presented in Chapter 7. Chapter 8 summarizes the study and ends with conclusions and recommendations for further research.

2 LITERATURE REVIEW ON CONTOUR RIDGES AND AGRICULTURAL RAINWATER HARVESTING

This chapter reviews available literature on rainwater harvesting in general and water conservation through contour ridges in particular.

2.1 Rainwater harvesting technology

2.1.1 Development of rainwater harvesting technology

Rainwater harvesting is a practice in which rainfall is collected and concentrated on smaller areas to enhance and prolong water availability for water supply and agricultural purposes (Li et al., 2000; Falkenmark et al., 2001; Prinz and Malik, 2002; Mbilinyi et al., 2005; Ncube et al., 2008). It is believed to have started more than 5000 years ago in Iraq with observations suggesting that it was in use in India and China some 4000 years ago (Pandey et al., 2000; Falkenmark et al., 2001). At present rainwater harvesting is practiced in many parts of the world particularly in India, Yemen, North and East Africa (Prinz and Malik, 2002).

Until the last quarter of the 20th century, the main application of rainwater harvesting techniques was domestic water supply (Li et al., 2000). Interest of scientists in the use of various rainwater harvesting techniques for agricultural purposes increased in the last quarter of the 20th century (Tsakiris, 1991; Li et al., 2000; Fulkenmark et al., 2001). Attention initially focused more on arid areas (Bruins et al., 1986) but later more work was carried out in semi-arid areas of India and later East and Southern Africa (Tsakiris, 1991; Hatibu and Mahoo, 1999; Li et al., 2000; Makurira et al., 2010).

Rainwater harvesting attracted a lot of attention from the donor community in the last two decades with several non-governmental organizations (NGOs) involved in promotion and implementation of rainwater harvesting systems in Zimbabwe and other Southern African countries. Many research projects such as Smallholder Systems Innovation (SSI) and the Challenge Programme for Water and Food (CPWF) carried out some research work in rainwater harvesting (Ncube et al., 2008; Makurira et al., 2010; Munamati and Nyagumbo,

2010, Mupangwa et al., 2011). These research outputs together with many before them contain important and relevant outputs that help to shape future research on rainwater harvesting in agricultural fields.

2.1.2 Types of rainwater harvesting systems

All rainwater harvesting systems have two main things in common. These are a catchment area where runoff is generated and a storage space where the runoff is collected and stored. The catchment area characteristics determine the amount of runoff that is generated. Some catchment areas such as roof and rock outcrop have high runoff coefficients. The runoff generated from such catchments is usually collected in storage tanks and used for domestic or supplemental irrigation. Other catchment areas have runoff generation governed by interaction of hydrological processes making estimation of runoff generation more challenging.

Rainwater harvesting types cover a wide range of systems that are intented for different purposes falling mainly in the domestic water supply and agricultural water use categories (Li et al., 2000; Prinz and Malik, 2002). Those falling in the domestic water use category comprise of a rainfall collection area (usually an impermeable surface such as roof areas or rock outcrops) and a storage tank. Water can be abstracted for use from the storage tank directly or through a pipe distribution system.

In the agricultural water use category, two main systems dominate. In one system water is collected from a permeable or semi permeable surface and either channelled directly to the crop growing area which is separate from the rainfall collection area or directed to a storage tank from where it is used for irrigation or other agricultural purposes such as animal watering (Li et al., 2000). A typical example of this system is shown in Figure 2-1. This system if accompanied by a storage tank has the advantage that it provides the farmer with control on when to use the water but has the disadvantage of requiring additional resources to build the storage tank/s and conveyance structures from the storage tanks to the point of use.

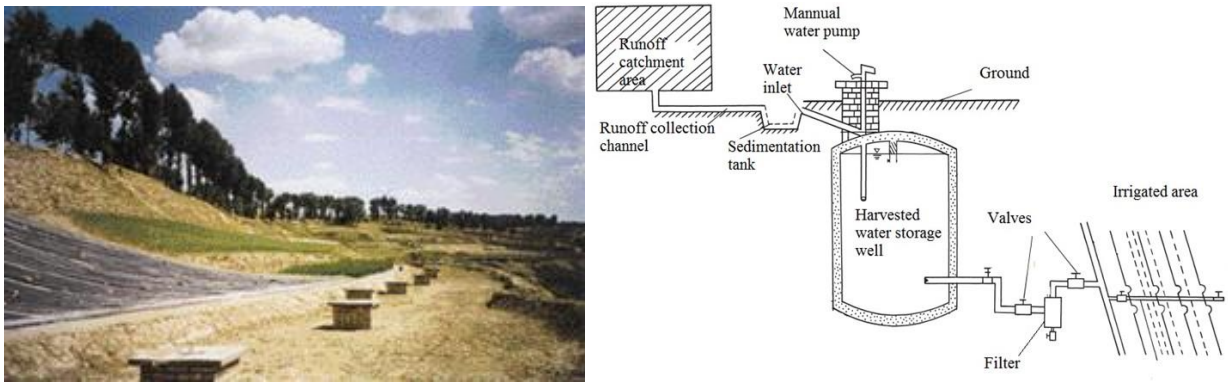

Figure 2-1: Rainwater harvesting from a plastic collection surface and storage in an underground tank (left) for crop irrigation as illustrated in the diagram (right) (source: Li et al, 2000).

In the other system of the agricultural water use category, the rainwater collected is stored in the root zone within the same area where it is collected and is often refered to as in-situ rainwater harvesting (FAO, 2000). Some examples of this system are shown in Figure 2-2. In-situ rainwater harvesting takes advantage of the runoff that is generated within the agricultural field. Technologies such as pot holing (basin planting), infiltration pits, fanya juus and contour ridges which are sometimes referred to as contour bunds focus on reducing runoff from the target field and increasing infiltration (Falkenmark et al., 2001). The infiltrated water is stored within the root zone of the field crops. These in-situ rainwater harvesting technologies may also benefit from rainwater harvested outside the crop field by directing runoff from grazing land, forested area, rock catchments and build up areas including roads and channelling it to cropped areas (Makurira et al, 2010; Laker, 2004). This is important in situations where the runoff generated from within the cropped area is insufficient to fill up soil moisture in the root zone. Details of a review of different types of rainwater harvesting systems in sub Saharan Africa can be found in Biazin (2012).

Figure 2-2: Examples of insitu rainwater harvesting systems: Potholing on the left (Source Mupangwa, 2007) and fanya juu on the right (Source Makurira, 2010)

2.1.3 Rainwater harvesting in the semi-arid regions of sub Saharan Africa

Semi-arid regions are characterised by low and unreliable rainfall often with mid-season dry spells (Tennant and Hewitson, 2002; Usman and Reason, 2004; Reason et al., 2005). In Southern and Eastern Africa most smallholder farmers in semi-arid areas are restricted to rain fed cropping and as in year 2000 stood at, Malawi, 90 %; Botswana, 76 %; Kenya, 85 %; and Zimbabwe, 70–80 %, of the population (Rockström, 2000). Successful crop yields under rain fed farming in most of the semi-arid areas of Southern and Eastern Africa are achieved in 2-3 years out of a 10 year period (Hatibu et al., 2003). This is expected to worsen under climate change conditions where the frequency of drought is expected to increase.

Crop failure in rain fed farming systems is caused more by the distribution of rainfall in the crop growing season than by the low seasonal amount (Rockström, 2000). Crop water requirements show that the threshold amount of water required for a crop to reach maturity is 300mm per growing season (Barron, 2004). However in many parts of semi-arid regions, total crop failure has been experienced due to water constraints where annual rainfall has been much larger than 300mm (Barron, 2004). This is mainly due to intra seasonal rainfall variability that is characterized by intra season dry spells that limit water availability at the plant root zone at critical crop growth stages. If water is made

available to the root zone during the dry spell say through supplemental irrigation or rainwater harvesting, then yield levels can be improved (Rockström, 2000).

Supplemental irrigation is used in many parts of the world in mitigation against effects of dry spells. India, China and Palestine are among the countries where various supplemental irrigation technologies are employed (Sbeih, undated). Hatibu and Mahoo (1999) showed that supplemental irrigation from rainwater harvesting in Tanzania significantly improved the yield of maize. In the semi-arid communal areas of South Africa supplemental irrigation through rainwater harvesting increased crop yield by 30 to 50% compared to conventional tillage method (Woyessa et al., 2006).

Supplemental irrigation requires storage facilities large enough to hold sufficient quantities of water and the means to abstract and apply the water to the field. The financial resources required to develop these storage and abstraction facilities are often beyond the means of most smallholder farmers in Southern Africa. This raises the need to focus on insitu rainwater harvesting technologies that can also be used to improve water availability to the root zone.

Despite the poor crop production levels that are experienced in most semi-arid regions there is still potential to obtain better yields if the water shortage problem experienced during the dry spell period can be solved. Rockstrom (2000) demonstrated the existence of this potential through a typical rainfall partitioning in semi-arid conditions of Sub-Saharan Africa and showed that non-productive water loses are as high as 70 – 80%. This high non-productive water loss provides an opportunity for improvement of food production in these areas if some of the water is rerouted to the root zone through adoption of appropriate technologies such as rainwater harvesting.

2.1.4 Adoption of rainwater harvesting by farmers

Despite the existence of various rainwater harvesting interventions, crop failure in smallholder farming and threats to water bodies due to sedimentation continue to be a major problem in Sub Saharan Africa. These problems are due to poor agronomic management practices used by farmers and/or failure to adopt appropriate interventions for given environmental conditions (Ziadat et al., 2006). Critchley et al. (1994) acknowledged the failure of soil and water conservation systems and established that much can be learned from indigenous soil and water conservation practices.

Mbilinyi et al. (2005) established that in Tanzania farmers hold substantial knowledge of rainwater haversting systems including knowledge on identification of potential sites for different types. Most of the farmers integrated different rainwater harvesting systems in one field most of which are soil and water conservation techniques. Mbilinyi et al. (2005) concluded that the indigenious knowledge was based on physical factors that include soil type, topography and distance from water sources.

Apart from poor rainfall conditions, soil nutrient deficiency is the other physical constraint to better yield in rain fed cropping systems. Studies in the Sahel (Hatibu et al., 2003) showed that soil nutrient deficit continues to be a more significant constraint than water deficit for annual precipitations as low as 300 mm. Another study by Zougmor´e et al (2004) found out that in Bukina Faso during eratic rainfall characterised by dry spells rainwater harvesting through stone bunds combined with composit provided suitable conditions for sorghum growth. In Zimbabwe Mupangwa (2010) established that application of nitrogen fertilizer at a rate of 10 $kgNha^{-1}$ on granitic sandy soils combined with double ploughing, ripper or planting basin systems improves maize yields during drought years. Therefore rainwater harvesting practices should be used in combination with proper nutrient management to realise improved yields.

Munamati and Nyagumbo (2010) also showed that socio economic factors play an important role in the performance of rainwater harvesting technologies and hence adoption of rainwater harvesting practices by farmers. In a study of the effectiveness of dead level contours for in situ rainwater harvesting and consequently on crop yield in Gwanda District of Zimbabwe, Munamati and Nyagumbo (2010) found out that dead level contours were more effective among more resourced farmers and among male headed households compared to resource poor and female headed households. This can be explained by the ability of well resourced farmers to combine good nutrient and crop management practises with rainwater harvesting practices.

In-situ rainwater harvesting has a better level of risk reduction than traditional farming practices without rainwater harvesting but has found low level of adoption due to high labour requirements and inappropriateness to certain conditions (Laker, 2004). Extension support provided by government departments or NGOs often recommends technologies for rainwater harvesting based on experience and trial and error rather than scientifically based techniques (Prinz and Malik, 2002). This may lead to unsatisfactory performance

of the technology and farmers abandoning the technology soon after withdrawal of the extension support. In Southern Africa in-situ rainwater harvesting has not been widely adopted although contour ridges have been used extensively for soil conservation while draining away water from the field (Hagmann, 1996). Adoption of contour ridges in Zimbabwe was enhanced by legislation that made it mandatory for farmers to construct contour ridges in their fields prior to independence. Recent adoption of contour ridges was driven by non-governmental organisations such as Practical Action (Munamati and Nyagumbo, 2010).

2.2 Rainwater harvesting through contour ridges

2.2.1 The standard contour ridge

Standard contour ridges are small earth structures constructed across the slopes on cultivated land with storage channels on the upper side of the earth structure (Figure 2-3). Their development in Zimbabwe was necessitated by soil erosion and they were thus designed to safely dispose off runoff and prevent rill and gulley erosion (Elwell, 1981; Mugabe, 2004).

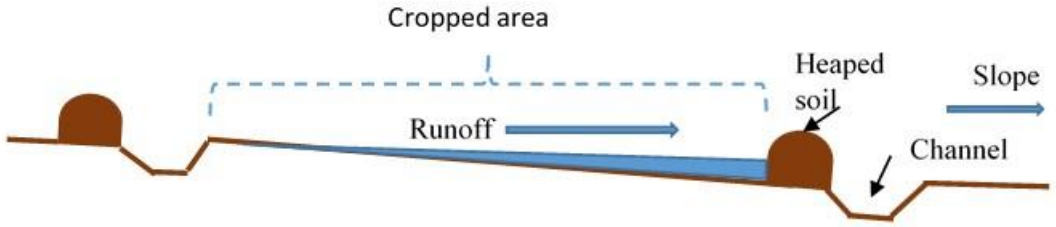

Cross section across a fanya juu

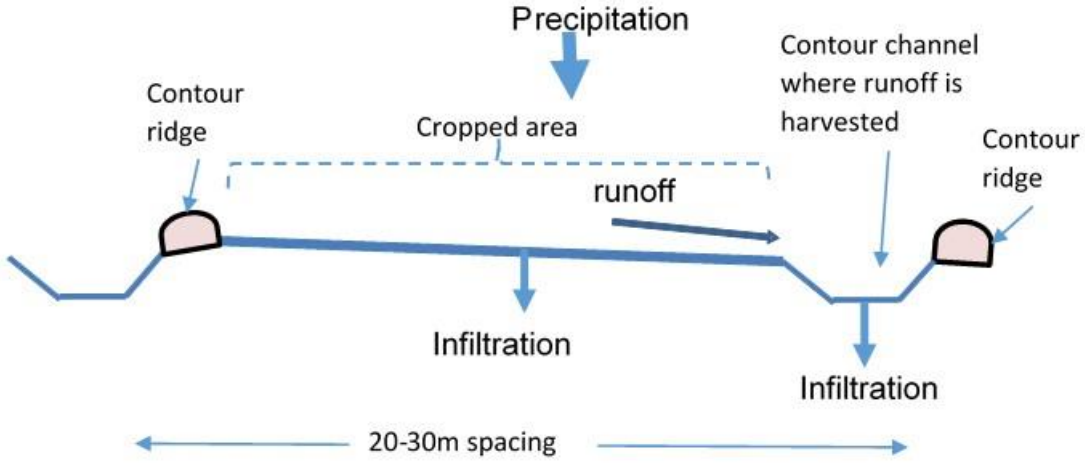

Cross section across a contour ridge

Figure 2-3: An illustration of the cross sectional area across a contour ridged field (bottom) contrasted from fanya juu at the top

The main objective for the construction of standard contour ridges is to reduce the erosive power of runoff flowing through the cultivated land resulting in reduction in soil erosion. This is achieved through interception of runoff which is then directed into grassed waterways where it drains to natural streams.

2.2.2 Limitations of standard contour ridges in some parts of Zimbabwe

Hagman (1996) established that standard contour ridges which were originally designed to control rill erosion were not effectively achieving their objective due to the inappropriateness of the technology to the semi-arid environment where they were imposed on the indigenous people. Their imposition was seen as colonial oppression and upon attainment of independence most smallholder farmers in communal areas failed to maintain them as expected. The study by Hagman (1996) which was carried out in the dry areas of Zimbabwe established that due to lack of maintainance, contour ridges were overflowing with water during heavy storms resulting in rill formation (Figure 2-4). Thus while the contour ridges were introduced to control soil erosion they ended up being one of the causes of rill formation which in some cases developed into gulleys.

Figure 2-4: Overflowing contour ridges resulting in rill formation (Source: Hagman (1996)

In some cases Hagman (1996) observed that, due to a ploughing practice in which farmers ploughed towards the centre of the field, depressions were formed upslope of contour ridge channels and downslope of the ridges (Figure 2-5). These depressions resulted in water retention and deposition of fine sediments as shown in Figure 2-6 . Such observations led Hagman (1996) to recommend retention of water through contour ridges that run along the contour lines later to be adopted as dead level contours (Mupangwa, 2006). This problem could also have been minimised by farmers alternating between ploughing towards the centre and away from the centre in different seasons.

Figure 2-5: Water retention in depressions due to ploughing towards the centre of the field (Source: Hagman (1996))

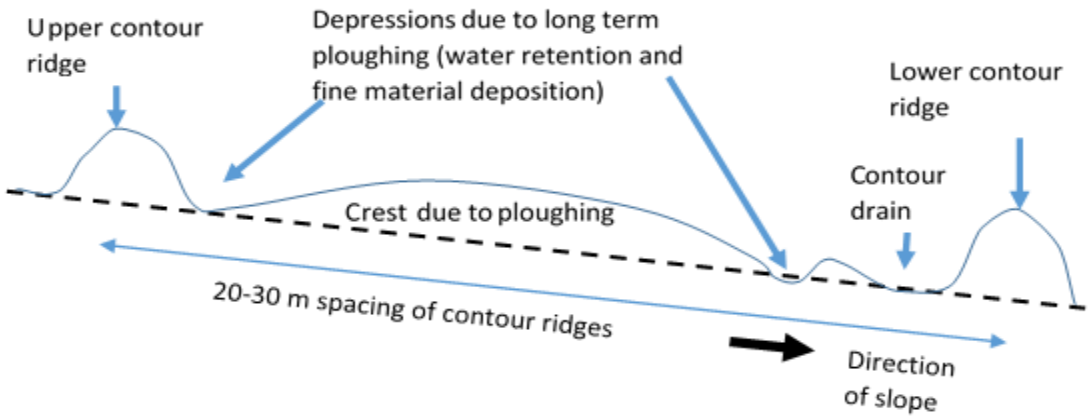

Figure 2-6: An illustration of change in surface profile after continuous ploughing towards the centre of the field (adapted from Hagman, 1996)

Imposition of contour ridges in many parts of Zimbabwe were done without studying the suitability of the practice on local conditions and without identification of modifications necessary to make them work (Hagmann, 1996). Imposition of farming practices was common in Zimbabwe's history. A similar case of imposition is draining of localised wetlands known as dambos in commercial farming areas resulting in serious gulley formation (MacFarlane, 1995). After realisation that serious gulley formation was taking place in dambos a legislation to outlaw cultivation in dambos was enacted despite a long history of successful farming in these areas by indigenous people. The indigenous people used to grow rice in the dambos during the rainy season and vegetables during the dry season using water obtained from shallow wells. The decision to drain dambos had a negative effect on the food security of the indigenous people who were now forced to grow maize as a staple food under conditions where the risk of failure was high.

While the focus of standard contour ridges was on soil erosion control through safely draining away water from the field, farmers in dry regions of Zimbabwe questioned the wisdom of draining away precious water in an area were crop failure was experienced due to shortage of water. Thus the current focus is now on retaining that water so as to

increase the amount of water added to the soil profile without compromising soil conservation.

2.2.3 Use of contour ridges for storing water

Published research on the use of contour ridges for storing water is limited and this study had to also consider grey literature to understand previous considerations in this respect. The use of contour ridges for storing water was previously proposed by Galletly (1980) who suggested that contour ridges be used for temporal storage after realizing that they were not efficient in preventing erosion as 10-20% of the soil eroded from the inter-contour ridge area is transported to the waterways and eventually to water bodies in the river system. Temporal storage would provide enough detention time to allow sedimentation to take place so as to prevent soil eroded from the field from leaving it and enter water bodies. Later the Queensland design manual (2004) pointed at the need to develop a design method that incorporates storage capacity of the contour ridges. Khlifi et al. (2010) carried out a study in Tunisia on the impact of contour ridges on soil fertility and established that they improve soil fertility and retain the soil in the field through deposition of fine sediments in the area upslope of them.

Use of contour ridges for storing water in Zimbabwe was driven by more frequent droughts in the last two decades leading to the adoption of dead level contour ridges (Munamati and Nyagumbo, 2010) in which the contour ridge is constructed at a zero gradient (Mwenge Kahinda et al., 2007; Mupangwa et al., 2006). These dead level contour ridges were implemented in the dry regions of Masvingo and Matebeleland South Provinces of Zimbabwe by nongovernmental organizations (NGOs), often on a massive scale.

Organizations implementing the dead level contours claimed success of the technology arguing the massive adoption by the farmers was an indication of their effectiveness of (Mutekwa and Kusangaya, 2006; Gumbo, 2006). However some researchers suggested that adoption alone does not imply effectiveness of the technology as the farmers may have been attracted by other factors (Hagman, 1996; Mupangwa et al., 2006). Non-governmental organizations often give away equipment for use in making the dead level contour ridges such as wheelbarrows, picks and shovels which eventually become part of the farmers' household equipment (Mupangwa et al., 2006).

Adoption of rainwater harvesting technologies depends among other factors on the benefits (in particular yield benefits) that are derived from the technology. Studies on the effect of agronomic practices on crop yield are many (Makurira, 2010, Mupangwa, 2009; Munodawafa and Zhou, 2008; Chibulu, 2007; Memon et al., 2007; Kusangaya et al., 2006; Sadras and Calvino, 2001). These studies are either through questionnaire surveys (Kusangaya et al., 2006), on station experiments (Mupangwa, 2009; Munodawafa and Zhou, 2008) or farmer based research (Makurira, 2010; Mupangwa, 2009). Maize is usually selected for yield assessment where water is considered a limiting factor. Maize is very sensitive to water stress and water shortage is likely to result in yield reduction. Thus many experimental studies on rain fed agriculture have used maize crop for assessing crop yield from different technological practices (Makurira; 2010, Mupangwa, 2009; Chibulu, 2007).

Several researchers have reported on the use of contour ridges for rainwater harvesting (Al Ali et al., 2008; Nasri et al., 2004; Mugabe 2002; Falkenmark et al., 2001;) but few have paid attention to the actual yield benefit derived from such rainwater harvesting. Among the few that have considered yield benefits of contour ridges are Kusangaya et al. (2006) who carried out a survey on the farmer's perception on the benefits of contour ridges on crop yield. The survey revealed that farmers were able to grow two crops per year where they would previously grow one crop. Mupangwa et al. (2010) studied crop yields from water conservation treatments of planting basins, ripper tillage and double ploughing on fields with contour ridges. The results however do not show the effect of contour ridges on crop yield as the effect of contour ridges was not isolated. No experimental study reporting on crop yield benefits for contour ridges has been found.

2.2.4 Research on rainwater harvesting by contour ridges

An attempt to provide evidence of the advantages of contour ridges in moisture retention was made by Mugabe (2004) who studied standard contour ridges where infiltration pits were incorporated to harvest runoff. The study was carried out in a semi-arid catchment during a period in which a seasonal rainfall of 625mm occurred. This study demonstrated the benefits of infiltration pits in standard contour ridge design. Mugabe (2004) found out that the field that was downstream of a standard contour ridge incorporated with infiltration pits had higher soil moisture (an increase of about 50% by end of the rainfall season) on average compared to the field that was downstream of a standard contour ridge without

infiltration pits. Mugabe (2004) recommended that further research was needed to establish the spacing and optimum depth of infiltration pits required under different soil types and slope as well as the effect of infiltration pits on crop yield. The first part of the recommendation relates to design of the standard contour ridges incorporating infiltration pits while the second relates to benefits accruing from adopting contour ridges with infiltration pits. This agrees with the study by Hagman (1996) who, although focusing on soil erosion, also established the need to set indicators of success for a technology as well as the need to modify the standard contour ridge design. Crop yield can be seen as a benefit of adopting a technology and as such one of the suitable indicators of success.

Another study on contour ridges in Zimbabwe was carried out by Mupangwa et al., (2011) who studied dead level contours and arrived at the conclusion that there was no significant improvement in soil moisture except for rainfall events as high as 60mm/day. The study was carried out in dead level contours incorporating infiltration pits in Gwanda District a dry part of the semi-arid Mzingwane catchment where average seasonal rainfall range from 200mm to 350mm. The study by Mupangwa *et al.* (2011) also concluded that dead level contours with infiltration pits had localised impact with soil moisture changes being observed at a distance of only about 3 m from the contour ridge suggesting a contour spacing of not more than 8m.

Mupangwa et al. (2011) recommended that further studies be focused on determining the rainfall threshold that would make contour ridges effective as well as other ways of utilising the limited soil moisture improvement that is realised from dead level contours. The areas of improvement that were suggested by Mupangwa et al. (2011) include strip cropping of food and fodder and deep rooted crops including drought tolerant agro forestry tree species. While the results of this study suggest that dead level contours are not effective as a rainwater harvesting technology the low rainfall received in the study area suggest that the low soil moisture improvement could have been due to the climatic conditions of the area rather than the technology itself. If there is no rainfall to harvest, one cannot expect a benefit from any rainwater harvesting technology. The areas that were proposed for further research suggest the need for modelling to investigate ‘what if’ scenarios before carrying out field experiments in areas such as Gwanda District where the study was carried out.

Away from Zimbabwe another study was carried out by Makurira et al. (2009) and Makurira (2010) in Tanzania in a bimodal climate on fanya juus where annual average rainfall ranges between 500mm and 800mm. A fanya juu is a type of contour ridge where the excavated soil is thrown up slope instead of down slope as is the case with contour ridges. The principle is to create a dam effect and allow infiltration in the cropped area. This can be contrasted with the contour ridge where the harvested rainwater is stored in the ridge channel where it infiltrates and travels to the root zone through seepage. The study by Makurira *et al.* (2009) established that the areas close to the fanya juu both upslope and downslope experienced higher moisture than the area away from the fanya juu (centre of field). The study also incorporated diversion of water from nearby catchment into the field through the fanya juu. Makurira *et al.* (2009) found out that diversion through the fanya juus resulted in further improvement of soil moisture in the field.

2.2.5 Lessons from previous studies on rainwater harvesting

The studies on rainwater harvesting by contour ridges reviewed in Section 2.2.4 did not make a comparison between the standard contour design that was developed for soil erosion control and the improved dead level contour design that retains water in the field. The studies also did not compare moisture between fields without contour ridges and those with contour ridges. In addition, previous studies did not assess the effect of soil type on the impact of contour ridges on soil moisture. Except the study by Makurira (2010) modelling of rainwater harvesting by contour ridges have been neglected in previous studies.

These gaps in the previous studies make it imperative to compare the soil moisture availability in a plot with dead level contours against one with the standard graded contour and one with no contour ridges in a single mode, semi-arid tropical climate condition.

Two of the three studies (Mugabe, 2004; Makurira et al., 2009) indicate soil moisture benefit from contour ridges while the third (Mupangwa et al., 2011) places doubt in soil moisture benefit from contour ridges. The study by Mupangwa et al. (2011) was carried out in a low rainfall area compared to the areas studied by Mugabe (2003) and Makurira et al. (2009) and therefore it can be concluded that benefits could not be established in seasons where rainfall was very low suggesting the possibility of a rainfall threshold below which no significant benefit can be realised. Although the contour ridges studied on these

three different locations are different, they operate on the same principle. Therefore, the difference in soil moisture benefit could be attributed to geophysical and climatic conditions.

The studies did not compare plots with dead level contour ridges with a control such as plots with no contour ridges nor plots with standard graded contour ridges. They relied on observing a moisture gradient from the contour ridge structure to the distance away from the structure across the field. There is a possibility that the results by Mupangwa (2011) could not show a benefit as the measurements were done once every two weeks which could have missed the downward movement of the zone of increased moisture across the field.

2.3 Design and modelling of contour ridges

Despite the long history of rainwater harvesting techniques dating back more than 5000 years the design of some of the in-situ rainwater harvesting techniques such as contour ridges is still not well developed. In Zimbabwe graded contour ridges were adapted from USA and were found to be effective for soil conservation through safely disposing off excess runoff from cultivated fields in high rainfall areas (Elwell, 1981). However they were applied right across all agro climatic regions of the country without considering the need to retain water in the field in regions that receive low rainfall (Hagmann and Murwira, 1996). The design was done with some parameters being adopted from the United States due to lack of local data (Elwell, 1981). Elwell (1981) emphasized the need for continued improvement of the design of contour ridges in order for them to remain relevant to the developments in agriculture.

The new focus in contour ridge design in which water is retained in the field implies contour ridges are now designed as a storage facility as opposed to previous focus when they were largely a conveyance channel. However there has been no guideline as to when dead level contours are appropriate and when the traditional standard graded contours should be adapted. Design data required to design contour ridges as a conveyance channel was controlled by maximum discharge that would need to be contained by the ridge channel without overtopping. Only peak discharge data was required for this design. Thus various methods for estimating peak discharge such as the rational method or Mitchell's method that is widely applied in Zimbabwe (Mitchell, 1974)

could be considered as adequate. The need to design the contour ridges for storing water implies the need to consider volumes of runoff and not just peak flows. In addition previous studies have shown that there are many factors such as presence of infiltration pits (Mugabe, 2004), diversion of water (Makurira et al., 2009) and rainfall amount (Mupangwa, 2011) that interact to determine the possible suitability of contour ridges for rainwater harvesting. These factors together with soil type occur differently at individual farmer's field. As a consequence of this, modelling would help to inform about the suitability of contour ridges without having to carry out field tests on soil moisture improvements on each field.

2.3.1 Modelling of rainwater harvesting

Modelling has been used to determine the impact of different rainwater harvesting technologies on soil moisture by many researchers (Boers et al., 1986a; Tsakiris, 1991; Hengdijk et al., 2005; Mwenge Kahinda, 2007; Makurira et al., 2009b). These researchers used different models some, specifically developed for rainwater harvesting, while others are general hydrological models that are usually used in combination with other models when modelling rainwater harvesting. This diversity in model types is described in the following few paragraphs.

Boers et al. (1986a) modelled micro-catchment rainwater harvesting in arid areas based on a water balance model. Micro-catchment rainwater harvesting is a method where runoff is collected from an adjacent catchment (the contributing catchment) about 100m in extent and directed to infiltrate and stored in the root zone of the crop growing area as shown in Figure 2-7 (Boers et al., 1986b; Tsakiris, 1991). The contributing catchment (CA) is usually small as it is often treated to reduce permeability using methods such as compaction or plastic covers (Li et al., 2000). It may also be a natural impermeable surface such as rock outcrops (Mwenge-Kahinda, 2007). The model involves carrying out a water balance analysis of the root zone of the crop growing (CG) area. The model was developed to analyze the performance of the micro catchment system in the arid climatic conditions and therefore is ideal for experimental conditions rather than for design purpose. The components of the water balance model used by Boers et al. (1986a) are determined from simple linear regression for runoff (R), direct measurements for rainfall (P) and evapotranspiration and simplified assumptions for deep percolation. Boers et al. (1986a) applied the water balance model in the arid zones of Israel and concluded that

the micro catchment technique can be beneficial in the desert fringes with loess soils, which form a surface crust that reduces infiltration and increase runoff from the CA, but not in extremely arid conditions where rainfall is too low. The water balance model neglected lateral moisture flow - a component that is presumed to benefit field crops in contour ridges rainwater harvesting techniques.

Tsakiris (1991) considered the design criteria for micro-catchment rainwater harvesting technique in the semi-arid Mediterranean climate of Tunisia. In this regard the water balance model approach used by Boers et al. (1986a) was inadequate without further improvement. A new model was needed to estimate the improvement in soil moisture from a situation where there is no micro catchment rainwater harvesting system to where a micro catchment rainwater harvesting system was implemented with a given ratio of CA to CG. It was established that the most important parameter is the ratio of the dimensions of the contributing area to those of the crop growing area. This required consideration of a wider range of rainfall events than those feasible under experimental conditions. To achieve this Tsakiris (1991) assumed the occurrence of a certain number of rainfall events within a given period and by extention the infiltration within the crop growing area was random and followed a Poisson distribution. A further assumption was that the contributing area was relatively impervious and as such runoff amount reaching the crop growing area was to a large extend also governed by the Poisson distribution. Therefore inflow into the root zone was estimated on the basis of Poisson distribution for both a situation when a micro catchment rainwater harvesting sytem is in place and when it is not in place. The Thornnwaite and Mather soil moisture depletion model (Tsakiris, 1991) was used to estimate the soil moisture uptake from the root zone. If the level of soil moisture at the beginning of the dry season is known the ratio of the required contributing area to the crop growing area can be determined. Tsikaris (1991) noted that though this method was not explicit, it was against the backdrop that in practice no design considerations are usually taken into account. While an effort was made to derive design criteria, the nature of rainwater harvesting technique investigated is different from contour ridges. The contributing area in contour ridges is pervious and the collected runoff is infiltration excess. The method does not recognise that the response may follow a different model considering that runoff generation depends on other factors such as soil type, soil moisture and rainfall intensity. Furthermore, the method developed does not allow for the investigation of the extent of lateral flow of the harvested water.

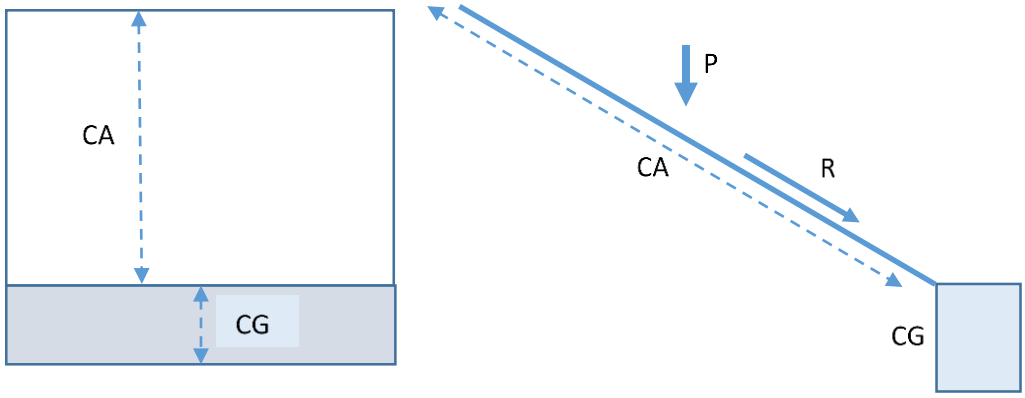

Figure 2-7: Plan and cross section of the schematic representation of a micro-catchment rainwater harvesting system (adapted from Tsikaris, 1991)

There are many hydrological models not specifically developed for rainwater harvesting that have been used to model rainwater harvesting some of which have been applied in modelling contour ridges and are discussed in section 2.3.2. One such model is the HYDRUS model which was used by Ruidisch (2013) to model water flow in a plastic mulched ridge cultivation system in South Korea and by Makurira (2010) to model rainwater harvesting by fanya juus. HYDRUS is a physically based model that simulates movement of water in both saturated and unsaturated porus media using a numerical solution of the Richards equation (Simunek, 1998, Simunek; 1999; Simunek, 2006). It has many applications including irrigation and drainage design, solute transport analysis, simulation of leachate in agriculture and waste dump sites, analysis and design of water barriers such as embankment dams and many others. It requires many parameters in particular soil hydraulic properties and data for calibration of other parameters that may not be measured in the field. Its application in modelling rainwater harvesting is not as wide as in the other areas. However it has been applied by Ruidisch (2013) to model water flow in a plastic mulched ridge cultivation system in South Korea. The results were satisfactory for one of the two sites modelled while on the second site the results were

less satisfactory. The poor performance was attributed to difficulty in capturing the real field conditions in the model such as unevenness of the ridges often having small depressions on top of the ridge and representation of soil hydraulic properties.

Other researchers have used GIS based methods to identify land suitable for rainwater harvesting (Mwenge Kahinda et al., 2008; Jasrotia et al., 2009). Mwenge Kahinda et al., (2008) developed a rainwater harvesting suitability model that combines physical, ecological, socio-economic and rainwater harvesting constraint factors to produce maps of areas that are suitable for rainwater harvesting in South Africa. The maps provided satisfactory information on areas that could be targeted for rainwater harvesting but cannot be used for individual farm scale rainwater harvesting design. Jasrotia et al., (2009) used GIS to generate thematic maps that included potential evapotranspiration, land use/land cover, soil map and slope and integrated them to identify sites suitable for rainwater harvesting structures. The results showed that 11% of the watershed area had suitable sites for rainwater harvesting structures.

There are also other models specifically developed for rainwater harvesting such as Parched-Thirst (predicting arable resource capture in hostile environments during the harvesting of incident rainfall in the semi-arid tropics). Development of Parched-Thirst was motivated by the need to enable transfer of experimental results for rainwater harvesting in space and time (Young et al., 2002). Parched-Thirst is a process based distributed model that couples runoff, soil moisture and crop growth models. It was tested in Tanzania with reported satisfactory results but has not been tested for contour ridges (Young et al., 2002). In the Olifants River basin, South Africa, Magombeyi et al. (2012) applied Parched-Thirst to model crop yield from rainwater harvesting by planting basins known locally as Chololo pits. The current farming practice was also modelled using Parched-Thirst and the results were compared. The results indicated that planting basins increased yield by up to five times that of current farming practices.

2.3.2 Modelling rainwater harvesting by contour ridges

Like general modelling of rainwater harvesting, modelling of contour ridges has been attempted using a variety of models in the past decade. These range from simple water balance to complex physically based distributed models. However these models have not

been specifically developed for contour ridges and have achieved success in varying degrees.

Hengsdijk et al. (2005) modelled the effect of stone contour ridges (bunds) on crop yield in Ethiopia using the World Food Studies dynamic crop growth simulation model (WOFOST) which simulates crop growth based on climatic conditions. It was assumed in this model that runoff reductions due to the stone bunds results in increased infiltration and that this moisture is then stored in the root zone and is available for crops. A daily water balance of the root zone was used by the model to illustrate the effects of stone bunds on water availability and hence yield changes. The results of this model were not compared with field observations. However the authors reported an increase in amount of infiltrating water of up to 50%. In terms of crop benefits incorporation of stone contour ridges resulted in increase in yield only when the sowing date was sub-optimum i.e. when water was a limiting factor to yield which is an indication of the effectiveness of the stone contour bunds.

Mwenge-Kahinda et al. (2007) used the Agricultural Production Systems SIMulator (APSIM) to model the impact of a rainwater harvesting system on reducing the gap between the actual yield and the optimum yield that could be realised when water and nutrients are not a constraint in semi-arid areas of Zimbabwe. The modelled rainwater harvesting system comprising of a micro catchment of a granite outcrop, dead level contours and infiltration pits for a smallholder farmer. Water from the different rainwater harvesting techniques including dead level contours was used for supplemental irrigation through manual application. Like the study by Hengdijk et al. (2005) the modelling focused on crop yield and was not compared with observations. Model results showed that when supplemental irrigation from rainwater harvesting was implemented the water productivity (yield of maize in kg/ cubic metre of water used) of the maize improved by 22% on average.

Makurira et al. (2009b) modelled moisture changes in a field where fanya juus were used as a rainwater harvesting technique in a semi-arid catchment in Tanzania and compared the results with field measurements. The model was based on the water balance equation of the root zone as shown in Equation 2-1. The input parameters in the model were either obtained from field measurements or from estimates using empirical methods. The model used by Makurira et al. (2009b) considered the whole area between fanya juus as one

plot and hence its results do not show simulations of sub plots within the field area. It also does not incorporate subsurface lateral flow (presumably this was considered negligible). Subsurface flow was observed by Mugabe (2004) to occur in contour ridges incorporating infiltration pits in Zimbabwe. The field studied by Mugabe (2004) was located between two contour ridges and plots close to the contour ridges had more moisture than those away from the ridges and it was concluded that the water that infiltrated in the infiltration pits was responsible for this change. Makurira (2009b) could have ignored the lateral flow since a fanya juu operates on the dam effect. The dam effect arises from the fact that the soil embankment of the fanya juu is constructed upslope of the trench and runoff is stopped by the embankment in the cropped area.

$$\frac{dS_u}{dt} + \frac{dS_s}{dt} = P - E_T - E_I - E_s - R_g - Q_s$$ Equation 2-1

Where:

$(dS_u)/dt$=rate of change of soil moisture in the root zone
$(dS_s)/dt$=Rate of change of surface water storage;
P=Precipitation on the cropped area during time step dt;
E_T=transpiration during time step dt.
E_I=Evaporation from interception during dt;
E_s=Evaporation from the soil during dt;
R_g=Groundwater recharge during dt;
Q_s=Surface runoff during dt.

Makurira (2010) applied HYDRUS2D model (Simunek et al., 2006) to model rainwater harvesting by fanya juus in the same field previously modelled by a water balance model (Makurira et al., 2009b) and compared the results from HYDRUS2D model against those of the water balance model. The results were in fair agreement although the water balance model performed better than the HYDRUS2Dmodel. The low performance of the HYDRUS2D model was due to the fact that it requires data on soil characteristics, slope, water input and boundary conditions which is costly and difficult to obtain. Where this data cannot be obtained the model has default functions to estimate these parameters when soil texture is defined which were used by Makurira (2010) for modelling rainwater harvesting by fanya juus.

2.3.3 Limitations in current approaches of modelling contour ridges

Models that were identified in this literature review as having been applied on rainwater harvesting in general and contour ridges in particular have not been specifically developed for contour ridges. Although each of the models can be applied to certain aspects of contour ridges there are other aspects that are important to functioning and design of contour ridges where the models may fail to represent adequately. Suitability of a hydrological model depends on how its perceptual component (hydrologist's perception or understanding of the processes taking place) and conceptual component (form of mathematical equations) capture the dominant processes in the system being modelled (Beven, 2000; McClynn et al., 2002; Butts et al., 2004; Dunn et al., 2007). Limited knowledge of the system may lead to important processes being left out which may result in an increase in uncertainty and inadequacy in the modelling (Chatfield, 1995; Wagener and Gupta, 2005). The perceptual and conceptual components of a model reflect the structural complexity of the model. Butts et al (2004) defines a model structure as the extent to which processes are described or coupled, numerical and spatial representations are descretised and physical attributes are interpreted and classified. Inadequacies in describing the hydrological processes and errors in estimating input variables and parameter values are the main causes of uncertainties in modelling (Willems, 2000; Jothityangkoon et al., 2001; Zehe and Sivapalan, 2007).

A model for rainwater harvesting by contour ridges requires a structure that captures the main processes driving rainwater harvesting by contour ridges and the ability to reduce or incorporate the uncertainty arising from input variables and parameter values. The main hydrological processes taking place in a contour ridged field occur in three main subzones of the rainwater harvesting systems. These subzones are the runoff generation area which is also the surface of the crop growing area, runoff receiving area which is largely the contour ridge channel and the root zone which is the soil horizon of the crop growing area. A suitable structure of a hydrological model for rainwater harvesting by contour ridges should consider that these three spatial areas and hydrological processes taking place within them are included in the model. This is why a water balance model covering only the runoff receiving area and ignoring the details of the water balance of the runoff generating area as well as ignoring the lateral soil moisture movement proves to be adequate for a micro catchment rainwater harvesting system (Boers et al., 1986a; Tsakiris, 1991) but not adequate for rainwater harvesting by contour ridges. Such a model

cannot handle infiltration within the same area where runoff is generated. The runoff generating area is often treated to reduce infiltration which is different from the case of contour ridges in which the runoff is generated from the crop growing area and any infiltration within that area is encouraged.

The aspect of infiltration taking place within the crop growing area is however captured by the water balance model developed by Makurira et al. (2009b). The structural weakness of this model arises from the fact that the model only deals with the water balance of the root zone and ignores water balance in the channel of the contour ridge. In addition, it does not incorporate subsurface lateral flow - a process that is considered important for the functioning of contour ridges in rainwater harvesting. In addition, it does not provide an estimate of runoff from rainfall, limiting its application to sites where runoff measurement would have been carried out. As previously alluded to methods of estimating runoff for standard graded contours are aimed at peak discharge while contour ridges designed for storing water would require discharges at all the various rainfall events. This makes modelling of rainfall runoff processes at field scale an important aspect and is discussed later in chapter 3 section 3.6. In that section different approaches for estimating runoff at field scale are considered and the fuzzy logic is identified as an applicable method for modelling runoff at field scale. Fuzzy logic is a method of handling systems with uncertain subsystem boundaries by grouping the subsystems into groups with defined boundaries and then determining the degree to which an aspect of the system belongs to each subsystem group. This is explained in greater detail in chapter 3 sub-section 3.4.2.

Although lateral subsurface flow of water is provided for in HYDRUS2D and has been applied by Makurira (2010) and by Ruidischa et al. (2013) its main weakness lies in the uncertainty arising from errors in estimating parameter values of the model. The parameters' values such as hydraulic conductivity are difficult to measure and they keep varying spatially and temporally (Heddadj and Gascuel-Odoux, 1999); (Sobieraj et al., 2002). The problem of uncertainty in estimating model parameters for the HYDRUS2D model can be seen in the studies where HYDRUS2D was applied to model lateral flow in rainwater harvesting by Makurira (2010) and Ruidisch (2013). One of the sites modelled by Ruidisch (2013) in South Korea had an underlying granite layer at a depth of 1m while the second site had a deep soil layer. The model results showed that lateral flow (as

shown by overall flow direction) was very strong in the field with an underlying granite rock at a depth of 1 m while on the other site with a deep soil layer the overall flow direction was vertical. When the results were compared with observations on the basis of measured pressure head it was found out that the model predicted the pressure head better at the site with underlying rock than at the site with a deeper soil layer. This agrees with the results obtained by Makurira (2010) in which HYDRUS2D was applied to model rainwater harvesting by fanya juus which were less satisfactory compared to the results from a water balance model. This indicates that there is high potential of uncertainty in the results of HYDRUS2D model if it is used to model areas with high spatial variability of soil and underlying rock arising from uncertainty of values of input parameters.

The problem of estimating values of input parameters and variables is not only restricted to HYDRUS2D model and other process based models but in most models that can be used for rainwater harvesting where the model is applied on sites without field experiments. The problem only increases in HYDRUS2D and other process based models owing to a large number of parameters associated with their physically based nature. The methods used to estimate the parameters and input values do not normally consider the impreciseness of the data. An example is the estimation of hydraulic conductivity which depends on soil type and soil moisture and affects runoff generation and infiltration rate (Vogel et al., 2001). Hydraulic conductivity also depends on macro porosity which is difficult if not impossible to measure but may sometimes result in the difference between hydraulic conductivity of two different soil types being difficult to establish (Sobieraj et al., 2002). Hydraulic conductivity that includes macro porosity would be better estimated as being high or low which is imprecise. Similarly where measurement of hydraulic conductivity is done indirectly such as through soil texture, it is much more realistic to specify it as low, moderate or high before assigning it a numerical value.

Another example is the estimation of runoff which depends on a number of factors such as soil type, soil moisture, rainfall intensity and rainfall duration (Ramos and Martı´nez-Casasnovas, 2006). Experimental sites rely on data measured on site while non experimental sites have the runoff estimated from empirical relations developed from the experimental sites. Even for experimental sites, the rainfall characteristics during data collection and experimentation may differ from those that may prevail in future.

Again another example is the uncertainties arising from the temporal variability of the rainfall data, which together with potential evapotranspiration is the main external forcing of the hydrological processes. Rainfall data is much more readily available on a daily temporal resolution yet the runoff amounts depend on rainfall amounts at subdaily time steps. Using daily rainfall requires disaggregation of the daily rainfall data to a subdaily time step. Patched-Thirst (Young et al., 2002) is the only rainwater harvesting model that was found to incorporate rainfall disaggregation. Development of Parched-Thirst model is presented and discussed in Young et al. (2002). It was mainly tested in Tanzania and Kenya with bimodal climate but details of rainfall disaggregation are not provided. As a result the suitability of the rainfall disaggregation in Parched-Thirst to unimodal climate of Southern Africa could not be ascertained from the literature. However a rainfall disaggregation model for application in South Africa was developed by Knoesen and Smithers (2009) who modified a rainfall disaggregation model initially developed by Boughton (2000) for Australia. The method relies on estimating the proportion of rainfall that falls in the hour of maximum precipitation followed by estimating the proportion of rainfall that falls in the remaining 23 hours of a day.

The socio economic conditions of smallholder farmers suggest that data collection would be restricted to data that is readily available such as soil type, evaporation and rainfall. This calls for an approach that deals with uncertainties while at the same time being able to model the basic conceptual structure of the processes taking place in the rainwater harvesting systems such as contour ridges. In addition to the water balance of the root zone that was considered by Makurira et al. (2009b), other spatial storages where water partitioning takes place such as the cropped surface area and the contour ridge channel need to be included in the modelling. A combination of a process based conceptual model and fuzzy logic approach could probably provide a model that meets these requirements. The search for an appropriate modelling approach incorporating uncertainties for modelling contour ridges is considered in Chapter 3.

2.4 Summary

Rainwater harvesting has a long history dating back to more than 5000 years ago. There are various types of rainwater harvesting technologies for both domestic and agricultural purposes. Adoption of some of the technologies by farmers is poor owing to

inappropriateness of the technologies to suit local conditions among other reasons. Despite the need to adapt technologies to local climatic and geophysical conditions, the absence of appropriate design guidelines for most rainwater harvesting technologies in general and contour ridges in particular remains a major challenge.

Most research has concentrated on proving that a technology improves water availability and yield but have neglected how the results can be transferred to other locations. With regard to contour ridges, there has been no comparison between dead level contours designed for water conservation and the traditional standard graded contour designed for soil conservation. A number of models that could be applied for modelling rainwater harvesting by contour ridges were identified but none was specifically developed for contour ridges.

3 A search for improved hydrological modelling applicable to contour ridges

The major factor that needs to guide the search for a hydrological model applicable to contour ridges is availability of data in individual farmer fields. Sufficient data for calibrating a model is mostly restricted to experimental fields. Farmers on non experimental fields are only able to collect limited data such as rainfall if they have raingauges on their farms. However some data can be collected from farmers through interview surveys that can complement experimental observations. Magombeyi et al. (2012) used this approach to collect data for modelling small holder farming systems.

If the model is to be useful for application to farmers' fields, which are mostly non experimental, an appropriate modelling framework is likely to be one used in ungauged catchments such as those that seek to converge process hydrology with statistical and empirical hydrology (Wagener, and Montanari, 2011). Process modelling is required to cater for interaction of the processes at different temporal and spatial scales which can be achieved by applying detailed distributed physically based models (Beven, 2000; Willems, 2000). Empirical models are suited to situations where data on the hydrological system is limited. In such a situation it is most likely unrealistic to apply process based modelling on its own.

Approaches for empirical models are mostly based on regression equations whose coefficients are determined through regression analysis of observed versus calculated data (Li et al., 2004; Walker and Tsubo, 2003a). The determination of the regression coefficients can be regarded as the calibration of this type of model and observed data is required to determine the regression coefficients. This means application of empirical models is limited to situations where regression coefficients have been established.

The application of the laws of physics, essentially the conservation of mass, momentum and energy, is fundamental to distributed physically based models (Beven, 2002). The explicit consideration of conservation of mass and momentum means that these models are physically meaningful and therefore produces correct results for the right reasons. However mass and momentum balance equations are expressed at point or

representative volume. This creates challenges of dealing with spatial variability in model calibration parameters. The calibration parameters of physically based models have a physical meaning to the system characteristics and hence often require measurement which can be restricted by resource availability.

Conceptual lumped models make use of simple mathematical relations to simulate real world behaviour. However variations within the entire spatial area are normally ignored during the modelling. Conceptual models are generally applied to surface hydrology more than in groundwater hydrology. A distinct class of models based on a combination of conceptual lumped models and distributed physically based models is the representative elementary watershed (REW) based models such as the CREW and REWASH (Zhang and Savenije, 2005). The REW approach is described in more detail in the following sub section.

3.1 The representative elementary watershed (REW) approach

The REW is a special group of models that combine principles of physically based models and those of the conceptual lumped models with the objective of developing a model that is directly applicable at the watershed scale (Reggiani et. al, 1998; Reggiani et. al, 1999; Reggiani et. al., 2001). It is based on an approach where the entire watershed is subdivided into smaller units each called a representative elementary watershed (REW). Reggiani et al. (1998, 1999) pioneered the concept of REW as an approach for developing catchment hydrological models applicable to all spatial and time scales (Reggiani and Schellekens, 2003). A REW is considered as a prismatic mantle whose boundary at the top is the atmosphere and at the bottom is an impermeable substratum or an assumed depth (Figure 3-1). The catchment area defining the common outlet of the unit completes the boundaries of a REW.

Reggiani et al. (1998) argued that distributed physically based models are based on equations that are developed for the point scale or control volume and then integrated over the entire basin. This gives rise to the extensive data requirements at the basin scale to reflect the physical processes taking place at the point scale as parameters of physically based models should have physical meaning to the system characteristics. Despite the parameters requiring extensive data with a physical meaning to the system characteristics a corresponding large number of parameter values are required for the

calibration process. Such a large number of parameter values means that an infinite combination of parameter values can yield the same model output. This leads to parameter estimation problem if the model is to remain physically based (Beven, 2001). Thus the REW approach was developed to address this problem as the equations under the REW approach are developed to reflect processes taking place at the REW scale.

3.1.1 The REW sub regions and balance equations for mass, momentum, energy and entropy

The volume of a REW enclosed by its boundaries is subdivided into sub regions based on different physical characteristics of water within each zone and typical time scales of various hydrological processes that are important at the basin scale (Reggiani and Schellekens, 2003). The hydrological processes are viewed in terms of all the basic functional components of a watershed which are recognisable as subregions of the REW (Figure 3-1). The establishment of the REW approach was necessitated by the need to develop physically based models that operate in a physically meaningful manner. This allows the applicability of the models in different environments unlike the lumped models that tend to be specific for certain regions or sites depending on the assumptions made prior to model development (Lee et al., 2005).

Five sub regions of the REW were identified as concentrated overland flow zone, saturated overland flow zone, channel reach zone, unsaturated zone and saturated zone (Reggiani and Schellekens, 2003). These sub zones provide a domain where hydrological flow processes are described and balance equations of mass, momentum, energy and entropy are developed. For example in the saturated zone the volume of the zone is occupied by soil and water while in the unsaturated zone it is occupied by soil water and gas and in the overland flow zone the volume is occupied by water. Reggiani et al. (1998) developed, through averaging, fundamental equations of mass, momentum, energy and entropy applicable directly at the REW scale and for each sub region.

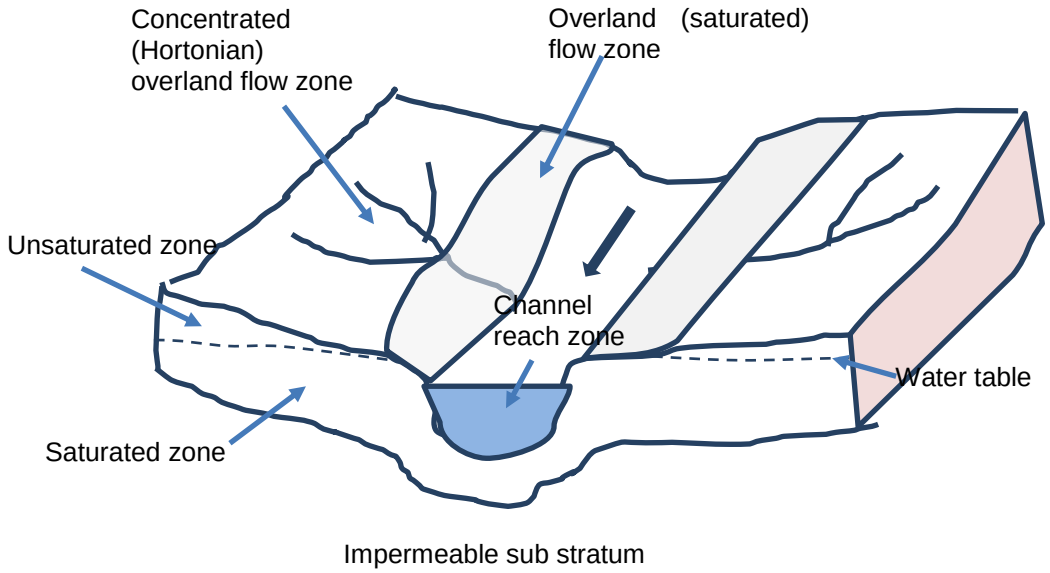

Figure 3-1: An Illustration of subregions forming a REW (adapted from Reggiani et. al, 1998)

The need to develop fundamental equations through averaging is in line with the concept of equifinality as discussed by Beven (2006). Equifinality is considered as a concept in which a hydrological model with many different parameter sets produces equally good outputs with each parameter set (Savenije, 2001; Beven, 2006). The disadvantage of this behaviour of models is that when certain characteristics of the catchment (space being modelled) change, the model will not produce the same output from the different parameter sets. This means that at the catchment scale some detailed hydrological processes will add no value to the desired output apart from confusion. The confusion arising from these detailed processes can be removed if the average process behaviour at that scale is considered (Savenije, 2001). Savenije (2001) illustrated how the process of averaging resulted in many physical laws such as the gas law and Ohm's law among others. Considering the gas law as an example, at a minute scale, where individual molecules are observable, the molecules move in a chaotic manner. However when observed at the scale of a gas container relationships among pressure, volume and temperature manifest. Savenije (2001) further argues that physically based hydrological models should be based on behaviour that is consistent at the scale of application. This supports the REW approach where the model is developed for the target catchment scale.

The REW approach enabled Reggiani et al. (1998) to develop for each sub region of the REW balance equations for mass, momentum, energy and entropy that are applicable at all spatial and time scales. Development of the balance equations was carried out using the second law of thermodynamics. In each volume of the sub regions of the REW the balance equation established is in the form shown in Equation 3-1 (Reggiani et al., 1999).

$$\frac{d}{dt}(\rho_{\propto}^{i} V_{\propto}^{i}) = \sum_{j \neq i} e_{\propto}^{ij} \qquad \text{Equation 3-1}$$

Where:

$\rho^{i}_{\propto}$ is the mass density of water at the $\propto$-phase occupying subregion i;
$V^{i}_{\propto}$ is the volume of subregion i filled by water in phase$\propto$;
$e^{ij}_{\propto}$ is mass exchange of water in phase $\propto$ between subregion i and subregion j.

The mass exchange components on the right hand side of the equation are general expressions to complete the balance equation and require that exact expressions known as closure relations be determined depending on the hydrological process that they represent. They are defined in terms of solvable variables and present the closure problem in the REW approach (Reggiani et al. 1999; Lee et al., 2005). The closure relations are required in all balance equations and should be expressed in terms of their relationship with known state variables of the sub regions (Lee et al., 2005).

3.1.2 Development of closure relations for the REW balance equations

Lee et al. (2005) developed closure relations for the balance equations of the sub regions of the REW and tested them for a catchment in Germany and concluded that although the model was able to predict the catchment fluxes fully, the closure relations needed testing in a wide range of physical and climatic conditions before they can be considered fully acceptable. Beven (2002) analysed and commented on the closure relations suggested by Reggiani et al. (1998) and noted that they involve coefficients that may be nonlinear and that ways of dealing with such coefficients had not been suggested. This problem was not solved by the closure relations developed by Lee et al. (2005).

Four approaches for developing closure relations were suggested by Lee et al. (2005) as an improvement of closure relations developed by Reggiani et al. (1998; 2000). These are field experiments, theoretical/analytical derivations, numerical experiments and

hybrid approaches. Field experiments produce empirical closure relations from field data. While this represents the intrinsic natural variability inherent in the catchment under study they may not be transferable as these relations may not be applicable in certain regions. Theoretical derivations provide meaningful closure relations that can enable use of physical and climatic properties of the catchment under study. However the development of closure relations, require simplifying assumptions about the processes taking place and the nature of heterogeneity of catchment properties such as physical and climatic parameters. The numerical approach methods make use of physically based hydrological models with well-defined boundary conditions to derive closure relations. They suffer the disadvantage of failing to deal with preferential flow pathways and non-linearity that is common in natural processes. The hybrid approach takes advantage of the methods discussed above to select convenient closure relations but there is no systematic approach to a hybrid approach.

3.1.3 Uniqueness, relevance and limitations of the REW approach in modelling contour ridges

The REW approach can be seen as a systematic way of building a hydrological model. This systematic approach can be summarised as involving three stages namely the discretisation of the system into the basic unit that contains all the fundamental processes found in the system being modelled, the identification of separate regions within which unique processes are taking place and constitution of mathematical relations known as closures to describe flux exchanges among these subregions.

Although a REW based model appears very similar to a conceptual lumped model what makes them different is that a REW has identifiable spatial regions or REW subzones (Reggiani and Schellekens, 2003) for which fluxes across their boundaries (closure relations) should be established in order to solve the balance equations for mass, momentum, energy and entropy of these regions. With respect to physically based distributed models the REW is identified by process descriptions developed directly at the REW scale as opposed to process descriptions that are developed at point scale that require discretised parameter descriptions (Zhang et al., 2005). This makes it not necessary to require highly variable soil parameter values required by physically based

models that are difficult and costly to obtain. With respect to lumped models the REW is identified by averaged parameter values.

REW based approaches have potential for modelling rainwater harvesting by contour ridges as the developed model is semi-distributed and physically based with characteristically identifiable subzones (Zhang et al., 2005). Where these subzones are found inadequate to describe the hydrological system more subzones have been proposed (Tian et al., 2006). As demonstrated by Lee et al. (2005) closure relations can be established using different methods which makes it convenient as availability of data can allow selection of best available closure relation. Thus the REW approach is more flexible than lumped conceptual models that are identified by a series of interconnected reservoirs (Reggiani et al., 1998) whose fluxes are represented by appropriate transfer functions. These transfer functions are generally lumped functions largely informed by data available for the site through calibration making them less applicable in ungauged sites. When one considers the situation of rainwater harvesting by contour ridges one realises that their suitability for an individual farmers field where experimental data was not collected may not be implemented with models whose transfer functions require calibration because data for such calibration does not exist.

With respect to physically based models the REW approach can be considered suitable for application to contour ridge modelling as it allows lumping of parameters where they are needed for the entire representative area thus reducing the need to obtain detailed data on parameter values. Despite the lumping approach that makes them similar to conceptual models, identification of subzones helps to capture the physical processes making it easy to relate to different sites.

While the REW approach has great potential for modelling contour ridges the approach is rigorous particularly in the development of balance equations of mass, momentum, energy and entropy and the corresponding closure relations (Reggiani and Schellekens, 2003). The constitution of the balance equations requires that consideration be made of the region to which the model is applied (Tian et al., 2006; Mou et al., 2008). Inclusion of momentum, energy and entropy equations add to the complexity of the model yet it may be convenient to include only mass balance equations. In this case the approach cannot be described as fundamentally REW as there are many other process based models that do that. Previous classification of modelling approach by researchers as being REW has

raised concern among readers. Vannametee et al. (2012) classified their modelling as having followed the REW approach which attracted criticism for its lack of embracing all the principles of REW. Later in an interactive comment Vannametee et al. (2013) conceded that their modelling was more of a Hydrological Response Unit (HRU) concept than a REW one. Therefore while it may be beneficial to borrow modelling ideas from the REW approach, a REW based model needs to incoprporate all the fundamental aspects of the approach. The most effective modelling approach for the problem at hand may however be a hybrid in which modelling aspects from different approaches are integrated.

3.2 Hybrid approaches in hydrological modelling

The main basis for selecting an acceptable model or developing one is the adequacy with which it will carry out the analysis and provide the required information. The model should obviously not violate physical principles at the scale of application and needs to be consistent with the observed data that may be available for the system being modelled (Beven, 2002).

Many researchers have combined different approaches to come up with models that meet these criteria with recent examples combining conceptual or process based principles with artificial intelligence techniques such as artificial neural networks (ANN) and fuzzy logic. Wen et al. (2014) combined adaptive network based fuzzy inference system with the physically based Hydrological Engineering Center-Hydrological Modelling System (HEC-HMS) model and obtained improved simulated river discharge in Kaoping River of Taiwan. Chen et al. (2015) used a hybrid of ANN and fuzzy logic combined with the continuity equation to model downstream river discharge. Badrzadeh et al. (2015) applied various computational intelligence models for runoff forecasting in Richmond River of Australia. Raghavendra and Deka (2014) give a comprehensive review of how support vector machines (SVMs) have been applied in hydrological modelling. SVMs is a statistical learning based technique that is used for classification and regression analysis. These hybrid approaches enable the model to deal with the problem of data scarcity while not violating the physical principles at the scale of application. This in turn helps in the incorporation and reduction of uncertainty in modelling.

3.3 Uncertainties in hydrological modelling

Uncertainty in hydrological modelling arises due to the inadequacy of the model structure, model parameter estimation and random variation as well as errors and inadequacy in observed variables (Chatfield, 1995; Butts et al., 2004; Wagener and Gupta, 2005). Uncertainty is introduced right at the moment use of modelling is conceived as the perceptual model is already a simplification of reality (Liu and Gupta, 2007). This means that a model structure that reduces uncertainty is one that can effectively model the whole range of conditions that occur.

Observed data has an effect on both parameter estimation and input (time series) variables. Estimation of parameters is an attempt to extract generalised information from observed data about the behaviour of the hydrological system being modelled (Wagener and Montanari, 2011). This means that observed data used for calibration may introduce uncertainty in addition to the method used to identify the parameters. Uncertainty in input variables may result from variables that are measured at different time steps or spatial scales when compared to the scale where the process being simulated takes place. For example rainfall can be measured at daily time scale and point scale but the runoff generation process could be measured at a smaller time step such as hourly or even smaller.

Uncertainties in flux based modelling such as REW modelling arise from estimation of fluxes across space boundaries such as REW sub regions. Closure relations that define flux exchanges among space boundaries introduce uncertainties as a result of their inadequacies in estimating the correct amounts. In addition boundary conditions together with initial conditions in subsurface flow are required to produce a unique solution of a hydrological model for a given process and for a particular site (Pinder and Celia, 2006) whose estimation also introduce uncertainty. Boundary conditions define the shape and boundary properties of a hydrological unit being represented by the governing equations and are represented by partial differential equations that can be solved using numerical methods (Freeze and Harlan, 1969). They are the edges of a hydrological unit where simulation will terminate or begin for a given time step.

The standard and general approach in defining boundary conditions in groundwater systems takes three different forms namely specified head conditions (Dirichlet

conditions), specified flux conditions (Neumann conditions) or specified head value dependent flux (Robbins conditions) sometimes known as specified leakage (Park and Leap, 2000; Pinder and Celia, 2006; Kresic, 2009). Lee et al. (2005) used specified head conditions and developed closure relations for these specified head conditions to model the Weiherbach catchment in Germany for a REW based model. Zhang et al. (2005) used constant flux boundary condition and no flow boundary condition for the modelling of runoff generation for a REW approach in the Reer River basin. Reggiani et al. (1999, 2000) proposed closure relations for boundary conditions which were considered by Lee et al. (2005) to be no flow flux boundaries.

Uncertainties in estimating fluxes across space boundaries such as the REW sub regions are related to the uncertainty related to the method used in the estimation of the respective flux such as infiltration and runoff. This is particularly so at smaller spatial and temporal scales. For example if one considers infiltration at a larger scale, the areas with very high infiltration rates will be compensated with areas with very low infiltration resulting in natural averaging of the infiltration processes (Corradini et al., 1998). Esteves and Lapetite (2003) attributed complexity of runoff to non-uniformity of runoff generation caused by spatial variability of infiltration capacity of the soil and existence of depression storage on the soil surface. Uncertainties are anticipated from variation in soil type, dependence of infiltration in soil moisture which in turn affect runoff generation and spatial and temporal variability of rainfall both in quantity, duration and in intensity (van de Giesen, 2000). This means that some of the runoff generated from upslope areas of a contour ridged field may infiltrate before reaching the contour ridge owing to portions of the field having less moisture than in the upslope subplots. Brocca et al. (2008) cited several researchers who showed that soil moisture content prior to a rainfall event has an effect on the runoff generation. It is therefore important to apply modelling methods that reduce or incorporate these uncertainties.

3.4 Approaches for incorporating uncertainties in hydrological modelling

3.4.1 Incorporating uncertainties in ungauged sites

In ungauged sites uncertainty is worsened by limited or no data to use for estimating model parameters or to assess model performance. Kapangaziwiri et al. (2009) and Kapangaziwiri et al. (2012) provide details of some of the approaches that were explored in South Africa to incorporate uncertainty in modelling ungauged sites. These are generally grouped into two, one focusing on reducing uncertainty in the estimation of model parameters and the other focusing on reducing uncertainty in the expected watershed functional behaviour (Wagener and Montanari 2011).

Estimation of model parameters for ungauged basins has in the past been achieved through regionalisation in which information on model parameters from gauged basins is extrapolated to ungauged sites (Kapangaziwiri et al., 2009). Kapangaziwiri et al. (2012) proposed an approach to incorporate uncertainty in modelling ungauged basins that is based on a local approach for a priori model parameter estimation from physical catchment characteristics, and a regional approach to regionalize signatures of catchment behaviour that can be used to constrain model outputs. In the prior model parameter estimation Kapangaziwiri et al. (2012) used catchment characteristics such as topography, soil texture and depth, geology and vegetation cover for the ungauged basin to estimate the model parameters. This could also be done using experience on feasible parameter ranges or formal equations to estimate moments of statistical distributions. Kapangaziwiri et al. (2012) defined a hydrological signature as an index of time series that define the basin's functional behaviour. Examples of indices used as hydrological signatures are base flow index and flow duration curves (Wagener and Montanari 2011). The estimated hydrological signature can then be used to provide feedback to the prior parameter estimation method to refine parameter estimation thus reducing uncertainty in ungauged sites.

The problem with this approach however lies with having data to establish the hydrological signature (Wagener and Montanari 2011). Information on hydrological signatures is not entirely unavailable but may occur in rather imprecise nature thereby

creating a challenge in linking it with an identified index that may give rise to the need to consider other approaches. French (1995) noted that uncertainty about imprecision and ambiguity gave rise to the field of fuzzy logic pioneered by Zadeh (1965) which has also been applied in hydrological modelling.

3.4.2 Incorporating uncertainty through fuzzy logic

The problem of uncertainty associated with input parameter estimation can be handled through fuzzy modelling (Zadeh, 1965, Mamdani, 1975, Takagi and Sugeno, 1985; Sen et al., 2005; Katambara and Ndiritu, 2009). Fuzzy modelling is a system of modelling based on fuzzy logic, a concept pioneered by Zadeh (1965). The concept of fuzzy logic involves grouping objects into classes or sets of similar characteristics and determining the degree (of membership) in which the object fits into the set. An object may partially belong to a given set of objects. To illustrate this point, suppose that one wants to estimate domestic water usage for a given settlement and has information that water usage is depended on whether a day is hot or not. It becomes necessary to find criteria for determining whether a day is hot or not and one possible criterion is temperature. Suppose then that a day with a temperature of 30^{o}C or higher is taken as a hot day. A day with a temperature of 29^{o}C is almost as hot as that with a temperature of 30^{o}C and therefore water consumption will be almost as high as that of a hot day. Fuzzy logic allows grouping this day (with a temperature of 29^{o}C) into the set of hot days by recognizing that it is nearly as hot. This is achieved through assigning the object (day) a value between 0 and 1 depending on whether it belongs to the set (is hot in which case the value becomes 1), does not (is cold in which case the value becomes 0) or in between (nearly cold or nearly hot in which case the value, x, takes a value between 0 and 1).

Fuzzy logic has wide application in many spheres of science where input data is imprecise. It has been used for load focus and control in the field of power supply (Poplawski, 2008). It has wide application in the field of aircraft engineering for control of flights (Ursu et al., 2001; Ursu I. and Ursu F., 2003; Kiyak, 2008) and has also application in business and financial management (Bojadziev G. and Bojadziev M., 2007).

Fuzzy logic has also been used in the field of water resources. Halkidis et al. (2009) used fuzzy logic to determine an analytical solution of a two-dimensional groundwater flow problem. Sen and Altunkaynak (2005) used a fuzzy model to estimate runoff and runoff

coefficient. Katambara and Ndiritu (2009) developed a fuzzy inference system for modelling streamflow. Hundecha et al. (2001) developed a fuzzy based rainfall runoff model which agreed fairly well with the process based HBV model and the observations and showed that in fuzzy logic fundamental knowledge of the underlying physical processes is not a pre-condition. Rather only knowledge of the factors that influence a process and a qualitative relationship between these factors and the process is required to be able to predict the process.

Fuzzy logic based modelling could be useful in rainwater harvesting systems given that extensive data collection required by process-based models makes modelling impractical for design purposes in most areas where rainwater harvesting systems are required for application. Given that rainwater harvesting is mainly applied in smallholder farmers data collection needs to be simple and easy so that either the farmers themselves or agricultural extension workers are able to collect it using inexpensive tools and instruments that are readily available. As pointed out by Elwell (2000) modellers need to decide whether the advantages of an improved accuracy achieved from using complex models are warranted given the complexity of simulation and the greatly expanded data requirements. The success of a model can be measured by how well the objective is achieved (French, 1995).

Several researchers (Hundecha et al., 2001; Sen and Altunkaynak, 2006; Katambara and Ndiritu, 2009) have used fuzzy approach to handle uncertainties in modelling runoff at river basin scale and achieved reasonably good results but little has been done towards incorporating uncertainties in modelling runoff at field scale. Therefore fuzzy logic approaches may be able to provide more accurate results given their ability to quantify fuzziness to suit the conditions of the situation. The development of a fuzzy model involves various stages that include collection of data, development of the fuzzy inference system and testing of the model. Details of the development of the fuzzy inference system and the fuzzy model structure are briefly described in section 3.5.

3.5 Identification of fuzzy model structure

A fuzzy model structure is general and independent of the system description (Takagi and Sugeno, 1985; Angelov and Filev, 2004) and has a basic structure as illustrated in

Figure 3-2 (Mehran, 2008). The three main building blocks are the input system, the fuzzy inference system and the output system.

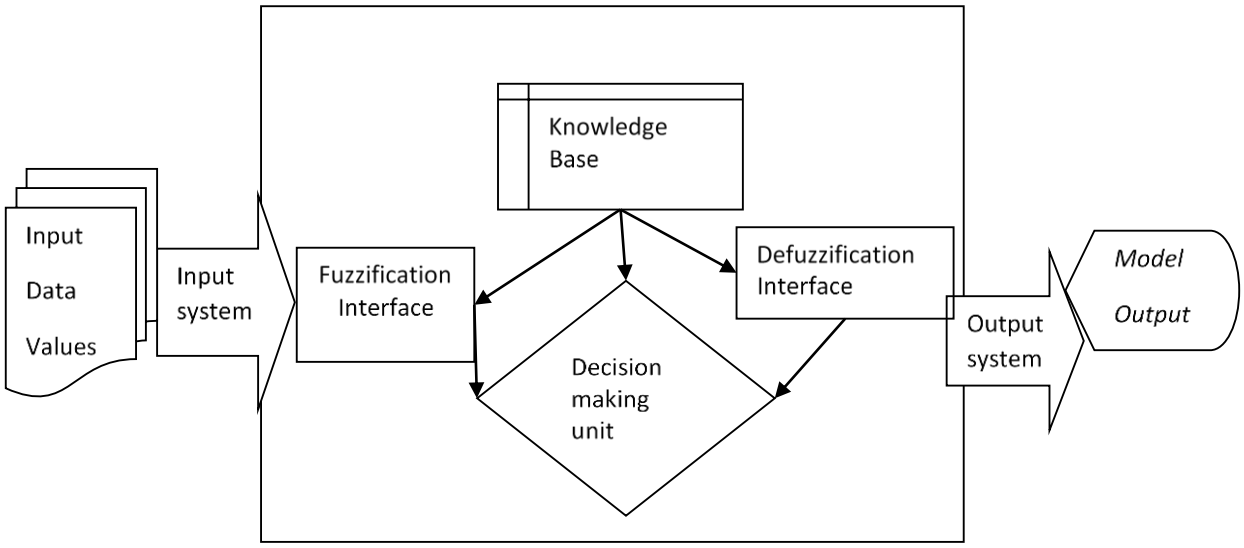

Figure 3-2: Basic structure of a fuzzy model (Adapted from Mehran, 2008)

The input system consists of the input data that is normally in number format which is changed by the input system to fuzzy language for use by the fuzzy inference system. The fuzzy inference system is the computational component that applies the fuzzy data to obtain the model output. The output system converts the model output which is normally in the fuzzy language to number format for use by decision makers.

3.5.1 Fuzzy input system

The first step in using fuzzy modelling for solving problems is to represent the problem in fuzzy terms. This is referred to as conceptualization in fuzzy terms. It means identifying or specifying a problem in linguistic terms and representing the parameters in linguistic variables. These linguistic variables are then grouped into continuous (and sometimes overlapping) classes based on continuous class membership values varying between 0 and 1 (Wilson and Burrough, 1999). The inference system mentioned above works with rules that are based on these membership values. Therefore the accuracy of a fuzzy model can be said to depend on the correct selection of membership values that are based on appropriate linguistic variables.

3.5.2 Fuzzy inference system

A fuzzy inference system contains functions that help map input variables such as previous soil moisture, soil classification and rainfall into output variables such as current moisture content. The mapping is achieved through simulating the output variables through operations that are based on IF (condition of input variable) THEN (condition of output variable) known as fuzzy rules. These rules form the rule data base and are stored in the knowledge base. The development of the rules takes into account the need to maintain continuity of the model response as a function of input variables so as to avoid discontinuities hence the need for continuous and sometimes overlapping functions. A decision making unit makes use of the data base to obtain the set of output variables given a set of input variables.

Many input variables can be used to determine one output variable and there are situations when many input variables are mapped into many output variables. This input-output mapping relation can be used to select an appropriate fuzzy inference system (FIS). Two fuzzy inference systems are generally used in fuzzy modelling. These are the Mamdani Rule based FIS and the Takagi-Sugeno, FIS (Jacquin and Shamseldin, 2009). Relationship between input parameters and output parameters and the rules that govern them can be of the multiple input single output (MISO) type or multiple input multiple output (MIMO) type (Jassbi et al., 2006). Mamdani-type FIS can be used for both MISO and MIMO type problems. The findings of Jassbi et al. (2006) recommend use of Mamdani FIS in MIMO type of input output type relations and Takagi-Sugeno for the MISO type of input output type relations. The Takagi-Sugeno FIS has computational advantage over the Mamdani FIS (Ying, 1999). However, the Mamdani FIS is simpler to understand and hence to develop. Where high level of computation is expected, a Takagi-Sugeno inference system is advantageous.

3.5.3 Fuzzy output system

The fuzzy output system consists of crisp sets corresponding to crisp input sets. This forms the model output that can be compared with observations during model calibration or verification or used for decision making in model application.

3.5.4 Identification of model parameters for the Takagi-Sugeno FIS

Fuzzy modelling involves subdividing the model space into overlapping subspaces each one associated with a sub model as shown in Figure 3-3. Each subspace is regarded as a cluster of data composed of many data points scattered around a focal point. This focal point is considered as the centre of the data cluster and is the focal point of the rule/rules associated with that cluster. The cluster's boundaries overlap such that every data point in the data series falls within at least one cluster (and sometimes in more than one cluster). The degree in which a data point belongs to a particular cluster is determined by its distance from the centre of the cluster.

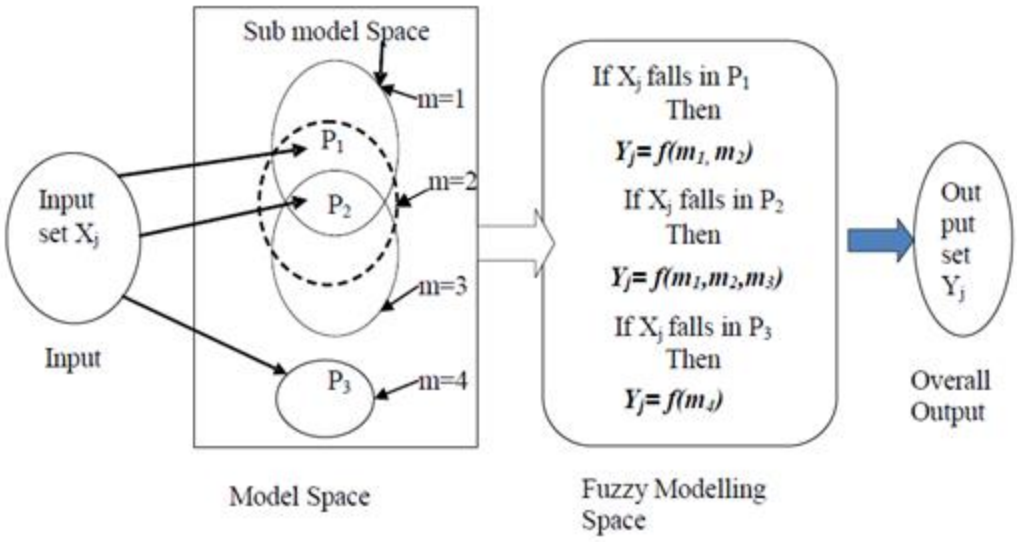

Figure 3-3: An illustration of a fuzzy model

The determination of clusters and their centres as well as the distance of each data point from the centre is an important aspect of fuzzy modelling. The determination of the data clusters is achieved through data clustering. Three main methods of data clustering used in fuzzy modelling are fuzzy C-Means method (Dembele and Kastner, 2003), Gustafson-Kessel method (Sarbu et al., 2007) and subtractive clustering method (Angelov and Filev, 2004; Katambara and Ndiritu, 2009). These methods are used for offline clustering i.e. when all the data is available and used for the determination of cluster centres. There are situations however where new data is used as it becomes available. For such situations

Angelov and Filev (2004) proposed an online clustering approach that is used for Evolving Takagi-Sugeno (ETS) models.

Data for a given time step is first classified according to the subspaces that it falls under. Often the data may fall in more than one subspace as is the case with data points P1 and P2 in Figure 3-3. In such cases, all sub models for the spaces that the data belongs are used to map (model) their respective partial model outputs which are then integrated to obtain the overall model output.

Each sub model can be represented by a general equation of the form shown in Equation 3-2 which is the general form of the Tagagi Sugeno fuzzy model (Katambara and Ndiritu, 2009; Gomez-Skamerta, 1997; Tagagi Sugeno, 1985). This equation consists of input variables and their coefficient parameters which are on the right hand side of the equation. If data points fall in a particular model sub space then the partial model (sub model) corresponding to that subspace is invoked.

$$R_i: If\ x_1\ is\ A_1\ and\ \dots\dots and\ x_k\ is\ A_k$$
$$then \qquad \text{Equation 3-2}$$

$$y_i = a_0 + a_1 x_1 + \cdots + a_k x_k$$

Where:

R_i is a specific model that is executed when certain conditions have been satisfied;
x_k is one of the independent variables required to make the prediction;
A_k is a certain subspace of variables x_k;
y_i is the partial model output;
a_k is the coefficient for variable x_k.

The search for data points that fall within a given model subspace and selection and running of the corresponding partial model is controlled by a fuzzy inference system. It consist of two components; the input (or antecedent) component and the output (consequent) component. The antecedent component inspects the data set and compares the data set with the model space in order to select the sub spaces under which the data set falls. This is achieved through establishing the degree of membership of the data set to each model subspace (Angelov and Palev, 2004). The consequent component predicts the partial model output and requires that the consequent parameters be

established first through calibration using methods such as the shuffled complex evolution method (Katambara and Ndiritu, 2009).

The model structure of Takagi-Sugeno FIS type identification is carried out iteratively with identification of model parameters. This is particularly so for the estimation of the focal point of the rules. This is achieved by determining cluster centres of the antecedent parameters. Each cluster centre is associated with a rule function based on Takagi-Sugeno fuzzy reasoning as shown in Equation 3-3 (Takagi and Sugeno, 1985).

R_i: $\boldsymbol{If}$; x_1 is A_1 and …… and x_k is A_k;

$\boldsymbol{then}$; Equation 3-3

$$y_i = a_0 + a_1 x_1 + \cdots + a_k x_k$$

Parameter identification of the Takagi-Sugeno model involves three main components (Takagi and Sugeno, 1985). The first one is the identification of variables constituting antecedent parameters of the model. The second is the identification of the membership functions of the antecedent parameters of the model. The third is the identification of the parameters in the consequent part.

Input variables of the antecedent part are presented in the “if” part of Equation 3-2. Not all these variables appear in every rule (Takagi and Sugeno, 1985). They are determined by how the fuzzy subspace is partitioned. Some processes have certain parameters being variables only at given environmental conditions. An input variable implies that its space is divided into subspaces that are defined around individual cluster centres.

Identification of parameters of the consequent part is a calibration process that involves establishing the coefficients of Equation 3-2. This is achieved by assuming a set of coefficient values and applying Equation 3-2 with these values to simulate the function value which is compared with observations against an objective function such as minimising the root mean square error (Takagi and Sugeno, 1985; Angelov and Filev, 2004). The identified parameter values can be optimised through use of efficient methods such as shuffled complex evolution method developed by Duan et al., (1992).

3.6 Potential for modelling field scale runoff using fuzzy logic

Chahinian et al. (2005) noted that most runoff models are either at catchment scale or point scale while few are available for modelling runoff at agricultural field scales. Most of these models simulate overland flow by first estimating infiltration amount from a rainfall event using physically based, conceptual or empirical methods (Corradini et al., 1997; Corradini et al., 1998; Chahinian et al., 2005). Infiltration is then subtracted from the precipitation with the remaining precipitation (infiltration excess) becoming runoff amount which is then routed to catchment outlet (Liu, 2004). Empirical models used to estimate runoff include the Φ index and the curve number method developed by the Soil Conservation Service, United States Department of Agriculture (USDA), (USDA-SCS, 1985). Garen and Moore (2005) discussed the misuse of the curve number approach when modelling runoff in agricultural fields particularly where runoff generation is dominated by infiltration excess (Hortonian flow) overland flow process. Typically the runoff generated in tropical semi-arid areas such as the low rainfall areas of Zimbabwe where contour ridges are used for rainwater harvesting is infiltration excess overland flow. Garen and Moore (2005) argued that the curve number system was developed using data that did not distinguish between components of runoff (infiltration excess or saturation excess) as it was developed to predict stream flow and not Hortonian overland flow.

Despite the existence of many forms of infiltration equations such as Horton's equation (1942), Green and Ampt equation (1914), Philip's equation (1947), Smith and Parlange's equation (1978) or Richard's equation (in Murty, 1970; Gifford, 1976; Maller and Sharma, 1981; Verma, 1982; El-Hames and Richards, 1995; Pachepsky et al., 2003), that may be used for computing runoff, infiltration still remains a difficult hydrological process to estimate. Chahinian et al. (2005) compared four models (based on Philips equation, Morel-Seytoux, Horton's equation and the curve number method) to simulate hortonian overland runoff and used a unit hydrograph as a transfer function. All the four poorly predicted low runoff from low rainfall intensities and from intermittent rainfall events. Therefore estimation of runoff based on models that first estimate infiltration and consider runoff as the remaining rainfall amount after infiltration is satisfied are prone to uncertainty in the estimation of infiltration giving rise to methods that also consider estimating runoff directly such as modelling runoff using linear regression modified using fuzzy logic.

Fuzzy modelling was used by several researchers for modelling runoff at river basin level. Hundecha et al. (2001) used fuzzy logic in which relative soil moisture was used as a guiding fuzzy rule to determine the proportion of rainfall that is converted to runoff in the Nercar River Catchment in Germany. The results compared well with those of the HBV model. Sen and Altunkaynak (2006) determined the runoff coefficients for the Rational method using fuzzy logic and obtained much better results than those from the average coefficient obtained by the regression method. Katambara and Ndiritu (2009) used a fuzzy model to estimate stream flow for the Letaba River in South Africa obtaining reasonably good results.

The alternative to physically based modelling when estimating runoff at field scale is linear regression modelling. Linear regression models have been found suitable for modelling runoff at field scale if runoff data for the site in question is available to develop the linear relationship (Walker and Tsubo, 2003b). A threshold linear model, such as Puturun shown in Equation 3-4 is a special case of a linear regression rainfall runoff model (Walker and Tsubo, 2003a). The model estimates runoff from rainfall events by considering that the runoff coefficient is a function of the rainfall amount. However the runoff coefficient values (e.g. 0; 0.05; 0.1 and 0.2 in Equation 3-4) are site specific or suitable for sites with similar conditions. Therefore runoff data for a site is required to calibrate a linear regression model so as to establish the runoff coefficients.

$$Q = \begin{cases} 0 & P \leq 15 \\ 0.05P \quad where & 15 < P \leq 25 \\ 0.1P & 25 < P \leq 50 \\ 0.2P & P > 50 \end{cases} mm/day \qquad \text{Equation 3-4}$$

Where
Q is runoff estimation (mm/day)
P is precipitation received (mm/day)

In situations where site data is not available such as for the purposes of designing contour ridges for each individual farmer's field linear regression models would not be suitable. However it is possible to develop linear models from sites were data is available and use them to model runoff in sites were data is limited using fuzzy modelling.

Researchers that developed linear and multiple regression equations include Li et al. (2004) who developed a series of linear regression and multiple linear regression equations for estimating runoff from different surface treatments in China. Li et al. (2004) established that multiple regression equations were useful in natural and cleared loess slope surfaces and that the input variables were rainfall amount and rainfall intensity. For artificial surfaces of concrete, asphalt and plastic linear regression equations using only rainfall amount as input variable were found to be suitable.

The Puturun model based only on one input variable (precipitation) can provide a good illustration of the potential of combining a set of equations to provide a good estimate of runoff. Equation 3-4 that represents the Puturun model can be stated in the form of "if rain falls within a certain range then runoff can be calculated by a given linear regression model". By applying the regression models of Equation 3-4 for given rainfall figures and strictly remaining within the boundaries defined by the regression models it can be seen from Table 3-1 that runoff from rainfall that falls on the upper boundaries of each sub model equation is under estimated while that which falls on the lower boundaries of each sub model equation is over estimated.

Table 3-1: Results of the PUTRUN linear regression model for selected rainfall figures

Precipitation (P) (mm/day)	If $P \leq 15$ Then $Q = 0$	If $15 < P \leq 25$ Then $Q = 0.05P$	If $25 < P \leq 50$ Then $Q = 0.1P$	If $P > 50$ Then $Q = 0.2P$
0	0			
14	0	0.7		
16		0.8		
24		1.2	2.4	
26		1.3	2.6	
49			4.9	9.8
51			5.1	10.2

However if one was to investigate how the runoff would change if the boundaries of the regression models were to be changed, for example by allowing them to overlap, one

would realise that allowing the boundaries of the regression model to overlap and then averaging the results from the overlapping equations provides more realistic runoff values than using a single regression model. Consider runoff generated from a rainfall amount of 49mm/day by the regression equations in the 4th and 5th columns of Table 3-1. The regression equation in the 4th column computes a runoff amount of 4.9mm while that of the 5th column computes a runoff of 9.8mm/day. If the two figures were to be averaged they would provide a runoff of 7.35mm/day. The runoff amount of 7.35mm/day is most likely to be more realistic than the amounted computed by the individual regression equations.

However it cannot be ascertained whether averaging the estimated runoff amounts by the separate regression equations is better than giving more weight to one of the equations. It can be argued further that if one knows the rainfall amounts for which each of the equations provides the best runoff estimate then the contribution of that regression equation on the runoff generated by a rainfall of 49mm/day can be related to how far the 49mm/day rainfall is from the best fit rainfall amount of the regression equation. This allows the regression equation that is closer to the rainfall amount whose runoff is being computed to have more influence on the result than those further away. At the same time it allows those regression equations further away to still influence the final computed runoff amount.

The overlapping boundaries recognise that each sub regression equation is applicable to a rainfall whose range has a fuzzy beginning and end value but having a rainfall amount where it gives the best result. Each rainfall amount within the range can therefore be defined in terms of its relation with the amount that gives the best result. The rainfall amount that gives the best result is the centre of the regression equation. The rainfall range is the group or cluster of rainfall figures associated with this centre and the relationship of any rainfall amount within this cluster with the centre is the degree of rainfall belonging to the cluster or the degree of membership. This conceptual understanding helps to define the regression equations in terms of fuzzy theory and therefore helps in modelling runoff using identified regression equations using fuzzy logic.

3.7 Summary

It was considered that a suitable model should include the rainfall partitioning processes taking place in the cropped area, the partitioning of the water harvested by the contour ridge and the partitioning of the soil moisture stored in the root zone. This proposal could be achieved by using an approach similar to the representative elementary watershed (REW) modelling in which the area between contour ridges is used as a basic spatial area containing the functionality of a contour ridged field. However it would not be ideal to consider the REW approach as the basis of developing a model for modelling rainwater harvesting by contour ridges unless all the fundamentals of the REW model are incorporated. It was therefore considered suitable to consider a hybrid approach that includes process based methods and fuzzy logic. Runoff, one of the main hydrological processes of a contour ridged field, could be modelled using a fuzzy approach based on Takagi-Sugeno fuzzy inference system (FIS) as there are many variables that would need to be determined by fuzzification. Subtractive clustering has computational advantages and helps reduce the number of clusters and hence rules needed for a fuzzy modelling system (Chopra et al., 2006) and is therefore selected for use in this study.

4 DESCRIPTION OF STUDY AREA AND STUDY METHODS

4.1 Introduction

This chapter presents the description of the methods that were used to collect and analyse data from field experiments carried out in Zhulube, a small left bank tributary sub-catchment of Mzingwane Catchment in Zimbabwe. The data collected during the field experiments together with data obtained from previous studies by Mugabe (2005) was also used to develop a model for investigating rainwater water harvesting by contour ridges as described in chapter 5.

Previous studies carried out in Zimbabwe by Mugabe (2005) provided data on field scale runoff and the corresponding rainfall amount for two different sites with different soil types. This data was used in developing a rainfall-runoff model for estimating runoff from the cropped field as described in chapter 5. However it was difficult to obtain some of the data from the study by Mupangwa (2008) which could have been useful in this rainfall runoff model. Mupangwa (2008) collected data on rainfall runoff processes at field scale in Gwanda and Insiza Districts.

There are several studies, carried out in Mzingwane Catchment in general and Zhulube Catchment in particular under the challenge programme for water and food (CPN 17) led by WaterNet, which contained some useful information on water resources availability and use, which was also used in this study (Sawunyama et al., 2004; Moyo, 2005; Munamati, 2005; Ngwenya, 2006; Dhliwayo, 2006; Dondofema, 2007; Mwamba, 2007; Mupangwa, 2010;). Among the studies that were carried out is the work that was done by Ngwenya (2006) and Dhliwayo (2006) who both collected data on infiltration where Ngwenya (2006) carried out field experiments in rangeland while Dhliwayo (2006) carried out field experiments in agricultural fields. More work was also done by Mupangwa (2009) on various tillage practices in Zhulube meso-catchment for which data on soil type was used in this study.

Mugabe (2004) studied graded contours with infiltration pits in Chivi District, Runde Catchment where mean annual rainfall is 550mm but did not study dead level contours with or without infiltration pits and also did not study graded contours without infiltration

pits. On the other hand Mupangwa (2011) studied dead level contours with and without infiltration pits in Gwanda District where mean annual rainfall is below 375mm but did not study graded contours. In both studies there was no control plot with any contour ridges. Given the difference in both the spatial and temporal scales of these studies it would not be reasonable to compare the water conservation abilities of graded contours and dead level contours on the basis of the two studies. Field experiments that enable comparison between graded contour ridges and dead level contour ridges with a control of a plot with no contour ridges was considered appropriate for this study. This part of the research focused on predicting water movement under conventional farmer managed practice and was therefore a farmer based action research.

4.2 Description of the field study area

4.2.1 Location of Zhulube Catchment

The study was carried out in ward 1 of Insiza District in Matabeleland South province of Zimbabwe on five field sites A to E. The ward falls within Zhulube a left bank small catchment of Mzingwane Catchment located at coordinates of 20^{o} 47’ South and 29^{o} 22’ East. The Mzingwane Catchment is found in the south western part of Zimbabwe and is part of the Limpopo River Basin (Figure 4-1). It is one of the seven administrative river systems in Zimbabwe. The river systems in Zimbabwe are derived from the hydrological catchment areas of major rivers in the country. Mzingwane catchment comprises all the rivers that fall within Zimbabwe and drains into the Limpopo River which is an international river basin shared by Botswana, Mozambique, South Africa and Zimbabwe.

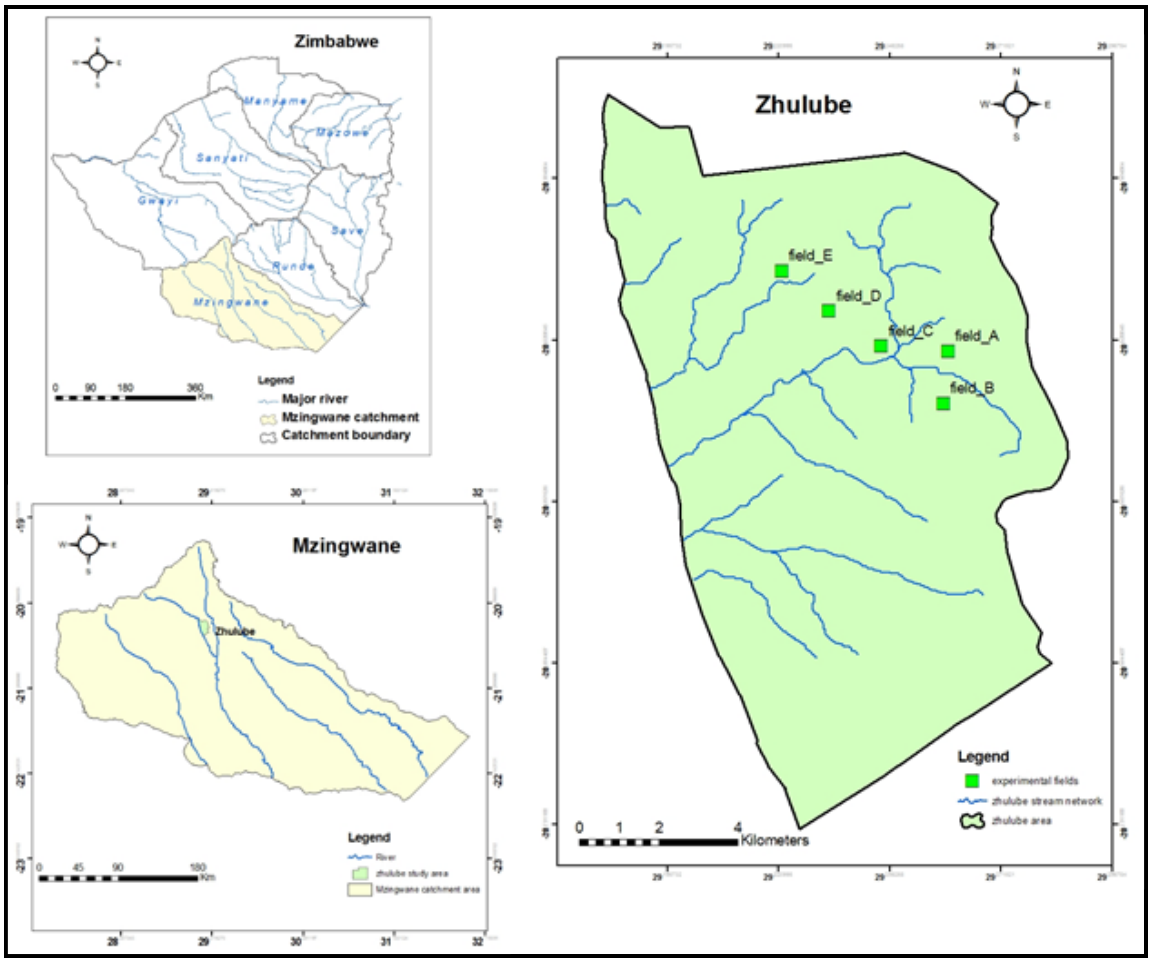

Figure 4-1: *Location of the study area (Zhulube) in Zimbabwe*

4.2.2 Geophysical conditions of Zhulube

Zhulube catchment is mountainous, covering an area of 21 km^2 upstream of an important small dam supporting a 40 ha irrigation scheme as shown in Figure 4-2. The middle part of Zhulube catchment is dominated by rain fed farming and grazing land. The slope is fairly steep ranging between 5% and 7%. Landscape degradation characterised by gulleying is widespread in the middle part of the catchment. A large significant gulley (Gobalidanke) has formed mid-stream between the hillslopes and the downstream Zhulube Dam (Figure 4-3) and efforts to reclaim the gulley proved difficult in the past (Dondofema, 2007). The gulley was developed following an increase in human activity such as livestock grazing and digging of fishing worms (Ngwenya, 2006; Dondofema, 2007).

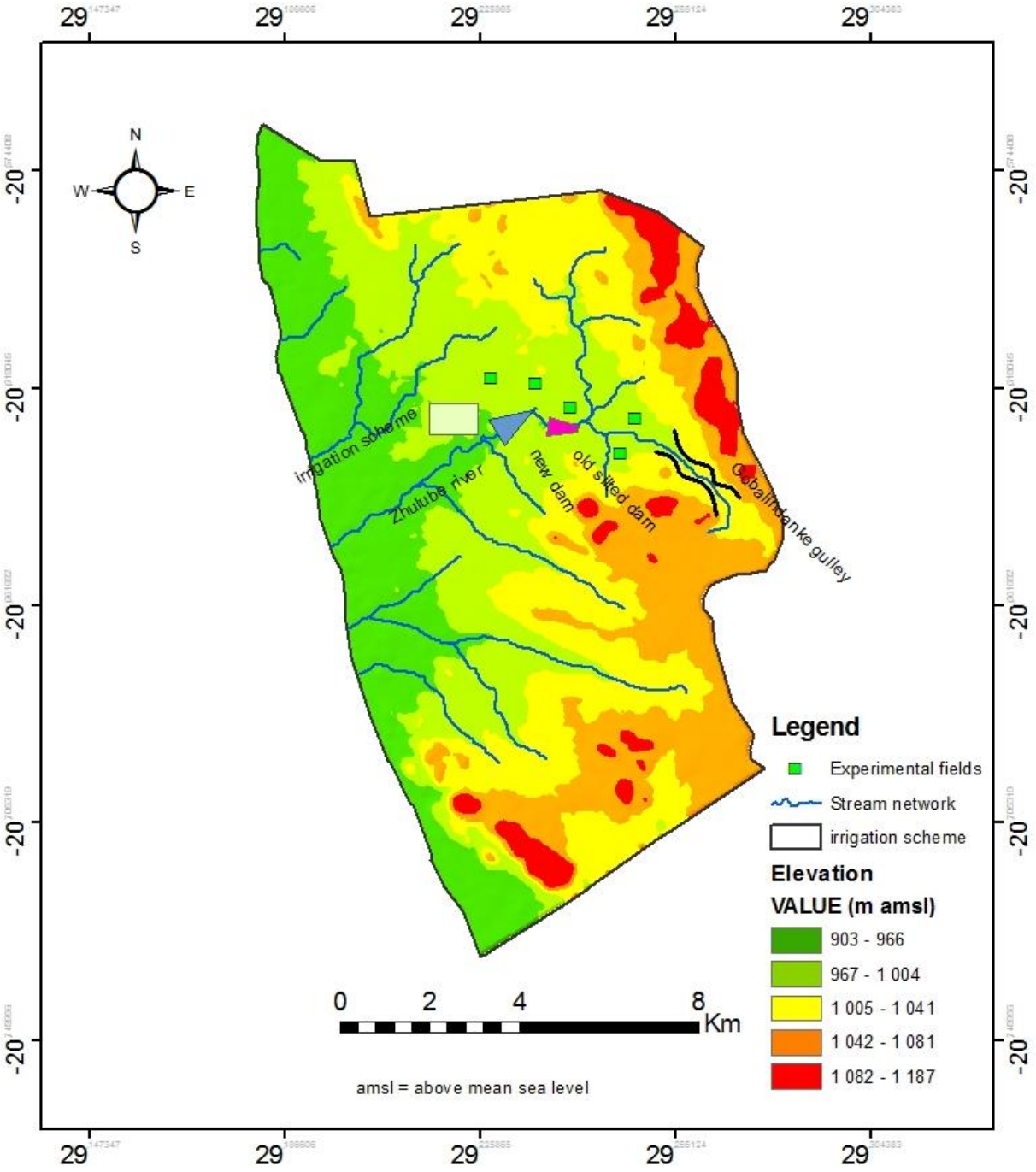

Figure 4-2: Zhulube catchment characteristics

The dam supporting the irrigation scheme is threatened with sedimentation from soil erosion emanating from up-stream and mid-stream erosion that leaves behind huge

gulleys. Already an old dam immediately upstream of the dam is full of sediments and was abandoned (Figure 4-4). Adoption of contour ridges in such a catchment could prove to be a very important soil and water conservation strategy as the ridges have the potential to reduce soil erosion and as a result sedimentation in the dam. However sustainability of the contour ridges depends on rain fed farmers deriving benefit from the practice. Thus the catchment was considered appropriate for research on the potential of water conservation from contour ridges.

Figure 4-3: Part of Gobalindanke Gulley and efforts to reclaim it

The vegetation in Zhulube catchment is dominated by acacia species and mopane (colophospermum) trees (Dondofema, 2007). The grass is made up of both perennial and annual species whose densities vary according to rainfall received each season (Ngwenya, 2006).

Figure 4-4: Silted Old Zhulube Dam abandoned after exessive land degradation in the catchment area

4.2.3 Climate and water resources

Mzingwane catchment falls within the semi-arid region of Zimbabwe where rainfall is low and unreliable with high temporal and spatial variability (Sawunyama, 2004; Rukuni, 2006). The rainfall is convective and is characterised by dry spells and frequent droughts (Moyo, 2005). The average annual rainfall ranges from a low of about 350 mm in the south west part of the catchment to about 630mm in the northern part of the catchment as shown in Figure 4-5.

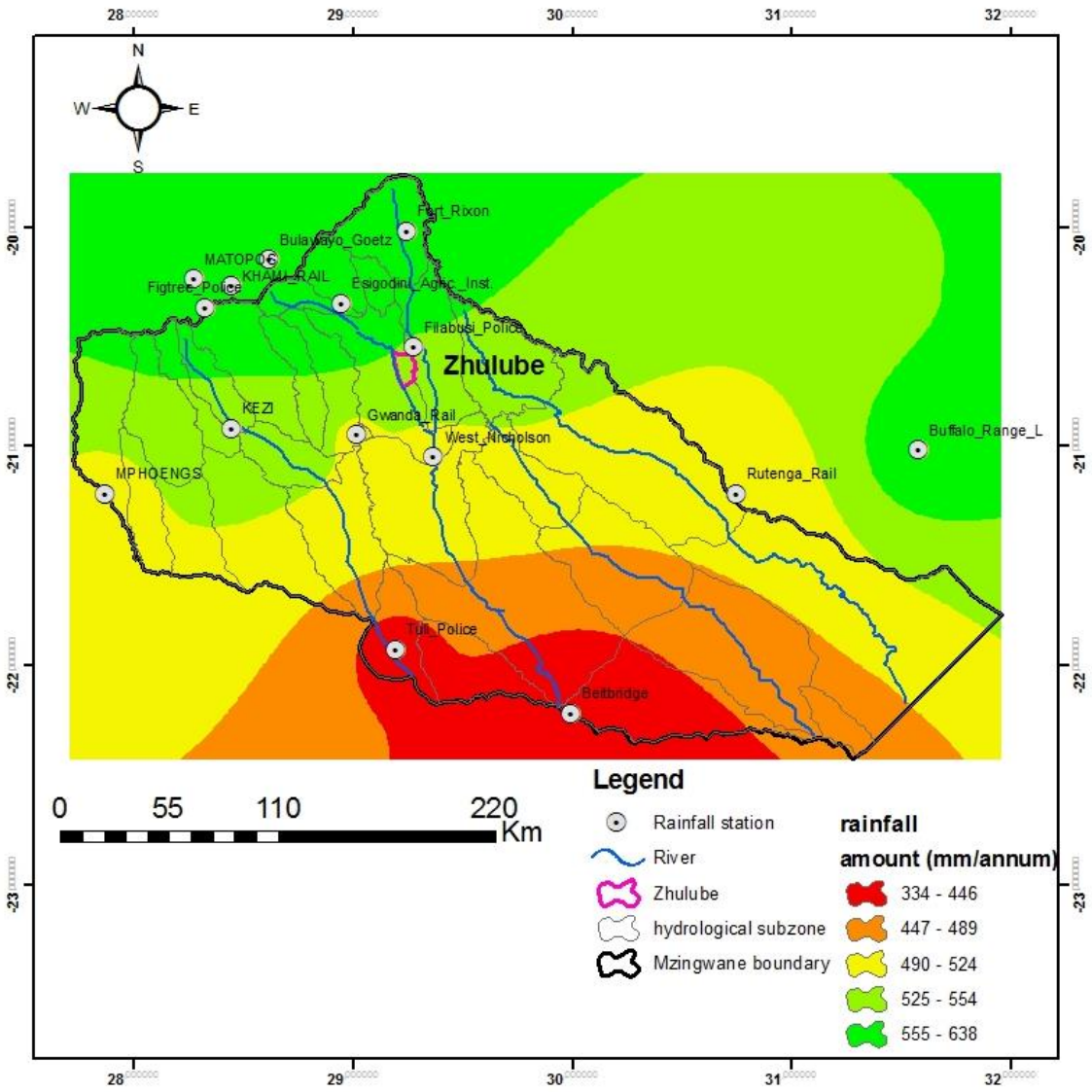

Figure 4-5: Spatial rainfall distribution in Mzingwane Catchment

While the average rain falls within the range in which crop production is possible there are several years where no crops are harvested at all owing to the high temporal variability (Figure 4-6 (a)). In areas where the annual rainfall averages 400mm the rainfall can be as low as below 200mm while in some few years it can reach 800mm. Zhulube catchment receives annual rainfall with an average of 540mm but has high deviation from the mean as shown by the rainfall at Filabusi a rainfall station about 20km from Zhulube (Figure 4-6 (b)).

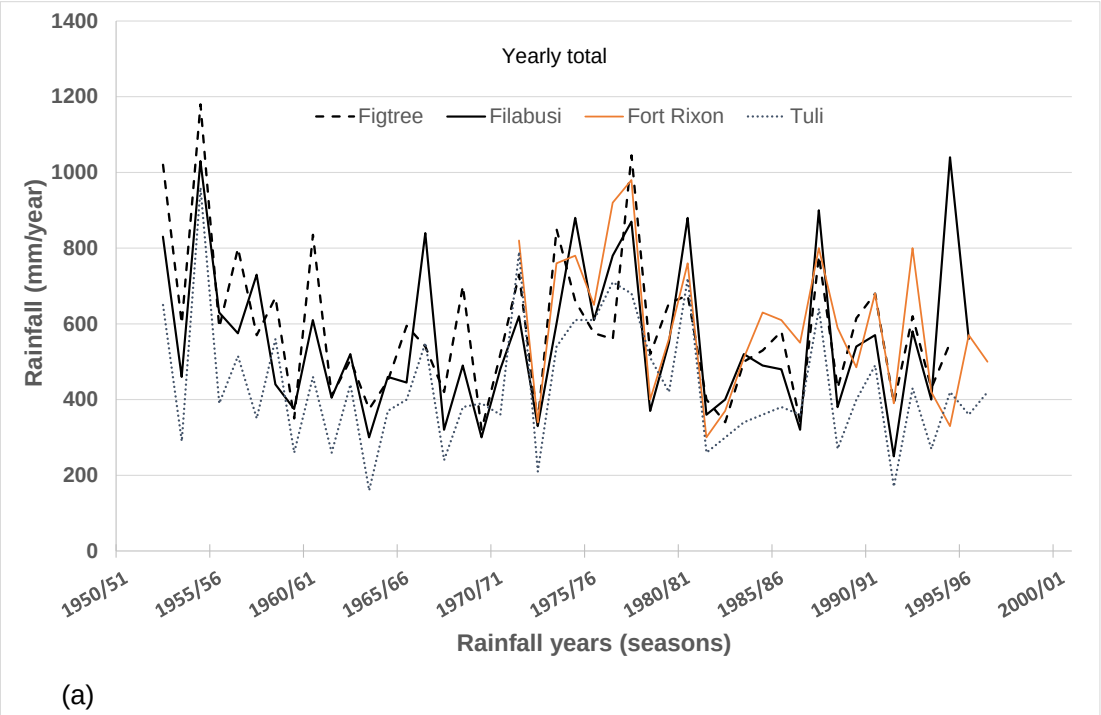

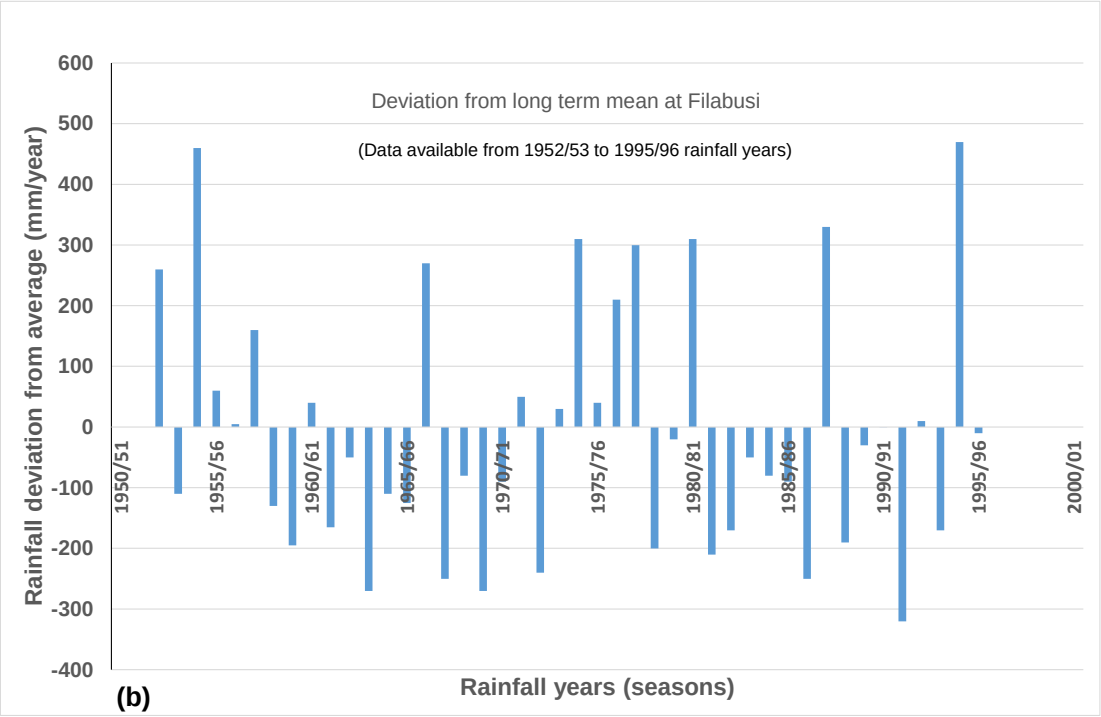

Figure 4-6: Temporal rainfall variability at selected rainfall stations in Mzingwane Catchment (a) and deviation from the mean at Filabusi Station (b)

There is also high intra-seasonal temporal variability experienced throughout the catchment as illustrated by the seasonal variation of rainfall of Zhulube for the year 2005/6 and 2006/7 shown in Figure 4-7. The rainfall is poorly distributed with frequent mid-season dry spells resulting in crop failures which discourage farmers from practicing rain fed farming (Chibulu, 2007). This high intra-seasonal temporal variability is largely responsible for crop failure in this catchment. As can be seen in Figure 4-7 the month of January received practically no rainfall during the year 2006/7. Such prolonged dry spell result in crop wilting and reduced yield and sometimes complete crop failure. The rainfall also occurs in sudden storms with high intensity that lead to high runoff and sediment generation from the degraded (eroded) land surface.

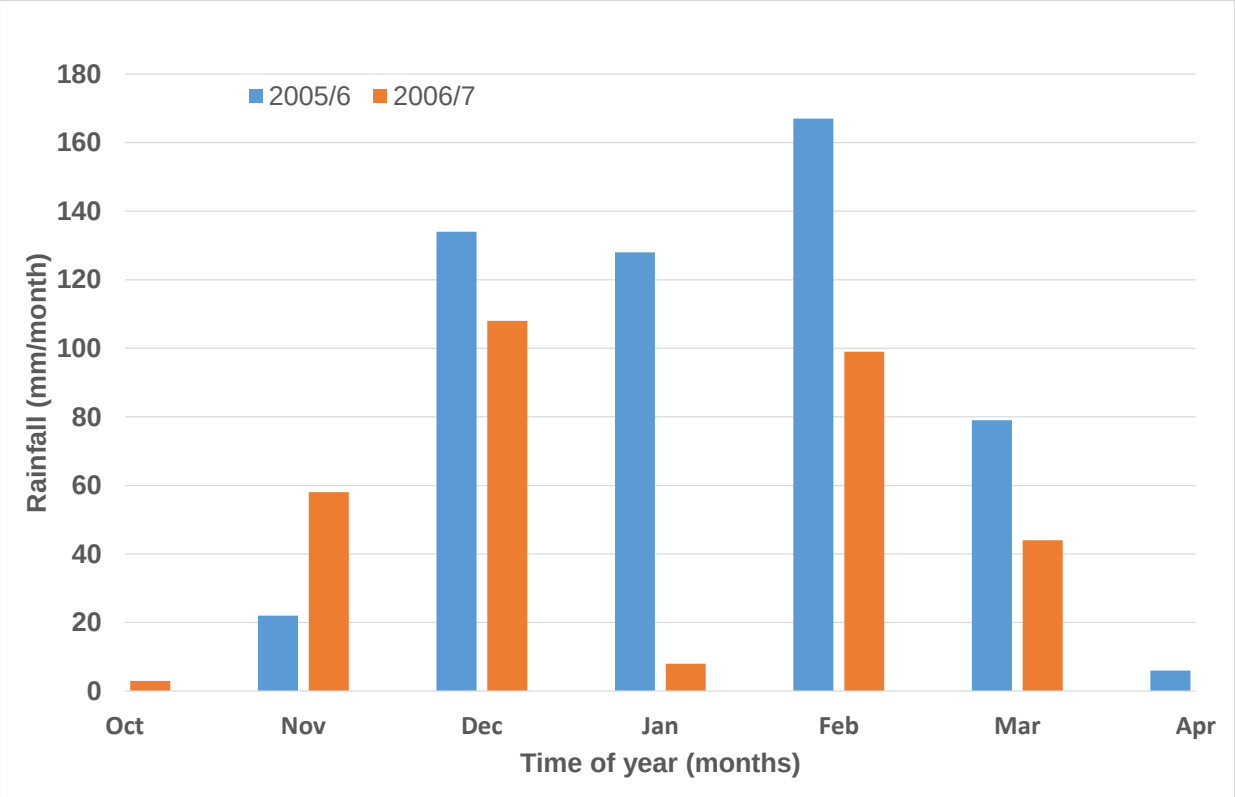

Figure 4-7: Intra-seasonal rainfall variation in Zhulube Catchment. (Source of Data: Ngwenya, 2006; Chibulu, 2007)

Surface runoff occurs for short durations following heavy rainfall storms but generally depends on rainfall intensity (Rukuni, 2006). In certain parts of the river system surface flow is largely limited to the rainfall season while during the dry period the riverbed is a thick alluvial aquifer storing some considerable amount of water (Sawunyama, 2005).

Some large rivers maintain flow during the dry season as subsurface flow in the river bed alluvial aquifer. These alluvial aquifers are a source of water for communities and are used to support small irrigation schemes for smallholder farmers in Mzingwane catchment (Munamati, 2005).

There are very few large dams (capacity > 1Million m^3) that have been constructed in the catchment (Table 4-1). These have a combined 10% risk yield of 350Mm^3/annum (DWR and ZINWA, 2007). However there are more than 1000 small dams found within the catchment whose capacities range from about 10 000m^3 to 100 000m^3 (Sawunyama et al., 2007). Water utilisation from these small dams is constrained by the high evaporation rates experienced in the catchment as the mean annual evaporation far exceeds mean annual rainfall. For example in Insiza District where Zhulube is found mean annual evaporation is 2000mm compared to mean annual rainfall of 470mm (Mamba, 2007). The topography does not provide many sites with deep valleys thus exposing most of the stored water to evaporation. If the reservoirs were deep, they could have provided large amounts of water as the proportion of evaporation loss would be much less. Therefore in Mzingwane Catchment a significant amount of the water stored in small dams is lost to evaporation thereby yielding low dry season water volumes. Besides the low surface water potential, Mzingwane catchment also has low potential groundwater mainly due to the predominant igneous rock formations found in the catchment (Moyo, 2005).

About 70% of the surface water from Mzingwane Catchment is used for urban water supply with the bulk going to Bulawayo, the second largest city in Zimbabwe. Only about 20% of the developed water resources are used for irrigation within Mzingwane Catchment. As a result of the low water resources availability in Mzingwane Catchment the extent of irrigated agriculture is very low, leaving most families vulnerable to food insecurity as they rely on rain fed farming.

Table 4-1: Distribution of dam sizes by capacity in Mzingwane Catchment

Dam Type	Large	Medium	Small	Small
Dam size (m^3)	>5Million	1 to 5 Million	0.1 to 1 Million	< 0.1 Million
Number of dams	20	10	205	>1 000

4.2.4 Soils and vegetation in Mzingwane Catchment

Vegetation in the Mzingwane catchment is dominated by acacia trees in light textured or well drained soils while mopane woodlands dominate the heavier textured or poorly drained soils (Dondofema, 2007). The soils in Mzingwane Catchment are light, well drained sandy soils associated with granite rock types that dominate the geology of the Catchment and heavier poorly drained sodic soils characteristic of areas dominated by Precambrian gneiss rocks with occasional dolerite intrusions where mopane trees are dominant. The light sandy soils have poor water holding capacity and high drainage rate due to high hydraulic conductivity while the heavier poorly drained sodic soils form a surface crust when wet which reduces infiltration rate (Abu-Awwad, 1997). Most of these soils are therefore considered not suitable for commercial irrigation systems although they are considered suitable for small scale traditional irrigation systems where water is applied manually by using watering cans. In sandy soils the high application rate of water in commercial irrigation systems means that more water is lost to deep percolation as the hydraulic conductivity is very high while in heavier poorly drained sodic soils the low infiltration rate due to the surface crust means that most of the water is lost as surface runoff.

4.2.5 Livelihood strategies in Mzingwane Catchment

The mopane trees dominant in Mzingwane Catchment play host to amacimbi, a tree borne butterfly lava that is well known in Zimbabwe for its nutritional value. The amacimbi are harvested from the mopane trees, dried and sold in many parts of the country, particularly in urban areas. Occurrence of amacimbi is seasonal and they form a major livelihood activity in many parts of Mzingwane catchment.

The catchment with its erratic rain falls under Zimbabwe's agro-ecological regions 4 and 5. Region 4 is considered suitable for livestock production while region 5 is considered suitable for wildlife management. Owing to the colonial legacy, most small scale farmers in Zimbabwe are found in these areas. Although livestock is the main livelihood in Mzingwane catchment, the people rely on rain fed farming for household food production (Rukuni, 2006). Land use in Zhulube is dominated by grazing with rain fed cultivation taking up 15% of the land (Dondofema, 2007). The main crop grown is maize. There is an irrigation scheme supplied with water from Zhulube Dam by gravity making it a

sustainable irrigation scheme (although it is under threat of sedimentation) growing maize, wheat and groundnuts (Maisiri, 2004). The land is generally degraded due to overgrazing and deforestation that has taken place over the years. Gold mining and panning is also practiced in part of the upstream catchment, resulting in further degradation.

Water users in Mzingwane catchment fall in various categories that include small and large scale commercial farmers; subsistence farmers (in pre-independence communal areas and post-independence resettlement areas), wildlife or game ranching and urban water users that include residential, industrial and mining uses (Munamati, 2005). Small scale irrigation for vegetable gardens is practiced near small dams where they exist. The small dams provide diverse livelihood activities to the communities ranging from livestock watering, brick moulding, grass for thatching and basketry, fishing and gardening which both provide families with food important for good nutrition, domestic water supply and recreation (Mamba, 2007).

4.3 Data collection and analysis for assessing effect of contour ridges on soil moisture

Five farmers were selected to provide fields for experimental work based on soil type, slope and willingness to participate in the study. The five farmers' fields were located as shown in Figure 4-1 on different soil types to enable comparison of results on different soil types. It was desirable that each field have a uniform slope, soil type and underlying geology to enable differences observed in soil moisture to be attributable to effect of contour ridges. This condition was difficult to meet in most farmers' fields within Zhulube catchment owing largely to the undulating topography of the area. This is typical of most small scale (communal) farming areas in Zimbabwe. The best possible sections of the field from those farmers who were willing to participate were however selected.

4.3.1 Plot design and replication

Two basic contour ridge designs were implemented in each field. One design retains runoff water in the field plot through contour ridges constructed along a zero gradient (DLC plot). The second drains runoff water away from the field plot through contour ridges constructed at a gradient of 5% (GC plot). The DLC plot was separated from the GC plot

by a plot with no contour ridges (NC plot) which was used as a control. Figure 4-8 illustrates the arrangement of the experimental plots in a farmer's field. Each experimental field contained these two types of contour ridges so that the effect of retaining runoff water and that of draining the runoff water could be established and compared to a plot without contour ridges.

Five fields were initially selected and instrumented. However, only two fields (field A and field B) eventually provided the main data owing to the commitment shown by the farmers and the contrasting soil type between these fields (Figure 4-9). Field A has loam soil and field B has sandy soil. Field C, field D and field E provided rainfall and runoff data that was used as independent sites to test the fuzzy rainfall runoff model whose development is described in chapter 5 section 5.4.

Runoff data feeding the contour ridges, rainfall on the fields and evaporation data was directly measured on site. Rainfall was measured daily using catch gauges installed at every field plot (Figure 4-10). Runoff measurement was carried out using runoff plots 2m wide running downslope from one contour ridge to the next as illustrated in Figure 4-8. The water collected into a graduated tank installed in the ground at the end of the runoff plot (the dotted circle in Figure 4-8). It is generally observed that evaporation does not vary much over small distances. Therefore only one standard class A evaporation pan whose location is indicated in Figure 4-9 was used to collect evaporation data.

Soil physical and chemical properties were determined in the laboratory at the University of Zimbabwe from soil samples collected from each field as described later in section 4.4.1. The laboratory tests carried out were sieve analysis to determine soil classification, water holding capacity test, pH test and nutrient tests to determine nitrogen, phosphorus and potassium content of the soil. The field density of the soil was measured using the sandy replacement method.

Soil moisture variation across the field was measured at the indicated positions during both the rainfall and the dry season as discussed in section 4.3.3.

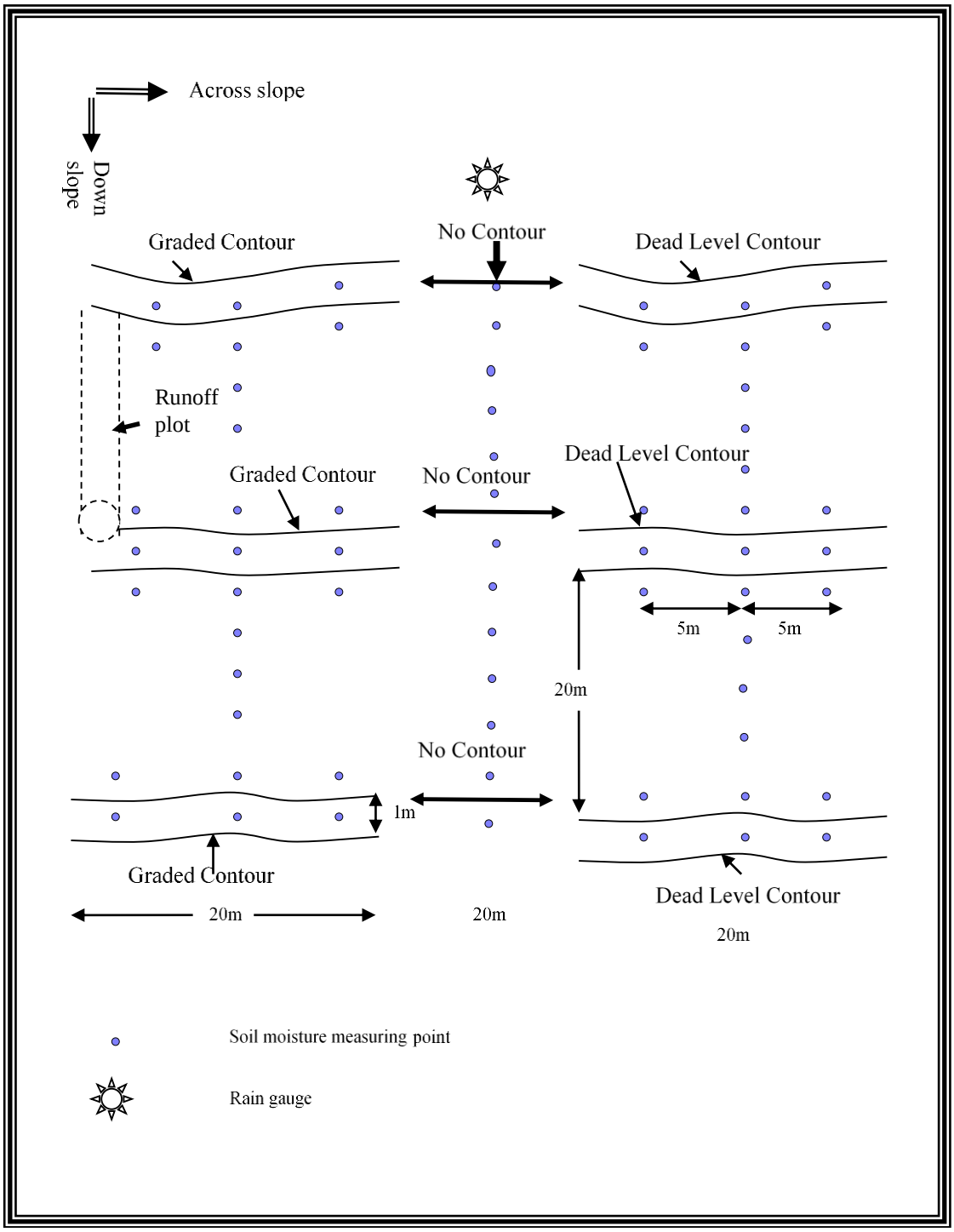

Figure 4-8: Arrangements of experimental plots in a farmer A's field

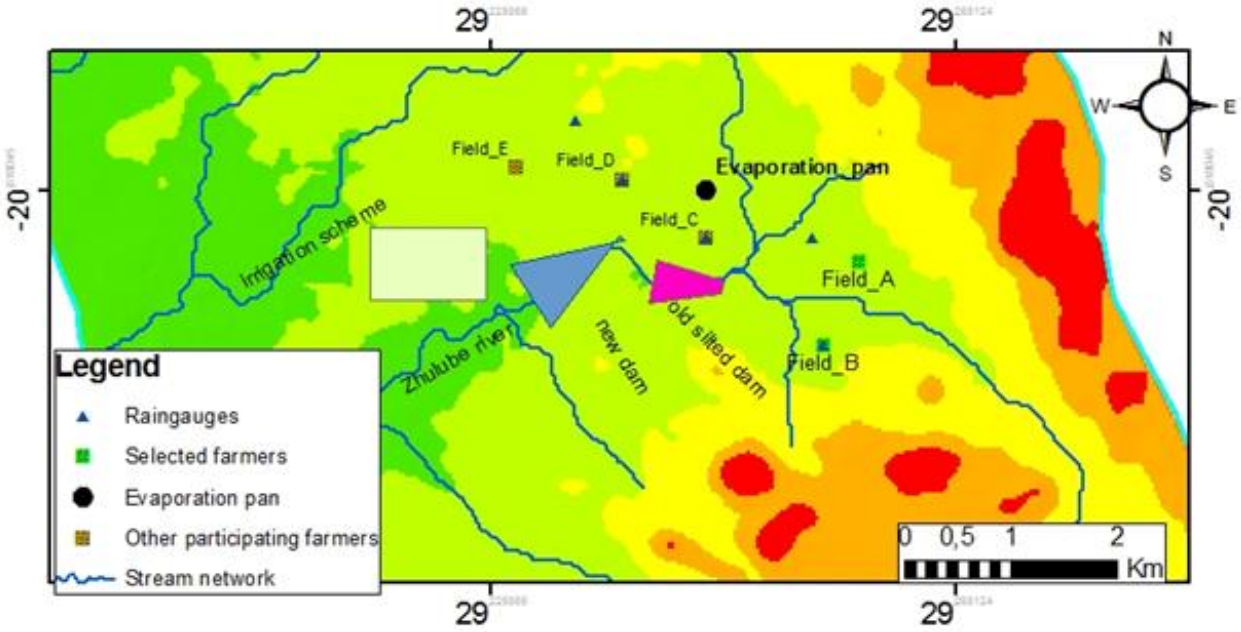

Figure 4-9: Location of data collection sites

Figure 4-10: A catch gauge used to measure rainfall installed in field C

4.3.2 Making Contour ridges

The contour ridges were made at the beginning of the rain season during the last week of October 2008 and first week of November 2008. The alignment of contour ridges was determined using an automatic leveling machine. In dead level contours the ridges were aligned along points of the same level while for standard graded contours a slope of 5% was used between successive points. The marked area was then ploughed using donkey drawn mouldboard ploughs which were also used during contour maintenance before the start of every rain season as shown in Figure 4-11. A shovel was then used to remove the soil from the channel to form the ridge (Figure 4-12). The channel was excavated to a depth of 300mm with a width of 1000mm. The excavated soil formed a ridge with a height of 500mm and a base width of 1000mm. Dead level contour ridge channels were blocked on the ends by constructing a small earth wall across the channel as shown in Figure 4-13 practically making them small dams /reservoirs in the field.

Figure 4-11: Use of donkey drawn mouldboard plough to losen the soil before shovelling during contour maintainance in filed A

Figure 4-12: A mouldboard ploughed contour ridge with the farmer's grandson posing for a photo illustrating shovelling during contour ridge making in field A

Figure 4-13: Constructed dead level contour ridge channels blocked at the end to retain the water

4.3.3 Instrumentation and data measurements

Access tubes were installed in January 2009 about two months after the commencement of the rain season due to delays in procurement. The seasonal rains had already started by the time the access tubes were installed. Access tubes were installed into the ground in each position where soil moisture data was required as illustrated in Figure 4-14 with part of the access tubes shown in Figure 4-15. It was anticipated that soil moisture would be influenced by the relative sampling position to the contour ridge. As a result the access tubes were installed across the field. It would have been desirable to have three transect sets of access tubes in each treatment. However this was not possible due to budgetary constraints. Only the places close to the contour ridge were installed with three sets of access tubes.

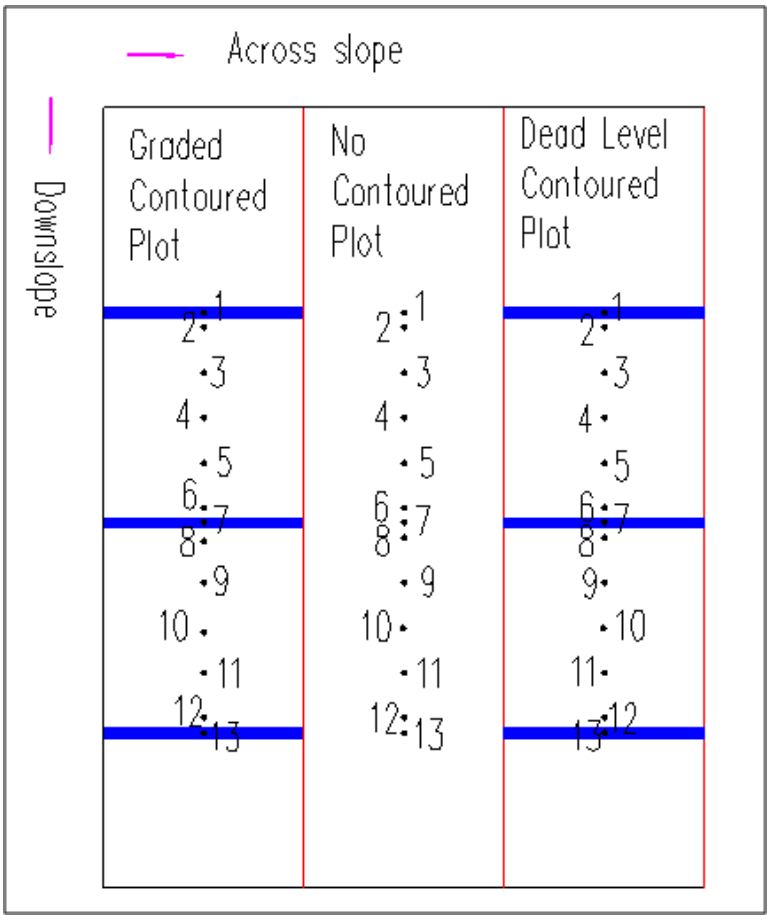

Figure 4-14: Moisture measurement locations (numbered) in the experimental plot with the contour ridge channel (number 1, 7 and 13)

Figure 4-15: Access tubes installed in the experimental plots of a loam soil (field A)

Table 4-2 gives the number of access tubes installed in each experimental plot of the two fields. The large number of access tubes installed in each field made it difficult to employ continuous soil moisture measuring methods as the cost was not affordable. Each access tube would have required individual soil moisture sensors and individual data loggers. Instead the method employed for soil moisture measurement used one soil moisture sensor that was used from one access tube to the next with the data recorded each time that was done.

Table 4-2: Number of access tubes installed in each experimental plot

Farmer	Plot type	Number of access tubes	Remarks
A	Dead level contour	27	13 on the centreline 7 on either side of the centreline
	No contour	13	All on the centreline
	Graded contour	27	13 on the centreline 7 on either side of the centreline
B	Dead level contour	23	11 on the centreline 6 on either side of the centreline
	No contour	9	All on the centreline
	Graded contour	23	11 on the centreline 6 on either side of the centreline
Total number of access tubes		122	

Soil moisture was measured using a Gopher Soil Moisture Profiler shown in Figure 4-16 (Charlesworth, 2005). This is an instrument that measures the moisture content of the

soil through measuring the dielectric constant of the soil plus water. An increase in the water content of a soil results in an increase in the dielectric constant of the soil plus water. The instrument uses a data logger for storing the data after measurement before the data is downloaded. This enabled use of the instrument by an assistant when the researcher was not available. To avoid losing data from the instrument through malfunctioning manual reading and recording was also carried out for every measurement.

Figure 4-16: Soil moisture measurement using the micro gopher instrument

Data collection started on 22 January 2009 and was continued until end of April 2011. However the data used for analysis was from May 2009 to end of April 2011 completing two years of soil moisture monitoring. Measurements were done on a weekly basis during the rainy season and once in two to three weeks during the dry season. The measurements were done for every 100mm depth starting with a depth of 100mm up to a depth of at least 600mm in field A where access tubes could not be installed any deeper

due to a rocky underlying profile. In field B, a sandy soil, the access tubes could be installed deeper and measurements were done up to 1000mm.

The soil moisture was measured as a percentage of the saturated soil moisture of the soil and converted to volumetric soil moisture in mm/horizon depth. The horizon depth was considered to be 200mm in the loam soil and 300mm in the sandy soil in order to create three soil horizons. The first zone represented top soil, the second subsoil and the last deep subsoil. Calibration of the instrument was done using data obtained through the gravimetric method of measuring soil moisture. This method involved obtaining a soil sample and weighing it immediately then drying it and weighing again when dry. The difference in weight indicates the weight of water in the soil.

Variation of soil moisture across the treatments was established by first subdividing each treatment into 4 subplots. For the DLC and GC treatments the contour ridge was considered as the 4^{th} subplot (subplot 4), the area below the contour ridge with a width of 5m was subplot 1, the middle of the contour ridge with a width of 10m was considered as subplot 2 and subplot 3 was the area upslope of the contour ridge with a width of 5m. The corresponding areas for the NC treatment which acted as the control were named in a similar fashion as the DLC and GC subplots. The average soil moisture for each subplot was computed and compared in a graphical plot and a t test was carried out to establish if there was a significant difference between each subplot and the middle subplot were the influence of the contour ridge was expected to be at its minimum. The comparison was carried out for a period after the fields had received large amounts of rainfall and after a dry spell. Large rainfall amounts were determined based on the observations by Mupangwa (2011) who observed evidence of lateral moisture movement from contour ridges after rainfall events of 40mm/day. The length of a dry spell was considered to be two weeks without rainfall exceeding the interception threshold in any of the days for the entire period as recommended by Chibulu (2007).

The seasonal accumulation of soil moisture in plots was determined using the soil moisture storage index as proposed by Nyagumbo (2002) and described in section 4.3.4.

4.3.4 Procedure for estimating soil water storage index

Accumulation of soil moisture over time was considered as a good measure of effectiveness of each treatment. While the soil moisture measurement was a point

measurement both in the spatial and temporal scale the moisture accumulation should be considered as storage represented by a depth of water accumulating in each treatment. Nyagumbo (2002) faced a similar problem when comparing soil moisture benefit of tillage practices. To solve this problem Nyagumbo (2002) developed a one dimensional soil moisture storage index (SWI) as a measure of the cumulative soil moisture stored in the soil profile during a growing season. The concept of SWI was therefore adopted and extended from one dimension to three dimensions (Figure 4-17). This was achieved by considering that a measurement from each access tube is representing an effective area around the access tube and weighting the SWI according to this area.

In the modified technique an average soil moisture storage index can be calculated by considering the different access tubes in grid format as given in Figure 4-17. An access tube point, P, is located at x_i, y_j. Soil moisture is measured at different depths within this tube and at different times. Each soil moisture measurement is done at location i, j, k and time n and is represented by $\theta_{i,j,k,n}$. The thickness of a layer represented by this measurement at depth z_k.is ∂z_k. In figure Figure 4-17 ∂z_1 is equal to 200mm while ∂z_2 is 200mm (i.e. 400mm -200mm).

Cumulative moisture content ($S_{i,j,n}$) for the whole soil profile at location i, j and time n, is given by Equation 4-1 and the effective time that this measurement represents is computed using Equation 4-2

$$\boldsymbol{S_{i,j,n} = \sum_{k=1}^{k_{max}} (\theta_{i,j,k,n}) \partial z_k}$$ Equation 4-1

$$\Delta t_n = \frac{t_{n+1} - t_{n-1}}{2}$$ Equation 4-2

Where

Δt_n is the effective time length interval on the nth measurement date;
t_{n+1} is the next measurement date after the measurement on the nth date;
t_{n-1} is the previous measurement date before the measurement on the nth date.

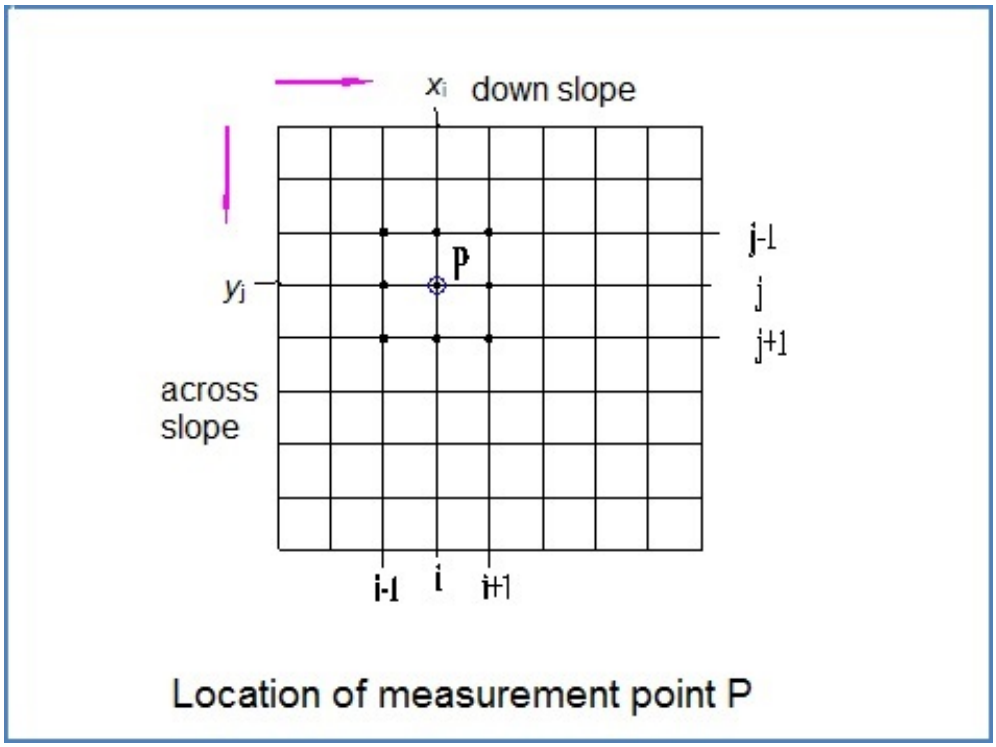

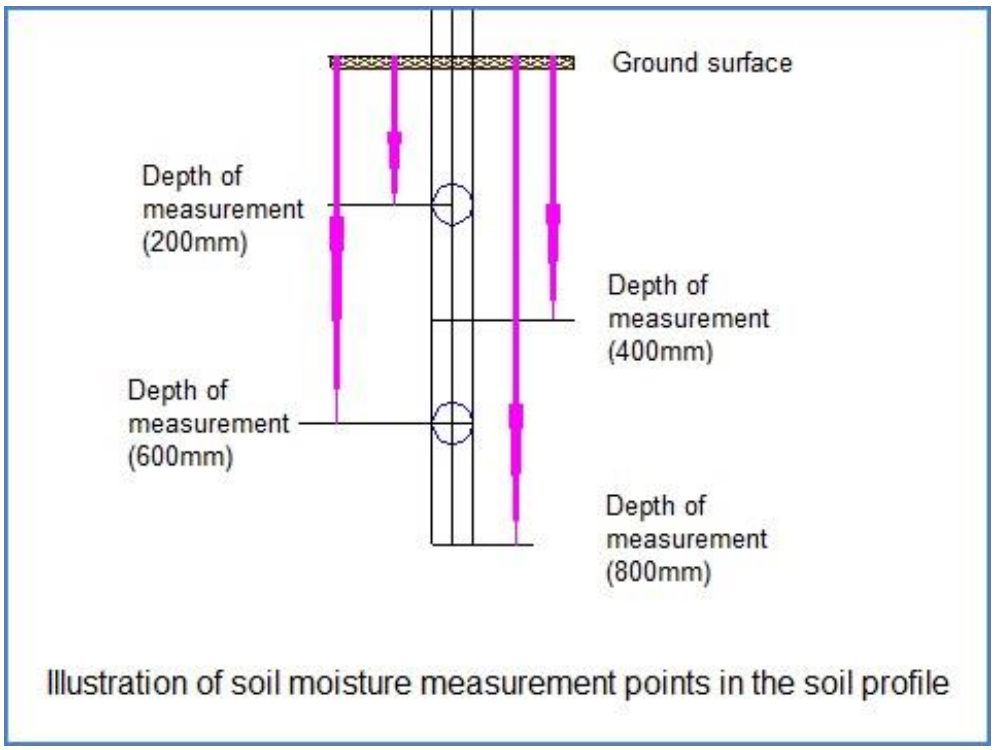

Figure 4-17: Three dimensional grid representation of soil measurement (Measurement point P {top} and vertical profile at P {bottom})

The soil water storage index ($SWI_{i,j,n}$) at location i,j and time n is thus represented by Equation 4-3;

$$\mathrm{SWI_{i,j,n}} = \sum_{l=1}^{n} \mathrm{S_{i,j,n}}\,\Delta \mathrm{t_n} \qquad \text{Equation 4-3}$$

The effective area represented by access tube i,j is given by Equation 4-4;

$$A_{i,j} = \left(\frac{x_{i+1} - x_{i-1}}{2}\right)\left(\frac{y_{j+1} - y_{j-1}}{2}\right) \qquad \text{Equation 4-4}$$

Where

$A_{i,j}$ is the area effectively represented by the soil moisture measured in the access tube located at i,j;
x_{i+1} is the distance to the next (i+1) access tube down slope;
x_{i-1} is the distance to the previous (i-1) access tube down slope;
y_{j+1} is the distance to next (j+1) access tube across slope;
y_{j-1} is the distance to the previous (j-1) access tube across slope;

The average SWI ($ASWI_n$) for the whole field plot at time n is therefore estimated using Equation 4-5.

$$ASWI_n = \frac{\sum_{i=1}^{i=i_{max}} \sum_{j=1}^{j=j_{max}} (SWI_{i,j,n})(A_{i,j})}{\sum_{i=1}^{i=i_{max}} \sum_{j=1}^{j=j_{max}} A_{i,j}} \qquad \text{Equation 4-5}$$

Each subplot had at least three access tubes and therefore three measurement points for each measurement date. With two areas between contour ridges at least six measuring points existed for each subplot type (Figure 4-18). The data was first analysed per subplot by comparing soil moisture among subplots of each treatment before combining the data from all the subplots within each treatment for the comparison of treatments.

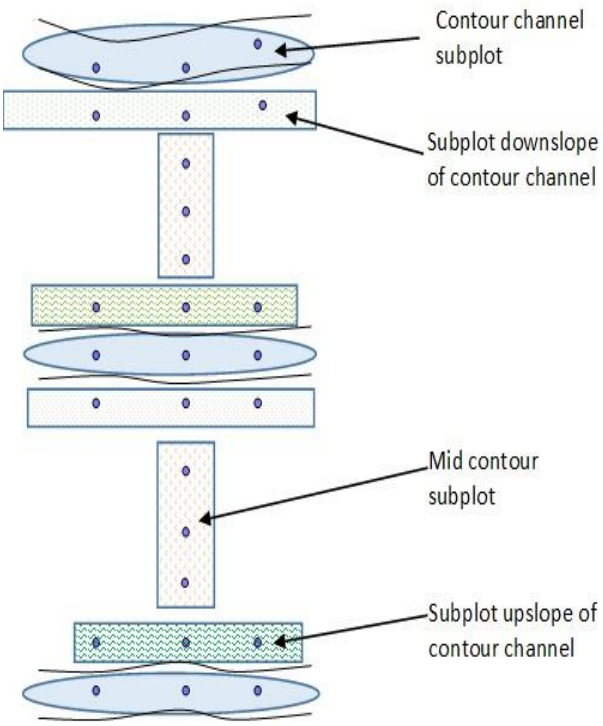

Figure 4-18: Soil moisture measurement locations used for spatial soil moisture analysis

Soil moisture data obtained within three days of a rainfall event greater than 40mm/day was considered for determining soil moisture after high rainfall for both loam and sandy soils. Soil moisture data obtained after a period of rainfall of at least 14 days was considered for determining the effect after a mid season dry spell. Rainfall events exceeding 40mm/day were observed by Mupangwa et al. (2011) to be effective in transferring water from a DLC ridge channel to the soil down slope.

4.4 Data collection and analysis to assess effect of contour ridges on crop yield

Maize crop was used to assess crop performance as it is sensitive to water availability and is also a staple food crop in Zimbabwe. The performance of the crop was assessed by monitoring crop growth and measuring biomass accumulation, grain and total yield. A

maize crop was planted in the plots between the contour ridges and managed by the farmers.

4.4.1 Soil sampling and measurement of physical and chemical properties

Differentiating the effect of treatment from that of soil properties was made difficult by high spatial variability of soil conditions even at very small distances. Replication of treatments was used to increase the quantity of data and reduce uncertainty caused by the spatial variability in soil conditions. Replication of treatment considers the variation of environmental conditions such as soil conditions as random events that require crop yield or any associated data to be treated as a random outcome whose population characteristics are affected only by the treatment. Replication was achieved by establishing in each subplot, two crop yield measurement areas each named a check plot as shown in Figure 4-19.

Each check plot measured 4m by 4m. Since the experimental fields had two areas that were bound by contour ridge channels it means each treatment (DLC, GC and NC) had a total of twelve check plots and four subplots. This was considered large enough to ensure the results reflect the effect of the treatment and was able to minimize the effect of local soil variations.

Table 4-3 shows the soil properties from the experimental fields before the start of the experiments. Five samples were collected from each field in a diagonal pattern one at the centre of the field and the others 5m away from each other along the diagonal line towards the centre. At each sample location two samples were collected one from top soil at a depth of 150mm and the other from the sub soil at a depth of 450mm. The samples were then analysed and the average values reported.

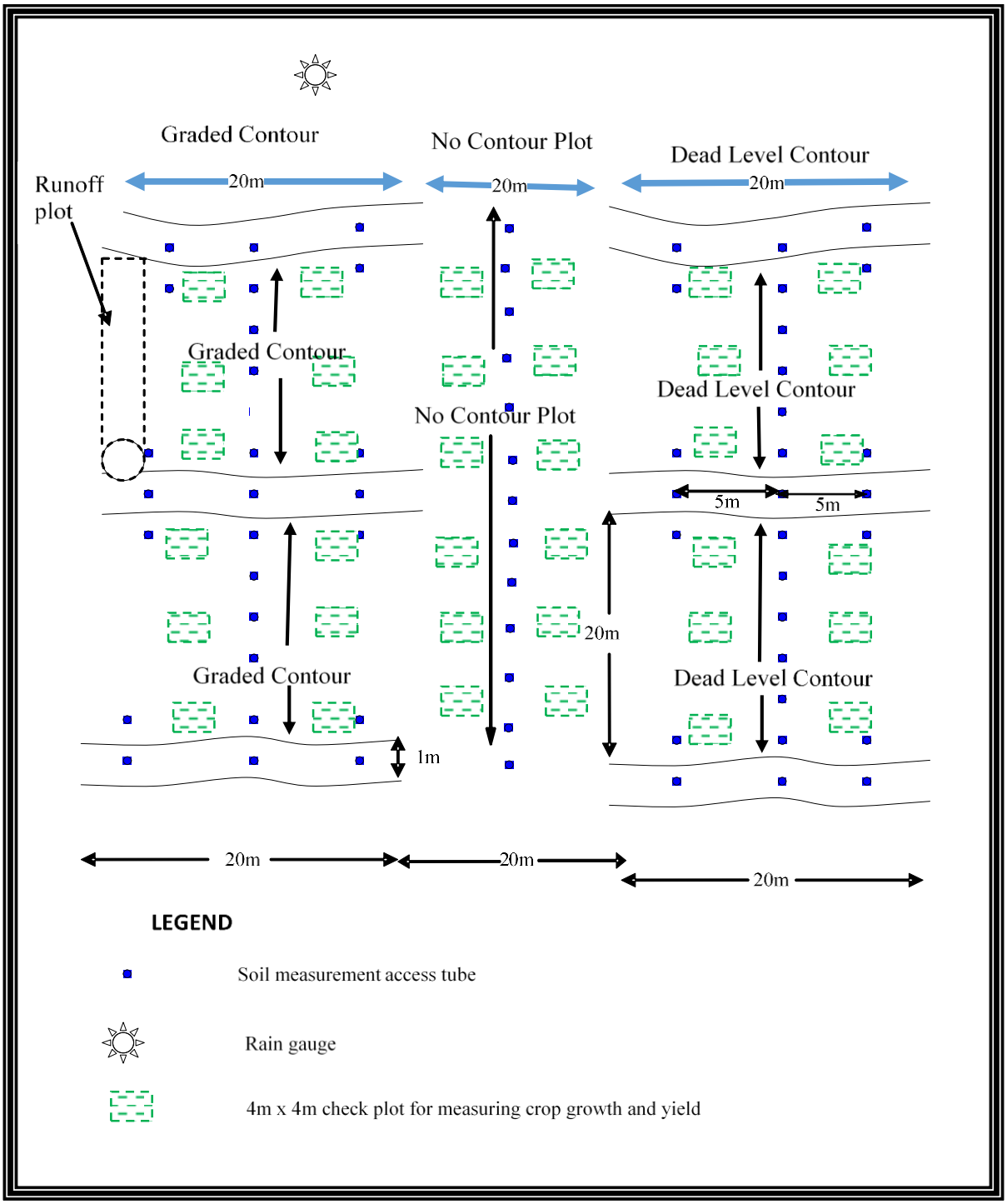

Figure 4-19: Location of check plots in an experimental farmer's field

Table 4-3: Physical and chemical soil properties from the experimental plots

Field	Textural class	pH ($CaCl_2$)	N (ppm)	P (ppm)	K (me%)	Clay content (me%)	Silt Content (%)	Sand content (%)	Water holding capacity (WHC) (mm)
Field A	Silt Loam	5.9	7	4	0.43	10	12	78	13.43
Field B	Sandy	5.3	12	6	0.39	3	2	95	4.85

In addition to the soil characteristics given in Table 4-3 other soil characteristic measurements that were carried out were field density and the soil moisture at saturation point, field capacity and at wilting point.

4.4.2 Procedure for crop growth data collection

Plant growth was measured using non-destructive methods carried out throughout the cropping season. These included measuring the crop height, counting number of leaves and crop leaf moisture content. Non-destructive methods of counting number of leaves and measuring plant height were used effectively by Memon et al. (2007) to assess the effect of sowing methods on growth of maize crop. Use of non-destructive methods was used to monitor plant growth so as to avoid destroying plants that would affect the yield. The research was farmer based and therefore the incentive for the farmers to participate was not only the long term knowledge transfer but also the grain that they would harvest at the end of the season. The method of monitoring crop growth through destructive methods such as above ground dry matter accumulation used by other researchers (Andrade, 1995) were considered inappropriate for a resource poor farmer based research.

At least 10 representative plants were selected at random from each check plot of a treatment. Crop heights were measured at least once every two weeks using a measuring tape. The height was taken as the distance between the ground and the highest point of the smallest (newest) leaf of the plant. During the same time the leaves on the selected plants were counted. Crop leaf moisture content was determined at the end of each of the dry spell periods. The dry spell selected for leaf moisture content determination was

that which occurred when the crop was close to flowering stage as this is the stage when the crop has high crop water requirements. Sample leaves were collected from plants selected in the manner described above. The leaves were weighed before being sun dried and weighed again until no change in weight could be noticed to obtain the dry weight of the leaves.

4.4.3 Procedure for maize crop yield data collection

The second measurement was destructive measurement carried out at the end of the cropping season. It involved cutting down the maize plant at harvesting and measuring the grain, inner cob and stover yield. The procedure that was followed in assessing the crop yield at the end of the crop growing season was adapted from IDRC-AFNET Project as used by Chibulu (2007). This procedure is described below.

1. The dimensions of each check were recorded in the field book crop assessment form as shown in Table 4-4. The dimensions are the same for all the nine check plots.
2. The number of plants and cobs in each check plot were counted & recorded in the appropriate row/column.
3. The stover was cut down and the cobs removed and weighed together with their grain. The cobs could not be separated from the grain since the experimental field constituted the main grain source for the farmers. In order to determine the constituent grain and inner cob weight, average cobs with grain were taken as a sample for both the determination of moisture content and for determining the proportion of grain and inner cobs.
4. Three to four average cobs were taken as a sample for moisture content determination and determination of the proportion of grain and inner cob. The cobs were weighed and the grain separated from the inner cobs and again weighed separately. Both grain and inner cobs were oven dried and weighed again for moisture content determination. These were averaged and recorded as the same figure for all the nine check plots of the treatment in the maize crop assessment form of Table 4-4.
5. Two to three stalks of stover were randomly selected from each check plot and chopped into smaller pieces. The pieces were weighed and placed in a plastic bag with the label of the check plot. The pieces were later weighed after drying for

moisture content determination averaged and recorded as same value for all the nine check plots.

Table 4-4: Maize Crop Assessment Form

Maize crop yield assessment form (Individual farmers trials only)

Name of Farmer---- R. Nkala Village ---------- Mpumelelo Ward ------- 1

Farming season --------- 2009/10 District ---------- Insiza

Date of sampling --------- 12 April, 2010 Recorded by ---------- Lewis Ndlovu

Treatment Graded contour late crop

Plot number as per sketch	1	2	3	4	5	6	7	8	9	Total	Average
Sub plot number	GC1	GC2	GC3	GC4	GC5	GC6	GC7	GC8	GC9		
Average width of 4 rows (m), (Average of at least 3 measurements)	4	4	4	4	4	4	4	4	4		
Length of check plot (m)	4	4	4	4	4	4	4	4	4		
Area of check plot (ha)	0,0016	0,0016	0,0016	0,0016	0,0016	0,0016	0,0016	0,0016	0,0016		
Number of plants in check plot	43	39	39	45	32	22	41	24	18		
Number of cobs	26	32	27	29	23	16	19	14	16		
Weight of cobs and grain in check plot together (kgs)	2,3	3,0	2,0	2,0	2,2	1,2	1,0	0,6	0,7		
Weight of sample cob and grain together (g)	183	183	183	183	183	183	183	183	183		
Weight of grain only from sample cob (g) (air dried)	140	140	140	140	140	140	140	140	140		
Moisture content of grain (% by mass)	15	15	15	15	15	15	15	15	15		
Initial weight of inner cobs (g)	43	43	43	43	43	43	43	43	43		
Moisture content of inner cob (%)	7	0	7	7	7	7	7	7	7		
Intial weight of stover (kgs), (at harvesting)	2,2	3,5	1,9	2	2,1	1,2	1,5	1	1		
Intial weight of sample stover (g), (at harvesting)	72,8	72,8	72,8	72,8	72,8	72,8	72,8	72,8	72,8		
Moisture content of stover (%)	9	9	9	9	9	9	9	9	9		
Grain yield (12.5% MC) (kg/plot)	1,71	2,23	1,49	1,49	1,64	0,89	0,74	0,45	0,52		
Population (Plants/ha)	26 875	24 375	24 375	28 125	20 000	13 750	25 625	15 000	11 250		
Dry grain yield (kgs/ha)	1 069	1 395	930	930	1 023	558	465	279	325	6 973	775
Dry stover yield (kgs/ha)	1 251	1 991	1 081	1 138	1 194	683	853	569	569	9 328	1 036
Dry inner cob yield (kgs/ha)	312	437	271	271	298	163	136	81	95	2 064	229
Total biomass (kgs/ha)	2 632	3 822	2 281	2 338	2 515	1 403	1 454	929	989	18 364	2 040

4.4.4 Characterization of rainfall seasons

The rainfall seasons were characterized as either a bad season, a fair season or a good season based on the criteria used by Chibulu (2007). The cropping season was described as being good, fair or bad based on the frequency of dry spells and the cumulative number of dry days experienced within 90 days after planting. The average growing period for a maize crop is considered as 90 days while the frequency and length of dry spells indicate water stress to the crop during the growing period. A dry day is defined as a day in which no rainfall or rainfall less than the interception amount is received. For the purpose of rainfall characterization interception was taken to be equal to the average evaporative demand of the study site which was found to be 4.3mm/day.

A bad season is a season in which at least 60 dry days out of 90 days after the planting date were experienced or three or more long dry spells lasting more than 21 days were experienced. A good season is a season in which less than 45 days of the 90 days were dry days and one or no long dry spell lasting 21 days were experienced. Any other season that does not fit the two criteria is a fair season.

4.4.5 Analysis of data for assessing effect of contour ridges on crop yield

The leaf moisture content was calculated from Equation 4-6.

$$lmc = \frac{wwl - wdl}{wdl} \times 100 \qquad \text{Equation 4-6}$$

Where:

$lmc\ is\ leaf\ moisture(\%)$
$wwl\ is\ weight\ of\ wet\ leaves(g)$
$wdl\ is\ weight\ of\ dry\ leaves(g)$

The moisture content of grain, inner cob and stover were calculated using Equation 4-7 with leaf moisture content replaced by moisture content of grain, inner cob and stover as the case may be. The weight of wet leaves and dry leaves were also replaced by the weight at harvest and the weight after drying of grain, inner cob and stover as was necessary.

The crop yield was considered to comprise of grain, inner cob and stover yield. While only grain is used for human consumption both inner cob and stover can be used for stock feed and therefore indirectly contribute to food security. Considering that the study area is a cattle rearing region it was considered necessary to include stock feed in the total yield of the crop. Grain yield, inner cob and stover yield were calculated separately and then added together to obtain the total yield. These separate yields were obtained using Equation 4-7. The total yield was obtained using Equation 4-8. The grain yield was calculated at 12% moisture content which is the moisture content at which harvesting of grain is recommended for good lasting storage. This is catered for by subtracting moisture content of grain from 112% instead of 100% moisture content in Equation 4-7(a). This means that mass of grain at storage is equal to 112% of mass of dry grain.

$$Y_{gc} = \frac{W_{sg}}{W_{sc}} \times W_{cc}\left(112 - mc_g\right)\% \qquad (a)$$

$$Y_{ic} = \frac{W_{sic}}{W_{sc}} \times W_{cc}(100 - mc_{ic})\% \qquad (b)$$

Equation 4-7

$$Y_{stc} = W_{stc}(100 - mc_{st})\% \qquad (c)$$

Where:

Y_{gc} is grain yield in check plot (kg/(check plot));
Y_{ic} is inner cob yield in check plot (kg/(check plot));
Y_{stc} is stover yield in check plot (kg/(check plot));
W_{cc} is weight of cobs (inner cobs and grain together) in check plot (kg) at harvest;
W_{sc} is weight of sample cob (inner cob and grain together) (kg) at harvest;
W_{sg} is weight of sample grain (kg) at harvest;
W_{sic} is weight of sample inner cob (kg) at harvest;
W_{stc} is weight of sample stover at harvest;
mc_g is moisture content of grain at harvest;
mc_{ic} is moisture content of inner cob at harvest;
mc_{st} is moisture content of stover at harvest.

$$Y_t = \left(Y_{gc} + Y_{ic} + Y_{stc}\right) \times \frac{10\,000}{A_c}$$

Equation 4-8

Where:

Y_t is the total yield (kg/ha);
A_c is area of check plot (m^2)

4.5 Statistical analysis of data

Comparison between subplots (representing position from contour ridge channel) or between treatments (DLC, GC NC) was done by carrying out an analysis of variance (ANOVA) at 95% confidence level. Statistical comparison for actual soil moisture was carried out on data measured on the same date for comparison of soil moisture after significant rain and after a dry spell. Time series soil moisture data analysis was carried out on cumulative soil moisture storage as represented by soil moisture storage index calculated using the method described in section 4.3.4. The statistical analysis was carried out using statistical package for social scientists (SPSS) version 16.

Analysis of variance (ANOVA) was also used to test the impact of DLC and GC on plant height, leaf moisture content, grain yield and total yield using the NC as a control. The spread of data was analysed by calculating the median, lower and upper quartiles. The statistical analysis was carried out using statistical package for social scientists (SPSS) version 16.

5 MODELLING RAINWATER HARVESTING BY CONTOUR RIDGES

5.1 Introduction

This chapter describes the development of the model that was used in this study for rainwater harvesting by contour ridges and how it was applied. The chapter starts by describing the modelling approach that was followed and how the approach relates to a contour ridged field. The model framework is then presented together with a description of the governing equations used in the model. Following this is a description of how the model was applied to model two farms where field experiments were carried out in Zhulube. Estimation of overland flow from daily rainfall data is treated as an important aspect of modelling rainwater harvesting by contour ridges and was modelled using a fuzzy logic approach which was developed as an extension of the linear regression model normally used for field-scale runoff estimation. The methods used to develop and test a fuzzy model for modelling overland flow runoff are described in this chapter. It was found realistic to formulate the fuzzy model with the mean rainfall intensity and duration for each rainfall event as inputs. However data at farm level setting is normally obtained in daily amounts and there was therefore need to disaggregate the daily rainfall data to mean hourly rainfall intensity of a specified sub-daily duration. The approach applied for rainfall disaggregation is described at the end of this chapter.

5.2 Selection of modelling approach

The model for rainwater harvesting by contour ridges was developed as a semi-distributed model that is based on a hybrid of process and statistical approaches.

A semi-distributed approach was selected so that the spatial distribution of runoff and soil moisture across a contour ridged field could be determined. This was achieved by dividing the area between contour ridges into a grid of subplots running from the upper contour to the lower contour as shown in Figure 5-1. The size of the subplots can be decided upon on the basis of the physical characteristics of the area so as to select areas with uniform characteristics so that the same parameters can be applied uniformly across the whole

subplot. In this study the fields selected for the experiments had uniform characteristics and the size of the subplot was selected to investigate effect of contour ridges on areas close to contour ridges upslope and downslope and at the middle of the field. This grid-based modelling enables the model to accumulate runoff as the area increases downwards across the field. Each subsequent subplot receives run-on water from an upper subplot and its runoff is discharged to the lower subplot. The concept of run on and runoff was used by Makurira (2010) to add runoff collected from an area surrounding a field with fanya juus into the fanya juu in Tanzania. With this concept, different subplots can have different infiltration amounts since the amounts of water available on the subplot surface are not set to the same value. In this way interaction of the components of the hydrological process within the contour ridged field would be better represented. The surface of each subplot contains one distinct component of the hydrological process of a contour ridged field. For example subplot 4 contains concentrated channel flow and it does not contain the overland flow that is contained in subplot 1, 2 and 3.

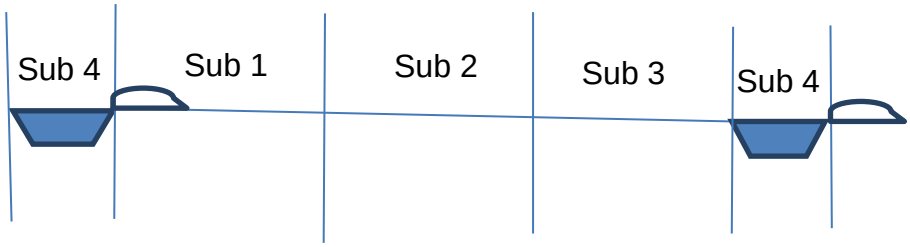

Figure 5-1: Subplots in a contour ridged field in which mass balance computations were carried out

Three horizons were defined in order to establish the vertical variation in moisture and eventually determine the flow to the groundwater system. The three soil horizons (horizon A, horizon B and horizon C) and the boundary layer below horizon C were defined by way of the depth and soil type for all the subplots. Horizon A represent the top soil while

horizon B and C represent the subsoil and deep soil layer. Two subsoil zones were also selected in order to provide a provision in the model to allow for significant variability within the subsoil horizons (e.g. a sand soil overlying a clay soil layer).

The distinct components of the hydrological system of a contour ridged field were identified in a manner analogous to the representative elementary watershed (REW) approach developed by Regianni et al. (1998) which is more systematic than other process based models. This identification was done to simplify the complexity of the hydrological process and select the main interactions among the processes that take place in a contour ridged field. This is against the background of difficulty in obtaining and handling detailed data that is typical in farm field conditions and the existence of a large number of hydrological fluxes occurring in a small area at varying temporal scales. These fluxes include precipitation, interception, infiltration, runoff, open water evaporation, evapotranspiration and seepage of soil moisture. Typical time scales at which the fluxes occur vary from as little as a few minutes for rainfall events to a few days for the seepage while spatial scales are in the order of hectares.

The difficulty in obtaining data at farm field scale is apparent given that a farm can be regarded as an ungauged area where normally no observed time series data exist. The high spatial variability in physical conditions such as soil type and temporal variability of climatic conditions such as rainfall intensity makes it difficult to transfer data from previously studied sites to each specific site requiring modelling. In addition for smallholder farms, financial and time constraints limit the type and quantity of data that may be obtained. This does not then favour the data intensive distributed physically based models where equations are derived at point scale and integrated over the modelled spatial area thereby requiring extensive data. The less data intensive lumped models would be considered appropriate for modelling in such situations. Therefore some statistical approaches were also considered appropriate in estimating some of the model inputs such as rainfall intensity and modelling runoff.

5.2.1 The contour-ridged field as a hydrological system.

Although a contour ridged field is not a watershed in the sense of a river system, the area between two contour ridges (Figure 5-2) was considered as analogous to a representative elementary watershed (REW) discussed in chapter 3 section 3.1. The analogy with a

REW was done in order to have a systematic identification of components of a hydrological system of a contour ridged field. This area was considered as the smallest representative control volume that contains all the functional components of the hydrological system of a contour ridged field that needed to be modelled. These functional components were identified based on physical characteristics and on the various time scales typical for the flow within each component.

Three hydrological components (sub-regions) within this representative contour ridged area were identified and described in a similar manner to three subzones out of the five REW subzones proposed by Reggiani et al. (1998) and later extended to six by Tian et al. (2006). The three were identified in REW terminology as overland flow, channel flow and unsaturated flow subzones located at the cropped area, the contour ridge channel and the root zone respectively as illustrated in Figure 5-2 and Figure 5-3. While these components of a hydrological system are not unique to the REW concept proposed by Reggiani et al. (1998) the presentation and grouping by Reggiani et al. (1998) makes it easy to follow and apply. The location of components in the spatial area of a contour ridged field helps in identifying water mass flows across their boundaries which in turn enables application of the principle of conservation of mass when developing mass balance equations.

5.2.2 Process interaction in the three subzones of a contour ridged field

The main processes in the cropped area are runoff generation, interception from vegetation, evaporation from detention storages and infiltration. These processes depend on soil moisture and soil type prevailing as the two have an effect on the infiltration rate as well as by the rainfall amount and intensity. Although precipitation and infiltration occur in the crop growing area as well as the contour ridge channel the two areas were considered to be separate from each other because the cropped area generates runoff while the contour ridge channel receives the generated runoff.

The contour ridge channel was identified as a channel flow zone because it experiences seepage of water from the channel to the surrounding unsaturated soil zone similar to what happens in a stream channel (Mugabe, 2004; Mupangwa, 2011). In addition the

surface water is in a concentrated form. The main processes in the contour ridge channel were identified as precipitation, infiltration and open water evaporation.

The root zone is the soil layer of interest where the crops grown derive their water. The bottom boundary of the root zone was considered as the root depth of the crops grown which in this study was the maize crop. The root depth of maize range from 0.4m to 1.4m depending on field conditions such as soil type and soil water availability (Gao and Lynch, 2016). Within this boundary and for the hydrogeology and the climatic conditions of the area under study the water table or impermeable horizon is always below the root depth. The main processes identified across the root zone boundaries are infiltration, evapotranspiration, seepage between root zone sub grids and percolation to groundwater system.

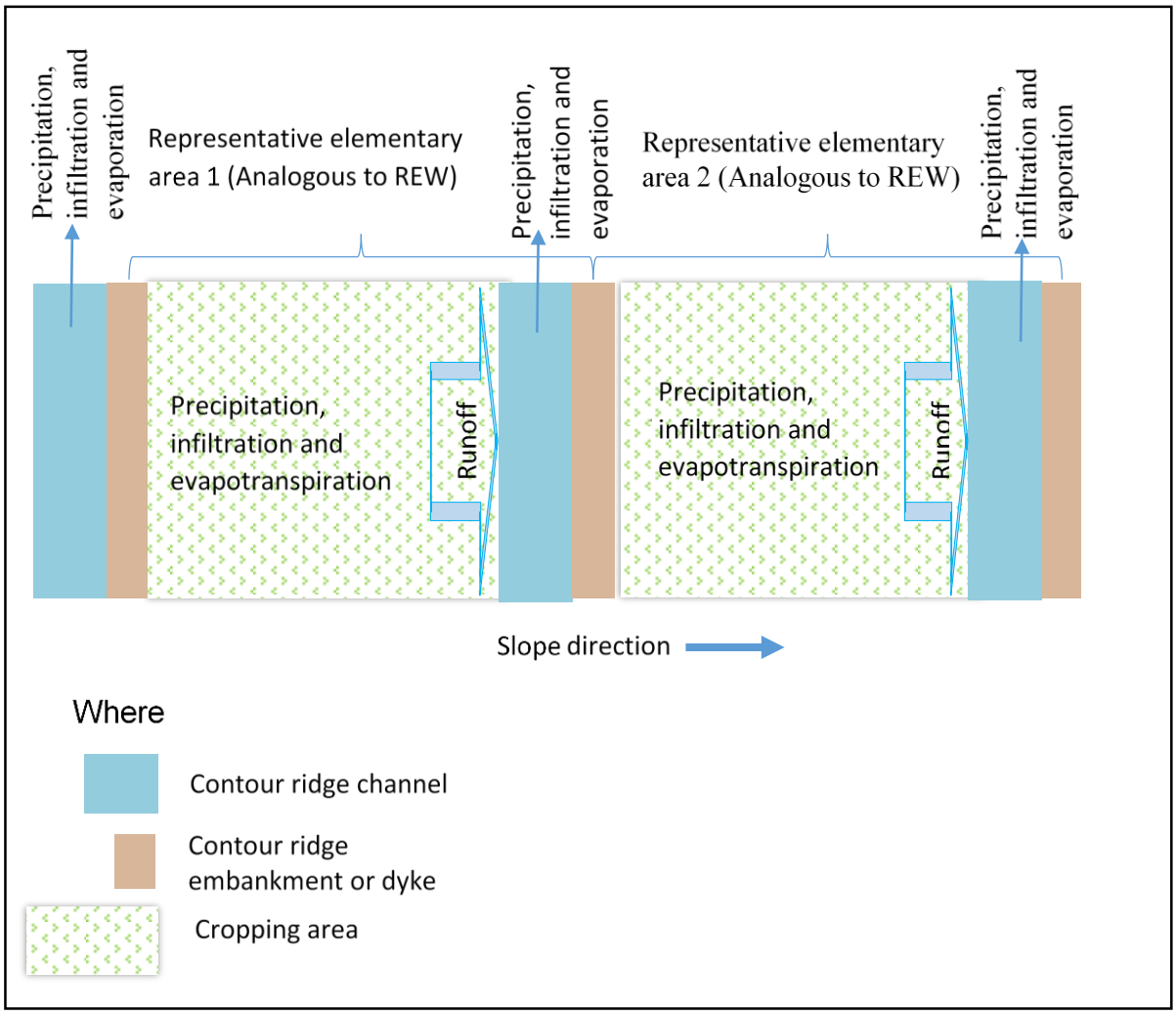

Figure 5-2: Representative surface area of a contour ridged field.

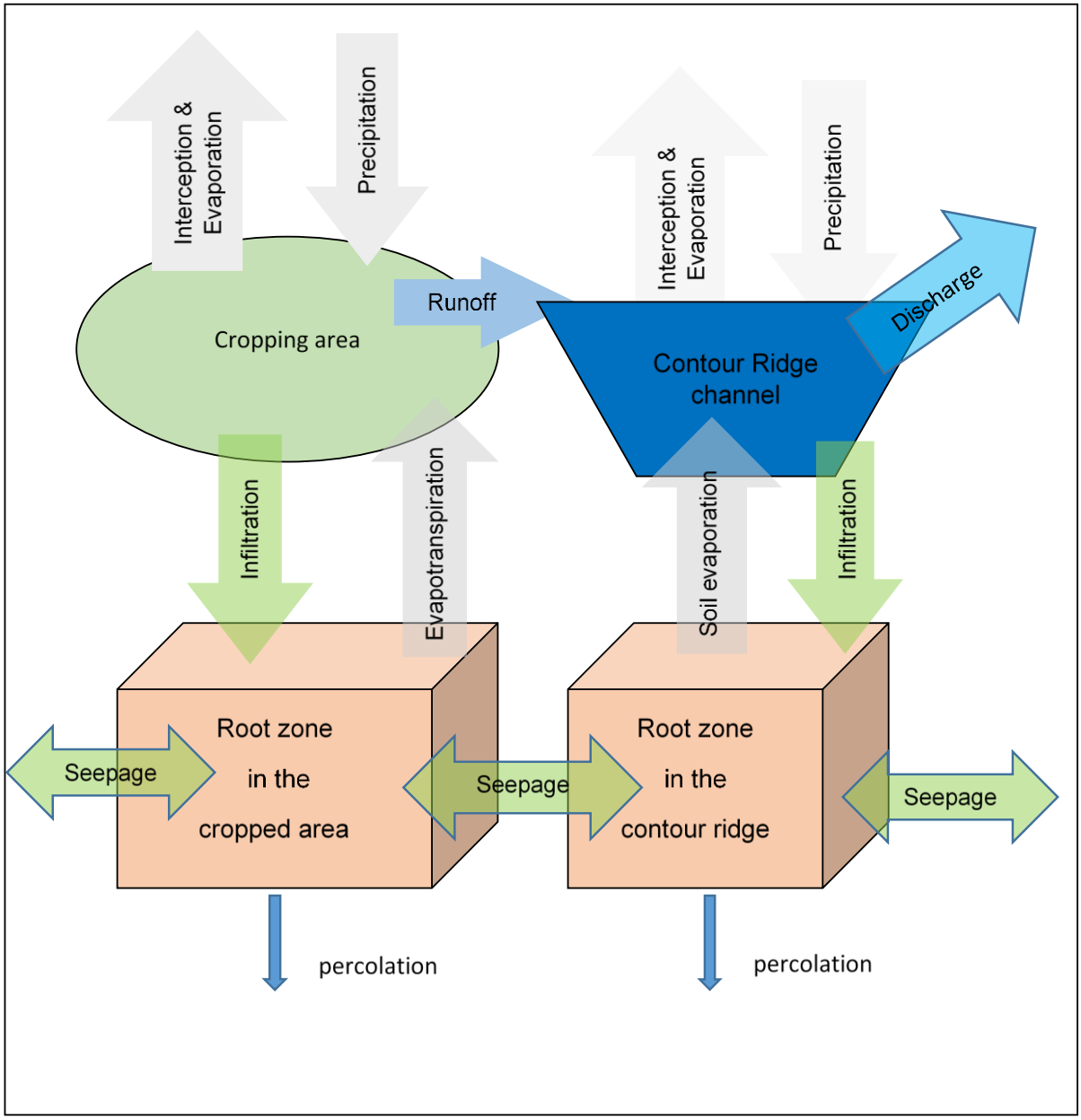

Figure 5-3: Representative cross sectional area of a contour ridged field

Some of the boundaries of subzones separate subzones from other subzones while others separate subzones from systems that are external to the representative system being modelled. The external systems that form boundaries with the modelled subzones are the atmosphere, groundwater and root zone of the areas adjacent to the area being modelled. The mass exchange across the external boundary with the atmosphere is through precipitation and evapotranspiration (including interception, open water

evaporation and soil evaporation) processes. Mass exchange across the external boundary with the groundwater system is through groundwater recharge and capillary rise processes. Mass exchange across the external boundary with the adjacent areas is through the seepage process.

Figure 5-4 shows the boundaries of the overland flow subzone in the cropped area across which mass exchange with the overland flow subzone takes place. These boundaries comprise of the atmosphere at the top (from where the rainfall originate), the root zone at the bottom (where infiltration takes place), top of contour ridge or the upslope edge of the field plot (where overspill water or run on enters the zone and runoff starts) and contour ridge channel or the down slope edge of the field plot (where runoff drains to).

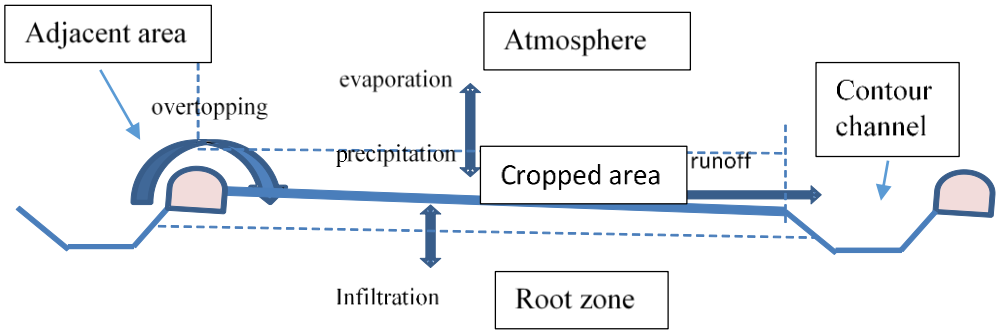

Figure 5-4: Boundaries of the overland flow subzone in the cropped area

The boundaries of the channel flow subzone are shown in Figure 5-5. These boundaries comprise of the atmosphere at the top (where rainfall and evaporation originates and terminates), root zone at the bottom of the channel (where infiltration takes place), cropped area sub plot on the up slope side of the contour ridge channel (where runoff originates) and contour ridge (which could be cropped) on the down slope side of the contour channel (where overtopping water terminates if the channel is undersized) and contour ridge channel edges at the upper end along the ridge (where diverted catchment

runoff originates if applicable) and contour ridge channel edges at the lower end along the ridge (where discharge from the channel takes place if the channel becomes full). The model assumes that there is no inflow into the channel flow zone from the area adjacent to the field but spillage from the channel flow zone to the adjacent field is catered for in the event the contour ridge channel is full.

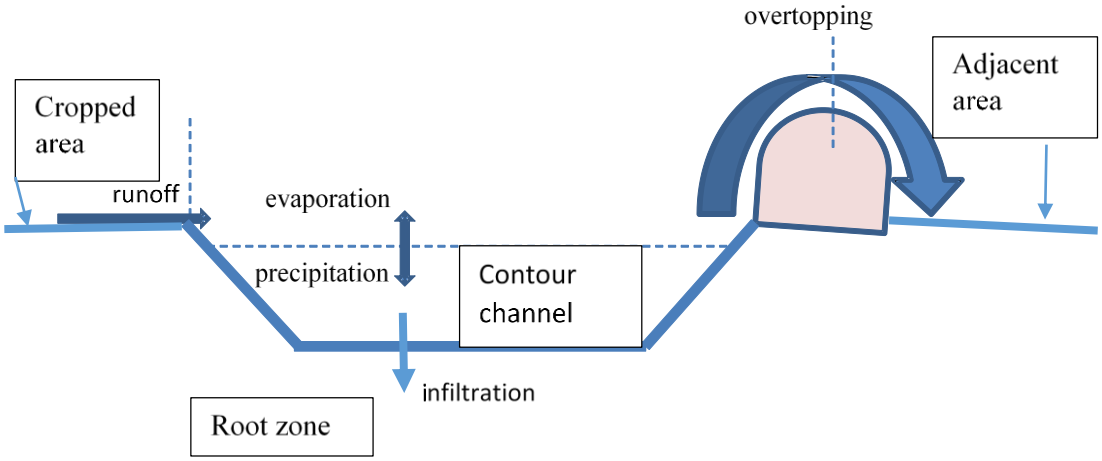

Figure 5-5: Boundaries of channel flow subzone in the contour ridge channel

Figure 5-6 shows the boundaries of the unsaturated flow zone in the root zone. The boundaries are the cropped surface area at the top (from where infiltration originate), the underlying layer at the bottom (where downward percolation water leaves the root zone and capillary water may originate), root zone of the adjacent area at the upslope (where exchange of seepage takes place) and root zone of the adjacent area down slope (where exchange of seepage takes place). Since the model bottom boundary is defined by the lower boundary of the root zone any exchange of water across this boundary is regarded as exchange with the groundwater system. Therefore capillary rise means water entering the root zone from the soil water below the root zone.

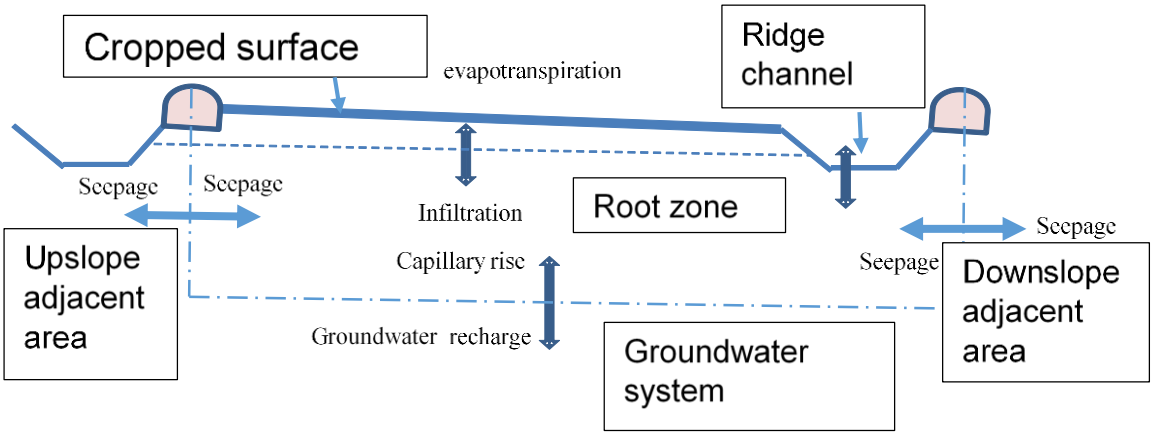

Figure 5-6: Boundaries of unsaturated flow subzone in the root zone

5.2.3 A hybrid of process and statistical approaches.

Each of the three distinct components of the hydrological system of a contour ridged field exchange mass flows of water through their system boundaries. Estimation of the mass flows across the system boundaries is important in completing the mass balance equation for each of the three distinct components. These mass balance equations include all the main processes taking place in the respective distinct components and are described in detail in section 5.3.2 to 5.3.4.

The determination of the components of the balance equations is necessary to enable the balance equations to be solved. They were determined using methods that were considered convenient for the conditions that prevail at farm level. These methods are a hybrid of process and statistical approaches as described in sections 5.3 to 5.6.

In developing the mass balance equations the partitioning of rainfall, runoff and soil moisture into various components was considered for the cropped area, contour ridge channel and the root zone respectively. Rainfall was partitioned into interception, runoff and infiltration components. Runoff harvested in the contour ridge was partitioned into infiltration, open water evaporation and discharge components. The infiltration component from the contour ridge channel is then transported to a field subplot where it adds on to the infiltrated water from rainfall partitioning to cause the effective change in moisture content through moisture redistribution. This soil moisture was then partitioned

into evapotranspiration, groundwater recharge through percolation and seepage to adjacent root zones. The water mass balance equations for each zone constitute the basis of the developed model and are presented in sub-sections 5.3.2, 5.3.3 and 5.3.4.

5.3 Description of the model and its operation

This section describes the main features of the model that was developed which is summarised in a flow diagram shown in Figure 5-7.

5.3.1 General description of the model

The model comprise of three modules namely rainfall partitioning, runoff partitioning and soil moisture partitioning for which mass balance equations were developed. These mass balance equations and their computations are presented and described in sub sections 5.3.2 to 5.3.4. Computation starts with the rainfall partitioning whose output from the mass balance analysis provides input variables into the runoff partitioning. Soil moisture partitioning computations are done last obtaining as this requires some of its input variables from the first two modules (rainfall partitioning and runoff partitioning modules). The main output from soil moisture partitioning is the soil moisture in the root zone which is used for the next time step for simulation of runoff in rainfall partitioning as well as initial soil moisture for soil moisture partitioning. The feedback of the information is represented by dotted lines in the model flow diagram of Figure 5-7.

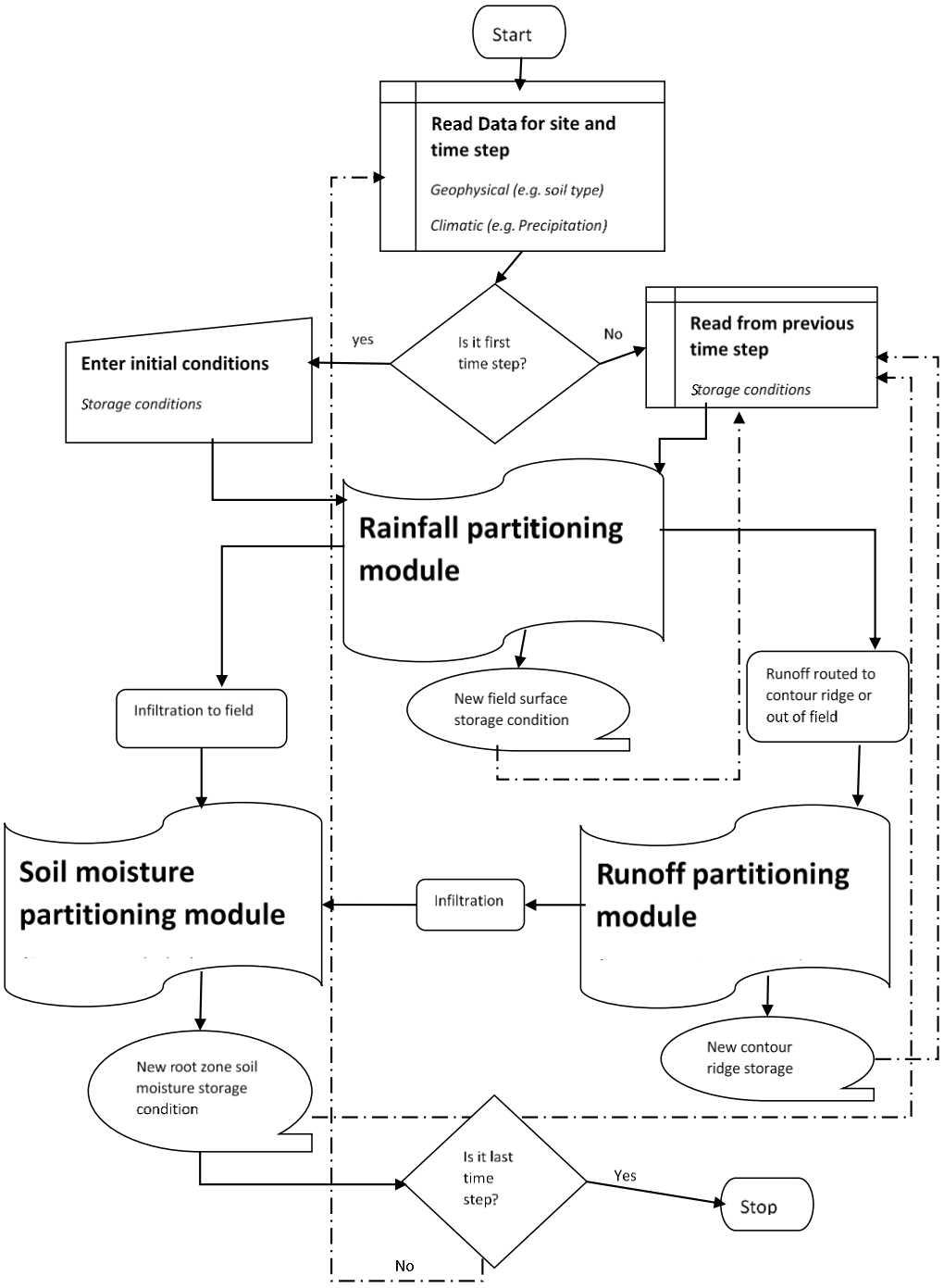

Figure 5-7: Modelling framework for the determination of soil moisture in a contoured field

5.3.2 Mass balance equations and computations for rainfall partitioning in the cropping area sub zone

The mass balance equation and the resultant closure relations required to solve the mass balance equation for rainfall partitioning in the cropping area are shown in Equation 5-1.

$$\frac{\Delta \varsigma}{\Delta t} = e^{rz} + e^{atm} + e^{ada} + e^{crc} \qquad \text{Equation 5-1}$$

Where:

$\Delta\varsigma/\Delta t$ is change in surface storage;
e^{atm} is exchange with atmosphere (precipitation and evaporation). Evaporation is represented by interception which is the water from precipitation that evaporates without taking part in other processes;
e^{ada} is exchange with adjacent subplot surface area (Run-on). Run-on is runoff from the subplot upslope of current subplot;
e^{crc} is exchange with the contour ridge channel (runoff); and
e^{rz} is exchange with the root zone (infiltration into horizon A of the subplot).

At the time scale of one day in which modelling was carried out, and the spatial scale of subplot at which mass balance was done, the change in surface storage of the cropped area was considered as zero. The time scale of one day is long enough to allow substantial infiltration to take place given that the root zone remains unsaturated in this semi arid area. The subplot spatial scale means very little accumulation of surface storage occurs and hence lead to little extra water that need to be infiltrated apart from that which infiltrates during the rainfall period.

Precipitation was measured on site during the study period as daily data. If the model is applied to investigate suitability of a site where site data is not available precipitation data can be obtained from a weather station nearest to the site under investigation. Although the model operated on a daily time step at which precipitation data was obtained runoff generation occurs at a subdaily time scale. Therefore the fuzzy logic method used to compute runoff described in section 5.4 required disaggregation of daily rainfall into a sub-daily time step. The hourly time step was selected and the rainfall input was thus the

mean hourly rainfall intensity (mm/hr) and the equivalent duration (hrs) over which it occurred. The disaggregation method is described in section 5.6.

Evaporation from the cropped surface area was considered to be made up of the rainfall water that is intercepted by crop leaves and stems lumped together with the rainfall water that is retained in surface detention storage. This is the concept of interception that was proposed by DeGroen and Savenije (2006) when they expanded the concept of interception to include all the evaporative fluxes that feed moisture back to the atmosphere from a rainfall event during and shortly after the event. This process is assumed to occur at a time scale of the order of a day. The lower limit of the interception is therefore determined by the amount of rainfall received for the day while the upper limit is determined by the potential evaporation (evaporative demand) of the day. When rainfall stops, interception storage is reduced by evaporation until there is no more storage or until the evaporative demand for the day is achieved. Estimation of interception was therefore based on Equation 5-2 (Makurira, 2009):

$$E_I = \min(P, E_D)$$ Equation 5-2

Where:

E_I (mm/d) is evaporation from interception which is evaporation from the cropped surface;
P (mm/d) is the precipitation measured for the day and
E_D (mm/d) is the evaporative demand.

Runoff from the cropped area was computed using the fuzzy model developed as described in section 5.4. The runoff generated in the cropped area was then used as a major determinant together with the rainfall amount in the water mass balance of the surface of the cropped area to compute the infiltration into the root zone.

Run-on to subplot 1 which is immediately downslope of the contour ridge channel was considered as zero since all runoff originates at the ridge of the upslope contour ridge channel and the contour ridge channel retains all the water unless the contour ridge is overtopped. For the remaining subplots, runoff from the subplot upslope of the one under consideration computed using the fuzzy logic approach was the run-on to the subplot

which is downslope of that under consideration. For example runoff from subplot 1 becomes run-on to subplot 2. The runoff from subplot 3 which is immediately upslope of the contour ridge channel becomes run-on into the contour ridge channel and is the rainwater harvested by the contour ridge channel.

The flux still undefined was then infiltration which was determined as the residual of the mass water balance equation since change in surface storage for the day was assumed to be zero. The infiltration computed by the rainfall partitioning becomes input into the water partitioning of the root zone.

5.3.3 Mass balance equations and computations for runoff partitioning in the contour ridge channel sub zone

The mass balance equation for runoff partitioning in the contour ridge is given by Equation 5-3.

$$\frac{\Delta \check{C}}{\Delta t} = e^{crz} + e^{atm} + e^{ca} + e^{ad} \qquad \text{Equation 5-3}$$

Where:

$\Delta \check{C}/\Delta t$ is change in contour ridge channel storage;
e^{crz} is exchange with channel root zone (infiltration);
e^{atm} is exchange with atmosphere (precipitation and evaporation);
e^{ca} is exchange with cropped area (run-on into contour ridge channel);
e^{ad} is exchange with adjacent area (discharge).

Precipitation was obtained from rainfall data measured on site as in the case with the cropped area for the rainfall partitioning. Open water evaporation was also obtained from site data measured using a standard evaporation pan. Run-on into the contour ridge was obtained using the method discussed in section 5.4 as is the case for rainfall partitioning.

Discharge from the contour ridge was considered to be zero for the dead level contours if the storage level in the channel is below full capacity and for this study no allowance was made for additional water coming from external catchments.

Infiltration was obtained by considering the top soil horizon in the contour ridge channel. The infiltration amount is limited by infiltration capacity of this horizon and the harvested

water stored within the contour ridge channel during the simulation day. If the harvested water is less than the infiltration capacity all the water infiltrates and if it is above the infiltration capacity infiltration takes place at the infiltration capacity rate. The excess water is then carried forward to the next time step as contour ridge storage. The infiltration capacities (Table 5-1) for the two study sites were obtained from the experimental work previously carried on the study site by Dhliwayo (2006) and Ngwenya (2006). These two studies carried out infiltrometer tests on fields in the study area with similar soil texture as for the two fields that were modelled. The capacities given in Table 5-1 are the averages of the loam and sandy soils from the study sites. Infiltration was therefore estimated using Equation 5-4.

$$F = \min(\check{C}, F_c) \qquad \text{Equation 5-4}$$

Where:

F (mm/d) is infiltration,
Č (mm/d) is harvested water stored within the contour ridge channel,
F_c (mm/d) is infiltration capacity for the contour ridge.

Table 5-1: Infiltration capacity of soils at the study site (Source: Dhliwayo, 2006)

Study Site	Soil type	Initial infiltration capacity (mm/hr) (Dhliwayo)	Steady state infiltration capacity (mm/hr)	FAO guideline for Initial infiltration capacity (mm/hr)
Field A	loam	12	0.8	10 - 20
Field B	sandy	35	15	25 - 50

The only unknown remaining from the mass balance equation for runoff partitioning becomes the storage volume in the contour channel at the end of the time step. The, infiltration into the root zone below the contour ridge becomes input into the soil moisture partitioning.

5.3.4 Mass balance equations and computations for the soil moisture partitioning in the root zone subzone

The mass balance equation for the root zone was developed for each subplot as illustrated in Figure 5-8. This figure illustrates how soil moisture was perceived to move

from a contour ridge to a subplot in the area between the ridges. Subplot 2 is used to show all the processes that take place in each of the other subplots (1 and 3) in the cropped area. Subplot 2 receives soil water from subplot 1 and transfers some to subplot 3. Some of the water flows downwards into the boundary layer while some is lost through evapotranspiration. The remaining amount of water is responsible for the change in storage. Water flows from the surface of subplot 2 into the root zone by infiltration and leaves the subplot into the atmosphere by evapotranspiration. If the boundary layer has more moisture than stored in the root zone of subplot 2 then water can flow from horizon boundary layer to the root zone of subplot 2 by capillary rise which is estimated using Equation 5-8. The flow according to Equation 5-8 takes place only if the moisture in the soil profile with higher moisture has moisture above field capacity. Water flow from subplot 3 to subplot 2 can also be possible if subplot 3 has higher moisture content than subplot 2 using the same assumption as that of water flowing from the boundary layer below the root zone to the root zone.

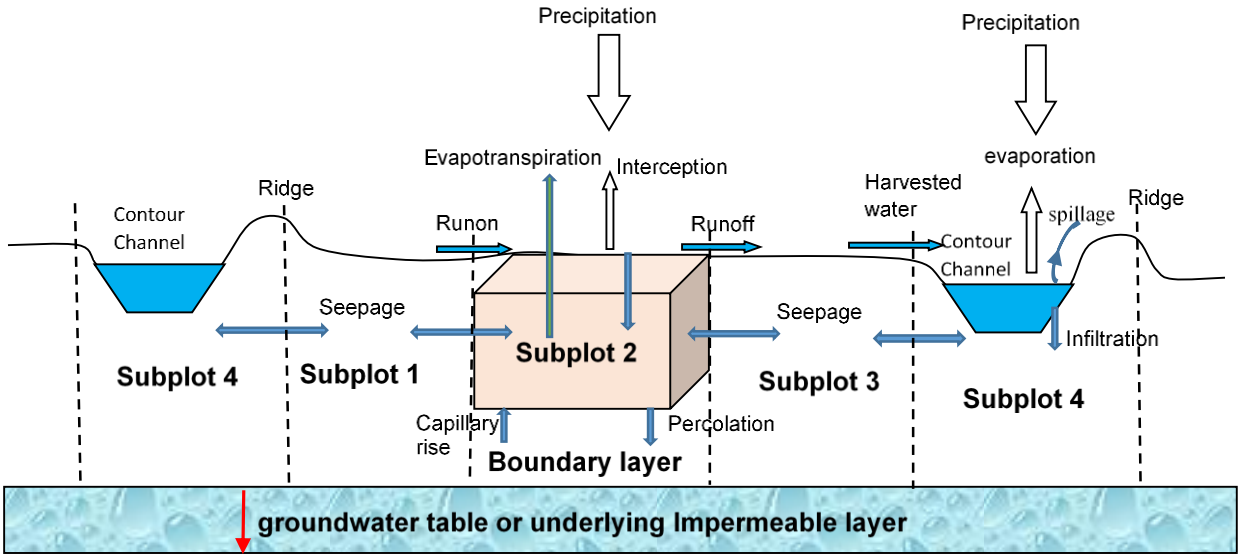

Figure 5-8: An illustration of soil water flow from a contour ridge to a sub plot

The water balance equation governing water movement in each subplot is given in Equation 5-5.

$$\frac{\Delta \boldsymbol{\theta}}{\Delta \boldsymbol{t}} = \boldsymbol{\theta_{m,t}} - \boldsymbol{\theta_{m,t-1}} = \boldsymbol{e^{ca}} + \boldsymbol{e^{atm}} + \boldsymbol{e^{as}} + \boldsymbol{e^{gw}} + \boldsymbol{e^{mp}}$$ Equation 5-5

Where:

$\Delta\theta/\Delta t$ is change in soil moisture during the time step;
$\theta_{m,t}$ is soil moisture in sub plot m at time t (current time);
$\theta_{m,t-1}$is soil moisture in sub plot m at time t-1 (previous time);
e^{ca} is exchange with croped area surface (infiltration);
e^{atm} is exchange with the atmosphere (evapotranspiration);
e^{as} is exchange with adjacent subplot (seepage);
e^{gw} is exchange with groundwater system (percolation);
e^{mp} is exchange with macropore spaces within the same subplot. Water stored within macropores cannot be accounted for when measuring soil moisture as it will be occupying large spaces within the soil structure and not the normal pore spaces. Appendix B shows how macropore storage was estimated in the model.

Infiltration for each time step was computed from the water balance of the rainfall partitioning in the cropped area as discussed previously in section 5.3.2. The evapotranspiration term includes both evaporation from soil and transpiration by the crops and was estimated by considering evaporation and transpiration processes separately in terms of the FAO-56 method as applied by Makurira et al. (2009) and Allen (2000). The transpiration component was estimated by Equation 5-6. Soil moisture fluxes including ET were assumed to be driven by the soil moisture storage levels at the beginning of the time step (which is the storage at end of the previous time step).

$$E_T = T_p f_{mt}$$ Equation 5-6

Where:

E_T is actual transpiration (mm/day);
T_p is potential transpiration when the crop has no moisture shortage and is given by $T_p=k_c\ k_p\ E_o$ where k_c and k_p are crop factor and pan factor respectively and E_o is pan evaporation;
f_{mt} is moisture stress factor which caters for a situation where soil moisture conditions are not sufficient to meet the transpiration needs of the crop. This is expressed as $f_{mt}=k\min((\theta_t-\theta_{wp}),1)$ where θ_t is soil moisture available in the root zone at the simulation time and θ_{wp} is soil moisture at which the crop start to wilt (soil moisture at wilting point) and k defines the proportional reduction to transpiration in the range of soil moisture within which transpiration takes place at a rate reduced by limited available soil moisture (Figure 5-9) and is given by $k=1/\{(1-p)(\theta_{fc}-\theta_{wp})\}$; where θ_{fc} is soil moisture at field capacity and p is soil water depletion fraction and is estimated as 0.6 for maize. The soil water depletion fraction is the fraction of readily available moisture (θ_{ram}) to soil moisture at field capacity (θ_{fc}) above which transpiration continues to occur at the potential rate until θ_{fc}. The soil moisture at field capacity shows the total moisture available to a crop within the soil profile (AM in Figure 5-9). Any soil moisture present in the soil profile above this is subject to drainage to the groundwater system up to saturated soil moisture (θ_{sat}).

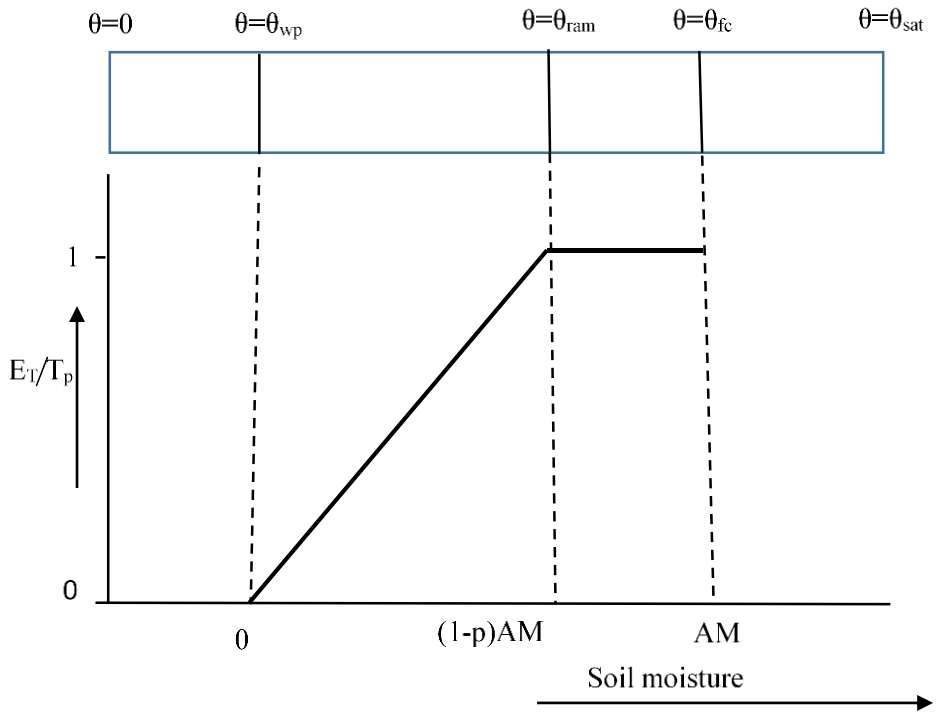

Figure 5-9: Relative evapotranspiration in relation to moisture availability in root zone

The evaporation component was estimated by Equation 5-7 (Makurira et al, 2009).

$$E_s = \max(1 - I_{LA}, 0)\, max\left(k_s k_p E_o - E_I, 0\right) f_{ms} \qquad \text{Equation 5-7}$$

Where:

E_s is soil evaporation (mm/day); I_{LA} is the leaf area index; E_I is evaporation from interception which has an effect of reducing evaporation demand in the atmosphere; k_s is soil evaporation factor (equivalent to crop factor in cropped areas); f_{ms} is moisture stress reduction factor given by $f_{ms}=\min(\exp((\theta_t - \theta_{sat})/b),1)$ where θ_{sat} is maximum soil moisture (which is soil moisture at saturation) in the root zone (mm) and b is a reduction scale (mm).

Makurira et al. (2009) used a reduction scale that was constant regardless of prevailing soil moisture. It was however discovered in this study that the reduction scale was dependent on the prevailing soil moisture. An appropriate formula for determining the

reduction scale was established and the results are given in chapter 7 section 7.2. The other parameters were obtained from literature (Makurira et al., 2009; Allen, 2000).

The vertical and lateral soil moisture fluxes were estimated using Equation 5-8.

$$\Phi_{m,t} = K_s F_z \frac{\partial \theta}{\partial x} \qquad \text{Equation 5-8}$$

Where:

$\Phi_{m,t}$ is soil moisture flux (flow) into or out of subplot m at time t; $\partial\theta/\partial x$ is the soil moisture gradient given by Equation 5-9 and K_s F_z is hydraulic conductivity and diffusivity of the soil.

$$\frac{\partial \theta}{\partial x} = \frac{\theta_{m,t} - \theta_{m+1,t-1}}{\Delta x} \qquad \text{Equation 5-9}$$

Where:

$\theta_{m,t-1}$ and $\theta_{m+1,t-1}$ are the soil moisture in subplot m and m+1 at end of time t and t-1 respectively and Δx is distance between the centre of subplots m_d and m_{d+1}

The hydraulic conductivity and diffusivity component K_s F_z varies with moisture content and depends on whether the subplot is drying or wetting. In order to cater for hysteresis in hydraulic conductivity Mahrt and Pan (1984) proposed a thin layer soil hydrology model in which the hydraulic conductivity of a layer of soil when drying would be based on the soil moisture of the lower layer and when wetting the hydraulic conductivity would be based on the soil moisture of the upper layer. This suggests that hydraulic conductivity and diffusivity is driven by the moisture gradient between two layers where moisture exchange is taking place. This concept was used to derive a representative relationship for the soil at the study site details of which are given in appendix A.

After initial runs of the model, adjustments were made to improve model performance by incorporating macropore spaces in the model. The macropore spaces would absorb more moisture when soil moisture increases above a certain moisture level which was assumed to be field capacity. The influence of macropores in soil moisture are reported by Clothier and Green (1994) who discussed how macro pore networks extending to the surface cause preferential transportation of irrigation water to higher depth resulting in poor

distribution of irrigation water in the rooting depth. During the rainy season Chiroco et al. (2010) suggested that lateral soil moisture redistribution is largely controlled by macro pore structure of the soil. The need to separate macropore storage from soil moisture storage also arises from the fact that soil moisture in the field experiments was measured through access tubes that are installed in the soil matrix therefore representing only the soil water stored in the spaces between soil particles and not water stored in large spaces such as those caused by burrowing animals. Details of the estimation of macropore storage are given in appendix B.

The water that infiltrates into the root zone of a sub plot in the cropped area or into the stratum below the contour ridge is lost from that root zone storage space through percolation to the ground water system, through evapotranspiration and seepage movement to the root zone of adjacent sub plots.

5.3.5 Model preparation, data requirements and operation

The model operates on a daily time step. However rainfall runoff processes at field scale occur at subdaily time scales. These subdaily processes were incorporated and modelled in fuzzy logic by disaggregating daily rainfall data to its equivalent average hourly rainfall intensity and rainfall duration for the day. Details of this disaggregation are given in section 5.6. The time series precipitation data required by the model is therefore in the form of mean daily rainfall intensity (mm/hr) and duration (hr) as well as evaporation data in the form of daily pan evaporation. The model also requires data on the number of time series data points and the planting date is incorporated as a number corresponding to the location of the planting date in the time series. Before the simulation of the first time step the model requires initial soil moisture for all the horizons of the root zone and for this study this was obtained from observed figures at the time when model simulation started. When modelling a site where no observations had been carried out the initial soil moisture can be derived from the expected soil moisture at the time simulation starts. For the subsequent time steps, the model derives the soil moisture required from the soil moisture simulated from the previous time step.

Computation of soil moisture partitioning is carried out in two parts. In the first part the computation considers vertical moisture redistribution while in the second part it considers lateral soil moisture redistribution.

In the vertical direction the soil moisture flux from a top soil horizon (horizon A) to a lower soil horizon (horizon B) is calculated using Equation 5-8 and Equation 5-9 in which $\theta_{m,t}$ is the soil moisture in horizon m (=A) at time t for the subplot and $\theta_{m+1,t-1}$ is the soil moisture in horizon m+1 (=B) at previous time step (t-1) for the same subplot.

The computation for the lateral soil moisture redistribution starts from subplot 1 which is immediately down slope of the contour ridge channel and continues until the upper half of the mid contour subplot. Again Equation 5-8 and Equation 5-9 is used to compute the soil moisture flux. For example when computing soil moisture flux from the contour ridge channel subplot to subplot 1 $\theta_{m,t}$ is the soil moisture in contour ridge subplot (m) at time t for a soil horizon and $\theta_{m+1,t-1}$ is the soil moisture in subplot 1 (m+1) at previous time step (t-1) for the same soil horizon. Similarly when computing soil moisture flux from subplot 1 to subplot 2 $\theta_{m,t}$ is the soil moisture in subplot 1 (m=1) at time t for a soil horizon and $\theta_{m+1,t-1}$ is the soil moisture in subplot 2 (m+1=2) at previous time step (t-1) for the same soil horizon. Subplot 2 is the mid contour subplot assumed to receive the least lateral flow owing to its proximity to the contour ridge channels. When computing lateral soil moisture flux from the contour ridge channel to the upslope subplot (subplot 3) $\theta_{m,t}$ is the soil moisture in the contour ridge subplot (m) at time t for a soil horizon and $\theta_{m+1,t-1}$ is the soil moisture in subplot 3 (m+1) at previous time step (t-1) for the same soil horizon.

5.4 Estimating runoff as an input for overland flow subzone using fuzzy logic

This section describes the development of a fuzzy runoff model applicable at field scale that was used to estimate runoff from the cropped area needed for the mass balance equation of rainfall partitioning discussed in sub section 5.3.2. This model can be used to generate field scale runoff data for other purposes as well.

Modelling of runoff in fuzzy logic at field scale was considered adequately applicable in this study as discussed in Section 3.6. Regression equations developed from different

conditions can be combined to provide a set of equations that can be used for estimating runoff in conditions where they were not developed. Examples of linear and multiple regression runoff models developed from site observations can be seen in Walker and Tsubo (2003a) and in Li *et al.* (2004). Such linear and multiple linear regression equations produced for specific conditions have limited application only to the conditions closely related to where they were developed. Fuzzy logic allows the quantification of the degree to which each of the regression equation is applicable to any condition where the equation was not developed.

The rest of this section presents the factors that were considered in the model development, followed by the description of the data that was used for model development and then the structure of the model is described in two parts. The first part describes the antecedent and the second the consequent component of the model. Lastly the methods used to verify the performance of the model are described.

5.4.1 Factors considered for the development of the field scale fuzzy rainfall runoff model

In developing the field scale fuzzy rainfall runoff model in this study it was assumed that runoff depends mainly on four variables namely rainfall duration, rainfall intensity, soil type and soil moisture conditions. Slope was not included as fuzzy logic modelling is data-based and the data that was available was from comparable slopes ranging from 3% to 5%. Vegetation cover for the experimental plots in Zhuluube was maize crop cover while for the additional dataset from Mutangi the cover was maize and woodland. The effect of the woodland was difficult to isolate and therefore it was assumed all vegetation was maize crop. This limitation may also affect the performance of the model.

In this study, the fuzzy model computes the runoff coefficient from input variables which is then used to compute the generated runoff by multiplying the rainfall amount by the runoff coefficient. The choice to determine a runoff coefficient rather than computing runoff directly from the input variables is favourable because the realistic range of runoff coefficients are not difficult to estimate and the limiting values of the runoff coefficient are also known (0 to 100%). A previous river basin scale rainfall runoff model by Hundecha

et al. (2001) applied a similar approach while Sen and Altunkaynak (2006) used fuzzy logic to compute runoff coefficient for the rational method.

Considering that a fuzzy model constitutes a certain number of partial models each representing a cluster where a data set is likely to fall into, the general partial model for computing runoff coefficient using the selected input variables was of the form of Equation 5-10.

$$q_{j,m} = c_{0,m} + c_{1,m}P_{ij} + c_{2,m}T_j + c_{3,m}\theta_j + c_{4,m}\alpha_{Nj} \qquad \text{Equation 5-10}$$

Where:
$q_{j,m}$ is normalised runoff coefficient (mm) contributed by partial model m during rainfall event j; $P_{i,j}$ is normalised rainfall intensity during rainfall event j (mm); T_j is normalised rainfall duration for rainfall event j (hours); θ_j is normalised root zone soil moisture during event j (mm); α_{Nj} is normalised soil parameter defining soil hydraulic conductivity as shown in Table 5-2 for event j and $c_{0,m}$,$c_{1,m}$, $c_{2,m}$, $c_{3,m}$ and $c_{4,m}$ are coefficients to input variables for cluster m.

Development of a fuzzy model involves two stages. The first stage is establishing the antecedent component of the model which involves determining the number of clusters and their focal points or cluster centres (Jacquin and Shamseldin, 2009). The second stage is the determination of the consequent component of the inference system which involves establishing the coefficient values for each cluster which represent a partial model.

The establishment of the antecedent component can be done through prior knowledge of the system which is used to determine the rules that make up the antecedent component or through determination of the clusters each representing a rule from available data. The earlier approach produces the rule based Mamdan fuzzy inference system (FIS) (Jacquin and Shamseldin, 2009) while the latter is the Takagi-Sugeno (TS) FIS. The cluster centre in the TS fuzzy model is therefore the focal point of the rule. All data points close to it requires that the rule is applied to a varying degree corresponding to the distance of the data point from the rule. The TS was selected for this study since there was no prior knowledge of the system behaviour that could form the basis of the rule base as is the case with the rule based Mamdan fuzzy inference system (FIS). Jassbi et al. (2006) also recommends the use of the Takagi-Sugeno FIS for the multiple input single output (MISO) type of input output type relations. The fuzzy model was typically developed as a MISO input output relation with the input comprising of rainfall intensity and duration, soil

moisture and soil type while the output was runoff. The identification of the TS FIS however requires suitable data to establish the appropriate number of clusters and locate their centres.

5.4.2 Data used for model development

Identification of both the antecedent and consequent components of a TS fuzzy model requires both input and output data that covers a wide spectrum so that all possible conditions are captured. This enables the establishment of an appropriate number of clusters and their centres. This means that the data required should include highly permeable soils and those with very little permeability, very low and very high rainfall intensities, short and long duration rainfall storms and very dry and very wet soils.

It was desirable that as much data as possible be used to improve the establishment of optimum number of clusters and location of their most appropriate centres. However the data needed to be a complete set that included all the variables in the model i.e. observed rainfall intensity, rainfall duration, soil moisture, soil type and runoff. Previous studies that included all these variables were difficult to establish and only data used by Mugabe (2005) in a study in Masvingo Province of Zimbabwe could be obtained. This complemented the data that was collected from the field during this study.

In both cases rainfall was recorded as daily rainfall amount from the rainfall intensity was approximated using the method described in section 5.6.

Data from 52 rainfall events was obtained from data that was collected from events that occurred over a period of 4 years at the two locations and was used for data clustering and for identification of consequent coefficients.

The data was first normalised before being used for identification of both the antecedent and consequent components using Equation 5-11. Data normalisation is important to bring different variables of the data which are in different dimensions to the same coordinate ranges falling within 0 to 1 (Katambara and Ndiritu, 2009). The minimum and maximum values of each variable contained in the data used for model development in this study are presented Table 7-1 in Chapter 7**.**

$$n_{i,k} = \frac{\left(x_{i,k} - x_{min,k}\right)}{\left(x_{max,k} - x_{min,k}\right)}$$ Equation 5-11

Where:
$n_{i,k}$ is normalised value of variable k for data step i; $x_{j,k}$ is data value for variable k at time i while min and max denote minimum and maximum value of variable k in the whole data range.

5.4.3 Identification of the antecedent component

The principle of fuzzy modelling following the Takagi Sugeno-Kang reasoning considers the system being modelled to be composed of multiple linear models each one mapping an input set X falling within a certain subspace of the input variable space into an output variable Y. The subspaces of the input variables X are defined by fuzzy boundaries meaning one set of input variable X may fall in more than one subspace. Each subspace is associated with a rule of the form given in Equation 3-2. That rule is the linear model associated with the subspace and needs to be identified. The identification of the rule involves establishing the centre of a cluster of data points that falls within the subspace of the rule. Thus antecedent component identification involves establishing the number of rules (number of clusters to which the points can be grouped) available for a given data set and establishing their focal points (the centres of the clusters).

Antecedent component identification was achieved through data clustering as detailed by Angelov and Palev, 2004) by identifying the number and location of cluster centres for the data that was available. The identification of cluster centres follows four main steps summarised below (Chiu 1994; Angelov and Palev, 2004; Katambara and Ndiritu, 2009);

i. Establishing the first cluster centre

The potential of a data point to be a cluster centre is measured by its proximity to other data points. A data point with many points close to it has a high potential compared to a data point with less points close to it. The potential of a data point is computed using Equation 5-12. Subtractive clustering starts by assuming that each data point is a potential cluster centre.

$$P_{i1} = \frac{1}{N}\sum_{i=1}^{N}\sum_{k=1}^{q} e^{-\frac{4}{r_a{}^2}\left\|x_{i,k}-x_{i1,k}\right\|^2}$$ Equation 5-12

Where:
$P_{i,1}$ is the potential of data point i to be the first cluster centre; N is the total number of data points; q is the total number of variables; $x_{i,k}$ is the variable k (rainfall intensity or duration, soil type or; moisture or runoff) at data point i which is considered as candidate cluster centre; $x_{i1,k}$ is variable k at the candidate cluster centre data point i1; r_a is a constant defining the radius of the neighbourhood of a data point.

The data point with the highest potential is taken as the first cluster centre and is taken as the reference potential.

ii. Establishing subsequent cluster centres

In order to establish subsequent cluster centres the potential of each data point is reduced by removing the effect of the previous cluster centre as shown in Equation 5-13. The data point that remains with the highest potential is taken as a candidate cluster centre and tested using the criteria described in the next step.

$$P_{i,j+1} = P_{i,j} - P_{cj}e^{-\frac{4}{r_b{}^2}\left\|x_{i,k}-x_{cj,k}\right\|^2}$$ Equation 5-13

Where:
$P_{i,j+1}$ is potential of data point i for candidate cluster centre j+1; $P_{i,j}$ is potential of data point i for cluster centre j; $P_{c,j}$ is cluster centre number j; r_b is a positive constant defining the closeness of cluster centres; $x_{cj,k}$ is the variable k at data point of the previous cluster centre j.

iii. Selection of a data point as a cluster centre

A data point is selected as a cluster centre if its potential falls above an upper threshold ($\bar{\varepsilon}^*$ P_{c1}), which is a function of the reference potential. If a candidate cluster centre is lower than the upper threshold but higher than a lower threshold ($\underline{\varepsilon}^*$ P_{c1}), it is a cluster centre if it satisfies the criteria defined by Equation 5-14.

$$\frac{d_{min}}{r_a} + \frac{P_{cj+1}}{P_{c1}} \geq 1$$ Equation 5-14

Where:
P_{cj+1} is the candidate cluster centre; d_{min} is the distance between candidate cluster centre and all previously established cluster centres.
If it does not, it is rejected as a cluster centre and the data point that remains with the highest potential becomes the next candidate cluster centre.

iv. Termination of the clustering process

The clustering process is terminated when the potential falls below a lower threshold (εP_{c1}) which is a function of the reference potential as shown in Equation 5-15.

$$P_{cj} < \varepsilon P_{c1}$$ Equation 5-15

Where:
ε is the rejection ratio.

5.4.4 Identification of consequent component of the inference system

The identification of the consequent parameters can be regarded as the calibration process of a fuzzy model as it is the establishment of the coefficients of the consequent (the then) part of the model. Consequent parameter identification was carried out using the shuffled complex evolution method, a powerful optimizer developed by Duan et al. (1992). The key features of the shuffled complex evolution (SCE) method are competitive evolution and complex shuffling. In the SCE method a selected number of candidate parameters (coefficients) is sampled from a viable range which constitutes the population of candidate parameters. The population is then divided into subpopulation groups or complexes which evolve independent of each other to form a new generation of complexes. The evolution process is based on replacement of parameters that produces poor function values with newly generated off springs which are generated based on the Nelder-Mead Simplex downhill search scheme (Duan et al., 1994). The evolved complexes are then mixed together and subdivided again into new complexes and the process is repeated until the population parameters converge to an optimum value. A complete description of the SCE method is found in Duan et al. (1992, 1994).

Convergence of the consequent parameters was determined by comparing the values of the parameters in the whole population. Each set of parameters in the population was used to compute its corresponding function value (soil moisture) for each of the data belonging to the cluster. The route mean square error (RMSE) of each parameter set was computed using Equation 5-16. The RMSE values were arranged in ascending order and the average error from the bottom half was compared to the average error from the top half. If the difference between the two errors was below a threshold value of 5% the parameters were considered to have converged. The 5% threshold was selected subjectively.

Objective function: $Minimize\ RMSE = \sqrt{\sum_{j=1}^{n}\left(\theta_{obs_i} - \theta_{sim_i}\right)^2}/n$ Equation 5-16

Where:
RMSE is the root mean square error, θ_{obs_i} and θ_{sim_i} is the observed and simulated soil moisture for data point i within the cluster and n is the number of data points in the cluster.

The SCE method was programmed in python and was run separately for each cluster centre that was established to obtain the set of coefficients for that cluster centre. Initial trial runs indicated that the model could not give realistic values of simulated runoff if some of the input variables lie outside the range of variables used in the calibration process.

5.4.5 Application of the field scale rainfall runoff fuzzy model

After the field scale rainfall runoff fuzzy model structure was determined using the methods described in section 5.4.2 to section 5.4.4 the model was set up. The model could be applied as a stand alone model estimating runoff at field scale for other purposes where data is limited or incorporated in other models. In this study the model was initially applied as a stand alone model in order to test its performance and was then incorporated in the contour ridge model for simulating the effect of contour ridges on soil moisture.

The model structure as represented by cluster centres that form the focal point of the partial models developed in this study using the method described in sub-section 5.4.3 are given in Table 7-2 in chapter 7. The consequent coefficient values needed to complete

the model structure by providing the specification of the partial model as given in the form of Equation 5-10 are given in Table 7-3 in chapter 7.

The model requires input variables for each rainfall event of one day duration. The variables for this model and the units of measurement are mean event rainfall intensity (mm/hr), mean event rainfall duration (hr), soil moisture at start of rainfall event (mm/m) and soil type (dimensionless index). The model works with data for each rainfall event one at a time.

The event data is first normalised using Equation 5-11 and the normalised data applied to compute partial model simulated runoff coefficient for each partial model. Computation of partial model simulated runoff coefficient requires that the degree to which the normalised event data set belongs to a partial model (cluster centre) be calculated using Equation 5-17. During model development the observed runoff was used for computing the degree of membership for each event. However during simulation only the input variables are used in computing the degree of membership as the runoff is an output of the model. The overall degree of membership was calculated using Equation 5-18. The overall degree of memberships provides the total weight of all the cluster centres.

$$\mathrm{DOM_{j,m}} = \exp\left(-\frac{4}{\mathrm{r_a}}\sum_{\mathrm{k=1}}^{\mathrm{P}}\left\|\mathrm{n_{j,k}} - \mathrm{c_{m,k}}\right\|^{\beta}\right) \qquad \text{Equation 5-17}$$

Where:
$\mathrm{DOM_{j,m}}$ is degree of membership of data point j belonging to partial model (cluster) m;$\mathrm{c_{m,k}}$is the normalised value of partial model (cluster centre) m for variable k; β is a constant related to the distribution of the input data; P is the total number of data points; ra is a constant denoting the spread of cluster centres; $\mathrm{n_{j,k}}$ is the normalised value of input variable k at data point j.

The partial output for each cluster centre was calculated using Equation 5-10 in sub section 5.4.1 and then combined using Equation 5-19 to obtain the overall normalised runoff coefficient. The combined model output was finally denormalized to yield the simulated relative runoff using Equation 5-20 and the corresponding runoff determined. Denormalization means converting the simulated normalised runoff coefficient which ranges from 0 to 1 to the actual runoff coefficient whose value ranges from 0% to 100%. This step could be left out in the case of this study where runoff coefficient was being

modelled but is important in the structure of the fuzzy model if runoff was being modelled directly.

$$\mathrm{SumDOM_j} = \sum_{m=1}^{M} \mathrm{Dom_{j,m}} \qquad \text{Equation 5-18}$$

Where: $\mathrm{SumDOM_j}$ is the overall degree of membership for all M clusters. The overall degree of memberships provides the total weight of all the cluster centres.

$$\mathrm{normq_j} = \sum_{m=1}^{M} \left(\mathrm{q_{j,m}} \times \frac{\mathrm{Dom_{t,m}}}{\mathrm{SumDOM_j}} \right) \qquad \text{Equation 5-19}$$

Where:
$\mathrm{normq_j}$ is the normalised runoff coefficient value for the data point j; $\mathrm{q_{j,m}}$ is partial normalised runoff coefficient for data point j computed by sub model m.

$$\mathrm{simq_j} = \mathrm{normq_j} \times \left(\mathrm{c_{max,ruoff}} - \mathrm{c_{min,runoff}} \right) + \mathrm{c_{min,runoff}} \qquad \text{Equation 5-20}$$

Where:
$\mathrm{simq_j}$ is the denormalised simulated runoff coefficient value for data point j; $\mathrm{c_{max,ruoff}}$ and $\mathrm{c_{min,runoff}}$ are the maximum and minimum runoff coefficients values from the data range used for calibration.

The final runoff (gross runoff) was obtained by multiplying the simulated runoff coefficient with rainfall amount.

5.5 Estimation of soil type as input data

The soil type was defined in the form of a soil parameter (α) related to hydraulic conductivity which was proposed by Jaafer et al. (1978) and can be estimated from the soil texture based on the particle size distribution as shown Table 5-2. The value of α is related to particle size distribution by Equation 5-21 and is widely used when estimating soil evaporation during the period when it is dry and evaporation rate becomes a function of hydraulic conductivity of the particular soil (Walker and Ogindo, 2003). Cumulative evaporation during this soil limiting stage is related to α by Equation 5-22 (Walker and Ogindo, 2003; Wallace et al., 1999; Mwendera and Feyen et al., 1997; Jaafer et al., 1978).

$$\propto = 0.374(\%clay) + 0.424(\%silt) + 0.386(\%sand) - 36.8$$ Equation 5-21

$$E_T = \sum_{t=1}^{T} \propto t^{1/2}$$ Equation 5-22

Where:

E_T is cumulative evaporation; α is assumed constant for any particular soil and is a function of soil diffusivity and t is the number of days after the start of evaporation (Walker and Ogindo, 2003; Wallace et al., 1999).

Table 5-2: Variation of hydraulic conductivity related parameter (α) with soil type (Jaafer et al., 1978)

Soil type	Particle size distribution			α
	Clay (%)	Silt (%)	Sandy (%)	
Sandy	4.0	8.7	87.3	1.68
Loam	17.0	31.8	51.2	2.89
Sandy loam	12.9	19.3	67.8	2.41
Silty clay loam	14.3	31.6	54.1	3.53
Silty clay loam	51.8	52.6	15.6	3.27
Silt loam1	27.8	46.6	25.6	3.36
Silt loam2	26.8	58.0	15.2	3.53
Clay loam	27.8	48.8	24.4	3.73
Silt loam3	20.6	59.4	20.0	3.73

5.6 Estimating rainfall intensity from daily rainfall amount

In order to adequately incorporate rainfall-runoff processes that occurred at field scale into the model there was need to establish the rainfall process at a sub daily scale. Rainfall runoff processes at field scale occur at time scales of 1 hour or less depending on the actual time the rainfall took place (Esteves and Lapetite, 2003; Le Bissonnais et al., 1998). Experiments have shown that runoff amount generated by each rainfall event varies with the rainfall intensity (Parsons and Stone, 2006; Li *et al*., 2004). This means that to

correctly represent the rainfall runoff processes at field scale the rainfall intensity and the rainfall duration should be incorporated into the model. Incorporation of rainfall intensity and duration in modelling runoff at field scale was previously done by Li *et al*. (2004) who developed regression equations to estimate runoff at field scale that used rainfall intensity and duration as input variables.

While the model was developed to use rainfall intensity and duration at an hourly time step most rainfall data is obtained as daily totals. This necessitated disaggregating the daily rainfall amounts to their equivalent rainfall intensity and duration per hour. The hourly time scale was selected subjectively considering the difficulty of rainfall disaggregation. It was also considered that even at small time scales such as 10 minutes duration rainfall amounts continue to change within the ten minute interval (McCartney et al., 1998). Hence the hourly interval was considered to be small enough to provide the rainfall characteristics of the day.

The mean rainfall intensity was estimated from given daily rainfall depths and was then used to obtain mean storm duration by dividing daily rainfall depth by the computed mean rainfall intensity. Two methods were used to establish rainfall intensity from daily rainfall amounts. The first method was developed by Knoesen and Smithers (2009) as a modification of the rainfall disaggregation model proposed by Boughton (2000). The other method was based on a modification of the method used by Kusumastuti et al., (2007) which was based on the stochastic rainfall generation model of Sivandran (2002).

There was no data to validate the rainfall intensity obtained using these method and the values of runoff and that of soil moisture obtained from the model were therefore used as the hydrological signature for the acceptability of these methods. Since the values of runoff and soil moisture were found to be within expected range both methods of estimating mean rainfall intensity were considered appropriate and acceptable for this study.

5.6.1 Rainfall disaggregation using random selection based on Boughton disaggregation model

The method developed for South Africa by Knoesen and Smithers (2009) was applied with modification to estimate the mean rainfall intensity which in turn was used to estimate the rainfall duration. The method involves determining the proportion (R) of rainfall that falls in the hour of maximum precipitation. Knoesen and Smithers (2009) determined the values of R from rainfall stations across the whole of South Africa and arranged the values within 20 range bins that were initially developed by Boughton (2000) for Australia as shown in Table 5-3. Sites with average R values falling in range bins with lower values of R generally receive long duration rainfall compared to sites that fall in range bins with higher values of R.

Table 5-3: The Proportion of daily rainfall falling in the hour of maximum precipitation range bins (source: Knoesen and Smithers, 2008)

No.	Range	No.	Range	No.	Range	No.	Range
1	0.0417–0.075	6	0.275–0.325	11	0.525–0.575	16	0.775–0.825
2	0.075–0.125	7	0.325–0.375	12	0.575–0.625	17	0.825–0.875
3	0.125–0.175	8	0.375–0.425	13	0.625–0.675	18	0.875–0.925
4	0.175–0.225	9	0.425–0.475	14	0.675–0.725	19	0.925–0.975
5	0.225–0.275	10	0.475–0.525	15	0.725–0.775	20	0.975–1.000

Knoesen and Smithers (2009) used the values to draw a map of the range bins within which all the areas in South Africa fall. This map was used to select the range bins for the areas falling in the Limpopo River Basins which were assumed to be range bins for the areas on the Zimbabwean side of the Limpopo within which the study area is found. These areas fell within range bin 9 and range bin 11 shown in Table 5-3.

For each rainfall event a value of R was randomly selected from within the range bins 9 to 11. This provided the fraction of rainfall that fell within the hour of maximum precipitation for that event. Once the fraction of daily total rainfall that fell in the hour of maximum precipitation was determined the fraction of daily total rainfall that fell in the

remaining 23 hours was determined by taking into account the remaining fraction of rainfall.

The following example of a daily rainfall amount of 25mm illustrates the disaggregation procedure.

1. The fraction of the 25mm that was received in the hour when maximum rainfall was obtained was randomly sampled from between 0.425 (the lower range of range bin 9) and 0.575 (the upper range of range bin 11).
2. Suppose a value of R=0.512 was selected. The remaining fraction was then 1-0.512 which is 0.488. The fraction of the rainfall falling within the next hour would then be sampled from 0 (as the next hour may have no rainfall) to 0.488 (being the maximum remaining fraction).
3. Suppose also that a value of R=0,456 had been selected instead of 0.512. The remaining fraction would then have been 1-0.456 which is 0.544. The fraction of rainfall falling within the next hour would then be sampled from 0 to 0,456 (as this is the fraction of rainfall falling in the hour of maximum precipitation).
4. Suppose for the second hour a value 0.378 was selected following a selection of 0.512 in the first hour. The cumulative R value becomes 0.89. The remaining maximum fraction of rainfall that can fall in the third hour is then 1-0.89 which is 0.11. Sampling for the third hour would therefore be done from 0 to 0.11. This means that the maximum R value for subsequent sampling hours was obtained by subtracting the cumulative R value from 1 and comparing it with the value of R falling in the hour of maximum precipitation. The minimum of the two values was taken as the maximum value. The minimum value was always considered as zero except for the hour of maximum precipitation as some hours may have zero rainfall. If the sampled value was below 0.0417, which is the R value when the rain falls uniformly for 24 hours, the fraction of that hour was taken as zero and the cumulative fraction for the next hour remained unchanged. If the cumulative fraction reaches 1 sampling ends. Suppose in this example 0.11 was sampled for the third hour then sampling would stop.
5. All the hours that contributed a fraction other than zero were added to come up with the rainfall duration for the event. The daily event rainfall amount was then

divided by the rainfall duration to obtain the mean rainfall intensity. In this example the rainfall duration would be 3 hours and the mean rainfall intensity would be obtained by dividing 25 by 3 giving 8.3mm/hour.

5.6.2 Rainfall disaggregation using an empirical approach

Rainfall intensity is considered to have two parts; one stochastic and the other deterministic (Willems, 2001; Kuczera *et al.*, 2006). Both the stochastic component and the deterministic component were estimated based on a modification of the method used by Kusumastuti *et al.*, (2007) which was based on the stochastic rainfall generation model of Sivandran (2002). The model used by Kusumastuti *et al.*, (2007) generates synthetic rainfall time series data containing discrete rainfall events whose arrival times, durations, average rainfall intensity and within-storm intensity patterns are all random governed by specified probability density functions such as the exponential distribution and a seasonal variation defined by a cosine function of the time of the year (in hours) as a fraction of the total number of hours in a year as shown in Equation 5-23.

$$\delta = \delta_s + \alpha_s cos\left\{\frac{2\pi}{\omega}(\tau - \tau_s)\right\} \qquad \text{Equation 5-23}$$

Where:
δ_s is the seasonally averaged storm duration; τ is the time of year in hours, τ_s is seasonal phase shift which is assumed to be 0; ω is the total number of time units in a year (i.e., ω=8760 hours) and α_s is the amplitude of the seasonal variation of storm duration,

Since storm duration and rainfall amount carries the hydrological signature for storm intensity, it was considered convenient for this study to compute mean rainfall intensity from daily rainfall amount using an exponential function as the probability density function that describes the data observed at the nearest meteorological stations of Bulawayo and Masvingo the results of which is shown in Section 7.2.1.

In order to incorporate seasonal rainfall characteristics it was considered appropriate to include the length of dry days prior to the rainfall event and the average number of dry days in a rainfall season in the cosine function instead of the time of year. Tennant and Hewitson (2002) showed that number of raindays relate to the total rainfall amounts received in South Africa during the summer season. This suggests that the number of dry

days prior to a rain event would also affect the rainfall characteristic of that event. As a result Equation 5-23 was modified by applying it to estimating the rainfall intensity component that is related to the rainfall characteristic related to the timing of the event. The timing of the event was included by considering average number of dry days in a season and the number of dry days prior to the rainfall event as given by Equation 5-24. The amplitude value was determined arbitraly based on field data and to ensure that the all the rain falls within the twenty four hour duration of a day.

$$I_t = \tau cos\left(\pi \frac{(\bar{d} - d)}{\bar{d}}\right)$$ Equation 5-24

Where:
I_t is the estimated mean rainfall intensity component related to timing of the event; d is the number of dry days between previous rain day event and current rain day event; τ is the amplitude of seasonal variation which was taken as 1 for all events with low rainfall amounts less than 36mm/day and -2 for events above 36mm/day; $\bar{d}$ is the average seasonal number of dry days.

The overall mean rainfall intensity for the event was then obtained by adding the two rainfall intensity components estimated by the exponential function (Equation 7-2 in section 7.2.1) and that by Equation 5-24. The contribution of equations 5-24 and 7-2 to estimate rainfall intensities using this method are shown in a time series data in appendix C.

5.7 Model performance and sensitivity analysis

Modelling often requires calibration in order to obtain acceptable performance. Calibration is the process of adjusting certain model parameters in order to improve the match between model outputs and observed measurements. Not all model parameters may require this adjustment as some parameters may not significantly alter model performance after being adjusted. As a result sensitivity analysis is often first carried out to establish which of the model parameters require calibration. Sensitivity analysis involves determining the impact of change in model parameter values to modelling performance. It differs from model calibration as it seeks to establish the parameters that impact on performance significantly while calibration is applied to establish parameter values that maximize performance.

In this study model results were compared to observed soil moisture to assess the performance of the model. The model performance was assessed using three model evaluation measures which are the Nash-Sutcliffe efficiency (NSE), the Percent bias (PBIAS) and coefficient of determination (R^2) details of which can be found in Moriasi et al. (2007). The NSE is a normalized statistic that determines the relative magnitude of the residual variance of the model simulation compared to the measured data variance. It is computed using Equation 5-25. The PBIAS measures the average tendency of the

simulation results being larger or smaller than the observed data and is computed using Equation 5-26. The R^2 is expressed as the squared ratio between the covariance and the multiplied standard deviations of the observed and predicted values as shown in Equation 5-27 (Krause et al., 2005).

$$NSE = 1 - \left[\frac{\sum_{i=1}^{n}\left(Y_{i,obs} - Y_{i,sim}\right)^2}{\sum_{i=1}^{n}(Y_{i.obs} - \overline{Y_{obs}})^2}\right] \qquad \text{Equation 5-25}$$

$$PBIAS = \left[\frac{\sum_{i=1}^{n}\left(Y_{i,obs} - Y_{i,sim}\right) \times (100)}{\sum_{i=1}^{n} Y_{i,obs}}\right] \qquad \text{Equation 5-26}$$

$$R^2 = \left[\frac{\sum_{i=1}^{n}\left(Y_{i,obs} - \overline{Y_{obs}}\right)\left(Y_{i,sim} - \overline{Y_{sim}}\right)}{\sqrt{\sum_{i=1}^{n}\left(Y_{i,obs} - \overline{Y_{obs}}\right)^2}\sqrt{\sum_{i=1}^{n}\left(Y_{i,sim} - \overline{Y_{sim}}\right)^2}}\right]^2 \qquad \text{Equation 5-27}$$

Where:
$Y_{i,obs}$ and $Y_{i,sim}$ are the observed and simulated values for data point I and $\overline{Y_{obs}}$ and $\overline{Y_{sim}}$ are observed and simulated mean values for all the data points.

Model performance evaluation measures are used for both sensitivity analysis and calibration. This is because in sensitivity analysis model parameters are adjusted just like in calibration then assessed to establish which parameter adjustments cause a significant change in model performance. On the other hand calibration requires adjustment to establish the value that maximizes model performance. In general the approach used to select and/or adjust model parmeters depends on computation costs and the parameter space in which the parameter adjustment has an impact on model output (van Griensven et al., 2006; Ndiritu, 2009). Parameters have both local and global impacts on model outputs. Local impacts refer to changes in model output due to variations in certain parameter values e.g. mean or maximum. Global impacts refer to changes in model outputs due to variations in parameter values from the whole possible parameter range.

A hybrid method of selecting the parameter space is often used in which local sampling methods are integrated into global sampling methods to reduce costs but at same time sample parmeters representative of the possible parameter range. Both sensitivity analysis and calibration can be carried out automatically or manually.

Automatic approach to sensitivity analysis or calibration is based on sampling of parameter values from an entire range of possible parameter values and possible parameter sets (van Griensven et al., 2006). In sensitivity analysis the approach is normally used to solve the problem of over parameterisation by identifying parameters that do not have a significant influence on modelling performance. The automatic approach involves sampling of a set of initial model parameters which are then varied using an automatic calibration method such as the shuffled complex evolution method until they convert to global values that optimize the set objective function. The process is repeated several times and each time the final set of parameters is recorded. Parameters that have low sensitivity will have high variation in their values as the process is repeated while those that are highly sensitive will have little variation. An application of automatic calibration approach in sensitivity analysis can be found in Ndiritu (2009). The automatic calibration approach is fast and therefore most suited to models that have a practical application as modellers or researchers will spend less time assessing the parameters that the model is sensitive to for a given application. However automatic model calibration may select parameter sets that do not make hydrological sense. This can be overcome by setting the range within which parameter search is carried out within the limits that are hydrologically meaningful. Another disadvantage of the automatic calibration is the need for an automatic calibrator such as the shuffled complex evolution method to be either incorporated in the model software or in a software that is compatible with the model software. Global sensitivity analyses such as those used in automatic modelling are not yet common in vadose zone modeling because they are difficult to implement (Skaggs et al., 2014).

The manual approach to sensitivity analysis modify selected input parameters while holding all other parameters constant (Hoyos and Cavalcante, 2015; Kumar et al., 2014). The values of modified input parameters are varied above and below those of the model determining the performance of the model in each case. If the change in model

performance corresponding to changes in a specific input parameter is large then the model is sensitive to the value of that input parameter and therefore that input parameter should be accurately estimated in order to reduce uncertainty in the modelling. On the other hand if the change in model performance is low when the value of the input parameter is changed then the model has low sensitivity to that input parameter. Manual model calibration is widely used for sensitivity analysis because of its simplicity.

Model sensitivity was carried out to establish input model parameters that require accurate estimation (calibration) in order to reduce uncertainty in the model output. The PBIAS was used as a model performance measure to assess the sensitivity of the model to variations in different parameters. For this study manual calibration approaches were therefore selected for their simplist. The model parameters were varied by increasing and decreasing them by 10%, 20% and 30% above and below that of the model parameters. Each time the model was run and the model performance in terms of the PBIAS was computed and was used to assess the sensitivity of the model. The sensitivity of the different parameters to model predictions was compared using the condition number which expresses the rate of change of the dependent variable with respect to the rate of change in the independent variables (Hoyos and Cavalcante, 2015). The condition number was calculated using Equation 5-28.

$$CN_p = \frac{\bar{p}}{D}\frac{\Delta D}{\Delta p} \qquad \text{Equation 5-28}$$

Where:
CN_p is the condition number for parameter p; $\bar{p}$ is the mean of the parameter p considered; ΔD is the change in the predictant D.

The model performance (PBIAS) each time the parameter value was changed was used to represent the predictant for calculation of the corresponding CN. To compare the sensitivity of the different parameters the difference between the highest and smallest CN was used as measure of the sensitivity with the parameter having a higher difference considered as being more sensitive.

6 FIELD ASSESSMENT OF WATER CONSERVATION THROUGH DEAD LEVEL CONTOUR RIDGES

This chapter presents results of field experimentation described in Section 4.3 to 4.4 on assessment of soil moisture and crop yield in fields where contour ridges were used for water conservation. The characteristics of the rainfall seasons during the study period are presented and discussed. This is followed by soil moisture assessment in which soil moisture variation across the fields of two different soil types were assessed in relation to the rainfall characteristics and comparison between treatments of dead level contours and graded contours for the two different soil types were made. The seasonal cumulative soil moisture in plots with different treatments of dead level contours and those with graded contours for the two different soil types are also compared. Finally, the results on the assessment of effect of contour ridges on the crop growth and yield are presented.

Comparison within treatments for both soil moisture and crop yield was done on different subplots defined by relative location to the contour ridge channel as shown in Figure 6-1. Subplot 2 is the area furthest from the contour ridges and was therefore assumed to have the least influence from the ridges as observed by Mugabe (2004). The study by Mugabe (2004) showed that soil moisture decreased away from contour ridges with infiltration pits. Within treatment comparison of the soil moisture at various locations away from the contour ridge was made by comparing the soil moisture of each subplot with that of mid contour subplot (subplot 2). As mentioned in section 4.5 comparison was done by carrying out a t-test at 95% confidence level. The data points for each test of significance ranged from a minimum of 12 to 24.

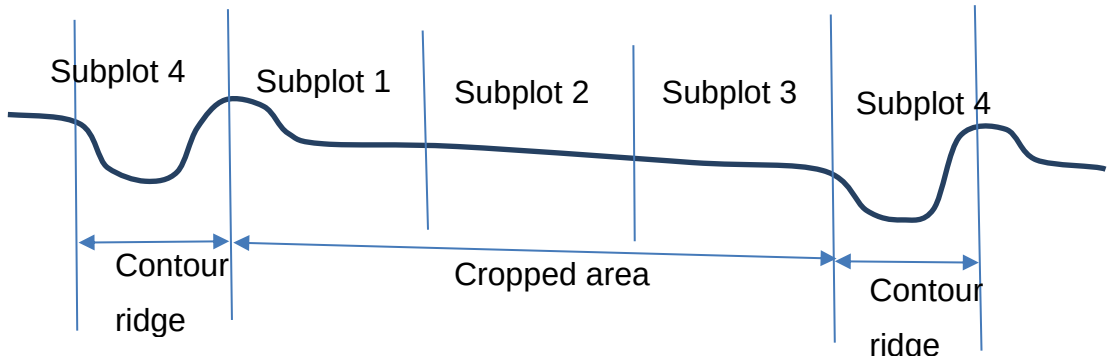

Figure 6-1: Location of subplots relative to contour ridge channel

6.1 Seasonal rainfall characteristics

Table 6-1 shows the rainfall amount received together with the rainfall characteristics during the three years of data collection from Nov 2008 to May 2011 rainfall year. The year 2008 to 2009 received good rainfall amount of 607mm compared to the long term average of 540mm while the years 2009 to 2010 and 2010 to 2011 received low rainfall amounts of 503mm and 512mm respectively.

All the seasons experienced long dry spells lasting 21 days or more. The dry spells received during the 2008/9 season had little effect on crop growth. The first dry spell lasted from 24 November 2008 to 23 December 2008. For farmers who had planted the crop water requirements were still small while some farmers had not planted yet when this dry spell was experienced. The second occurred from 01 April 2009 to 03 May 2009. This was when most crops had matured. During the crop growing period in the 2009/10 season two long dry spells occurred. The first was from 13 December 2009 to 4 January 2010 and the second from 6 January 2010 to 18 February 2010 with some small rainfall events with a total rainfall amount of 25mm received during the period 27 to 30 January 2010. In the 2010/11 season between planting and harvesting two mid-season dry spells were experienced. The first was a short one lasting 13 days from 18 December 2010 to

1 January 2011. The second was long lasting 30 days from 25 January 2011 to 24 February 2011 and this destroyed crops in the area.

Table 6-1: Rainfall amount and dry spell characteristics during the data collection period

Rainfall Year	Seasonal rainfall (mm)	No. of 7 day Dry Spells	No. of 10 day Dry Spells	No. of 14 day Dry Spells	No. of 21 day Dry Spells
2008 to 2009	607	8	5	3	2
2009 to 2010	503	10	8	4	2
2010 to 2011	512	7	5	3	3

The year 2009/10 that received the least seasonal rainfall amount also had the most frequent dry spells lasting seven, ten and fourteen days or longer. This season also had the least rainfall amount during the critical month of January (Figure 6-2) but had more rainfall received later in the season (March, April and May) compared to the other two seasons.

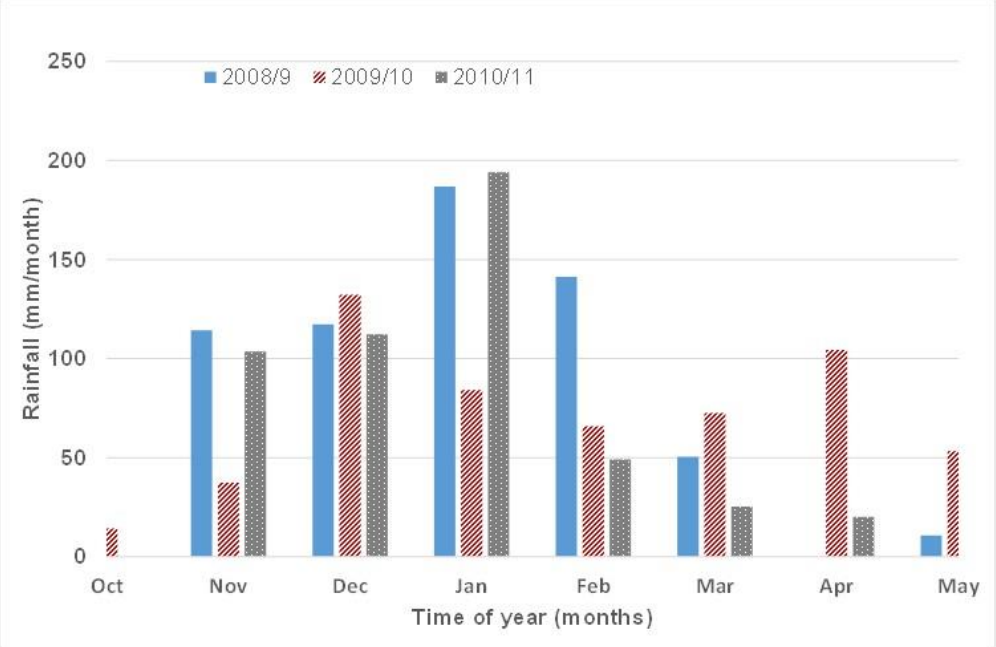

Figure 6-2: Intraseasonal rainfall variability during the study period

6.2 Assessment of soil moisture conservation by dead level contour (DLC) and standard graded contour (GC)

Statistical comparison for actual soil moisture was carried out on data measured on the same date while for time series soil moisture data statistical comparison was carried out on cumulative soil moisture storage as represented by soil moisture storage index. Comparisons were first carried out within treatments and then between treatments for each soil type.

6.2.1 Variation of soil moisture across a loam soil field with contour ridges (field A)

Graphs of soil moisture variation in the soil horizons for different subplots of the loam soil for field A described in chapter 4 section 4.3 and subplots positions shown in Figure 6-1 are shown in Figure 6-3 (a) - (c) (DLC) for the dead level contour, Figure 6-5 (a) - (c) (NC) for the no contour and Figure 6-7(a) - (c) (GC) for the standard graded contour treatments. The soil moisture for each of the treatment is the average of all the subplots of that treatment i.e. from the upper, the middle and the lower subplot.

The DLC treatment subplot 4 which is along the contour ridge channel has the highest soil moisture for the top two horizons (Horizon A and B) to a depth of 400mm while subplot 2 representing the middle portion of the treatment has the lowest soil moisture. After a prolonged dry spell it was only the subplot immediately upslope of the contour ridge (subplot 3) that showed soil moisture significantly higher than the mid contour subplot and only in horizon C ($p=0.014$). The soil moisture after receiving high rainfall amount showed that subplot 3 had a weaker significantly higher soil moisture than the mid contour subplot in horizon C ($p=0.034$). The soil moisture of subplot 3 for horizon A and B was not significantly higher than the mid contour subplot ($p>0.5$) (see appendix C). In addition all the other subplots had their soil moisture not significantly higher than the mid contour subplots in all horizons both after receiving high rainfall amounts and after a dry spell ($p>0.5$).

Subplot 3 which is the area upslope of the contour ridge indicates the highest soil moisture for the area between contour ridge channels which suggest that the mechanism that influenced the soil moisture is largely the damming effect than subsurface flow. Figure

6-4 shows that when the contour ridge was full, some runoff water would be held back by the ridge within the cropped area and infiltrate there explaining the higher levels of moisture for subplot 3.

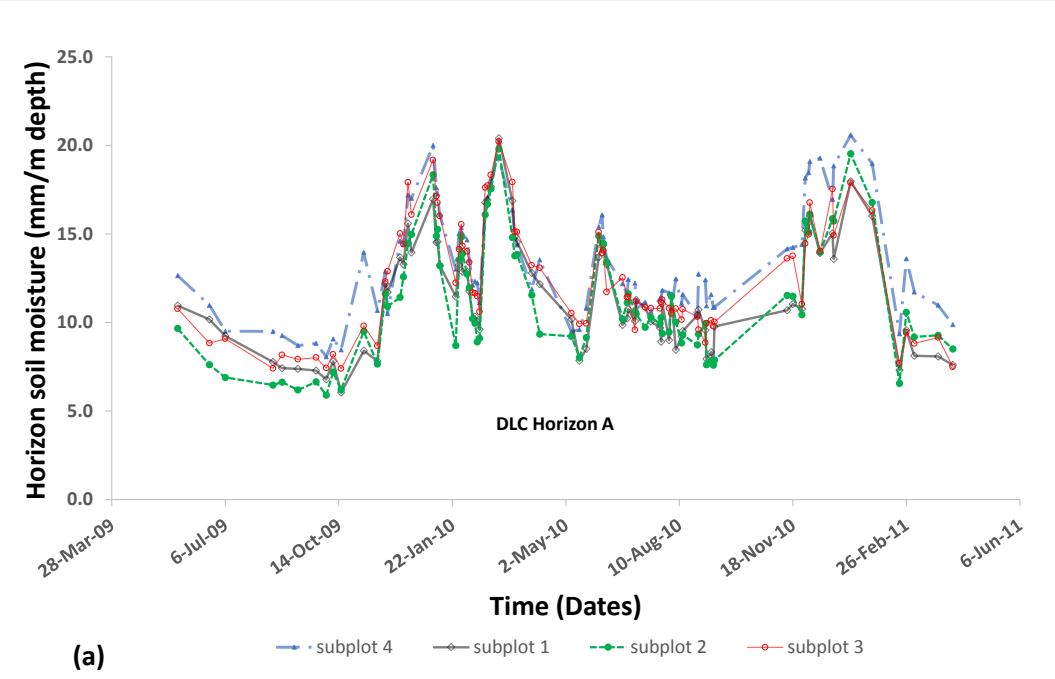

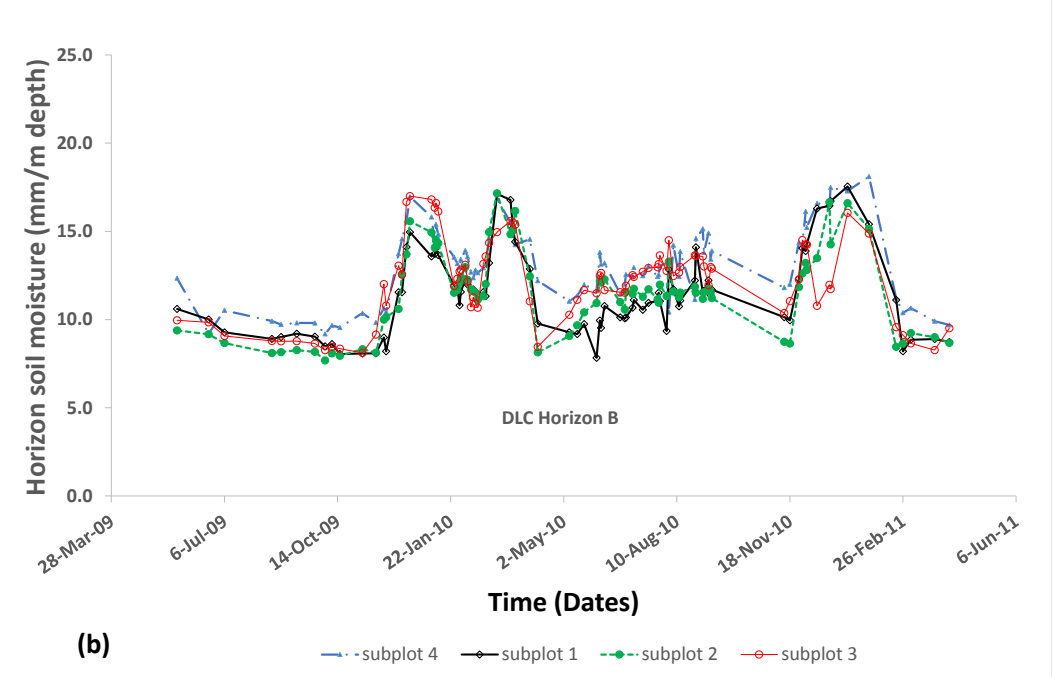

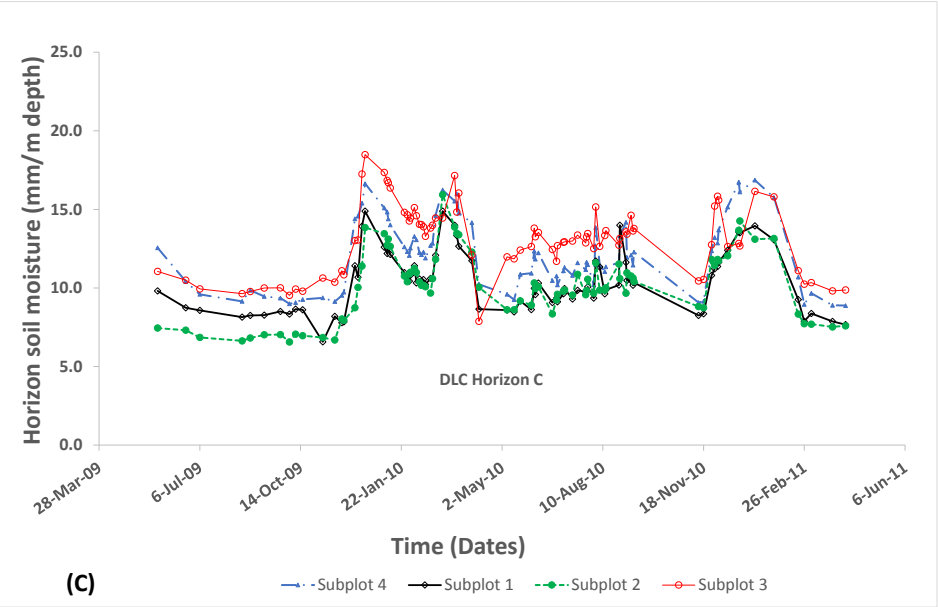

Figure 6-3: Subplots variation of soil moisture for the DLC plots in field A

Figure 6-4: A picture of DLC full of harvested water in field A. *(Photo taken before access tubes were installed).*

The NC plots show that the soil moisture in the subplot corresponding to the contour ridge subplot (subplot 4) was significantly higher than the subplot corresponding to the mid contour subplot (subplot 2) for horizon C ($p<0.05$) (Figure 6-5). The subplot corresponding

to the subplot immediately downslope of contour ridge (subplot 1) in horizon C and the subplot corresponding to the subplot immediately upslope of the contour ridge in horizon B had their soil moisture significantly less than the mid contour subplot ($p<0.05$). Given the experimental design in which the NC treatment was located close to the DLC treatment (Figure 6-6) it is possible that the higher soil moisture experienced in the subplot corresponding to the contour ridge could have been due to infiltration of water from the DLC ridges. It was also evident that during ploughing the farmers would leave the subplot corresponding to the contour ridges unploughed.

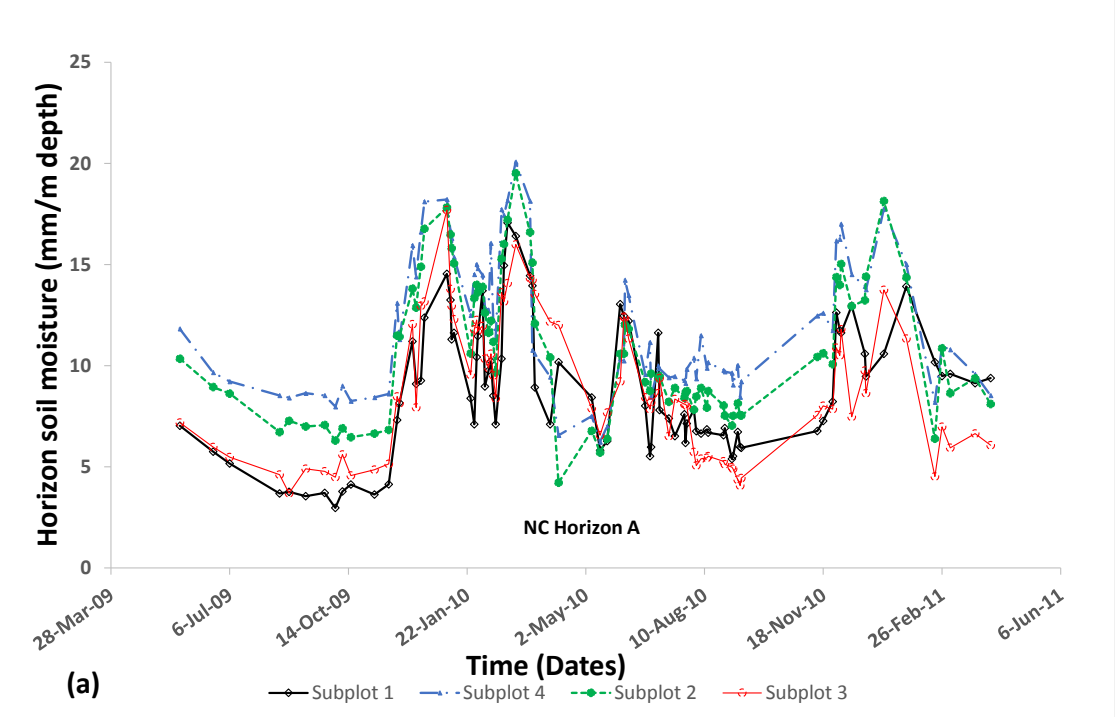

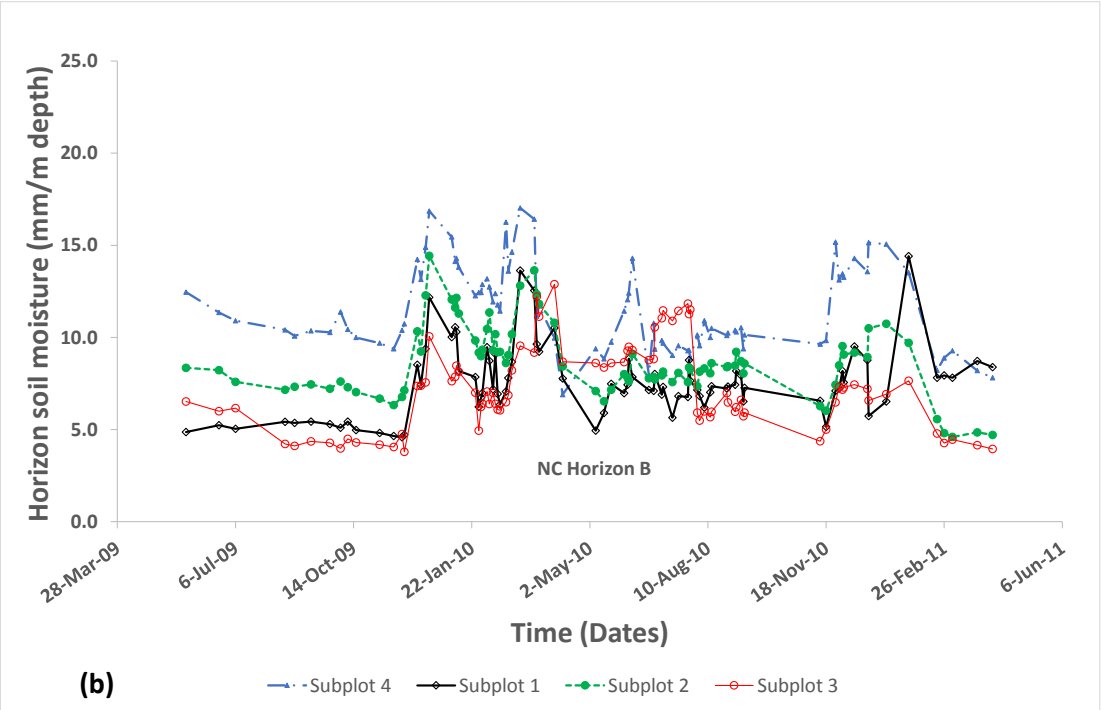

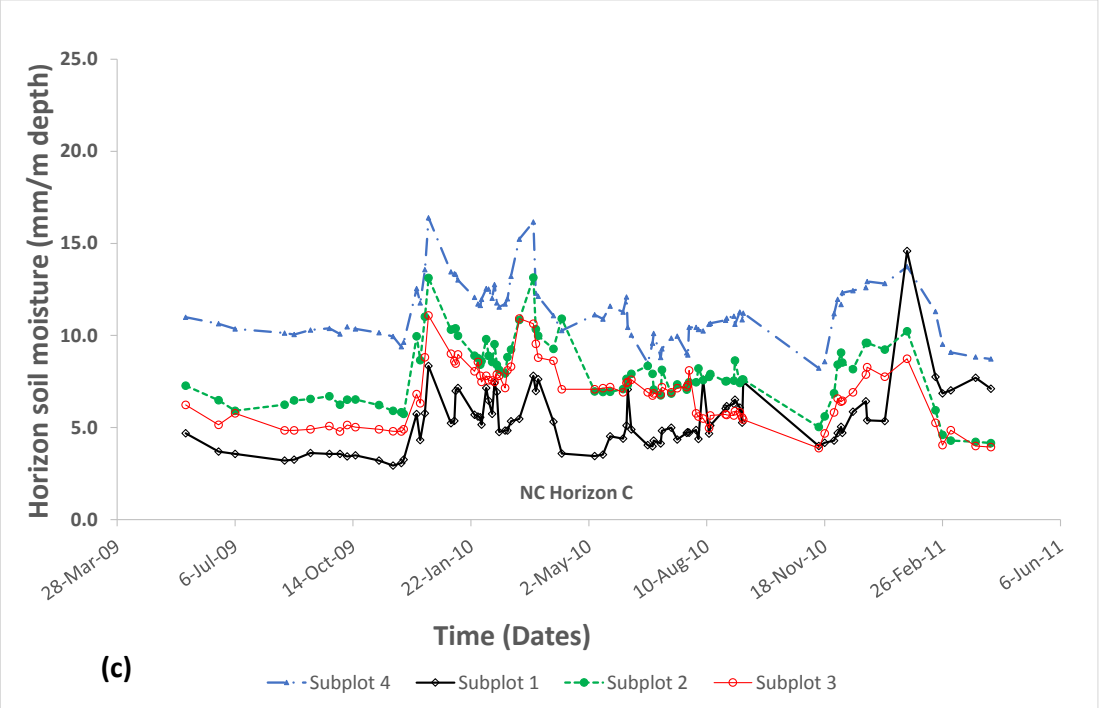

Figure 6-5: Subplots variation of soil moisture for the NC plots in field A

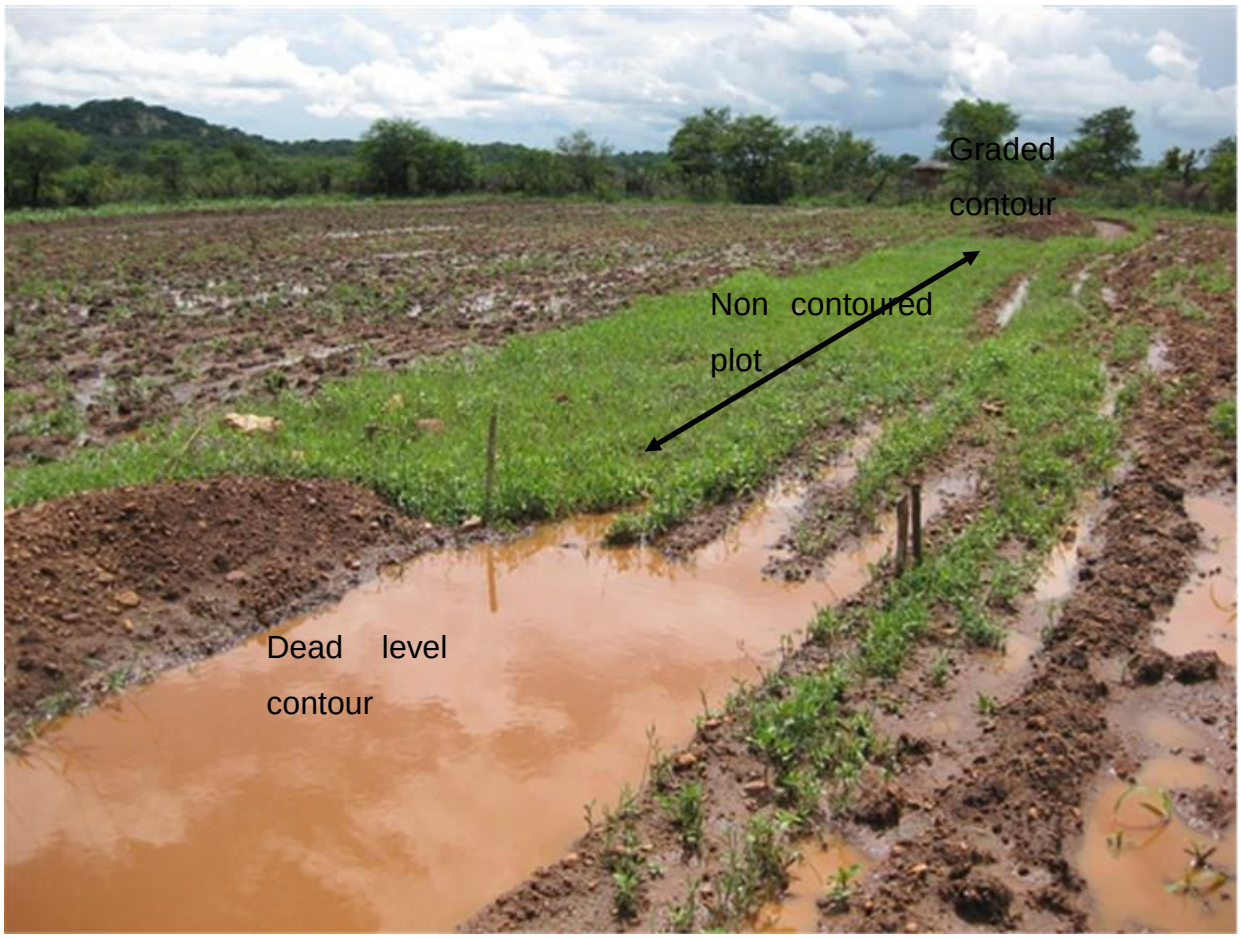

Figure 6-6: Proximity of non contoured plot (green grass) to the dead level contour plot (with water) and the graded contoured plot (with no water further up) in field A. *(Photo taken before access tubes were installed)*

In the GC plots subplot 3 distinctly has the worst soil moisture when compared to the rest of the subplots (Figure 6-7). When compared to the mid contour subplot (subplot 2) the contour ridge subplot (subplot 4) soil moisture for horizon A and that of the subplot immediately upslope of contour ridge (subplot 3) for horizon B and C were significantly lower than the mid contour subplot ($p<0.05$). This suggests the effect of draining water away by the graded contour ridge has a significant influence on the low moisture levels.

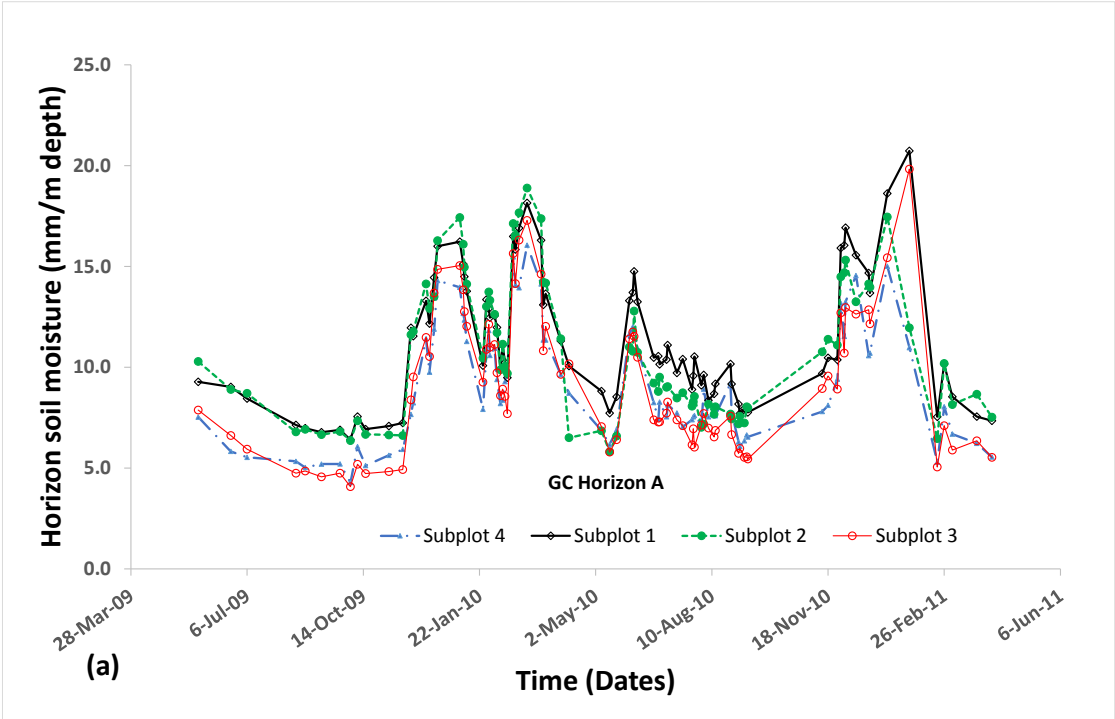
Horizon soil moisture (mm/m depth)
25.0
20.0
15.0
10.0
5.0
0.0
GC Horizon A
Subplot 4
Subplot 1
Subplot 2
Subplot 3
28-Mar-09
6-Jul-09
14-Oct-09
22-Jan-10
2-May-10
10-Aug-10
18-Nov-10
26-Feb-11
6-Jun-11
(a)
Time (Dates)

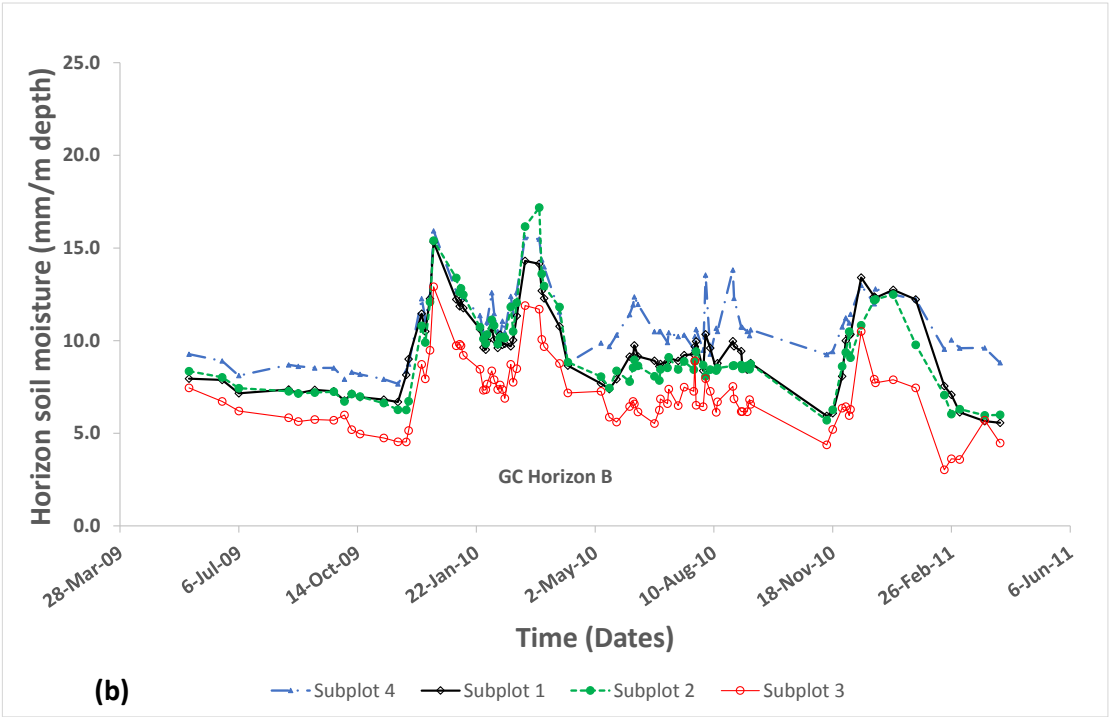
Horizon soil moisture (mm/m depth)
25.0
20.0
15.0
10.0
5.0
0.0
GC Horizon B
28-Mar-09
6-Jul-09
14-Oct-09
22-Jan-10
2-May-10
10-Aug-10
18-Nov-10
26-Feb-11
6-Jun-11
Time (Dates)
(b)
Subplot 4
Subplot 1
Subplot 2
Subplot 3

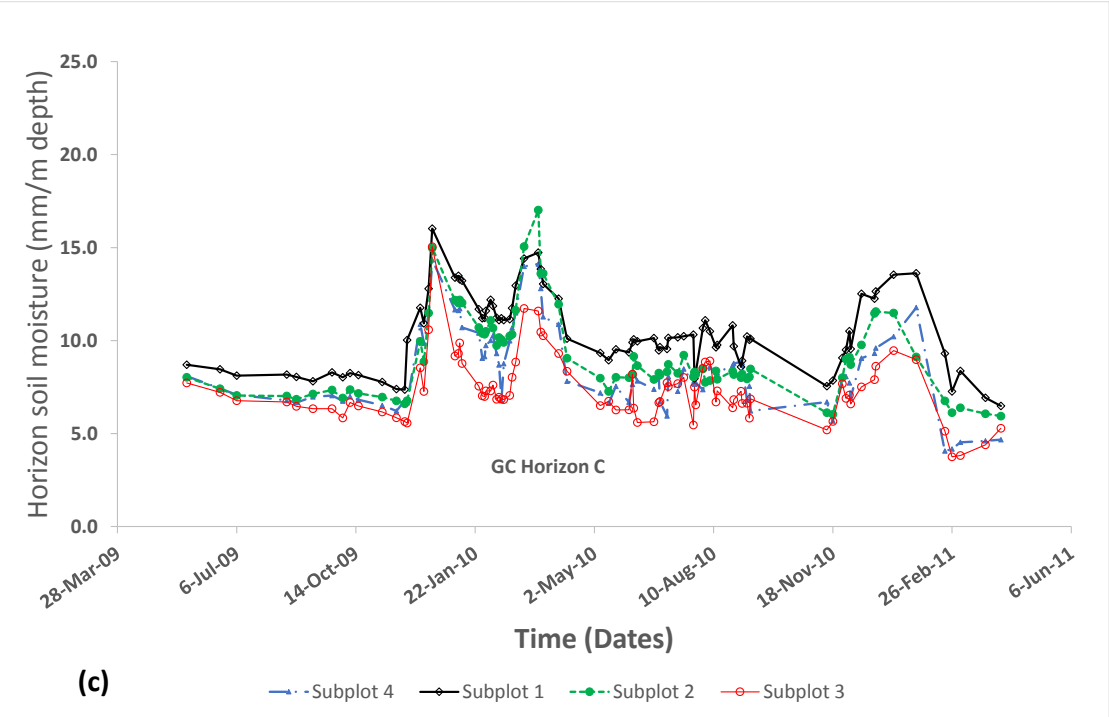

Figure 6-7: Subplots variation of soil moisture for the GC plots in field A

6.2.2 Variation of soil moisture across a sandy soil field with contour ridges (field B)

Field B with a sandy soil shows different soil moisture variation from field A. The soil moisture in all the subplots of field B is generally the same and there is no subplot that is distinctly higher or lower than the others in all the three treatments and throughout all the three soil horizons (Figure 6-8).

After a dry spell that occurred from the soil moisture in all subplots in the DLC treatment was not significantly different from soil moisture in the mid contour subplot for horizon A and horizon C ($p>0.05$). It was only in horizon B that soil moisture in the subplots immediately downslope (subplot 1) and upslope of the contour ridge (subplot 3) that soil moisture was significantly different from that in the mid contour subplot ($p<0.05$). After receiving large amount of rainfall the soil moisture was only significantly lower ($p<0.05$) than the mid contour subplot soil moisture for horizon B in the subplot immediately above the contour ridge (subplot 3). In all the other subplots the soil moisture was statistically similar to that in the mid contour subplot ($p>0.05$).

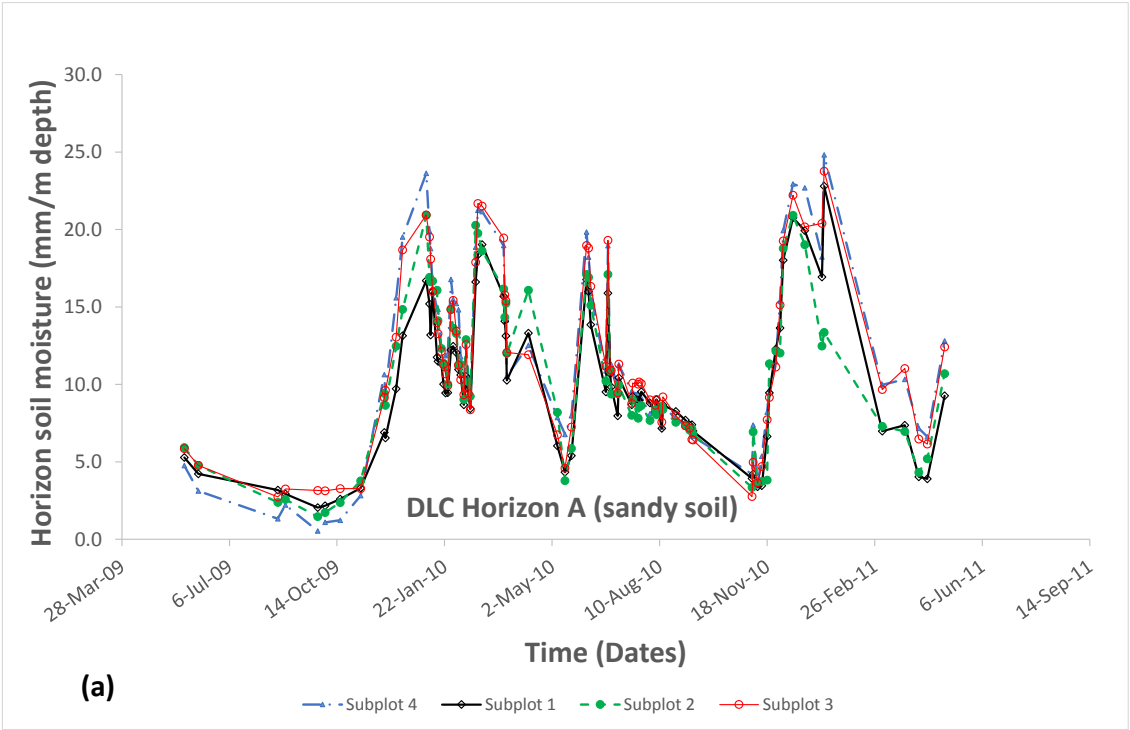
Horizon soil moisture (mm/m depth)
30.0
25.0
20.0
15.0
10.0
5.0
0.0
DLC Horizon A (sandy soil)
28-Mar-09
6-Jul-09
14-Oct-09
22-Jan-10
2-May-10
10-Aug-10
18-Nov-10
26-Feb-11
6-Jun-11
14-Sep-11
Time (Dates)
(a)
Subplot 4
Subplot 1
Subplot 2
Subplot 3

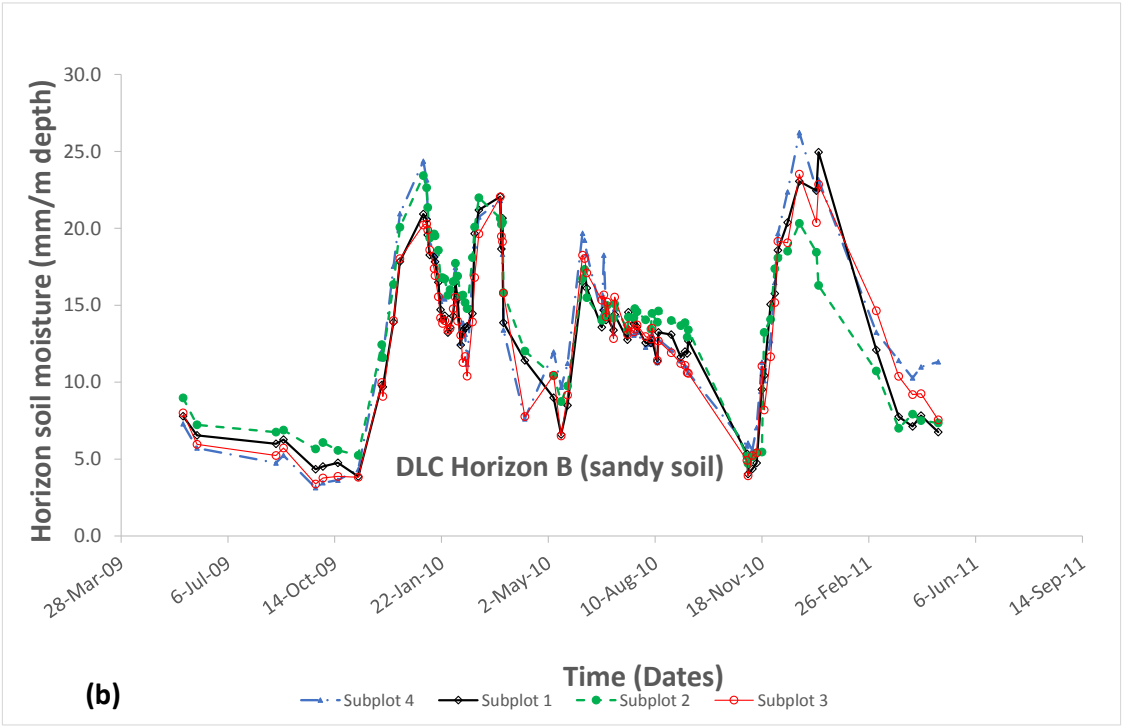
Horizon soil moisture (mm/m depth)
30.0
25.0
20.0
15.0
10.0
5.0
0.0
DLC Horizon B (sandy soil)
28-Mar-09
6-Jul-09
14-Oct-09
22-Jan-10
2-May-10
10-Aug-10
18-Nov-10
26-Feb-11
6-Jun-11
14-Sep-11
Time (Dates)
(b)
Subplot 4
Subplot 1
Subplot 2
Subplot 3

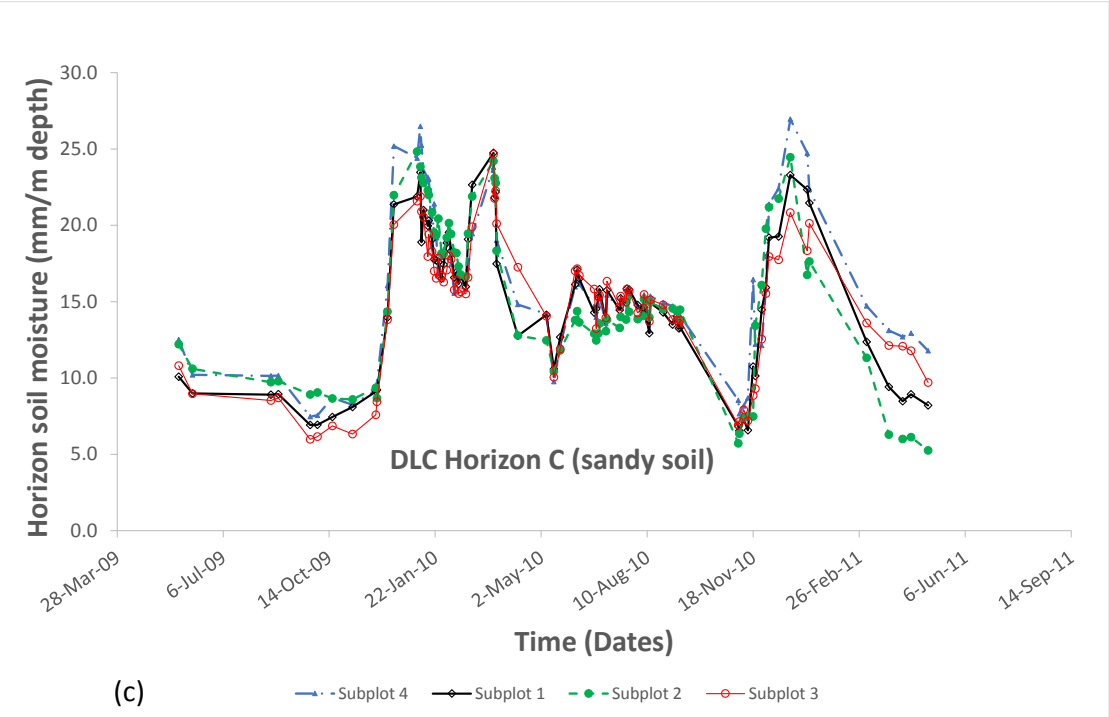

Figure 6-8: Subplots variation of soil moisture for the DLC plots in field B

After a dry spell the soil moisture in all subplots of NC plots (Figure 6-9 (a) and (b)) was also not significantly different from the corresponding mid contour subplot for horizon A and B. However in horizon C, soil moisture (Figure 6-9 (c)) for the corresponding subplots to those immediately upslope (subplot 3) and downslope (subplot 1) of the contour ridges were significantly higher than the mid contour subplot. After receiving large amounts of rainfall the soil moisture was significantly higher than the mid contour subplot in the subplots corresponding to the areas immediately upslope (subplot 3) and downslope (subplot 1) of the contour ridges and only for horizon C.

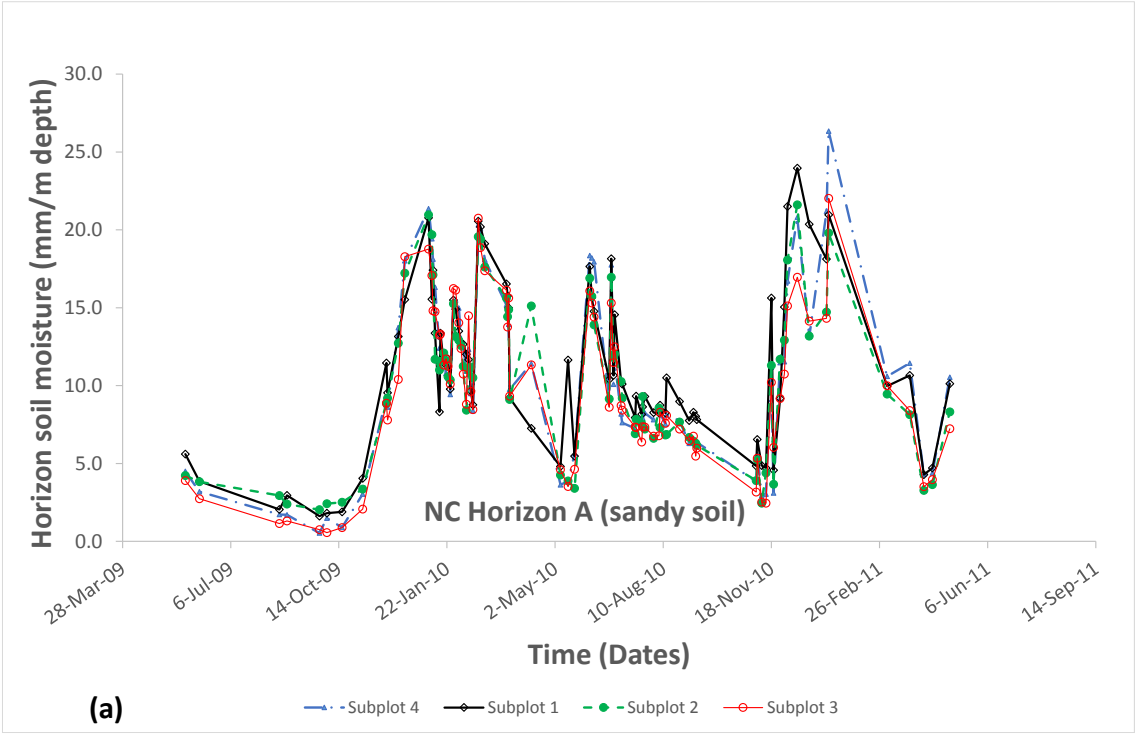
Horizon soil moisture (mm/m depth)
30.0
25.0
20.0
15.0
10.0
5.0
0.0
NC Horizon A (sandy soil)
28-Mar-09
6-Jul-09
14-Oct-09
22-Jan-10
2-May-10
10-Aug-10
18-Nov-10
26-Feb-11
6-Jun-11
14-Sep-11
Time (Dates)
Subplot 4
Subplot 1
Subplot 2
Subplot 3

(a)

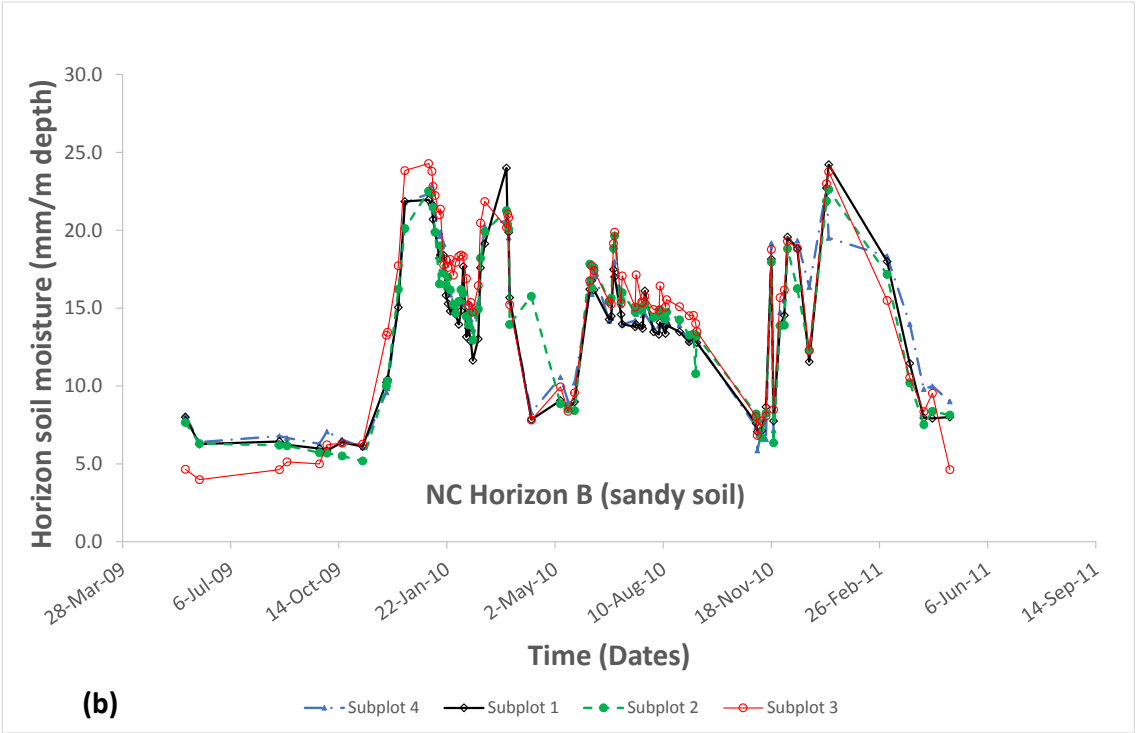
Horizon soil moisture (mm/m depth)
30.0
25.0
20.0
15.0
10.0
5.0
0.0
NC Horizon B (sandy soil)
28-Mar-09
6-Jul-09
14-Oct-09
22-Jan-10
2-May-10
10-Aug-10
18-Nov-10
26-Feb-11
6-Jun-11
14-Sep-11
Time (Dates)
Subplot 4
Subplot 1
Subplot 2
Subplot 3

(b)

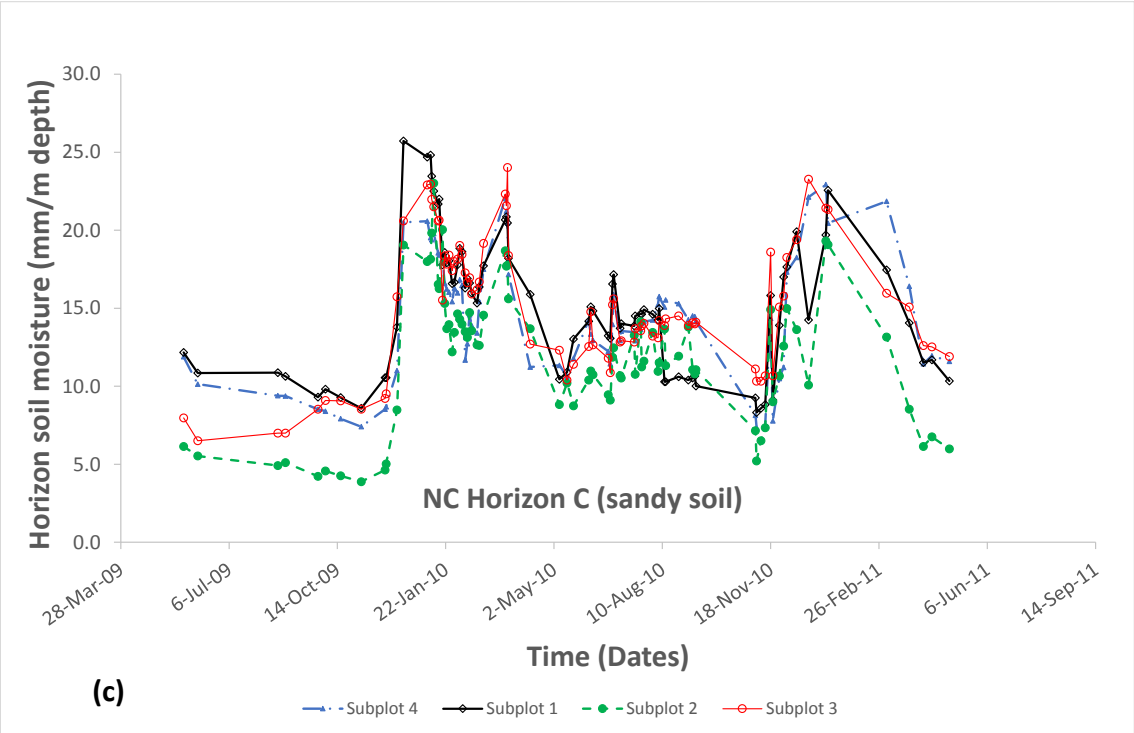

Figure 6-9: Subplots variation of soil moisture for the NC treatment in field B

In the graded contour treatment the contour ridge channel (subplot 4) had soil moisture that is significantly lower than that of the mid contour ridge in horizon B and C. The subplot immediately upslope of the contour ridge channel (subplot 3) had its soil moisture significantly lower than the mid contour subplot only in horizon B. All the other horizons had no significant difference in soil moisture with the mid contour subplot. Figure 6-10 shows the variation of soil moisture in the three horizons.

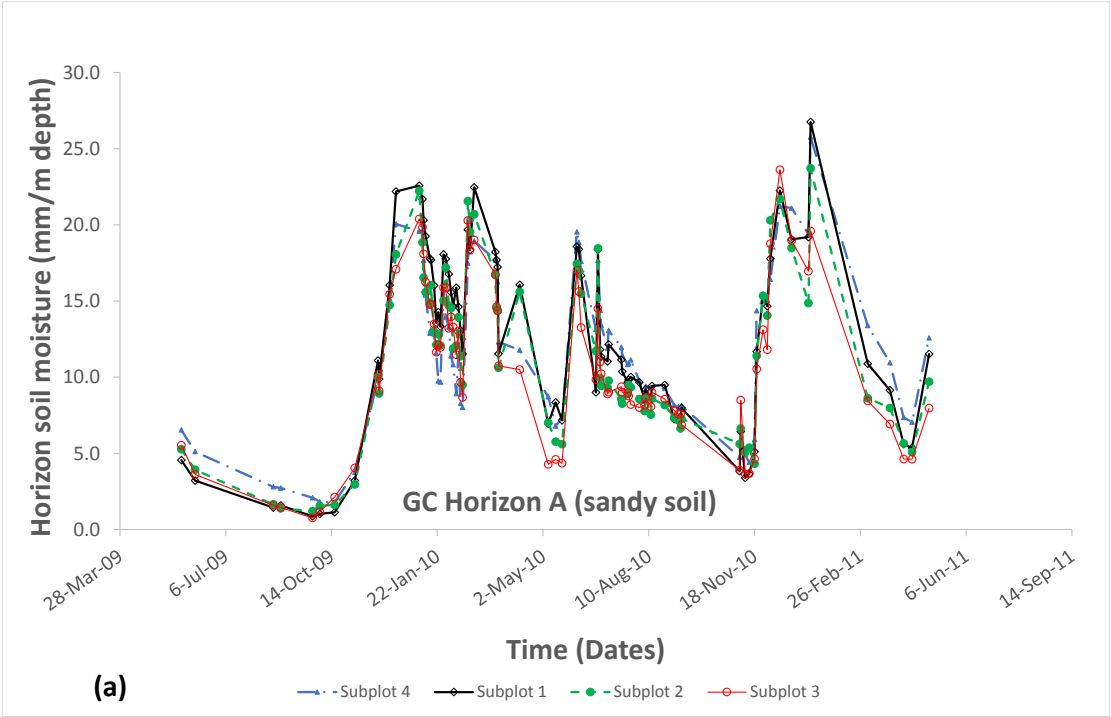
Horizon soil moisture (mm/m depth)
30.0
25.0
20.0
15.0
10.0
5.0
0.0
GC Horizon A (sandy soil)
28-Mar-09
6-Jul-09
14-Oct-09
22-Jan-10
2-May-10
10-Aug-10
18-Nov-10
26-Feb-11
6-Jun-11
14-Sep-11
Time (Dates)
Subplot 4
Subplot 1
Subplot 2
Subplot 3

(a)

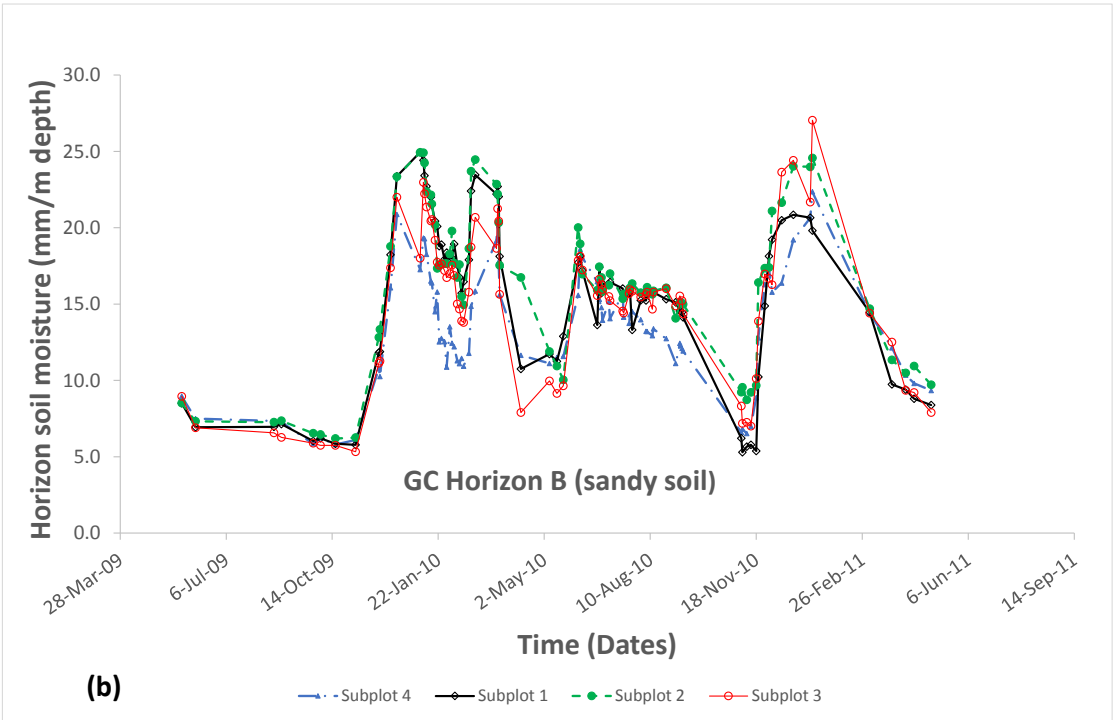
Horizon soil moisture (mm/m depth)
30.0
25.0
20.0
15.0
10.0
5.0
0.0
GC Horizon B (sandy soil)
28-Mar-09
6-Jul-09
14-Oct-09
22-Jan-10
2-May-10
10-Aug-10
18-Nov-10
26-Feb-11
6-Jun-11
14-Sep-11
Time (Dates)
Subplot 4
Subplot 1
Subplot 2
Subplot 3

(b)

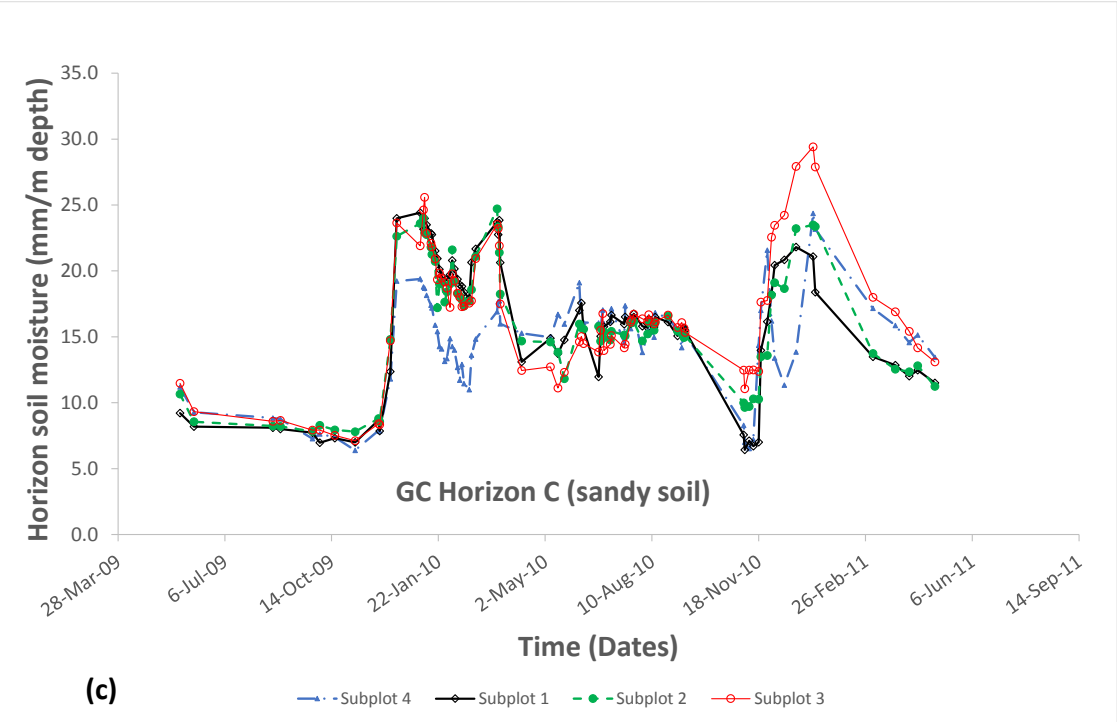

Figure 6-10: Subplots variation of soil moisture for the GC plots in field B

6.2.3 Comparison of soil moisture conservation between treatments for a loam soil (Field A)

Figure 6-11 shows the average soil moisture for all the subplots in the three treatments for field A. DLC plots showed distinctly higher soil moisture than the other two treatments whose soil moisture looks close to each other in all the three horizons. In all the three horizons the DLC treatment had its soil moisture significantly higher than both the NC and GC treatments ($p<0.05$). However the GC had soil moisture not significantly different from NC ($p>0.05$).

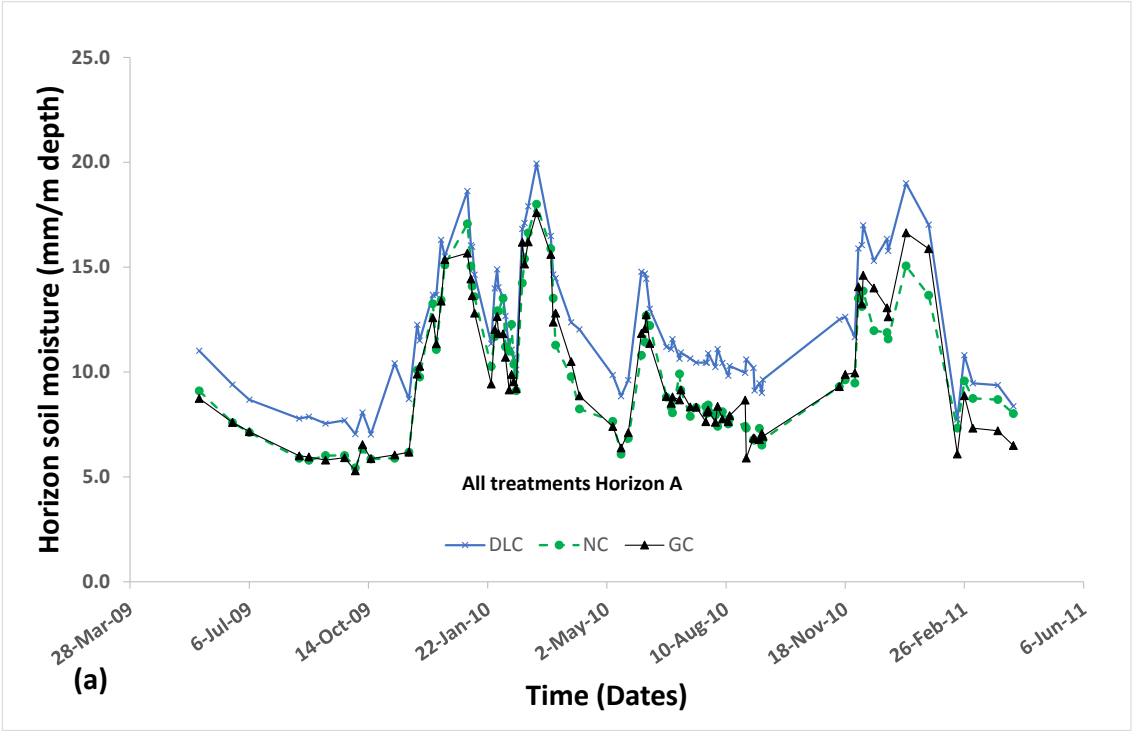
Horizon soil moisture (mm/m depth)
25.0
20.0
15.0
10.0
5.0
0.0
All treatments Horizon A
DLC
NC
GC
28-Mar-09
6-Jul-09
14-Oct-09
22-Jan-10
2-May-10
10-Aug-10
18-Nov-10
26-Feb-11
6-Jun-11
(a)
Time (Dates)

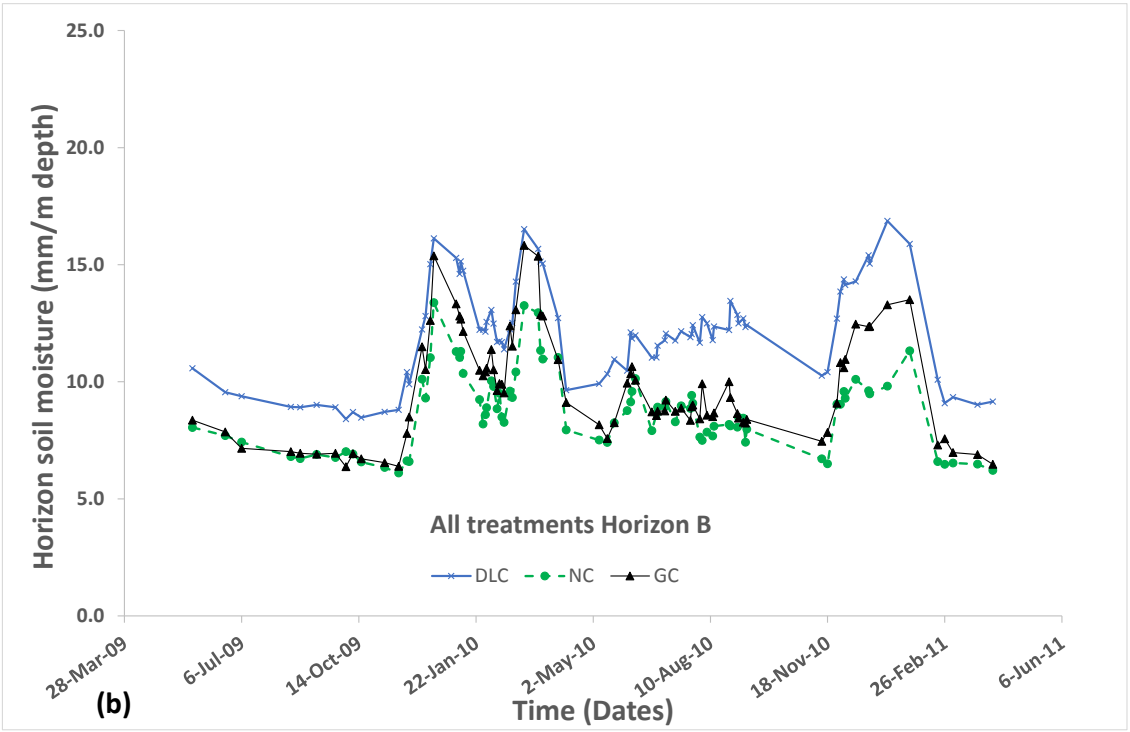
Horizon soil moisture (mm/m depth)
25.0
20.0
15.0
10.0
5.0
0.0
All treatments Horizon B
DLC
NC
GC
28-Mar-09
6-Jul-09
14-Oct-09
22-Jan-10
2-May-10
10-Aug-10
18-Nov-10
26-Feb-11
6-Jun-11
(b)
Time (Dates)

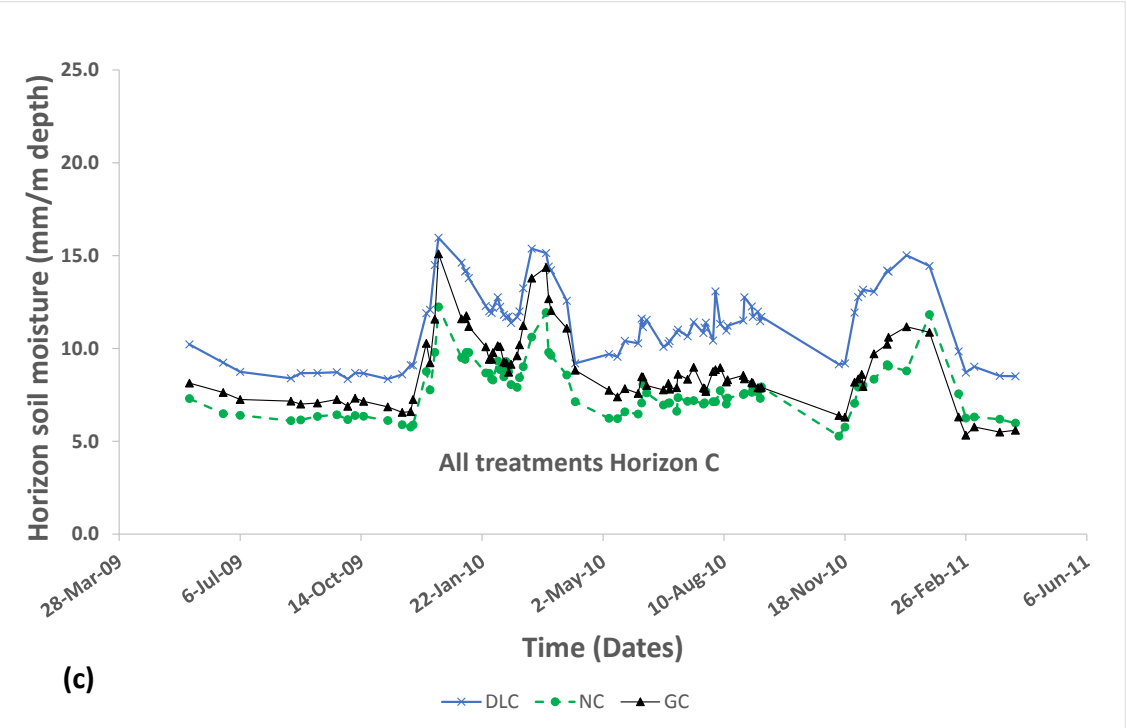

Figure 6-11: Variation of soil moisture for the three treatments in field A

Comparison of soil moisture among treatments in field A measured 3 days after the plots received a high rainfall amount of 60 mm/day which occurred on 05 January 2010 and after a dry spell lasting 3 weeks on 25 January 2010 is shown in Table 6-2.

In the loam soil the DLC plots had the highest soil moisture 3 days after a high rainfall amount was received which was significantly higher than that of the NC treatment ($p=0.000$) and the GC treatment ($p=0.000$). However the soil moisture in the GC treatment was not significantly higher than that in the NC treatment ($p=0.273$). Even after a dry spell lasting 3 weeks the DLC treatment continued to have the highest soil moisture (Table 6-3) which was significantly higher than both the GC and the NC treatments ($p=0.000$). Again after the dry spell GC treatment had its soil moisture not significantly higher than the NC treatment ($p=0.189$).

A comparison of soil moisture with position across the field for data from all the treatments (Table 6-2 bottom) shows the influence of contour ridges. The soil moisture from the position along the contour ridge channel was significantly higher that that from positions

along the cropped area upper and middle plot. The separate influence of each treatment are shown in Table 6-3 which shows the soil moisture variation among subplot positions for the different treatments.

Table 6-2 Comparison of soil moisture among treatments (top) and subplot position (bottom) in field A after significant rain and a dry spell

Treatment (All positions)	**Mean soil moisture (mm/0.2m depth)**	
	Sign Rain	**Dry Spell**
DLC	16.5[a]	12.1[a]
GC	13.2[b]	9.6[b]
NC	12.7[b]	9.2[b]

Position (All treatments)	**Mean soil moisture (mm/0.2m depth)**	
	Sign Rain	**Dry Spell**
Contour channel	15.4[a]	10.9[a]
cropped area upper plot	13.3[b]	10.1[b]
cropped area middle plot	13.6[b]	10.0[b]
cropped area lower plot	14.1[a,b]	10.4[a,b]

Table 6-3 Comparison of interaction between position in subplot and treatment on soil moisture in field A after significant rain and a dry spell

Treatment	**Position**	**Mean soil moisture (mm/0.2 m depth)**	
		Sign Rain	**Dry Spell**
DLC	Contour channel	16.2	12.5
	cropped area upper plot	14.8	11.3
	cropped area middle plot	16.2	11.3
	cropped area lower plot	18.8	13.4
GC	Contour channel	12.6	9.7
	cropped area upper plot	14.3	10.8
	cropped area middle plot	13.1	9.9
	cropped area lower plot	12.7	8.2
NC	Contour channel	13.6	10.5
	cropped area upper plot	10.6	8
	cropped area middle plot	11.9	8.8
	cropped area lower plot	14.6	9.7

6.2.4 Comparison of soil moisture conservation between treatments for a sandy soil (Field B)

Unlike in field A, comparison of treatments (Figure 6-12) shows that in field B, all treatments had soil moisture variation close to each other for all the three soil horizons. In addition there is no one treatment that distinctly gave higher or lower soil moisture. This trend was maintained in all the three soil horizons that were monitored. This suggest that both DLC and GC have no effect on soil moisture in sandy soils.

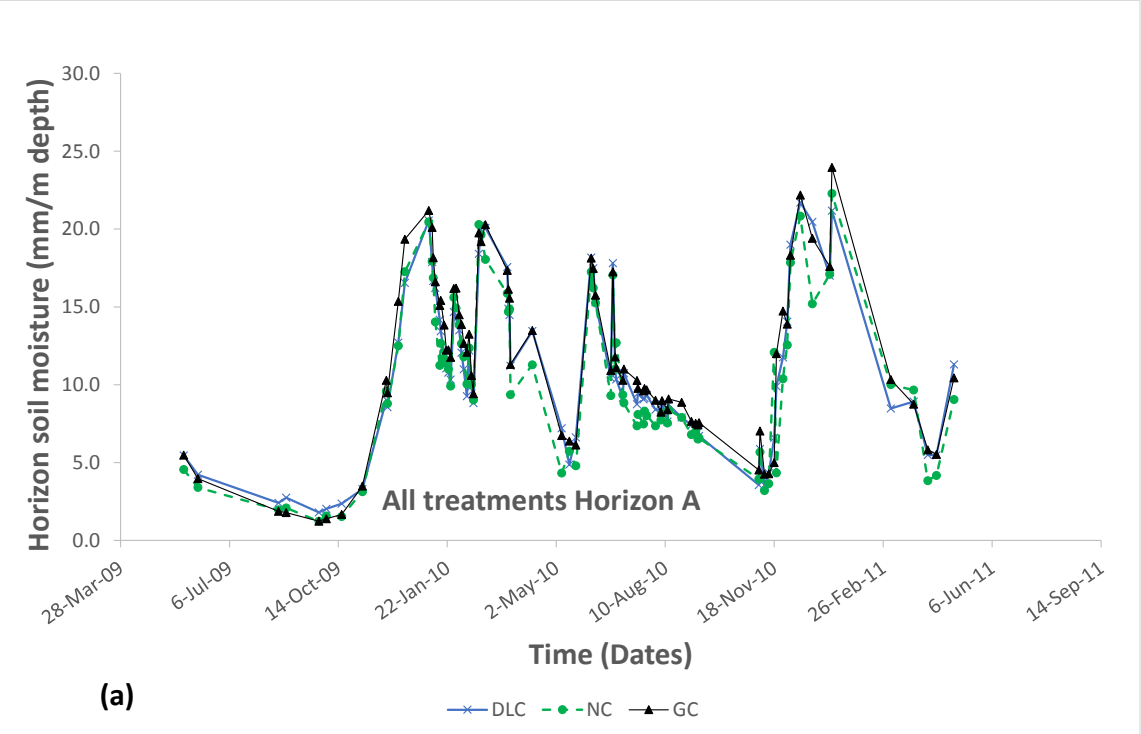

(a)

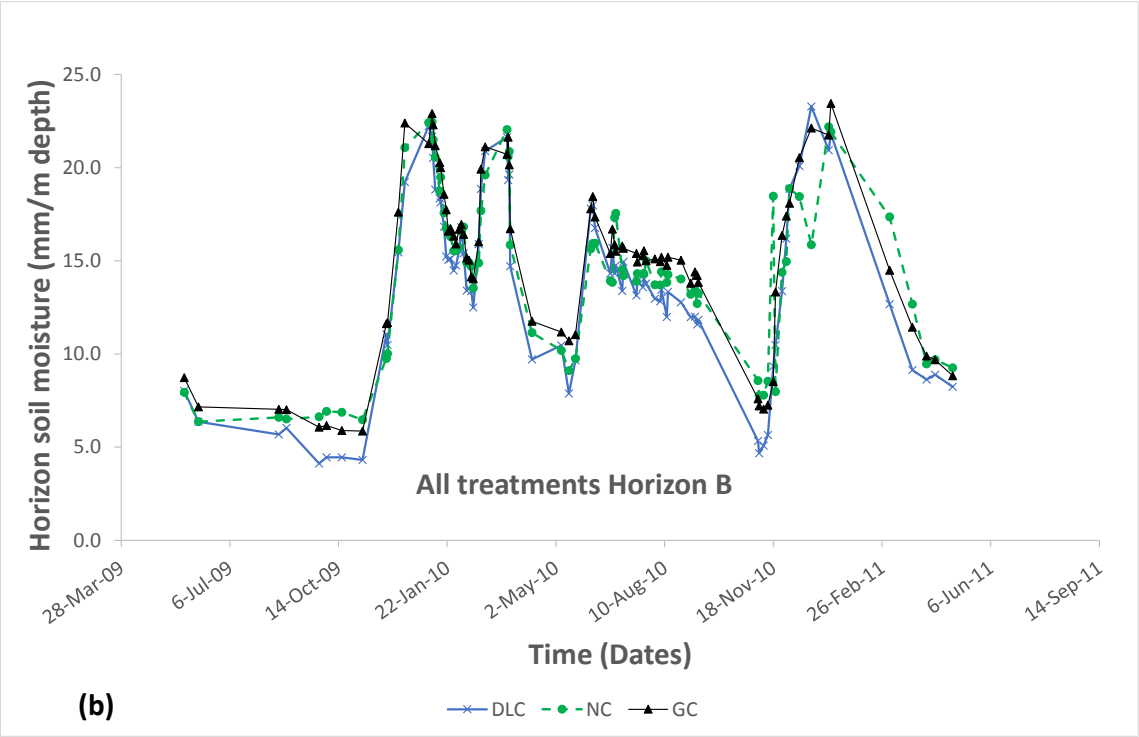

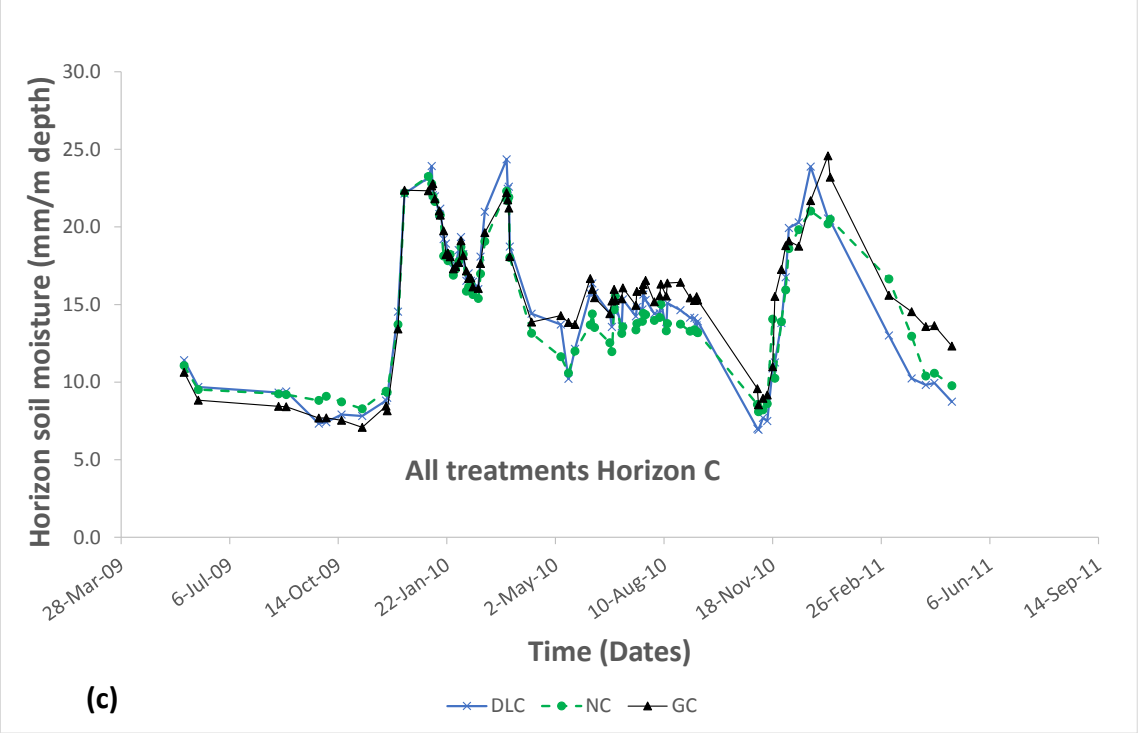

Figure 6-12: Variation of soil moisture for the three treatments in field B

Soil moisture variation among treatments and among subplot position in the sandy soil, measured 3 days after the plots received a high rainfall amount of 60 mm/day which

occurred on 05 January 2010 and after a dry spell lasting 3 weeks on 25 January 2010, is shown in Table 6-2. In Table 6-3 the effect of interaction between treatment and position is presented.

After the high rainfall the soil moisture in both the DLC and GC was not significantly different from the NC treatment in all the soil horizons (p=0.912 and 0.836 respectively). The soil moisture for the DLC was also not significantly different (p=0.751) from that of the GC. The trend remained the same after a dry spell in which no significant difference in soil moisture for the DLC when compared to GC and NC (p=0.147 and 0.061 respectively). However GC treatment had a significantly higher soil moisture content when compared to the NC treatment (p=0.001). This observation is considered an indication that there could have been other factors affecting soil moisture since the GC did not obtain any significantly higher soil moisture than the NC after the high rainfall. The overall results from field B suggest that both DLC and GC had no effect on soil moisture.

Table 6-4: Comparison of soil moisture among subplots and treatments in the sandy soil after significant rain

Treatment	**Mean soil moisture (mm/0.2m depth)**	
	Sign Rain	**Dry Spell**
DLC	21.4[a]	14.4[a]
GC	21.5[a]	15.3[a,b]
NC	21.4[a]	13.7[a]

Position (All treatments)	**Mean soil moisture (mm/0.2m depth)**	
	Sign Rain	**Dry Spell**
Contour channel	21.5[a]	14.0[a]
cropped area upper plot	22.3[a,b]	15.6[b]
cropped area middle plot	21.0[a]	15.0[a,b]
cropped area lower plot	20.9[a]	13.4[a]

Table 6-5: Comparison of soil moisture among subplots and treatments in the sandy soil after significant rain

Treatment	Position	Mean soil moisture (mm/0.2 m depth)	
		Sign Rain	Dry Spell
DLC	Contour channel	22.7	14.4
	cropped area upper plot	20.2	15.2
	cropped area middle plot	20.7	14.7
	cropped area lower plot	21.9	13.4
GC	Contour channel	20.5	14.3
	cropped area upper plot	24.0	16.9
	cropped area middle plot	21.3	16.3
	cropped area lower plot	20.3	13.9
NC	Contour channel	21.3	13.3
	cropped area upper plot	22.7	14.7
	cropped area middle plot	21.1	14.1
	cropped area lower plot	20.7	12.8

6.2.5 Seasonal cumulative soil moisture storage

Field A

The cumulative soil moisture storage in the loam soil represented by the average soil water index (ASWI) shown in Table 6-6 showed that treatment had a significant effect on the cumulative soil moisture storage during both the 2009/10 season (p=0.001) and the 2010/11 season (p=0.000). However position had no significant effect on cumulative soil moisture storage during the 2009/10 season (p=0.724) but showed a significant effect during the 2010/11 season (p=0.003). Table 6-7 indicates results of interaction between treatment and position on cumulative soil moisture storage which had no significant effect during 2009/10 season (p=0.281) but inconclusive during the 2010/11 season (p=0.054).

Comparison of cumulative soil moisture among treatments showed that in the loam soil the DLC plot had significantly high soil moisture storage compared to both NC and GC treatments during both the 2009/10 season (p=0.002 and p=0.000 respectively) and 2010/11 season (p=0.000 and p=0.000 respectively). On the other hand the cumulative soil moisture storage of the GC was not significantly different from that of the NC plot during both the 2009/10 (p=0.582) and 2010/11 (p=0.749) seasons.

Table 6-6: Comparison of cumulative soil moisture among treatments and subplot positions for the loam soil.

Treatment (All Positions)	**Mean ASWI (mm days)**	
	2009/10 season	**2010/11 season**
DLC	30199[a]	20596[a]
GC	24082[b]	15138[b]
NC	24994[b]	14810[b]

Position (All treatments)	**Mean ASWI (mm days)**	
	2009/10 season	2010/11 season
Contour channel	27690[a]	19385[a]
cropped area upper plot	26137[a]	16946[b]
cropped area middle plot	26283[a]	16217[b]
cropped area lower plot	25590[a]	14845[b]

Table 6-7: Mean values of soil moisture index (SWI) showing interaction between treatment and position for the loam soil.

Treatment	**Position**	**Mean value (mm days)**	
		2009/10 season	**2010/11 season**
DLC	Contour channel	32614	23011
	cropped area upper plot	28484	19594
	cropped area middle plot	27160	18847
	cropped area lower plot	32540	20932
GC	Contour channel	25131	15365
	cropped area upper plot	27086	17071
	cropped area middle plot	26365	15602
	cropped area lower plot	21392	12515
NC	Contour channel	25325	19780
	cropped area upper plot	22839	14174
	cropped area middle plot	25325	14202
	cropped area lower plot	22839	11089

Field B

Table 6-8 shows the variation of cumulative soil moisture among the three different treatments and among different subplot positions. Treatment had no significant effect on cumulative soil moisture in the sandy soil during both the 2009/10 season (p=0.062) and 2010/11 season (p=0.084). Equally, position had also no siginificant difference during the two seasons 2009/10 (p=687) and 2010/11 (p=0.212). The interaction between treatment and position (Table 6-9) also had no significant effect on cumulative soil moisture storage for both 2009/10 (p=0.189) season and 2010/11 season (p=0.687).

DLC had its cumulative soil moisture storage not significantly lower than that of NC treatment during both 2009/10 (p=0.133) and 2010/11 (p=0.164) seasons. The DLC also had its seasonal cumulative soil moisture storage not significantly different from the GC treatment during the 2009/10 season (p=0.393) but significantly lower seasonal cumulative soil moisture storage in the 2010/11 season (p=0.028). The 2010/11 rainfall season received higher rainfall when compared to the 2009/10 season particularly during the month of January in which dry spells are normally expected. This suggests that there was subsurface flow that could have influenced the soil moisture in the GC plot.

Table 6-8: Comparison of cumulative soil moisture among treatments and subplot positions for sandy soil.

Treatment (All Positions)	**Mean ASWI (mm days)**	
	2009/10 season	**2010/11 season**
DLC	30949[a]	24917[a]
GC	31915[a,b]	27369[a,b]
NC	29237[a]	26454[b]

Position (All treatments)	**Mean ASWI (mm days)**	
	2009/10 season	2010/11 season
Contour channel	30212[a]	27712[a]
cropped area upper plot	31131[a]	25532[a]
cropped area middle plot	31372[a]	25263[a]
cropped area lower plot	30089[a]	26478[a]

Table 6-9: T test for the sandy soil during the 2010/2011 rainfall season

Treatment	Position	Mean value (mm days)	
		2009/10 season	2010/11 season
DLC	Contour channel	33121	28489
	cropped area upper plot	30181	23473
	cropped area middle plot	30940	22947
	cropped area lower plot	29555	24758
GC	Contour channel	28421	27894
	cropped area upper plot	34083	26763
	cropped area middle plot	33312	26894
	cropped area lower plot	31847	27923
NC	Contour channel	29095	26754
	cropped area upper plot	29128	26359
	cropped area middle plot	29862	25949
	cropped area lower plot	28864	26754

6.3 Effect of rainwater harvesting by contour ridges on growth and yield of maize crop

This section presents the results of the assessment of the effect of contour ridges on the growth and yield of a maize crop. Although field data collection started in the rainfall season 2008/9 the harvested data was not done according to the sample check plots that were used for the other two rainfall seasons. As a result only yield data for the 2009/10 and 2010/11 seasons were analysed.

6.3.1 Crop growth

Figure 6-13(a) presents variation of plant height on a loam soil during the growing season of 2009/10. The cumulative rainfall is also presented on the same graph to show when dry spells occurred. The cumulative rainfall graph shows two distinct dry spell periods during the crop growing period. At the start of the second dry spell on 08 January 2010 the average plant height in the treatments was DLC (236mm), NC (235mm) and GC (234mm) indicating closely related plant heights. By the end of the dry spell on 22 February 2010 the average plant height in DLC plot had changed to 1 353mm compared to 1 257mm in the control plot and 999mm in the GC plot. The difference in plant height between the DLC and the control changed from 0.4% before the dry spell to 7.6% after the dry spell showing the influence of the increased soil moisture observed in the DLC when compared to NC. The same trend was not observed in the sandy soil shown in Figure 6-14 (b).

The average number of leaves for the different treatments as the season progressed is given in Table 6-10. While number of leaves is not significantly different for the different treatments DLC had the highest number of leaves compared to the other treatments.

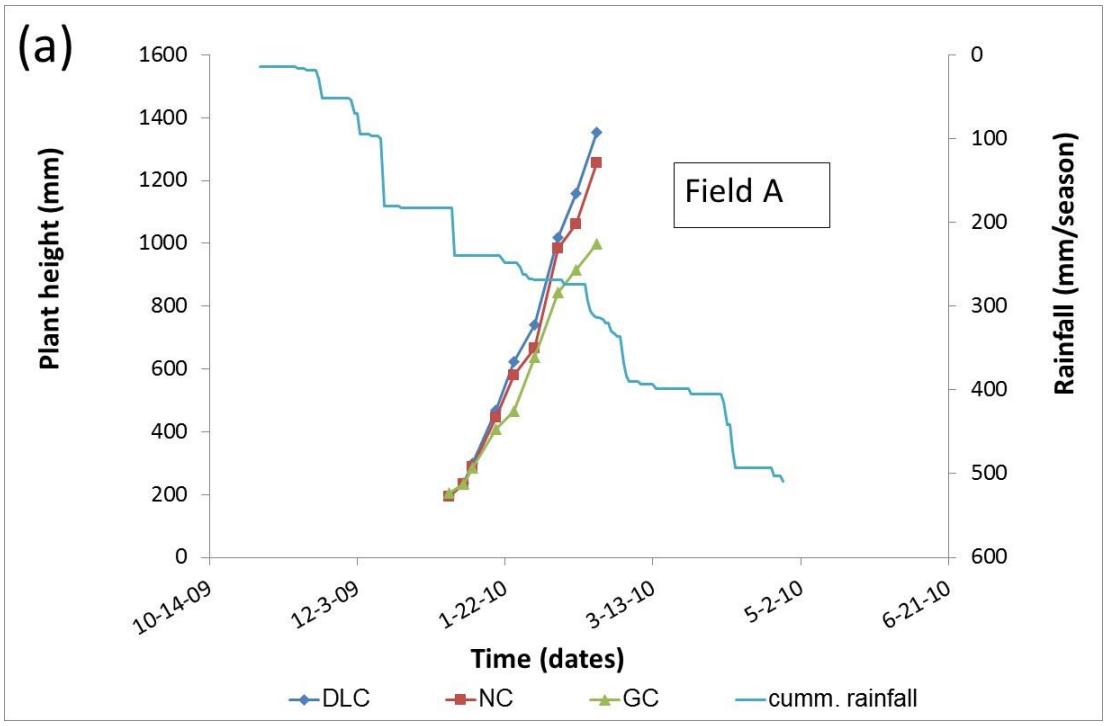

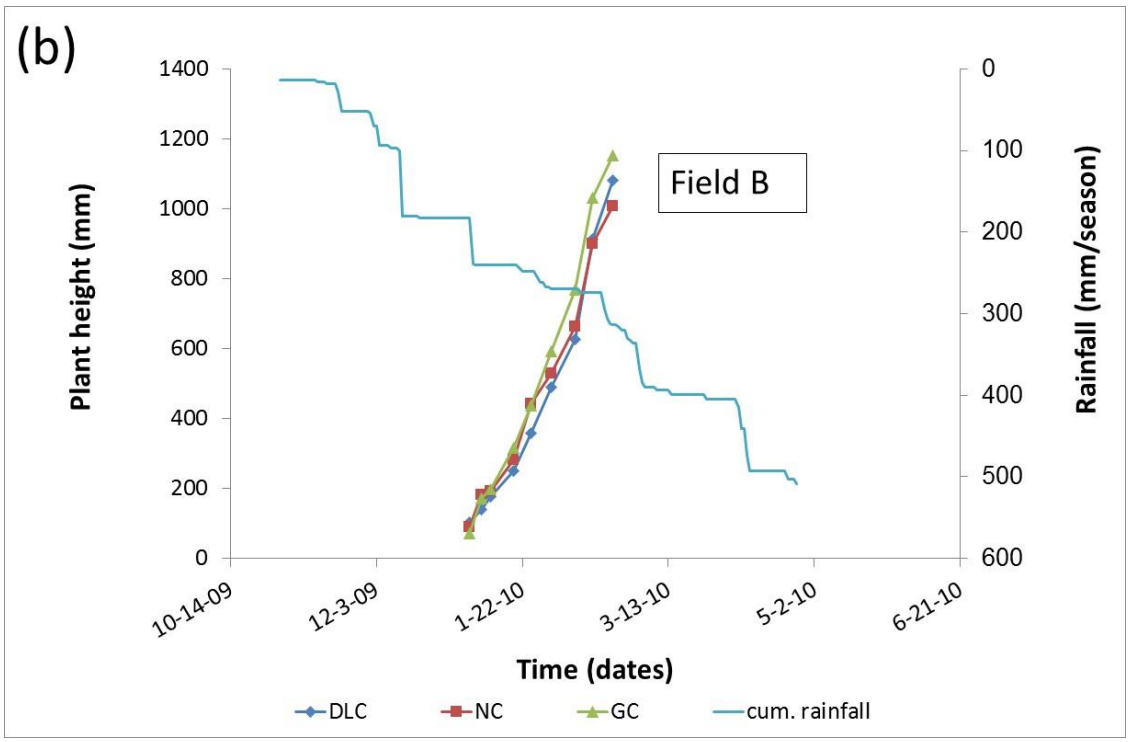

Figure 6-13: Variation of plant height on a a loam soil (a) and sandy soil (b) during the 2009/10 growing season

Table 6-10: Average number of leaves per plant on a loam soil as the 2009/10

Time (date)	2009-12-29	2010-01-22	2010-02-05	2010-02-20
Treatment	Number of leaves at counting date (as above)			
DLC	5	11.7	11.8	8
NC	5	9	10.2	6.2
GC	5	9.6	10	7.3

Figure 6-14 (a) shows the average moisture content of maize leaves expressed as a percentage of leaf dry matter for the loam soil. Ten leaves (one per plant) were sampled from each of the 12 check plot. The DLC had significantly more ($P<0.05$) leaf moisture content (average of 325% of dry matter) compared to the control (average of 292% of dry matter) while the leaf moisture content (average of 261% of dry matter) in the GC plot was not significantly lower than in the control ($p>0.05$). Figure 6-14 (b) shows the average moisture content of maize leaves expressed as a percentage of leaf dry matter for the sandy soil. The difference among the three treatments is insignificant ($p>0.05$) with the GC plot showing the highest leaf moisture content (average of 343% of dry matter) when compared to DLC (average of 334% of dry matter) and the NC (average of 342% of dry matter).

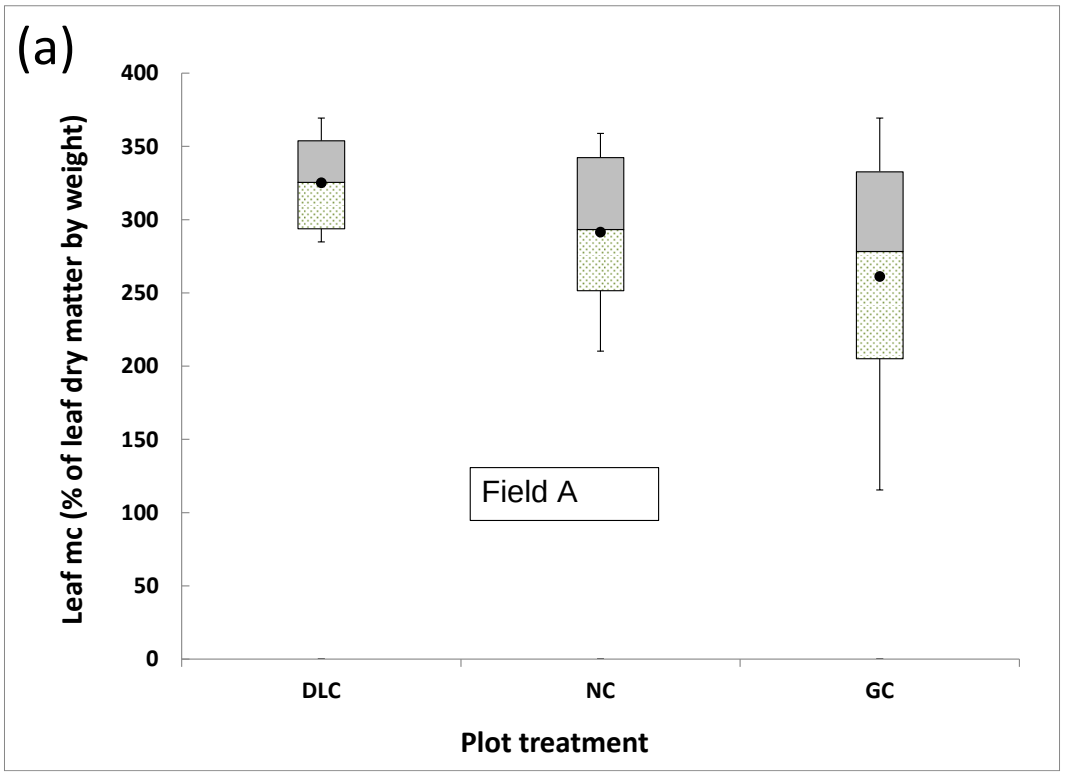

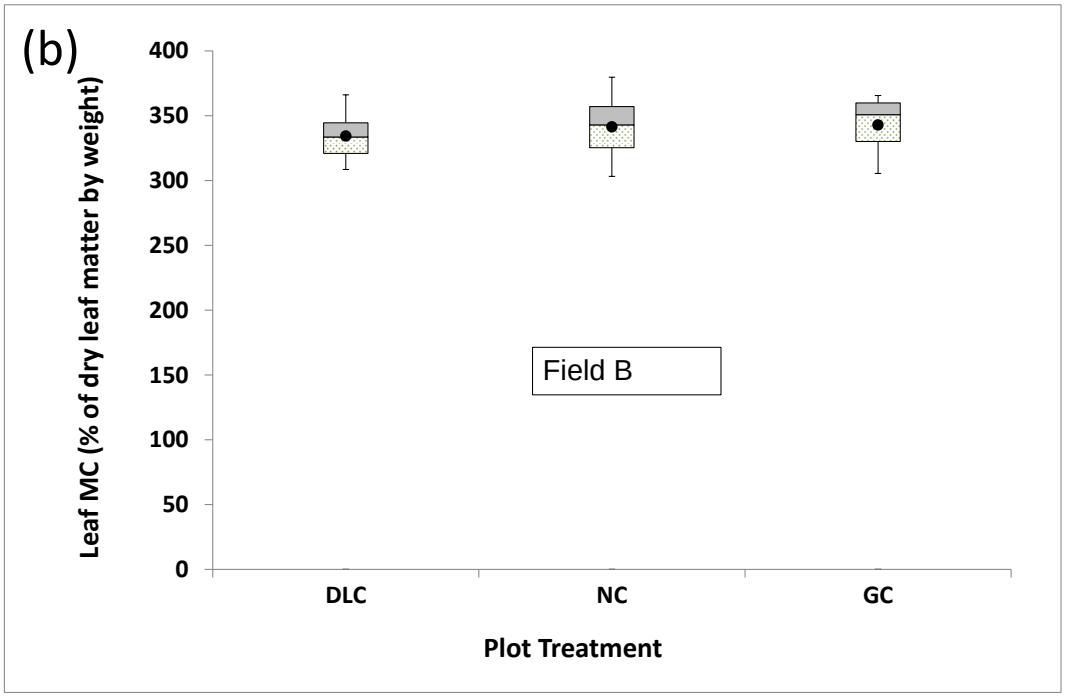

Figure 6-14: Variation of leaf moisture content for the different treatments at the end of a three week dry spell in field A (a) and field B (b).

6.3.2 Crop yield

The average seasonal grain and total yield for the 2009/10 and 2010/11 farming season from the loam and sandy soil are shown in Table 6-11. The DLC plot had the highest grain yield of 973kg/ha in the loam soil compared to 869kg/ha in the NC plot and 446 kg/ha observed in the GC plot. The sandy soil showed a different situation with DLC having the highest yield of 1073 kg/ha and the least yield of 820kg/ha observed on the NC plot and the GC having 1052kg/ha.

Table 6-11: Average Grain and total yield for the different treatments for the 2009/10 and 2010/11 farming season.

Treatment	DLC grain yield (kg/ha)	DLC total yield (kg/ha)	NC grain yield (kg/ha)	NC total yield (kg/ha)	GC grain yield (kg/ha)	GC total yield (kg/ha)
Field A	973	3 249	869	3 282	446	2 246
Field B	1 073	2 737	820	1 959	1 052	2404

The average grain yield for the 2009/10 and 2010/11 growing seasons for the loam soil and sandy soil is shown in Figure 6-15a and Figure 6-15b respectively. The total crop yield for a loam soil for the three treatments is shown in Figure 6-16a while that for the sandy soil is shown in Figure 6-16b. The data points were derived from 12 check plots for two seasons resulting in 24 data points per treatment. The yield in the loam soil followed the same trend as that shown by the leaf moisture content. The DLC plot had the highest yield followed by the NC plot while the GC plot yield was the lowest. The difference in yield between the GC and the NC plot was insignificant while that for the DLC and the NC plot was significant ($p = 0.018$).

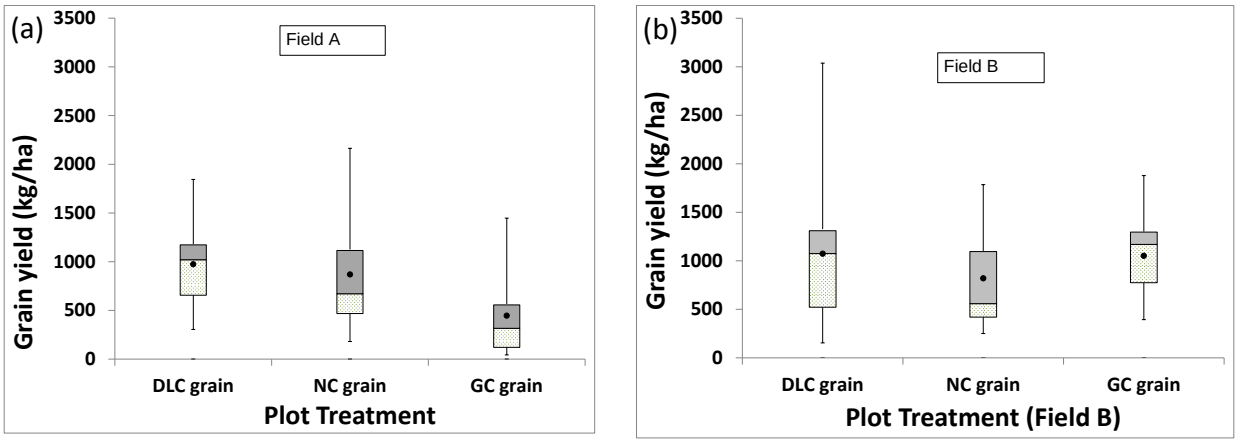

Figure 6-15: Combined grain yield for 2009/10 and 2010/11 seasons from field A (a) and field B (b).

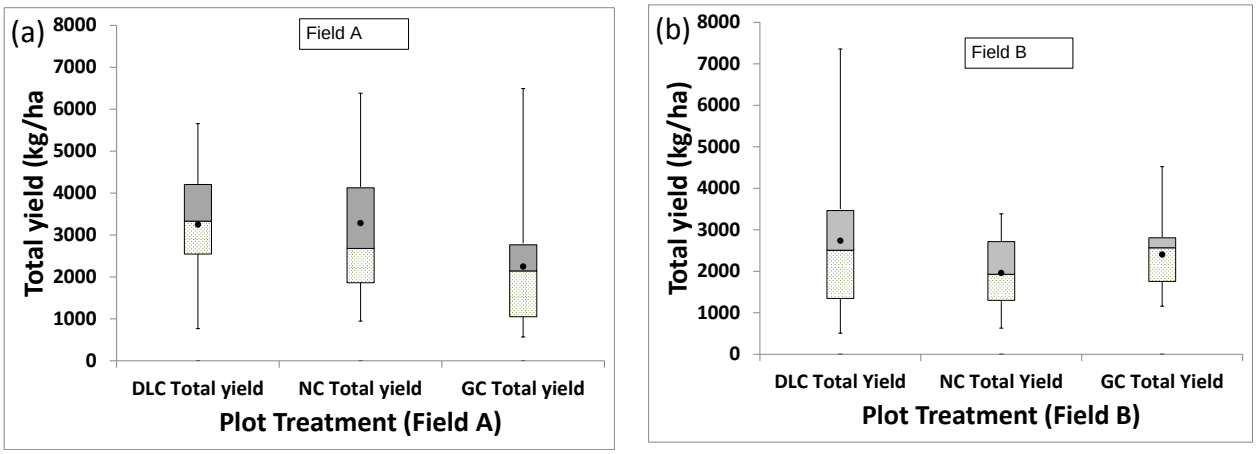

Figure 6-16: Combined total yield for 2009/10 and 2010/11 seasons from field A (a) and field B (b).

6.4 Discussion

In the loam soil, the soil moisture after a dry spell in subplot 1 was higher (although not significantly ($p>0.05$)) than the soil moisture in subplot 2 in all the three horizons. However after large rainfall amounts, the soil moisture in subplot 1 was lower than in subplot 2 although not significant ($p>0.05$) in all the three soil horizons. The increase in soil moisture as distance increases downslope after receiving large amounts of rainfall is in agreement with the damming effect as observed in Figure 6-4. Since the same pattern is not followed after the dry spell it shows that a separate process results in the increase in soil moisture

in subplot 1 than subplot 2. This suggests that there was some subsurface lateral flow from the contour ridges to subplot 1 which agrees with the observations of Mugabe (2004) and Mupangwa et al. (2011).

The DLC plots were able to conserve soil moisture more than GC and NC in the loam soils. The soil moisture in DLC plots is more uniformly distributed as demonstrated by subplot soil moisture that is close to each other. The high levels of soil moisture found in the subplot upslope of the ridge (subplot 3) indicate that soil moisture improvement due to DLC is more through infiltration of harvested runoff than through seepage of infiltrated runoff. This suggests that shallow dead level contours with high ridges could be more effective than deep ridges. However the fact that the subplot downslope (subplot 1) of the ridge showed more moisture than the middle subplot (subplot 2) indicates that there was soil moisture increase through seepage.

On the basis of experimental results on available soil water index (ASWI) it has been shown that dead level contours significantly retain more water compared to graded contours and also compared to having no contours in the field. The moisture retained by dead level contours is concentrated in areas around the contour ridges. The design of contour ridges for water conservation needs to consider that when dead level contours are constructed in the field, moisture tends to accumulate close to the contour ridge both upslope and downslope. It is necessary to be able to predict the extent of area in which significant moisture improvement will take place as a result of the dead level contours. In addition, the level of improvement is also important to assist farmers in their decision of crops to grow in areas where dead level contours have been constructed. This calls for a model that can be used to predict the soil moisture storage for a field taking into account the field's geophysical conditions.

The observation that two out of three seasons for which data for the study was collected were bad seasons agreed with long term records from the area as represented by the rainfall station at Filabusi 17 km away from the study sites. Mupangwa (2008) carried out an analysis of dry spells in Matebeleland South and found out that rainfall data from Filabusi station showed that the probability of occurrence of dry spells lasting 14 days or more is 90% and that of 21 days or more is 60 to 80%.

Plant height during the second dry spell had a significant difference between the treatments suggesting the DLC were able to avail water to the maize crop. This agrees

with results obtained by Memon et al. (2007) who demonstrated that farm management practices had effect on plant height.

The different yield obtained from the three treatments is less pronounced for the sandy soil although the DLC still performed better than the other two. These results compare favorably with those obtained by Munodawafa and Zhou (2008) on station trials in similar conditions in Zimbabwe. The yield from DLC plots could have been higher for the loam soil had it not been for the termites that were cutting down some of the plants. The presence of termites could be attributed to higher soil moisture levels that were evident in these plots (Mutsamba and Nyagumbo, 2010).

The results of non-destructive methods for measuring crop growth agreed favourably with the crop yield results. This suggest that these methods can be useful for monitoring crop growth and measuring effect of a farming practice such as contour ridges on crop yield.

This chapter has shown that DLC significantly improves moisture content in loam soils which leads to improved crop yield. This was demonstrated by the DLC plot having higher moisture than the GC and NC plots. However DLC did not show the same effect on sandy soils.

7 CONTOUR RIDGE RAINWATER HARVESTING MODEL IMPLEMENTATION AND TESTING

This chapter starts by presenting the results of the fuzzy modelling for estimating field scale runoff that was developed in this study as described in Chapter 5. It is necessary to consider these results first since the runoff is an input into the rainfall partitioning module of the overall model. The overall model is used to estimate soil moisture for the two farm plots used in the field experimentation and a comparison of the modelled soil moisture with the field measurements is done. Finally, the overall model implementation and modelling performance are discussed.

7.1 Modelling runoff harvested by contour ridges using fuzzy logic approach

This section presents the implementation and performance of the developed field scale rainfall runoff fuzzy model. The first subsection presents results of the developed fuzzy inference system made up of the identified model structure and the estimated consequent parameters. A fuzzy model structure is considered to present the number of rules that control the fuzzy inference system which is the decision making part of the model. The number of rules is the same as the number of the cluster centres that were identified during data clustering. Each of the identified clusters could be interpreted as containing a group of data points exhibiting similar physical characteristics whose behaviour is controlled by the fuzzy rule associated with the corresponding identified cluster centre.

In the same subsection, the estimated consequent parameters for each sub model are also presented. The consequent parameters are the coefficients of the input variables in the general fuzzy model that makes it unique to each of the specific fuzzy rule. The identification of the consequent parameters completes the full identification of the fuzzy inference system. The last subsection compares the runoffs from the fuzzy model with those measured in the field.

7.1.1 The developed fuzzy inference system

The data that was used for developing the fuzzy inference system was limited by the need to have rainfall events that contained all the four variables that were used for the fuzzy model namely rainfall, soil type, soil moisture and runoff measured at field scale as described in chapter 5 section 5.4.

Rainfall events in the semi-arid areas of Zimbabwe are rare thus the number of rainfall events in field experiments where both soil moisture and field scale runoff were measured were limited. Furthermore measurement of soil moisture and runoff on the two catchments where the data was obtained was constrained by lack of automatic measuring instruments due to resource constraints further limiting data availability. Data was available from two different semi arid catchments of Zimbabwe described in chapter 5 section 5.4.2. These data gave 52 data points for the modelling that matched the criteria. This was considered to be reasonably adequate for the fuzzy logic modelling. The minimum and maximum values of each of the variables from the 52 data points used for the modelling are shown in Table 7-1.

Table 7-1: Minimum and maximum variable values used for normalising and denormalising data

Variable	Minimum value	Maximum value
Runoff coefficient (%)	0.0	100.0
Rainfall duration (hours)	0.0	19.86
Rainfall intensity (mm/hour)	0.0	6.35
Soil moisture (mm)	3.0	35.0
Soil type (index)	1.68	3.73

Following subtractive data clustering, five cluster centres shown in Table 7-2 were established, each cluster centre forming the focal point of a sub model of the inference system. The value for each variable of a cluster centre in Table 7-2 indicates the relative position of the cluster centre in the range of possible values of the variable. For example rainfall duration can range from all the rainfall falling in one hour to rainfall spread over the whole 24 hour period of the day. Cluster centre number 1 implies that it is applicable to rainfall events in which rain falls during short durations clustered around 1.7 hours

(0.072 of 24 hours = 1.7 hours) while cluster centre number 3 is for rainfall events that fall over very long periods clustered around18.5 hours. Similarly cluster 1 is applicable to events where rain falls on soil that is very wet while cluster 5 is for rainfall events falling on soil that is very dry. The values of the cluster centres on the scale of 0 to 1 could have been influenced by the maximum values of the variables that were used for normalising the data (Table 7-1). The cluster values for runoff coefficient and rainfall duration are based on a well established range as both the minimum value and maximum value are known with certainty. Both have a minimum value of zero when the rainfall event produces no runoff and when the rainfall occurs for a few seconds which becomes zero on a time scale of 1 hour. The maximum theoretical value of runoff coefficient is 100 (%) which occurs when all the rainfall is turned into runoff while the maximum theoretical value of rainfall duration is 24 (hours) which occurs when rainfall is received throughout the day. However the maximum theoretical value of rainfall intensity is the maximum value that was obtained from the data range used for data clustering and there is a probability that such a rainfall intensity can be exceeded. The maximum value of soil moisture was that obtained from the data range and could be exceeded in reality.

Table 7-2: Normalised cluster centre values after data clustering

Cluster number (m)	Runoff coefficient ($c_{0,m}$)	Rain duration (T)	Rain intensity (P_i)	Soil moisture (θ)	Soil type (α_N)
1	0.390	0.072	1.000	0.969	1.000
2	0.171	0.242	0.531	0.328	0.666
3	0.412	0.771	0.263	0.734	1.000
4	0.616	0.367	0.735	0.906	1.000
5	0.020	0.572	0.422	0.094	0.010

Figure 7-1 illustrates the clustering results graphically clearly showing the range of runoff coefficients that can be generated. It shows location of the runoff coefficient and the four input variables for each sub model represented by a cluster centre on a scale of 0 to 1.

The five cluster centres can be interpreted in linguistic fuzzy terms to establish the corresponding five fuzzy rules as presented in the following paragraphs.

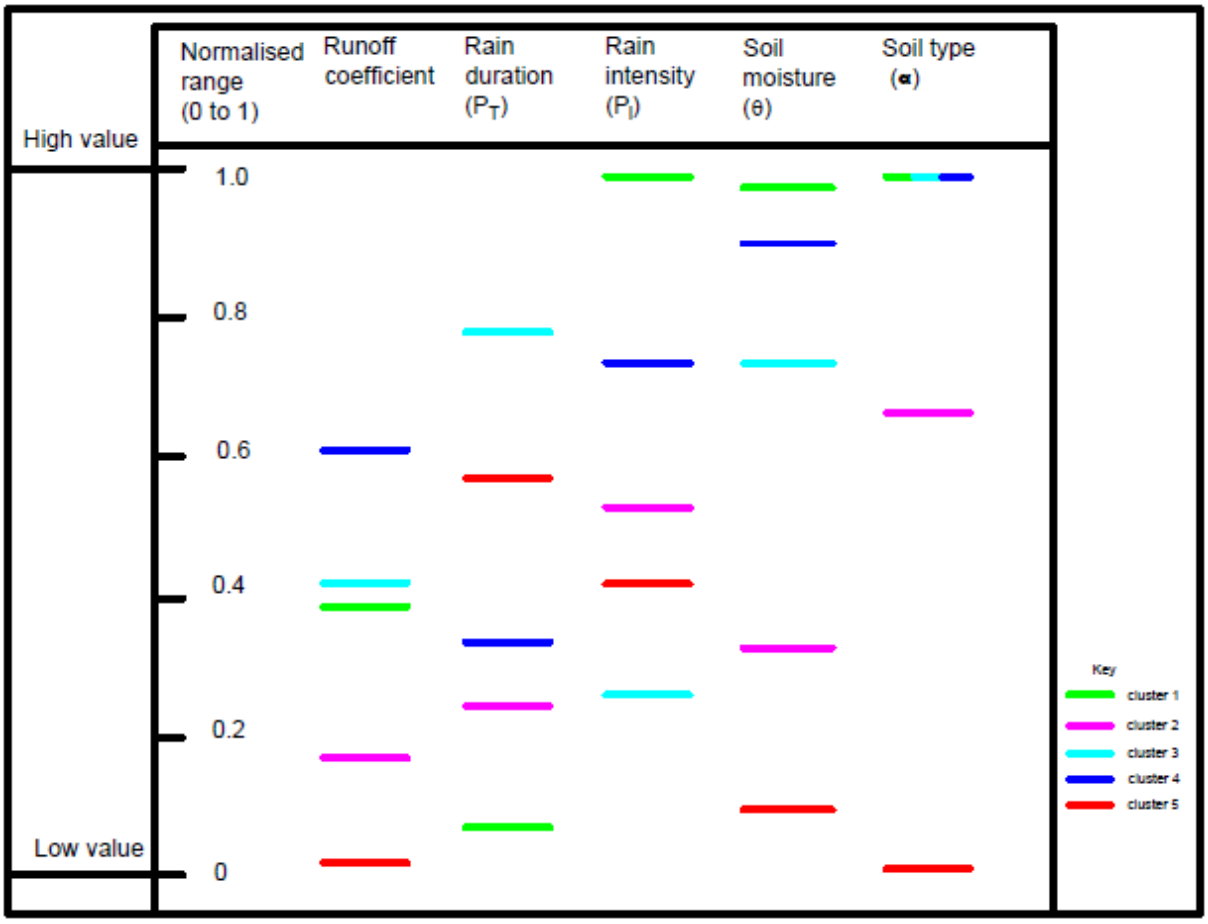

Figure 7-1: The variation of the input variables for the cluster centres

The spread of data points for cluster centre 1 indicates the physical characteristics of the variables that form the focal point for fuzzy sub model 1. This cluster centre represents heavy textured soils as the value of soil type is high. It also represents a situation where both the soil moisture and rainfall intensity are both high as their corresponding values are equally high. However despite representing high conditions of soil moisture and rainfall intensity falling on heavy textured soil that favours high runoff generation the cluster centre represents a cluster of events in which rain falls for a short duration as the

value of rainfall duration is small. This means that during that short rainfall period the infiltration rate would still be high given that infiltration rate exponentially decreases with the rainfall period. This result in low proportion of rainfall that is converted to runoff and hence the runoff coefficient for this cluster is nearly average (39%). Therefore rule 1 of the fuzzy model can be defined as follows: ***fuzzy rule 1:*** **A heavy textured (clay loam) soil that receives high rainfall intensity falling for a very short duration on soil with high soil moisture generates slightly below average runoff**.

The values of variables constituting cluster centre 2 are much lower when compared to those of cluster centre 1 except for the rainfall duration value which is relatively higher. This cluster centre represents rainfall falling relatively on dry soil with rainfall intensity that is not very high. This favours high infiltration which explains why the runoff coefficient associated with this cluster is low (17.1%). This suggests that rule 2 of the fuzzy model can be stated as follows: ***fuzzy rule 2:*** **A loamy soil that receives above average rainfall intensity falling for a short duration on soil with low soil moisture generates low runoff.**

The spread of values of variables making up cluster centre 3 indicate that while the rainfall duration increased to a level where infiltration capacity would be expected to reduce thereby allowing more runoff to be generated the rainfall intensity was low compared to cluster 1 and 2. This means the low rate of rainfall intensity allowed for drainage of water from top soil horizon thereby creating reduced runoff generation than that suggested by the long rainfall period. Despite this disadvantage of the location of the cluster centre the runoff coefficient (41.2%) that results from this cluster suggest average runoff is generated under these conditions. The corresponding rule for the fuzzy model is suggested as follows: ***fuzzy rule 3:*** **A clay loam soil that receives low rainfall intensity falling for a long period on soil with high soil moisture generates nearly average runoff.**

A typical situation where high runoff is generated is shown under conditions of cluster 4. While rainfall duration for cluster 4 is average compared to all the five clusters the runoff coefficient (61.6%) is highest owing to the high values of rainfall intensity, soil moisture and a heavy textured soil that have low hydraulic conductivity. The rainfall intensity, soil moisture and soil texture of the soil for cluster 4 are comparable to cluster 1. However the higher rainfall duration in cluster 4 suggests that the infiltration capacity of the soil reduced

as the rainfall event progresses resulting in more runoff being generated compared to that which is generated under cluster 1. Therefore rule 4 for the fuzzy model could be described as follows: ***fuzzy rule 4:*** **A heavy textured soil (clay loam soil) that receives high rainfall intensity falling for nearly average period on soil with high soil moisture generates high runoff.**

The influence of soil conditions and properties on the runoff amount generated is demonstrated by the distribution of input variables for cluster centre 5. The rainfall duration is fairly high which would suggest sufficient time to reduce infiltration capacity while rainfall intensity is above that of cluster 3. However the rainfall with such characteristics that would suggest average runoff generation falls on dry light textured soil. A soil with such conditions has a very high infiltration capacity that remains high during the rainfall event as the infiltrating water quickly drains away resulting in very low runoff being generated. This results in a very low runoff coefficient value (2%). Thus the last rule for the fuzzy model is described as follows: ***fuzzy rule 5:*** **A sandy soil that receives average rainfall intensity falling for an average duration on soil with low soil moisture generates very low runoff.**

The SCE optimization guidelines provided by Duan et al. (1994) were successfully applied in identifying the consequent parameters of the fuzzy model (see Equation 5-18 reproduced in Equation 7-1). All the five sub models met the convergence criterion that was set for this study of the average value of RMSE for best top half and the least bottom half falling within 5% (see section 5.4.4 in Chapter 5).

The consequent coefficient,$c_{i,m}$, for each of the sub models with focal points (cluster centres) presented in Table 7-2 are shown in Table 7-3. The coefficients (Table 7-3) were applied to the general model of Equation 7-1 for each of the corresponding cluster centres shown in Table 7-2. The corresponding runoff coefficients which were obtained from this calibrated fuzzy model were compared to the runoff coefficient that was established during data clustering for the corresponding cluster centre and the results are shown in Figure 7-2. The results show that the consequent parameters of the fuzzy model provide a very good estimate of the runoff coefficients. The model was therefore tested on the data set that was used for developing the model and from another data set obtained from independent sites, the results of which are presented in the next sub section.

$$q_{j,m} = c_{0,m} + c_{1,m}T_j + c_{2,m}P_{i,j} + c_{3,m}\theta_j + c_{4,m}\alpha_{N,j}$$ Equation 7-1

Where:
$q_{j,m}$ is normalised runoff coefficient contributed by partial model m during rainfall event j in; T_j is normalised mean rainfall duration (hours) for rainfall event j; $P_{i,j}$ is normalised mean rainfall intensity(mm/hour) during rainfall event j; θ_j is normalised root zone soil moisture (mm) at the start of rainfall event j; $\alpha_{N,j}$ is normalised soil parameter defining soil characteristic (type) for rainfall event j; $c_{0,m}$ is a constant for partial model m; $c_{1,m}$, $c_{2,m}$, $c_{3,m}$ and $c_{4,m}$ are coefficients to input variables for partial model m.

Table 7-3: Model consequent coefficients from shuffled complex Evolution calibration

Sub model Number	Constant ($c_{0,m}$)	rain duration ($c_{1,m}$)	rain intensity ($c_{2,m}$)	soil moisture ($c_{3,m}$)	soil type ($c_{4,m}$)
1	0.042	0.107	0.163	0.129	0.089
2	-0.244	0.266	0.280	0.238	0.187
3	-0.021	0.181	0.181	0.136	0.144
4	0.027	0.270	0.059	0.208	0.271
5	-0.008	0.020	0.020	0.021	0.304

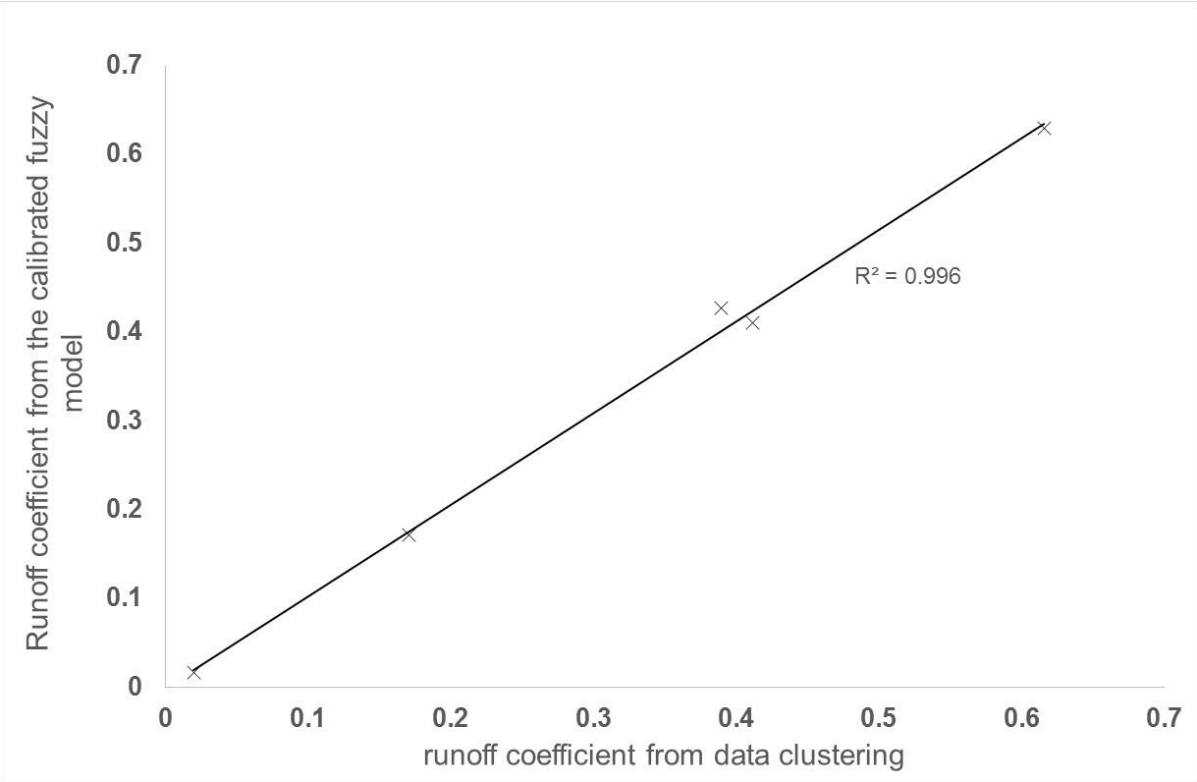

Figure 7-2: Comparison of runoff coefficient figures established from calibrated fuzzy model with those established from data clustering

7.1.2 Field scale rainfall runoff fuzzy model simulation results

Figure 7-3 shows the results of runoff simulated by the field scale rainfall runoff fuzzy model using the same data that was used for developing the model plotted against the observed runoff. The daily rainfall figures were disaggregated to mean rainfall intensity and the corresponding rainfall duration based on the range bin random sampling method described in section 5.6.1. The results indicate a good estimate of runoff with a coefficient of determination of R^2=0.69.

Figure 7-4 shows the model results in which the simulated runoff values are plotted against the observed runoff values for the same data used for model development but with the mean rainfall intensity and rainfall duration estimated using an empirical approach as described in section 5.6.2. The coefficient of determination for this simulation is better with R^2=0.75 and was subsequently used for disaggregating rainfall data used in the modelling.

The two results show that the model is able to simulate observed runoff well although there is considerable scatter of the data points. This is not unexpected and could be due to inaccuracies in the estimation of rainfall intensities and soil moisture values, the limited data available and the assumptions inherent in applying fuzzy modeling to the complex rainfall-runoff process. The availability of soil moisture data at a weekly time interval may have limited the ability of the modelling to adequately incorporate antecedent soil moisture. In addition, the form of the sub model (Equation 7-1) assumed a linear relationship between the output (runoff) and the input variables (rainfall intensity, rainfall duration, and soil moisture and type). Besides the considerable scatter of the data points the low runoff figures are also not well simulated. Again this could have been caused by the constant parameter in the sub model which gets more pronounced at low values.

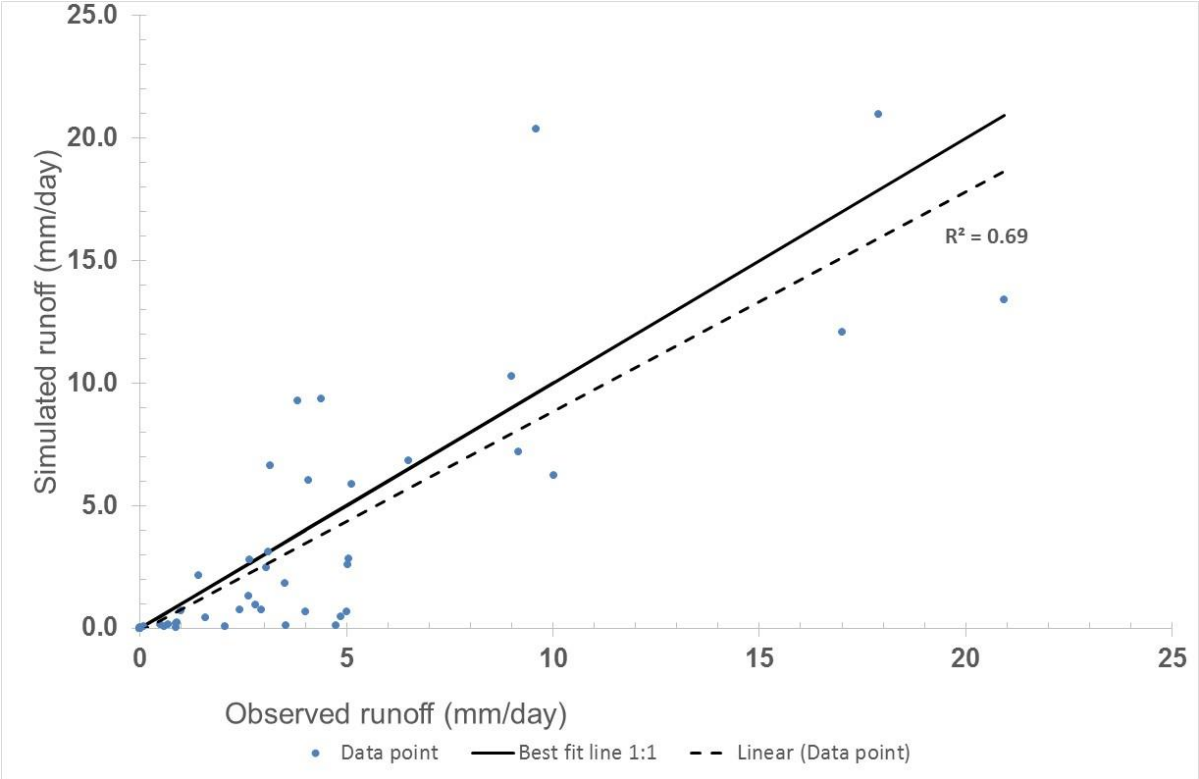

Figure 7-3: Simulated runoff using rainfall disaggregated using rainfall disaggregated by the range Bins method (Boughton, 2000)

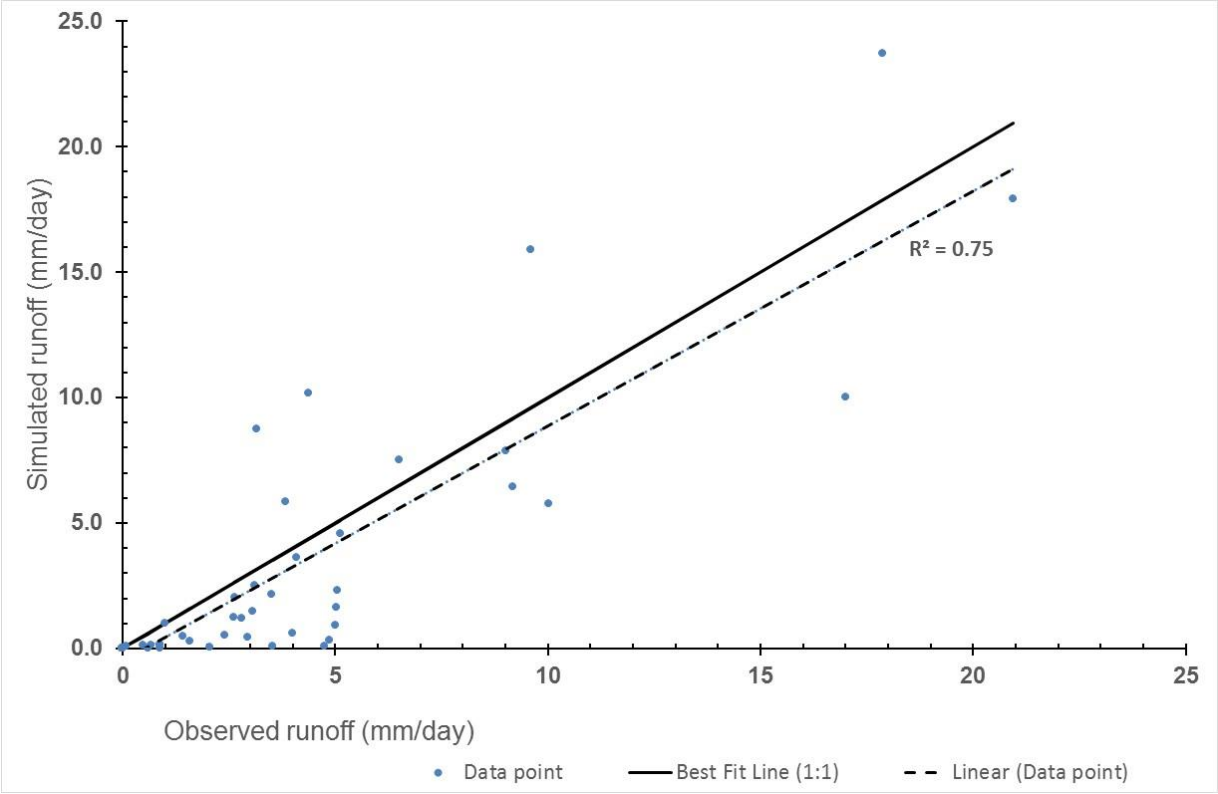

Figure 7-4: Comparison of simulated runoff against observed runoff using rainfall disaggregated by an empirical approach

Figure 7-5 shows a plot of simulated values plotted against observed values for two independent sites located in Zhulube catchment shown as field C and field D in Figure 4-9 (chapter 4). The results with a coefficient of determination, R^2 of 0.68 shows that the modelling was fairly successful. The linear fit on Figure 7-5 with an intercept of 1.27 and gradient of 1.36 is an additional indicator of model performance. This shows that the model generally overestimated the simulated runoff. As previously suggested this could be due to the fact that the sub models of equation 7-1 assumes a linear relationship between the output and the input variables. A search for the correct form of the submodels could improve the performance of the model.

Table 7-4 shows a summary of the performance of the Field scale rainfall runoff fuzzy model using the same data as in model development and data obtained from the

independent sites. It can be seen that the model performance was nearly the same for both sites.

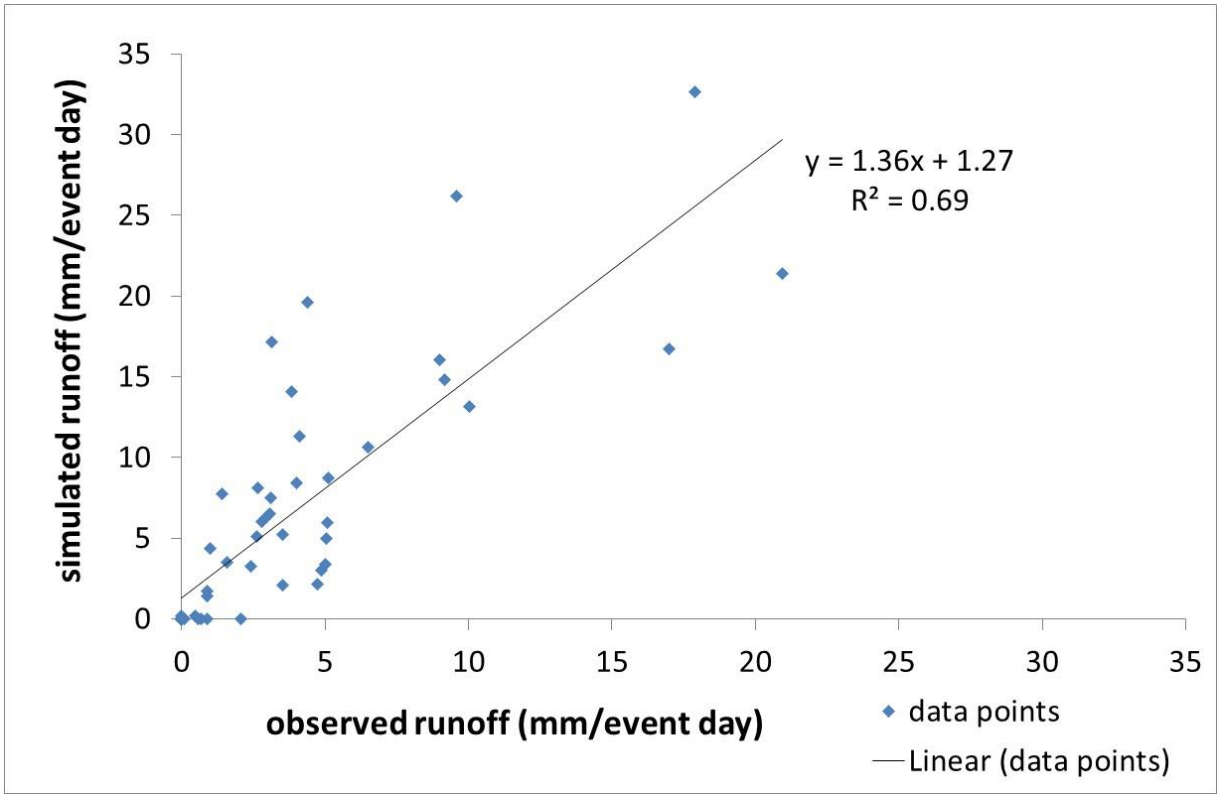

Figure 7-5: Comparison of simulated runoff against observed runoff for a different data set from an independent site

Table 7-4: Field scale rainfall runoff fuzzy model performance

Model performance criteria	Data used in model development	Separate data from that used in model development	Model Performance Rating	
			Best	Satisfactory
Coefficient of determination	0.747	0.675	1	0.5
Nash–Sutcliffe efficiency (NSE)	0.673	0.615	1	0.5
Percent bias (%) (PBIAS)	20.3	18.9	0	<15 to 55

7.2 Modelling soil moisture changes in a field with contour ridges

This section presents the results of the modelling of rainwater harvesting by contour ridges. Its performance was tested using observed soil moisture. It also demonstrates its application through determining the water partitioning in the three hydrological subzones of a contour ridged field that were identified in chapter 5. It ends with a discussion of possible improvements to design of contour ridges.

7.2.1 Input data and estimated parameters

Model input time series data was limited by observed records of rainfall and pan evaporation that were done from November 2008 to 31 May 2011. This data together with the observed soil moisture data per subplot in the DLC of both field A and field B are shown in A. Rainfall data was observed and recorded as daily totals and was disaggregated into mean rainfall intensity and duration for each rainfall day using the method described in Chapter 5 Section 5.6.2. Transpiration and soil evaporation were determined from the evaporative demand of the day using pan evaporation as an indicator of the evaporative demand of the day.

The plot of data on daily rainfall totals and rainfall intensity obtained from the Meteorological stations nearest to the study site of Masvingo (about 100km east of study site) and Bulawayo (about 80km north west of study site) where records could be obtained is shown in Figure 7-7. The data that could be obtained from the meteorological stations was limited and only a few points were ploted to provide the general relationship between daily rainfall amount and average rainfall intensity. The data points are scattered around an exponential curve represented by Equation 7-2. The deviation of the data points from this exponential curve are estimated by Equation 5-24 in chapter 5. The rainfall intensity used as input data in the model was then estimated by adding the result of Equation 7-2 to that of Equation 5-24 in chapter 5.

$$I_e = 3.51e^{-0.004P}$$ Equation 7-2

Where:
I_e is the estimated rainfall intensity for a daily rainfall amount P.

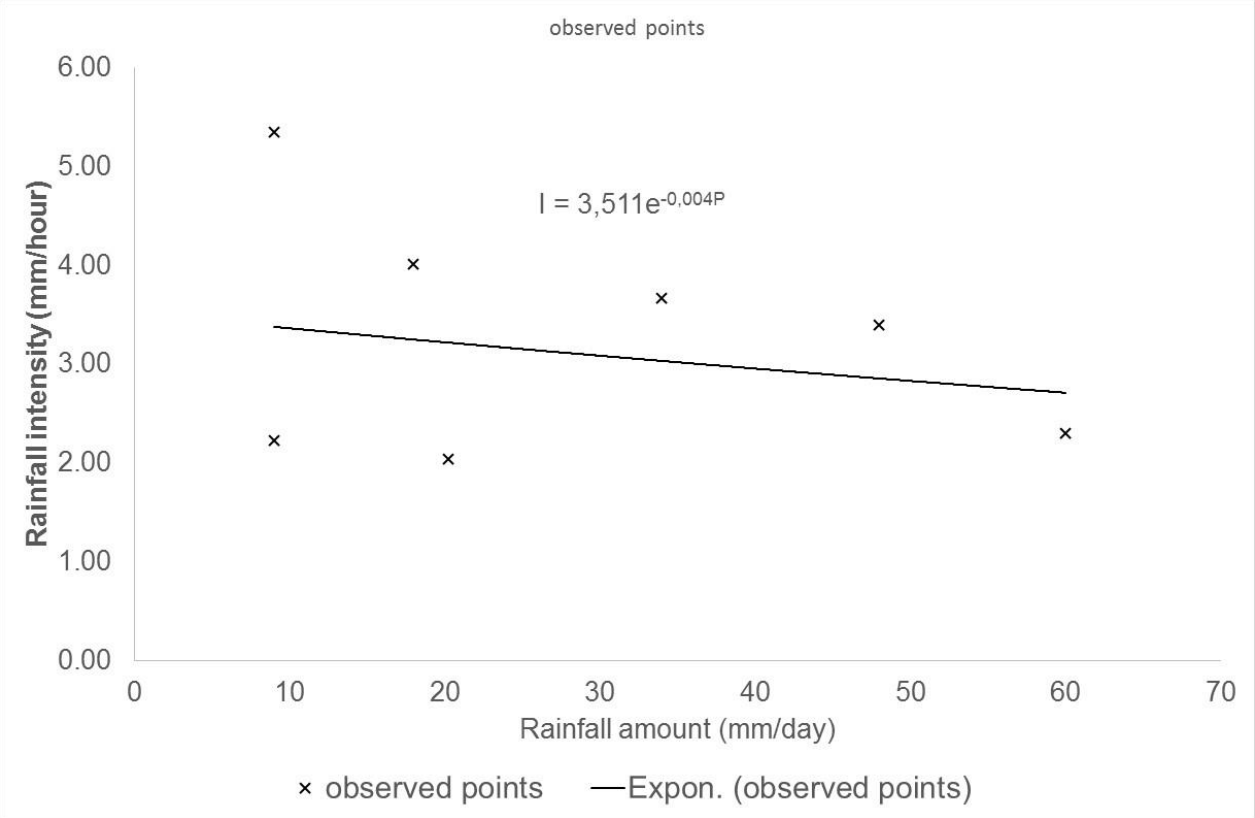

Figure 7-7: Variation of mean rainfall intensity with rainfall amount

The hydraulic conductivity and diffusivity with soil was estimated using an empirical equation which was based on the assumed dependents of unsaturated hydraulic conductivity on soil moisture gradient in line with Mahrt and Pan (1984) thin layer soil hydrology model. The empirical equation was developed from data obtained from the study site. The empirical relation is shown in Figure 7-8. Details of how the observed data were used to develop this empirical relation are given in appendix A.

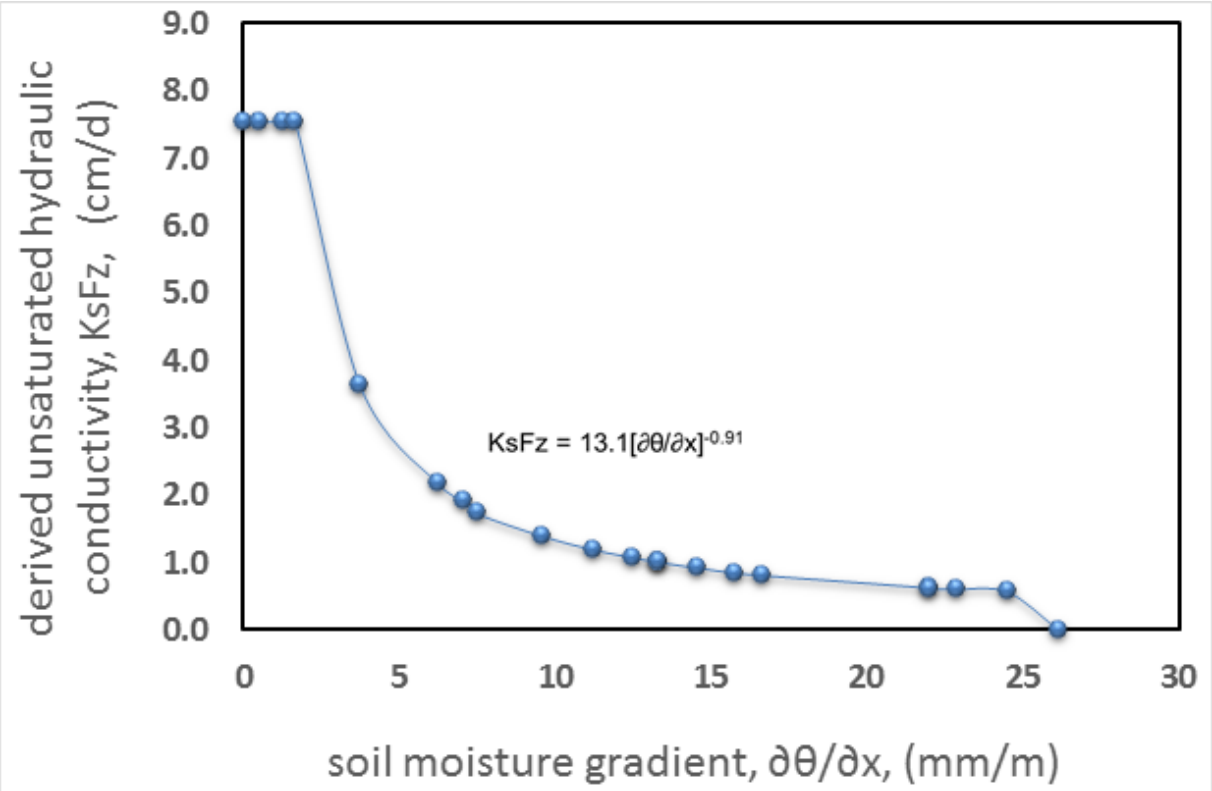

Figure 7-8: Variation of derived unsaturated hydraulic conductivity with soil moisture gradient using data from site

Soil evaporation proved to be critical to the model performance. Unlike transpiration which ends at wilting point soil evaporation ends before wilting point with the reduction in soil evaporation due to soil moisture stress being controlled by an exponential function that includes a reduction scale parameter as described in Equation 5-7 (Makurira et al, 2009). Both the reduction scale and the soil moisture at which soil evaporation stops were considered as values that needed to be established in the study as they could not be established from literature. Data for the first growing season (2009/10) during which soil moisture data was obtained was used to determine the best values of the soil moisture at which soil evaporation stops and the applicable reduction scale. The data for the second growing season (2010/11) was then used to verify the model. The soil moisture per root zone was obtained by averaging the soil moisture of the three soil horizons (A to C) each comprising 200mm. The loam soil of farm A has a shallow depth averaging 600mm.

7.2.2 Sensitivity analysis of the model

A sensitivity analysis was carried out to establish the sensitivity of the model output to variations to the model parameter values using the method described in chapter 5 section 5.7. The model parameters that were considered for sensitivity analysis were those that influence soil moisture. These were grouped into those that relate to soil water retention and those related to loss of water from the soil through evapotransipiration. The soil water retention parameters considered were infiltration capacity of the soil, soil moisture at field capacity and soil moisture at wilting point (Equation 5-4 and Equation 5-6). The infiltration capacity determines how fast the water infiltrates into the soil while the soil moisture at field capacity and at wilting point determine the water available for evapotranspiration. Model parameters influencing water loss during evapotranspiration that were considered were the pan evaporation factor, soil water depletion fraction, soil evaporation factor and the reduction scale (Equation 5-6 and Equation 5-7).

Figure 7-9 shows the graphical representation of the sensitivity of the model outputs to input parameter values represented by the PBIAS at different parameter values. The model outputs showed highest sensitivity to variation of the value of soil moisture at field capacity followed by variation in the value of the reduction scale. The next model parameter to influence model output was the pan evaporation factor. The soil evaporation factor and the soil water depletion fraction (p fraction) had moderate sensitivity while the model showed no sensitivity to infiltration capacity and soil moisture at wilting point.

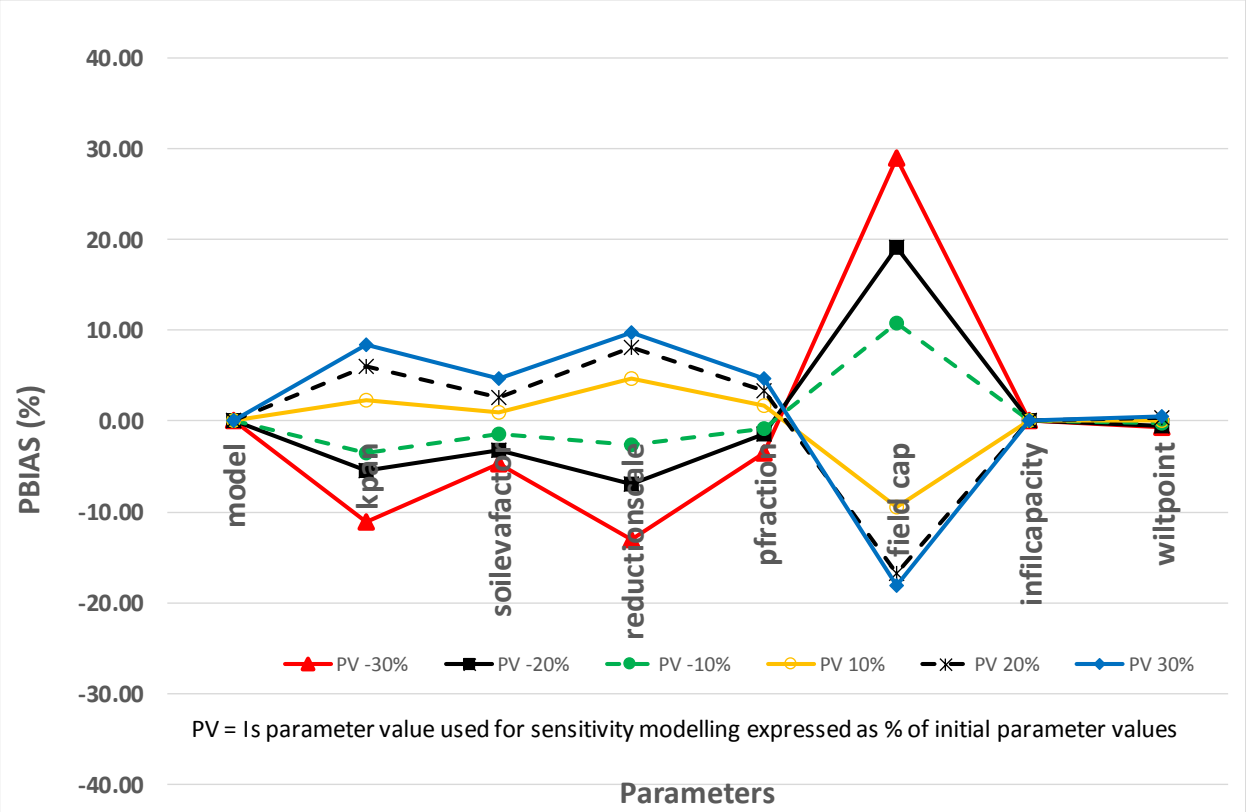

Figure 7-9: Sensitivity of model output to input parameters

Comparison of the sensitivity of the different parameters was done using the condition number as described in section 5.7 (Hoyos and Cavalcante, 2015). Generally the higher the condition number the more sensitive the model is to the parameter. The difference between the smallest and the largest CN value for each parameter was calculated and recorded as Delta CN in Table 7-5. The Delta CN was used to compare the sensitivity of the different parameters with the parameter having the highest value regarded as the most sensitive and that with the least value as the least sensitive. The reduction scale with a DeltaCN of 101 and the pan evaporation factor with a DeltaCN of 99 were found to be the most sensitive values. The model was also found to be moderately sensitive to soil moisture at field capacity with DeltaCN of 56. The soil evaporation factor (DeltaCN of 3.5) and soil water depletion fraction (DeltaCN of 3.8) showed low sensitivity. Of the three most sensitive model parameters the soil moisture at field capacity can be established from soil samples in the laboratory thus reducing uncertainity in the model. The pan evaporation factor is well established and uncertainity reduction depends on correct installation of the evaporation pan in the field. The method for establishing the correct

value of the reduction scale is not well established. An investigation to establish the best way of estmating the reduction scale was therefore carried out in and the results are given in section 7.2.3.

Table 7-5: Comparison of parameter sensitivity using the condition number

Model Parameter	minimum CN	maximum CN	deltaCN
kpan	-100.7	-1.6	99.1
soilevafactor	-4.5	-1	3.5
reductionscale	-64.1	37	101.1
pfraction	-4.6	-0.8	3.8
fcapacity	-50	5.5	55.5
wiltpoint	-0.3	-0.1	0.2
infilcapacity	0	0	0

7.2.3 Model sensitivity to the reduction scale

Figure 7-10 shows modelled soil moisture plotted against observed soil moisture for the 2009/10 growing season for three different values of the reduction scale. Figure 7-10(a) is for a reduction scale of 6, Figure 7-10(b) for a reduction scale of 7.5 and Figure 7-10(c) for a reduction scale of 12. The model generally overestimated the soil moisture as can be seen from the graph and this is confirmed by the model performance tests based on percent bias reported in Table 7-6. Although a reduction scale of 12 gives the best percent bias values it can be seen from the graph that in terms of the soil moisture simulation during the dry season the model underestimated the soil moisture when compared to the observed values and therefore compensated for the overestimation during the wet season in computing the bias. The results on Figure 7-10 showed that a constant reduction scale was not appropriate and a variable reduction scale based on prevailing soil moisture was then considered. After some trials, a satisfactory reduction scale was found to be equivalent to the prevailing profile soil moisture minus half the wilting point soil moisture. This provided considerably better results in terms of all the model performance criteria as seen in Table 7-6 and clearly seen graphically in Figure 7-11.

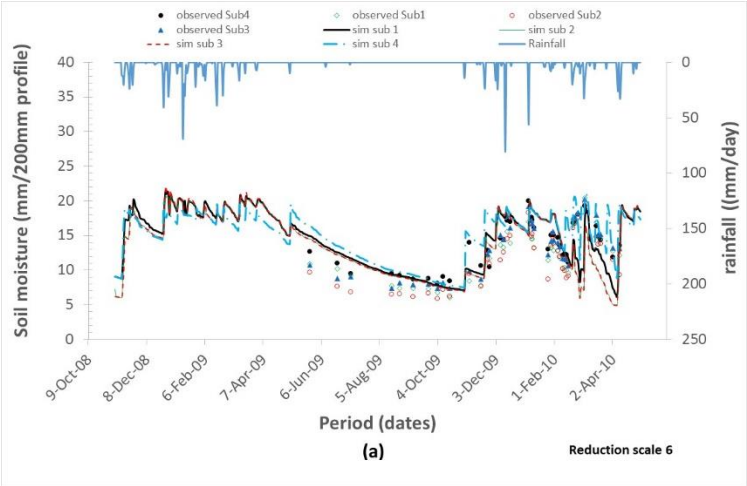

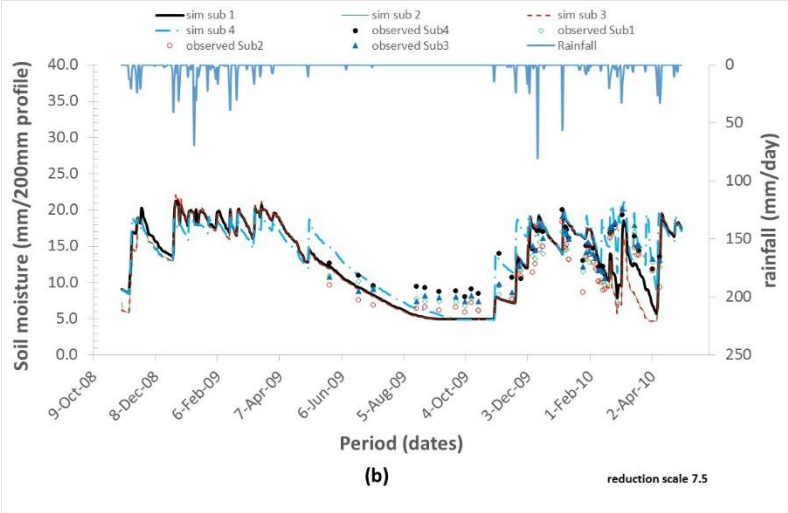

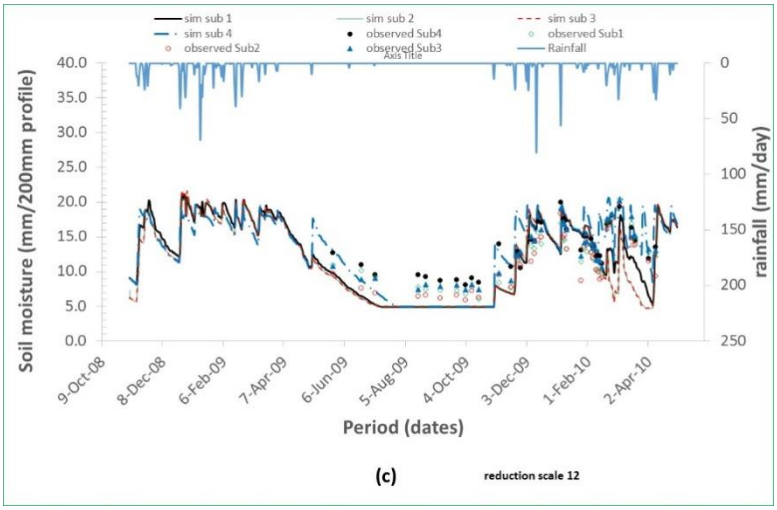

Figure 7-10: Modelled soil moisture compared to observed moisture in the DLC plot for constant reduction scale

Table 7-6: Model perfomance results for different values of reduction scales

Model performance criteria	Reduction scale				Model Performance Rating	
	6	7.5	12	Variable*	Best	Satisfactory
Nash–Sutcliffe efficiency (NSE)	0.346	0.424	0.430	0.657	1	0.5
Percent bias (%) (PBIAS)	-18.0	-6.9	-1.42	-1.28	0	<15 to 55

* Variable Reduction scale = Profile moisture-0.5×wilting point

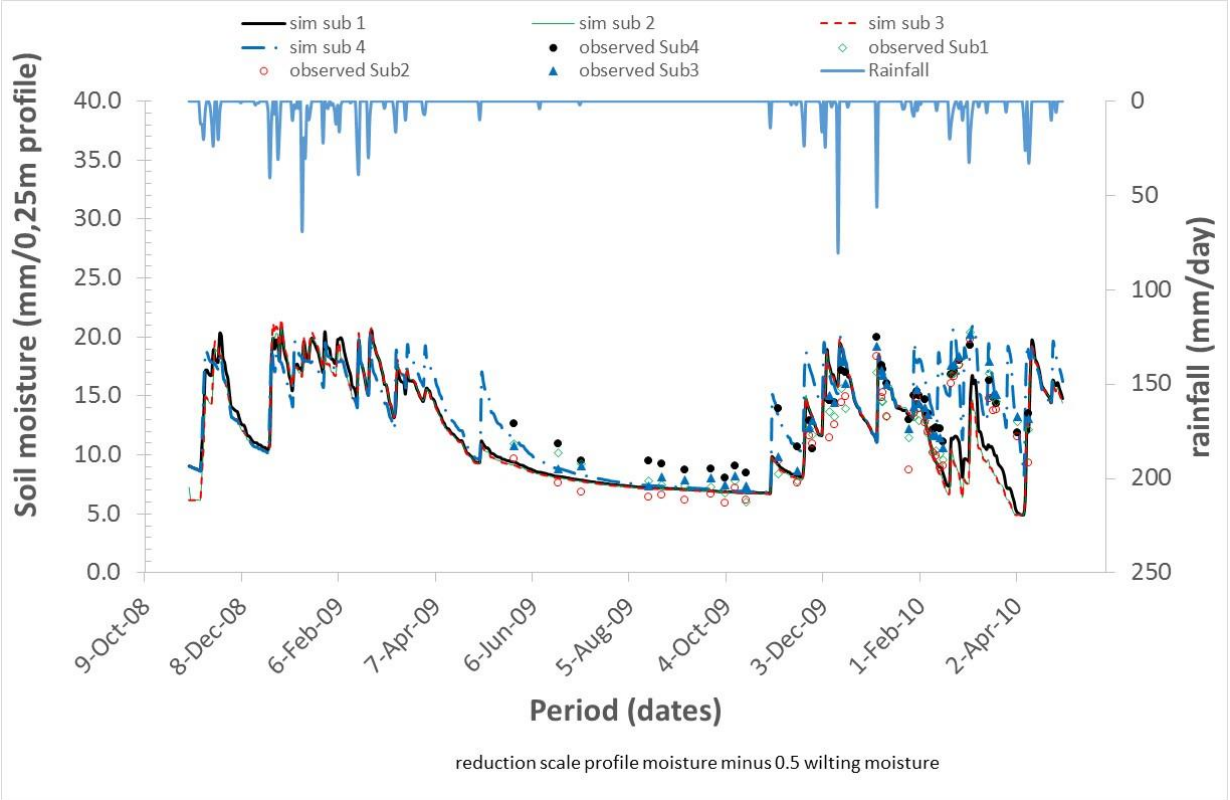

Figure 7-11: Modelled soil moisture compared to observed moisture in the DLC plot for a reduction scale based on prevailing soil moisture

7.2.4 Contour Ridge Model output and performance

Running the model during the second growing season of 2010/2011 as part of model verification showed that the model performance remained good as can be seen in Figure

7-12 and Table 7-7. The model however underestimated values in the verification stage as indicated by the percent bias performance criterion while the other model performance criteria remained very good.

The model was again applied to model the soil moisture in a contour ridged sandy soil (farm B) without further calibration and the results are shown in Figure 7-13 and the model performance in Table 7-7. The model showed good performance comparable to the performance when modelling the loam soil (farm A).

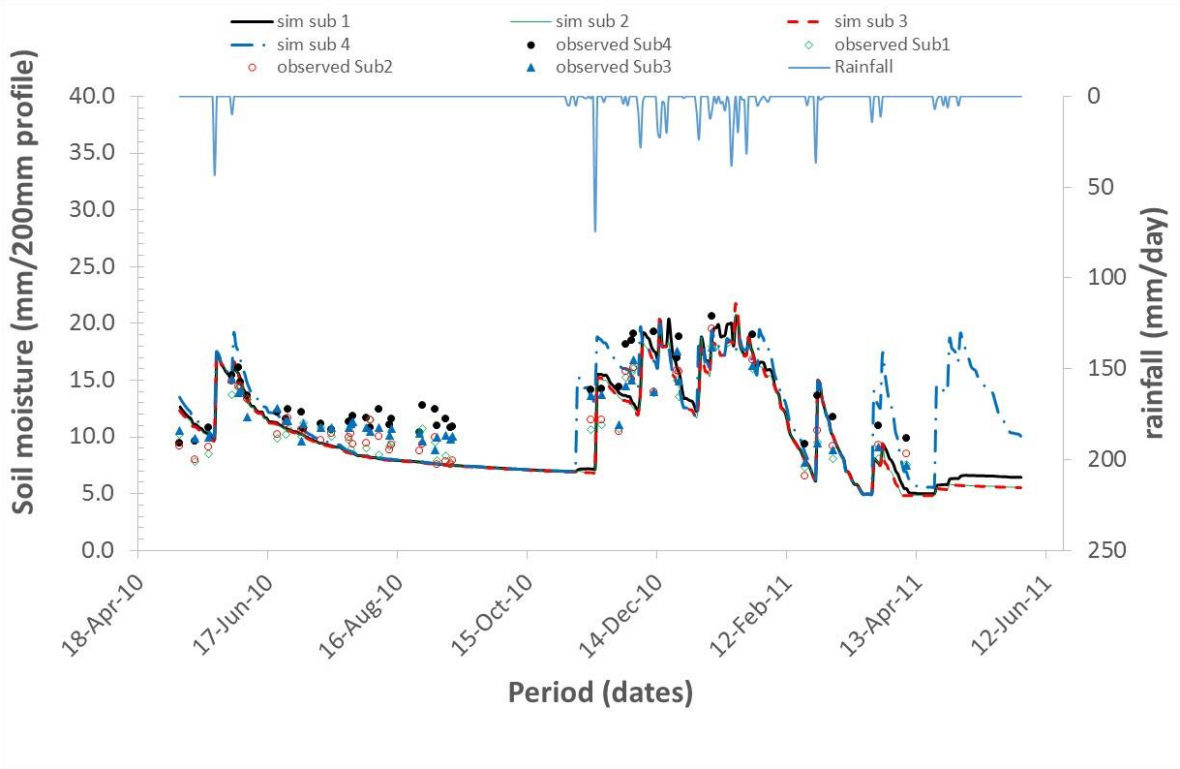

Figure 7-12: Results of model verification for the second growing season Farm A

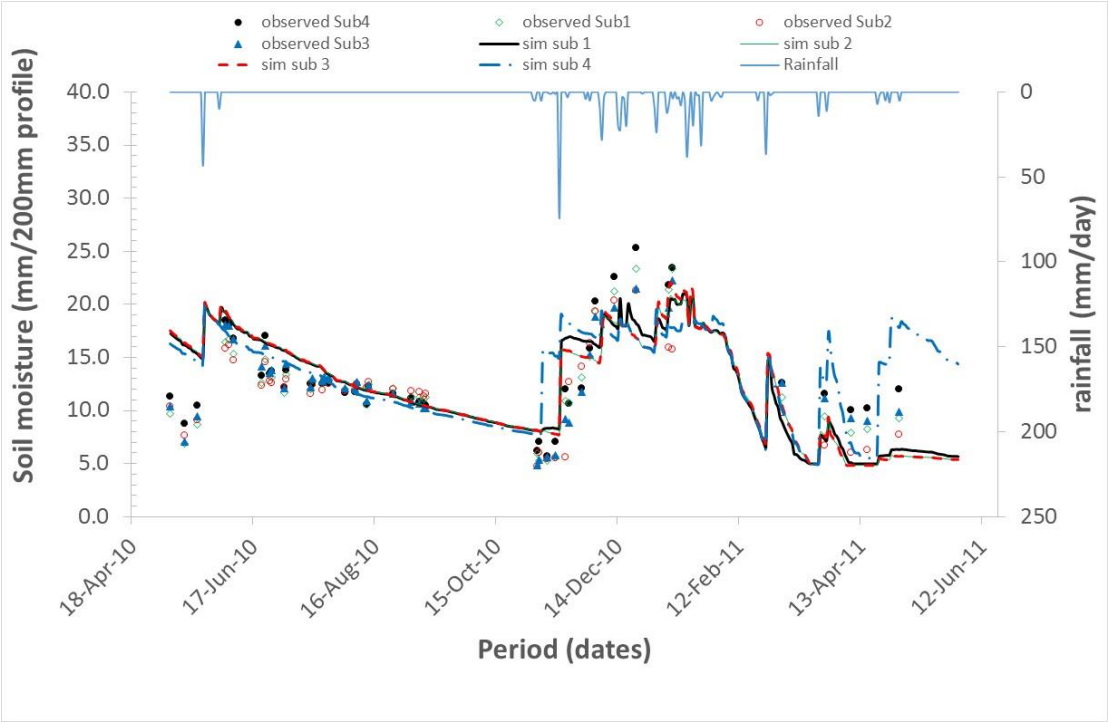

Figure 7-13: Results of model verification for the second growing season Farm B

Table 7-7: Results of model performance test for different data at Farm A and Farm B

Model performance criteria	Model after Calibration (setting reduction scale) Farm A	Model verification Farm A	Model verification Farm B
Nash–Sutcliffe efficiency (NSE)	0.657	0.522	0.622
Percent bias (PBIAS)	-1.28	6.1	-5.3
Root mean square error observed standard deviation (RSR)	0.586	0.627	0.615

7.3 Application of model to assess water partitioning in the subregions of a contour ridged field

Table 7-8 shows the model results summarising the mass balance of the water in the three subplots constituting the cropped area of the dead level contour treatment of field

A (with loam soil). Runoff (R_{off}) generation and infiltration (F) increases with subplot location downslope from the contour ridge. R_{off} generated in the upper subplot becomes run-on (R_{on}) for the downslope subplot adding on to the water of the downslope subplot. This is why the R_{off} and F of the downslope subplot become higher than the upper subplot. Table 7-9 shows the similar results for field B (with sandy soil) where the runoff amount is much less compared to that in field A. In both cases the mass balance results are presented as a depth meaning that the water volume is spread over the area per metre width of each subplot. This means over a length of 6.7m for subplot 1, 2 and 3 and 0.9m (the contour contour channel width) for the contour channel.

Table 7-8: Modelled annual water mass balance in the cropped area of contour ridged field A (loam soil) in Zhulube Catchment averaged over the 2008/2009 to 2010/2011 seasons

Water flux (See # below)	P (mm)	R_{on} (mm)	Total influx (mm)	I (mm)	R_{off} (mm)	F (mm)	Total outflux (mm)
Upper subplot (subplot 1)	567	0	567	197.2	118	251.8	567
Mid-contour subplot (subplot 2)	567	118	685	197.2	165	322.8	685
Lower subplot (subplot 3)	567	165	732	197.2	189.8	345.0	732

Water flux notations: P is Precipitation; R_{on} is Surface run-on to the subplot; I is Interception from the subplot; R_{off} is Surface runoff from the subplot; F is Infiltration

Table 7-9: Modelled annual water mass balance in the cropped area of contour ridged field B (sandy soil) in Zhulube Catchment averaged over the 2008/2009 to 2010/2011 seasons

Water flux (See # below)	P (mm)	R_{on} (mm)	Total influx (mm)	I (mm)	R_{off} (mm)	F (mm)	Total outflux (mm)
Upper subplot (subplot 1)	567	0	567	197	39	330	567
Mid-contour subplot (subplot 2)	567	39	606	197	49	360	606
Lower subplot (subplot 3)	567	49	616	197	51	368	616

Table 7-10 and Table 7-11 show the results of the runoff partitioning in the contour ridge for field A and field B respectively. These results are summed from the model outputs on a daily time step to provide the annual total. The model did not cater for the sub daily processes in the contour ridge channel. However the runoff which was an input to the runoff partitioning in the contour ridge channel was modelled incoporating sub daily processes in the form of rainfall intensity. In addition spillage was catered for, although at a daily time step (Equation 5-3), thus the model was expected to pick spillage if it occured. During field observations throughout the three rain seasons there were no heavy rains that caused the DLC contour ridges to spill and the model results also showed that there was no spillage. This is an additional indicator that the modelling was realistic.

In the loom soil (field A) the runoff from the cropped area above the contour ridge channel was more than the precipitation that directly fell on the contour ridge channel. This resulted in a total infiltration within the channel that was 2.1 times more than the rainfall amount. While the average infiltration in the subplot downstream of the contour ridge channel was 252mm/season that in the contour ridge channel was modelled as 1381mm/season. This shows more water available within the contour ridge channel or the area around it compared to the adjacent subplot. The availability of this water for crop production would depend on the processes that take place on the water once it has infiltrated from the contour ridge channel. This was determined by assessing the soil moisture partitioning in the root zone of the contour ridge channel and the adjacent cropped field subplots as presented in Table 7-12. On the other hand in the sandy soil (field B) the total infiltration in the contour ridge channel is almost the same as the

precipitation amount received and is not very much different from infiltration within the cropped area.

In the loam soil (field A) the run-on to the contour ridge is greater than the precipitation on the contour ridge channel because the runoff is estimated from subplot 3 where it is generated with a width of 6.2m (three subplots and one contour ridge over 20 m spacing) and then accumulated over the contour ridge channel with a width of 900mm. Effectively a 1177mm run-on to the contour ridge channel is equivalent to 190mm runoff from subplot 3.

Table 7-10: Model results of annual water mass balance in the contour ridge channel of a contour ridged field A in Zhulube Catchment averaged over the 2008/2009 to 2010/2011 seasons

Water flux (See *# below)	P (mm)	R_{on} (mm)	Total influx	E_c (mm)	I (mm)	R_{off} (mm)	F (mm)	Total out flux
Amount (mm/for 3 seasons)	1701	3531	5232	561	528	0	4143	5232
Average (mm/ season)	567	1177	1744	187	176	0	1381	1744
Average (% of Precipitation)	100	208	308	33	31	0	244	308

 # Water flux notation: P is Precipitation, R_{on} is Surface run-on to the contour ridge channel, E_c is Evaporation (open water) from the contour ridge channel, I is Interception (from soil surface) from the contour ridge channel, R_{off} is Surface (spillage) runoff from the contour ridge channel and F is Infiltration from contour ridge channel.

Table 7-11: Model results of annual water mass balance in the contour ridge channel of a contour ridged field B in Zhulube Catchment averaged over the 2008/2009 to 2010/2011 seasons

Water flux (See *# below)	P (mm)	R_{on} (mm)	Total influx	E_c (mm)	I (mm)	R_{off} (mm)	F (mm)	Total out flux
Amount (mm/for 3 seasons)	1701	918	2619	411	512	0	1696	2619
Average (mm/ season)	567	306	873	137	171	0	565	873
Average (% of Precipitation)	100	54	154	24	30	0	100	154

The results of modelling soil moisture in the root zone of a loam soil (Farm A) are shown in Table 7-12 while those from a sandy soil (Farm B) are shown in Table 7-13. The results show that most of the water that was harvested by the contour ridge channel was lost to groundwater recharge in the subplot immediately downslope of the contour ridge channel and possibly through macropore spaces to either downslope subplots or to groundwater recharge. The contribution of the lateral flow to the downslope subplot (subplot 1) was about 25% of the infiltration that took place in that subplot. The value of 785mm is spread over 900 mm width while the subplots are 6.2m. So the actual change in moisture over the downstream subplot was effectively modelled as 63mm but could have been 126mm if all the water was transferred to downslope subplot. However field observations as shown by spatial distribution of soil moisture presented in Chapter 6 suggested that the damming effect contibuted more to spatial differences in soil moisture than lateral flow (seepage). When comparing the results from the loam soil and the sandy soil the model does not clearly show this effect which suggest that it requires further improvements to correctly model the damming effect.

Table 7-12: Model results for annual water mass balance in the root zone of a contour ridged field A in Zhulube Catchment averaged over the 2008/2009 to 2010/2011 seasons.

Water flux (See **# below)	F (mm)	L_{in} (mm)	Total influx	T (mm)	E_s (mm)	G (mm)	L_{out} (mm)	M_p (mm)	Total out flux
Upper subplot (subplot 1)	251.8	63	315	49.1	131.8	54	27.2	53	315
Mid-contour subplot (subplot 2)	322.8	12	335	43.5	146	116	0	29.3	335
Lower subplot (subplot 3)	345	55	400	45.1	149.4	164	0	41.5	400
Contour ridge channel (subplot 4)	1381	0	1381	44	153.4	349	785	49.4	1381

 # Water flux notation: F is Infiltration into the root zone, L_{in} is Influx from the adjacent subplot, L_{out} is Outflux to adjacent subplot, T is Transpiration from the root zone, E_s is Evaporation from the soil in the root zone, Mp is Outflow through macroopores and G is Flow to groundwater system.

Table 7-13: Model results for soil moisture partitioning in the root zone of a contour ridged field B in Zhulube Catchment averaged over the 2008/2009 to 2010/2011 seasons.

Water flux (See **# below)	F (mm)	L_{in} (mm)	Total influx	T (mm)	E_s (mm)	G (mm)	L_{out} (mm)	M_p (mm)	Total out flux
Upper subplot (subplot 1)	330	18	348	66	71	65	13	133	348
Mid-contour subplot (subplot 2)	360	18	378	61	68	65	0	184	378
Lower subplot (subplot 3)	368	18	386	61	70	65	5	186	386
Contour ridge channel (subplot 4)	565	0	565	95	70	181	198	22	565

7.4 Discussion of results

The number of cluster centres obtained in the fuzzy modelling was considered to be the optimum for the available data. If more data was available a different number of cluster centres could probably have been obtained. Katambara and Ndiritu (2009) identified ten cluster centres for a similar fuzzy model developed for the Letaba River streamflow modelling.

The correlation coefficients of 0.76 and 0.68 between observed and simulated runoff per day event obtained from the model agree favourably with the values obtained by Zere et al. (2005) of 0.58 to 0.74 for a conventional tilled maize field in the Free State Province of South Africa. The data used by Zere et al. (2005) was obtained over 18 years.

The performance of the rainfall runoff modelling was constrained by lack of data to improve the developed fuzzy model given the scarcity of historical runoff data at field scale. The data points used were clearly too few to develop a good model as it was only obtained for a few years. Field scale data is mormally only corrected during experiments unlike for catchment scale data that can be obtained from national data bases were it is archived after long term collection. Thus model development at catchment scale have more rainfall runoff data to use in the development. Despite the poor data this study demonstrated that with adequate data say for a national project a fuzzy logic has potential to adequately model runoff at field scale as it can capture the important factors that affect

runoff generation such as soil type, rainfall intensity and duration and antcedant soil moisture.

The soil moisture model appears to have performed reasonably well. The model performance with NSE value of 0.66 and PBias value of -1.3% compare favourably with the results obtained by Ruidisch *et al.* (2013) who modelled ridge cultivation in South Korea using HYDRUS 2D model whose performance on a similar soil (loam) in which NSE value of 0.48 and PBIAS of 12% were obtained. The model performance falls within the general satisfactory range for modelling as proposed by Moriasis et al (2007) while that of Ruidisch *et al.* (2013) is just satisfactory. Further the model provided consistent performance considering that when applied to a sandy soil the NSE value was 0.62 and PBIAS was -5.3% which is not much different from the performance on the loam soil. This is against the performance of the HYDRUS 2D model used by Ruidisch *et al.* (2013) which gave a performance range of NSE=0.48 and PBIAS=12% on one site and NSE=0.79 and PBIAS=2% on the other where the soil was characterised by a granitic bedrock layer at 1 m depth. Similar modelling by Makurira et al. (2009) and Makurira (2010) in Tanzania does not indicate the model performance in terms of evaluation criteria. However based on the graphical presentation of the model results, the modelling here appears to have performed better.

The simulated infiltration amounts ranging from 250mm to 350mm and observed total dry matter yield ranging from 1 959kg/ha to 3 282kg/ha gives further indications of the performance of the model. Abu-Zreig and Tamimi (2011) in a study for rainwater harvesting in Jordan established an empirical relation between infiltrated rainfall amount and dry matter yield of native vegetation and grasses. A threshold infiltration amount of 113mm was required before any yield could be realised. After this threshold amount a further infiltration of 1mm would result in an average yield of 24kg per ha. If the same threshold infiltration is assumed an average dry matter yield of 14kg/mm of infiltration was realised in this study. Although the dry matter yield per mm of infiltration in this study is lower than that observed by Abu-Zreig and Tamimi (2011) the difference could be attributed to the fact that for this study the yield was for only stover and grain while the study by Abu-Zreig and Tamimi (2011) the yield was for native vegetation and grasses. In addition the climatic conditions of the study sites are different. Therefore overall the dry matter yield can be considered to be comparable.

Although the soil moisture modelling developed in this study appears to have simulated the soil moisture reasonably well it still requires further improvements as can be seen from the model performance. The sensitivity analysis has shown that the model performance depends on how well the model will estimate the water losses particularly through evapotranspiration. While the evapotransipiration process is well understood its estimation is difficult in situations were there is insufficient amount of water in the soil which happens when the soil moisture is less than field capacity. Thus the correct estimation of both the field capacity and the evapotranspiration rate at periods when soil moisture is below field capacity is the main area of the model that caused uncertainity in the results. This means application of the model would require that the field capacity soil moisture be measured from the field rather than be estimated from soil texture. This study has clearly shown that the reduction scale is a function of the prevailing soil moisture. This needs verification in other modelling exercises that uses the same equation that applies the reduction scale and to establish the best formula for estimating the reduction scale.

Available data made it difficult to assess how accurately the model was able to simulate groundwater recharge. This would have been possible if say there was data on water table fluctuations within the modelled area. Thus the effect of estimation of vertical and lateral flow rate on the model output cannot be verified. This could also affect the model performance.

The soil moisture model performance could also have been affected by the estimation of flows into the macropore spaces which was based on the assumption that macropore spaces would reduce with an increase in moisture content of the soil. In practice some water could occupy macro pore spaces and may also be transported through macro pore structures of the soil leaving the macropore spaces being controlled by the macropore conductivity. Chiroco *et al.* (2010) suggested that lateral soil moisture redistribution during the rainy season is largely controlled by macro pore structure of the soil. Clothier and Green (1994) discussed how macro pore networks extending to the surface cause preferential transportation of irrigation water to higher depth resulting in poor distribution of irrigation water in the rooting depth.

Despite the model limitations it can still assist in design of contour ridges given that application of the model can show the spatial distribution of runoff generation and soil

moisture in the area between contour ridges. Design decisions that can be assisted by the model are contour ridge spacing which are considered to be affected by the need to control soil erosion, contour ridge channel dimensions which are considered to be affected by the need to retain water and effective use of a contour ridged field which depends on the water fluxes and the soil moisture distribution in a contour ridged field.

Soil erosion is related to the erosive power of the water which means the higher the runoff depth the higher the erosive power. If the spacing between contour ridges is too large more runoff accumulates before reaching the downward contour ridge resulting in erosion taking place. The model provides runoff results spatially distributed to the area between contour ridges. If the runoff depth of the downslope subplot exceeds a certain runoff depth threshold that is considered to cause erosion it therefore means with respect to soil conservation the spacing for contour ridges is too large and should be reduced.

The runoff partitioning that is done by the model shows how the water harvested by the contour ridge channel is distributed into various components. If the channel dimensions are too small the spillage component would be large signifying undersizing of the contour ridge channel. This would suggest that the contour ridge channel dimensions should be increased.

The soil moisture partitioning that takes place within the contour ridged field can also be estimated which may help in identifying possible improvements in the design that may be made such as that shown in Figure 7-14. For example the model results suggest that the lateral outflow from the contour ridge in the loam soil of 785.2mm is largely lost to groundwater recharge and macro porosity in subplot 1. It can therefore be argued that a mechanism to effectively transfer water harvested by the contour ridge channels is required if increased benefits are to be realised from rainwater harvesting by contour ridges. Such a mechanism could be based on imitating macropore fractures say by introducing perforated pipes leading from the contour ridge channel to downslope subplots that will carry the harvested runoff and allow it to infiltrate in the downslope subplots. These perforated pipes would act in a similar manner to that of drip irrigation systems as illustrated in Figure 7-14 but would require the size of perforations to be investigated in order to prevent the pipes from being blocked. This would result in more even distribution of harvested water and as a result reduce unproductive water loses by

reducing groundwater recharge and increasing transpiration. Drip irrigation systems are an efficient method of applying irrigation water to crops (Maisiri, 2004).

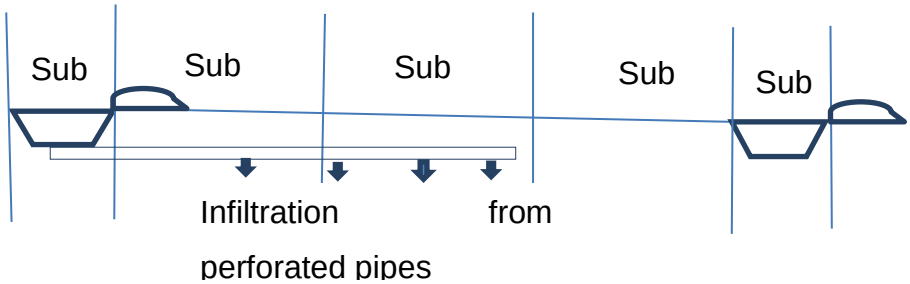

Figure 7-14: An illustration of perforated pipes proposed to transfer moisture from contour ridge channel to downslope subplots

The spatial soil moisture distribution in the contour ridged field may also be used to determine application of the field by deciding the cropping pattern. For example the areas located close to the contour ridge channel may be used for crops with a higher water demand while those further away may be used for more drought tolerant crops. The model helps to identify the spatial areas that should be targeted for the different types of crops. Researchers have shown that the contour ridged channel area can be used for cropping such as planting of cassava in a fanya juu channel (Makurira et al, 2009a).

While the model developed in this study provides reasonable results, it still fails to adequately show difference in soil moisture between subplots to the extent that was shown in observations. This limits the application of the model for design of contour ridges. The spatial distribution of soil moisture assists in matching the contour ridge spacing with crop water requirements. For example where the contour ridges are used for strip cropping the area close to the contour ridge could be used for a crop with higher crop water requirements. The soil moisture distribution could help to determine the area that would be planted with that crop. The limitation of the model could be because the model was developed without considering momentum and energy during rainfall partitioning in the cropped area. This affects the retention time of runoff within a subplot and hence the infiltration that takes place in that subplot.

8 CONCLUSIONS AND RECOMMENDATIONS

8.1 Conclusions

The main focus of this study was to investigate rainwater harvesting by contour ridges and develop a model for assisting in the design of contour ridges for water conservation. The use of contour ridges in Zimbabwe dates back to the 1950s when the practice was imported from USA and imposed on farmers as a soil conservation practice. The imported practice was designed essentially to safely drain away water from the field using graded contours. It was however found to be inappropriate in the low rainfall areas of Zimbabwe leading to adoption of dead level contours to retain the runoff within the field.

This study has extended the work that was carried out by Mugabe (2004) and by Mupangwa et al. (2011) by assessing the performance of dead level contour ridges in different soil types and comparing with the conventional graded contour ridges. The study further demonstrated the link among runoff generation, soil moisture improvement and a significant increase in crop yield in loam soils while in sandy soils contour ridges were found to have no significant effect on increase in crop yield. The study developed a field scale fuzzy rainfall runoff model for estimating runoff generation at field scale and a soil moisture simulation model based on process and fuzzy logic concepts. The model was formulated with three subsystems namely rainfall partitioning, runoff partitioning and moisture partitioning that corresponds to three subzones of a representative elementary watershed proposed by Reggiani et al. (1998). These three subsystems reflect the various hydrological processes taking place in a contour ridged field. Mass balance equations for each of the three subzones were developed and the methods that were used to estimate the components of each mass balance equation were described. One of the key components, the runoff generated from the cropped field which is then harvested by the contour ridge channels, was estimated using fuzzy logic. The application of fuzzy logic was considered for estimating runoff because it incorporates uncertainty and fuzziness that arise from description of variables that affect runoff generation such as soil type, soil moisture and rainfall characteristics comprising rainfall intensity and duration.

Field data for the study were obtained from experiments carried out in the semi-arid area of Zhulube which is located in Mzingwane Catchment, Matebeleland South Province of Zimbabwe. The experiment comprised of three farmer managed field plots containing Dead Level Contours (DLC) ridges, Graded Contours (GC) ridges and No Contour ridges on two fields; one with loam soil and the other with sandy soil. The data was collected for three seasons from November 2008 to May 2011.

The field observations showed that in loam soils DLC significantly improved soil moisture when compared to GC or having no contours at all ($P<0.05$). However, the GC plots had soil moisture not significantly different from the NC plots ($p>0.05$). The improvement in soil moisture was found to be due to generation of runoff in the loam soil which was harvested by DLC contour ridges which did not happen in the GC and NC plots. In the sandy soil field no significant improvement in soil moisture was realised in the DLC plot when compared to GC and NC plot. A significant increase in yield was also observed in the loam soil with DLC application but not in the sandy soil in agreement with the observed effects of DLC on soil moisture. The loam soil had a yield of 973kg/ha compared to 869kg/ha in the NC plot and 446 kg/ha observed in the GC plot. On the sandy soil the yield was 1073kg/ha compared to 820kg/ha in NC plot and 1052kg/ha in GC plot.

A rainfall runoff model for estimating runoff generated at field scale was developed in this study using fuzzy logic. Fuzzy modelling was found to provide an effective way of estimating daily runoff generated at field scale with the use of minimum data that can easily be obtained from different farmers' fields. While this fuzzy rainfall runoff model uses rainfall input variable in the form of hourly rainfall intensity and rainfall duration the rainfall data is readily available in the form of daily rainfall amounts. Rainfall disaggregation was done using two methods, the range bin method proposed by Boughton (2000) and modified for South Africa by Knoesen and Smithers (2009) and an approach based on a modification of the method used by Kusumastuti et al. (2007).

Using the method of subtractive clustering, five fuzzy submodels were established. These fuzzy submodels were found to correspond to linguistic description of how runoff is generated at field scale. Calibration of the fuzzy model was done by estimating the consequent coefficients of each of the five fuzzy submodels by applying the popular shuffled complex evolution method. The model was applied for rainfall events observed at four different fields performed reasonably well with the coefficient of determination of

0.75, a Nash-Sutcliffe Efficiency of 0.67 and overall percent bias of 14.2% to 20.3%. The model was then validated by applying it on rainfall events observed on two independent fields and again it performed reasonably well with the coefficient of determination of 0.68, the Nash-Sutcliffe Efficiency ranging from 0.62 and overall underestimation of runoff shown by a percent bias of 18.9%.

The fuzzy rainfall runoff model was integrated into a model for simulating soil moisture in a contour ridged field which was also developed in this study based on a hybrid of process and fuzzy logic approaches. The model was tested against soil moisture observed from two field sites, one with a loam soil and the other with a sandy soil. Data from the loam soil observed during the period November 2008 to April 2010 was used for model development while that from May 2010 to May 2011 and the data observed form the sandy soil for the period November 2008 to May 2011 was used for model verification. The overall model performance of the developed model was reasonably good with a Nash-Sutcliffe Efficiency of 0.657, overall percent bias of -1.28 and a Root mean square error observed standard deviation of 0.586. The model continued to perform well during verification with Nash-Sutcliffe Efficiency of 0.522, overall percent bias of 6.1 and a Root mean square error observed standard deviation of 0.627 on the loam soil and Nash-Sutcliffe Efficiency of 0.622, overall percent bias of -5.3 and a Root mean square error observed standard deviation of 0.615 on the sandy soil.

Soil moisture modelling results for the loam soil indicate that infiltration from rainfall partitioning within the area between contour ridges is highest in the area upstream of the contour ridge channel as runoff accumulates in this area. This is in line with field observation in this study which revealed that the area upslope of the contour ridge channel had the highest soil moisture. However in the sandy soil the modelled infiltration is highest in the area upslope of the contour ridge while observations do not suggest the same. The infiltrated water could have been fast drained from the root zone as the modelled results suggest that in the contour ridge channel there was more ground water recharge than lateral subsurface flow.

Based on the design of contour ridges spaced at 20m intervals implemented in the field work of this study, the runoff amount received by the contour ridges was estimated to be 43% more than the rainfall that directly falls on the contour ridge channel. The water that directly falls in the contour ridge channel from rainfall together with that which is harvested

from runoff generated in the upslope subplots is partitioned into evaporation from the channel and infiltration into the soil in the contour ridge channel. No overflow of contour ridge channel was experienced and hence the runoff received by the contour ridge and the rainfall either evaporated or infiltrated within the contour ridge channel. The water that infiltrates was estimated as 2.1 times the rainfall that directly falls on the contour ridge channel while that which evaporates as only 0.3 of the rainfall amount. The extra water infiltrating in the contour ridge is what runs off from the field to the contour ridge.

Although the modelling found that a high amount of water infiltrates into the soil in the contour ridge channel a large proportion of about 37% of the infiltrated water was lost to the ground water system in the area immediately downslope of the contour ridge channel and is not used for productive purposes. The modelling also found out that some of the water could have been lost through the macropore system to groundwater or to downslope areas.

The results of this study have shown that contour ridges are am important rainwater harvesting technique that improves both soil moisture and crop yield. In addition this study has produced a model that estimate runoff at field scale and estimate soil moisture in a field where rainwater harvesting by contour ridges have been applied. This helps improving understanding of how contour ridges improve soil moisture and can assist in helping field officers in selecting fields where optimum benefits from contour ridges can be obtained. The sensitivity analysis of the soil moisture modelling indicated that use of the model would require field data for soil moisture at field capacity and that it is affected by estimation of evapotranspiration. This helps researchers in this field of study to know the key factors that affect soil moisture depletion when soil moisture is below field capacity.

8.2 Recommendations

Although the field study design involved replicated soil moisture and crop yield measurements, it was carried out on two fields at one geographical site. A replication of the study on different geographical sites with different soil types is required to further evaluate the effectiveness of dead level contours for rainwater harvesting in different conditions.

The fuzzy model developed in this study to estimate runoff generation was based on limited rainfall and runoff data. The modelling needs to be updated when more data is available to especially improve the fuzzy inference system.

The model on soil moisture partitioning was based on a hybrid of process and fuzzy approaches. Although it has performed reasonably well, the methods of estimating some of the processes such as macropore flows were from the literature as field measurements were not available. Future studies should consider exploring field experiments for validating or improving such methods for estimation of these processes. In addition to these suggested improvements to the methods for estimation of these processes, the model structure of can also be improved. One of the suggested improvements to the model structure relates to the effect of slope in a contour ridged field. This could be improved by considering the representative elementary watershed approach in which conservation of momentum and energy will also be incorporated in addition to the conservation of mass that was included in the modelling in this study. This would ensure incorporation of forces acting in the contour ridge field in which the slope will be included.

9 REFERENCES

Abu-Awwad, A. M., 1997.Water infiltration and redistribution within soilsaffected by a surface crust, Journal of Arid Environments, Vol. 37 page 231–242.

Abu-Zreig M., Attom M. and Hamash N., 2000. Rainfall harvesting using sandy ditches in Jordan; Agricultural Water Management 46 pg 183-192, ELSEVIER.

Abu-Zreig M., Attom M. and Hamash N., 2000.Rainfall harvesting using sandy ditches in Jordan; Agricultural Water Management 46 pg 183-192, ELSEVIER.

Al Ali Y., Touma J., Zante P., Nasri S. and Albergel J., 2008. Water and sediment balances of a contour bench terracing system in a semi-arid cultivated zone (El Gouazine, Central Tunisia), Hydrological Sciences 53 (4) pg. 883-892, IAHS.

Allen R. G., 2000. Using the FAO-56 dual crop coefficient method over an irrigated region as part of an evapotranspiration intercomparison study. *Journal of hydrology, Vol. 229*, pg.27-41.

Andrade F. H., 1995. Analysis of growth and yield of maize, sunflower and soyabean grown at Balcarce, Argentina, Field Crops Research, Volume 41, pages 1-12, Elsevier Ltd.

Angelov P. P. and Filev D. P., 2004. An Approach to Online Identification of Takagi-Sugeno Fuzzy Models, IEEE Transactions on systems, man, and cybernetics—Part b: Cybernetics, Vol. 34, no. 1, pg. 484-498.

Barron J., 2004. Dry spell mitigation to upgrade semi-arid rain fed agriculture: Water harvesting and soil nutrient management for smallholder maize cultivation in Machakos, Kenya, PhD Thesis, Stockholm University.

Beven K., J., 2002. Towards an alternative blueprint for a physically based digitally simulated hydrologic response modelling system, Hydrological processes, Vol. 16, page 189-206, John Wiley and Sons, Ltd.

Beven K. J., 2001. Rainfall – Runoff Modelling: The Primer, John Wiley & Sons Ltd, West Sussex, England.

Beven K. J., 2004. Robert E. Horton's perceptual model of infiltration processes, Hydrological Processes, vol. 18 pg. 3447-3460, HP Today.

Biazin B., Sterk G., Temesgen M., Abdulkedir A. and Stroosnijder L., 2012. Rainwater harvesting and management in rainfed agricultural systemsin sub-Saharan Africa – A review, Physics and Chemistry of the Earth Vol. 47–48 pg. 139–151.

Boers Th. M., Zondervan K. and Ben-Asher J., 1986. Micro-Catchment-Water-Harvesting (MCWH) for Arid Zone Development, Agricultural Water Management, Vol. 12, Page 21-39, Elsevier Science Publishers, Amsterdam.

Bojadziev G. and Bojadziev M., 2007. Fuzzy logic for business, finance and management, 2nd Edition, World Scientific Publishing Company.

Boughton, W., 2000. A model for disaggregating daily to hourly rainfalls for design flood estimation. Report 00/15, Cooperative Research Centre for Catchment Hydrology, Monash University, Clayton, Victoria, Australia.

Brocca L., Melone F. and Moramarco T., 2008. On the estimation of antecedent wetness conditions in rainfall-runoff modelling, Hydrological processes, Vol. 22, page 629-42, Wiley InterScience, John Wiley and Sons, Ltd.

Brooks RH, Corey AT. 1964. Hydraulic properties of porous media.Hydrology Paper No. 3, Fort Collins, Colorado: Colorado State University; p. 27.

Bruins H. J., Evenari M.and Nessler U., 1986. Rainwater-harvesting agriculture for food production in arid zones: the challenge of the African famine, Applied Geographv, vol.6, pg. 13-32.

Butterworth J.A., Mugabe F., Simmonds L. P. and Hodnett M. G., 1999. Hydrological processes and water resources management in a dryland environment II: Surface redistribution of rainfall within fields, Hydrology and Earth System Sciences, Vol 3, pg. 333-343.

Chahinian N., Moussa R., Andrieux P. and Voltz M., 2005. Comparison of infiltration models to simulate flood events at field scale, Journal of Hydrology, Vol. 306, pg. 191-214, Science Direct, Elsevier.

Charlesworth P., 2005. Irrigation insights number 1, Soil Water Monitoring, An information package, 2nd Edition, Land and Water Australia, National Programme for Sustainable Irrigation, Canberra ACT 2601, ISBN: 192086568, www.lwa.gov.au.

Chibulu, B. 2007. Effect of rainfall variability on crop yield under semi-arid conditions at sub-catchment level, MSc Thesis (unpublished), University of Zimbabwe.

Chirico G. B., Medina H. and Romano N., 2010. Functional Evaluation of PTF prediction uncertainty: An application at hillslope scale, Geoderma, Vol. 155, pg. 193-202, Elsever Ltd.

Chiu S. L., 1994. Fuzzy model identification based on cluster estimation, Journal of Intelligent and Fuzzy Systems, Vol. 2, pg. 267-278. John Wiley and Sons, Inc.

Clothier B. E. and Green S. R., 1994. Rootzone Processes and the efficient use ofirrigation water, Agricultural Water Management Vol. 25, pg. 1-12, Elsevier.

Corradini C., Morbidelli R. and Melone F., 1998. On the interaction between infiltration and Hortonian runoff, Journal of Hydrology, Vol. 204.pg. 52-67, Elsevier.

Corradini C., Melone F. and Smith R. E., 1997. A unified model for infiltration and redistribution during complex rainfall patterns, Journal of Hydrology, Vol. 192, pg. 104-124, Elsevier Science.

Critchley W. R. S, Reij C. and Willcocks T. J., 1994. Indigenous soil and water conservation: A review of the state of knowledge and prospects for building on traditions, Land Degradation and Rehabilitation, vol. 5, page 293-314, John Wiley and Sons, Ltd.

de Groen M. M. and Savenije H. H. G., 2006. A monthly interception equation based on the statistical characteristics of daily rainfall, Water Resources Research, Vol. 42, pg. W2417 to W2427, American Geophysical Union.

Delin G. N., Healy R. W., Landon M. K. and Bohlke J. K., 2000. Effects of topography and soil properties on recharge at two sites in an agricultural field, Journal of the American Water Association, vol 36 No. 6 pg. 1401-1416, American Water Resources Association.

Dhliwayo C. T., 2006. An on farm comparison of conservation agriculture practices and conventional farmer practices on soil hydrology and maize yield. MSc Thesis, University of Zimbabwe, Harare.

Dondofema F., 2007. Relationships between gulley characteristics and environmental factors in the Zhulube Meso-Catchment: Implications for Water Resources Management, MSc Thesis, University of Zimbabwe, Harare.

Duan Q. Y., Gupta V. K. AND Sorooshian S. Communicated by Dixon L. C. W., 1992. Shuffled Complex Evolution Approach for Effective and Efficient Global Minimization, Journal of optimization theory and applications: vol. 76, no. 3, pg. 501-521.

Duan Q. Y., Sorooshian S., Gupta V. K., 1994. Optimal use of the SCE-UA global optimization method for calibrating watershed models, Journal of Hydrology Vol. 158 pg. 265-284.El-Hames A. S. and Richards K. S., 1995. Technical Note: Testing the numerical difficulty applying Richards' equation to sandy and clayey soils, Journal of Hydrology, Vol. 167, pg. 381-391, Elsevier Science.

Elwell H. A., 1981.Contour Layout Design, Department of Conservation and Extension, Government Printers, Harare, Zimbabwe.

Esteves M. and Lapetite J., M., 2003. A multi-scale approach of runoff generation in a Sahelian gully catchment: a case study in Niger, Catena, Vol. 50, pg. 255-271, Elsevier Science B.V.

Falkenmark M., Fox P., Persson G. and Rockstrom J., 2001. Water harvesting for upgrading rainfed agriculture, Problem analysis and research needs, Stockholm International Water Institute, Stockholm, ISBN 91-974183-0-7.

FAO, 2000. Manual on integrated soil management and conservation practices, FAO Land and Water Bulletin 8, ISBN 92-5-104417-1, Food and Agriculture Organisation of the United Nations, Rome.FAO, extract, www.fao.org/ag/ags/agse/7mo/69/chap10_2.pdf - Similar pages.

Feras M. Ziadat, Butros I Hattar and Akram S. Baqain, 2006. farmers verification of improved land-use alternatives in transitional Badia of Jordan, Renewable Agriculture and Food Systems, 21(4) pg. 207-215, CAB International.

Fiedler and Ramirez, 2000. A numerical method for simulating discontinuous shallow flow over an infiltrating surface, International Journal for Numerical Methods in Fluids, Int. J. Numer. Meth. Fluids 2000; 32:219-240.

Ganoulis J., 2006. Comparative Risk Assessment and Environmental Decision Making, NATO Science Series, Vol 38, Springer Netherlands.

Gao Y. and Lynch J. P., 2016. Reduced crown root number improves water acquisition under water deficit stress in maize (Zea mays L.), Journal of Experimental Botany, Oxford University Press, pg. 1-13.

Garen D. C. and Moore D. S., 2005. Curve number hydrology in water quality modeling: uses, abuses, and future directions, Journal of the American Water Resources Association (JAWRA), Vo. 41, No. 2, pg. 377-388.Gifford G. F., 1976. Applicability of some infiltration formulae to rangeland infiltration data, Journal of Hydrology, Vol. 28, pg. 1-11, Elsevier Scientific Publishing Company, Amsterdam.

Gumbo. D, 2006. Dead Level Contours, Technical Paper, Practical Action, http://practicalaction.org/practicalanswers.

Hagmann J., 1996. Mechanical soil conservation with contour ridges: cure for, or cause of, rill erosion? Land Degradation and Development Vol. 7, pg. 145-160.

Hatibu N. and Mahoo H. 1999. Rainwater harvesting technologies for agricultural production: A case for Dodoma, Tanzania, *Conservation tillage with animal traction.* A resource book of the Animal Traction Network for Eastern and Southern Africa (ATNESA). Harare. Zimbabwe. pg. 173-.

Hatibu N., Young M. D. B, Gowing J.W., Mahoo H. F. and Mzirai O. B., 2003. Developing Improved Dryland Cropping Systems For Maize In Semi-Arid Tanzania. Part 1: Experimental Evidence For The Benefits Of Rainwater Harvesting, *Expl Agric*, volume 39, pg. 279–292 C_ *2003 Cambridge University Press.*

Heddadj D. and Gascuel-Odoux C., 1999. Topographic and seasonal variations of unsaturated hydraulic conductivity as measured by tension disc infiltrometers at the field scale, European Journal of Soil Science, Vol. 50, pg. 275-283.

Hengsdijk H., Meijerink G. W. and Mosugu M. E., 2005. Modelling the effect of three soil and water conservation practices in Tigray, Ethiopia, Agriculture, Ecosystems and Environment, Vol. 105, pg. 29-40.

Hoyos E. M. and Cavalcante A. L. B., 2015. Sensitivity Analysis of One-Dimensional Infiltration Models, EJGA, Vol. 20., Bund. 10, pg. 4313-4324.

Hundencha Y., Bardossy A. and Theisen H. W., 2001. Development of a fuzzy logic-based rainfall-runoff model, Hydrological Sciences, Journal-des Sciences Hydrologiques, Vol. 46, Issue 3, pg. 363-376.

Jacquin A. P. and Shamseldin A. Y., 2009. Review of the application of fuzzy inference systems in river flow forecasting, Journal of Hydroinformatics, Vol. 11, pg. 202-210.

Jaafer, M. N., Kanemasu, E. T., Powers, W. L., 1978. Estimating soil factors for nine Kansas soils used in an evaporatranspiration model, Transactions Kansas Academic Science, Vol. 81 page 57-63.

Jasrotia A. S., Majhi A. and Singh S., 2009. Water Balance Approach for Rainwater Harvestingusing Remote Sensing and GIS Techniques, Jammu Himalaya, India, Water Resources Management, 23., pg. 3035–3055.

Jassbi J. J., Serra P. J. A., Ribeiro R. A. and Donati A., 2006. A comparison of mandani and sugeno inference systems for a space fault detection application, World Automation Congress (WAC) (2006), July 24-26, Budapest, Hungary.

Kapangaziwiri E., Hughes D. A. and Wagener T., 2009. Towards the development of a consistent uncertainty framework for hydrological predictions in South Africa, New Approaches to Hydrological Prediction in Data-sparse Regions (Proc. of Symposium HS.2 at the Joint IAHS & IAH Convention, Hyderabad, India, September 2009). IAHS Publ. 333., pg 84-93.

Kapangaziwiri E., Hughes D. A. and Wagener T., 2012. Incorporating uncertainty in hydrological predictions for gauged and ungauged basins in southern Africa, Hydrological Sciences Journal, 57:5, 1000-1019, DOI: 10.1080/02626667.2012.690881.

Katambara Z. and Ndiritu J., 2009. A fuzzy inference system for modelling streamflow: Case of Letaba River, South Africa, Physics and Chemistry of the Earth, Vol. 34, pg. 688–700.

Kaufmann, G., 2003. Modelling unsaturated flow in an evolving karst aquifer. *Journal of Hydrology, 276*, pg. 53–70.

Keskin M. E, Terzi O and Taylan D, 2004. Fuzzy logic model approaches to daily pan evaporation estimation in Western Turkey, Hydrological Sciences – Journal –des Sciences Hydrologiques 49 (6) pg. 1001-1010.

Keskin M. E., Terzi O. and Taylan D., 2004. Fuzzy logic model approaches to daily pan evaporation estimation in Western Turkey, Hydrological Sciences – Journal –des Sciences Hydrologiques 49 (6) pg. 1001-1010.

Khlifi S., Arfa H., D'beya L. B. D., Ghedhoui S. and Baccouche S., 2010. Effects of Contour Ridge Benches on Several Physical and Chemical Soil Characteristics at the El Ghrifettes Site (Zaghouan, Tunisia)., Arid Land Research and Management, Vol. 24, Issue 3, pg. 196-212.

Klaassen W., Bosveld F. and de Water W., 1998. Water storage and evaporation as constituents of rainfall interception, Journal of Hydrology, Vol. 212-213, page 36-50.

Knoesen D and Smithers J, 2009. The development and assessment of a daily rainfall disaggregation model for South Africa, Hydrological Sciences Journal, Vol. 54, issue 2, pg. 217-233, DOI: 10.1623/hysj.54.2.217.

Konukcu F., 2007. Modification of the Penman method for computing bare soil evaporation, Hydrological Processes, Vol. 21, Page 3627-3634, Wiley InterScience.

Krause P., Boyle D. P., Base F., 2005. Comparison of dierent eiency criteria for hydrological model assessment. Advances in Geosciences, European Geosciences Union (EGU), Vol. 5, pg.89-97.

Kuczera G., Kavetski D., Franks S. and Thyer M., 2006. Towards a Bayesian total error analysis of conceptual rainfall-runoff models: Characterising model error using storm-dependent parameters, Journal of Hydrology Vol. 331, pg. 161– 177.

Kumar R., Shankar V. and Jat M. K., 2014. Sensitivity Analysis of Nonlinear Model Parameters in a Multilayer Root Zone, Journal of Hydrologic Engineering, ASCE, Vol. 19, No. 2. Pg. 462-471.

Kusumastuti D.I. Struthers I., Sivapalan M., and Reynolds D. A., 2007. Threshold effects in catchment storm response and the occurrence and magnitude of flood events: implications for flood frequency, Hydrol. Earth Syst. Sci., Vol. 11, page 1515–1528, European Geosciences Union.

Laker M. C., 2004. Development of a general strategy for optimising the efficient use of primary water resources for effective alleviation of rural poverty, WRC Report No.KV 149/04. WRC, Pretoria.

Le Bissonnais Y., Benkhadra H., Chaplot V., Fox D. King D. and Daroussin J., 1998. Crusting, runoff and sheet erosion on silty loamy soils at various scales and upscaling from m 2 to small catchments, Soil & Tillage Research Vol. 46 page 69-80, Elsevier Science.

Lee H., Sivapalan M. and Zehe E., 2005. Representative elementary watershed (REW) approach, A new blueprint for distributed hydrological modelling at the catchment scale: Development of closure relations, Prediction in Ugauged Basins: Approaches for Canada's Cold Regions.

Li F., Cook S., Geballe G. T. and Burch W. R. Jr, 2000. Rainwater Harvesting Agriculture: An Integrated System for Water Management on Rainfed Land in China's Semiarid Areas, Ambio Vol. 29 No. 8, pg. 477-483., Royal Swedish Academy of Sciences.

Li X-Y., Xie Z-K. and Yan X-K., 2004. Runoff characteristics of artificial catchment materials for rainwater harvesting in the semi arid regions of China, Agricultural Water Management.Vol. 65 page 211–224.

Liu, Y., and Gupta H. V., 2007. Uncertainty in hydrologic modeling: Toward an integrated data assimilation framework, Water Resour. Res., 43, W07401, doi:10.1029/2006WR005756.

Liu Z. and Todini E., 2002. Towards a comprehensive physically based rainfall-runoff model, Hydrology and Earth System Sciences, 6(5), pg. 797-817, European Geophysical Society.

Liu, Q. Q., Chen L., Li J. C. and Singh V. P., 2004. Two-dimensional kinematic wave model of overland-flow. Journal of Hydrology, Vol. 291, pg. 28-41, Science Direct, Elservier.

Liu, Y. P., 2006. Fluxes through the bottom boundary of the root zone in silty soils: Parametric approaches to estimate groundwater contribution and percolation. *Agricultural water management, 84*, pg. 27-40.

Mabula M. C., 1995. Mechanics of water movement in soils: A re-examination of basic principles, PhD Thesis, University of Witwatersrand, Johannesburg.

Magombeyi M. S., Morardet S., Taigbenu A. E. and Cheron C., 2012. Food insecurity of smallholder farming systems in B72A catchment in the Olifants River Basin, South Africa, African Journal of Agricultural Research Vol. 7(2), pp. 278-297.

Makurira, H., 2010. Water Productivity in rainfed Agriculture: redrawing the rainbow ofwater to achieve food security in rainfed smallholder systems, PhD thesis, UNESCOIHE, Taylor & Francis Group.

Makurira H., Savinije H. H. G and Uhlenbrook S., 2009b. Modelling field scale water partitioning using on site observations in a sub-Saharan rainfed agriculture, Hydrology and Earth System Sciences Discussions, 6, pg. 5537-5563.

Makurira H., Savenije H. H. G, Unhlenbrook S, Rockstrom J and Senzanje A, 2009a. Investigating the water balance of on-farm techniques for improved crop productivity in rainfed systems: A case study of Makanya catchment Tanzania, Physics and Chemistry of the Earth, vol 34 pg. 93-98, Elsevier.

Mallants, D. M., 1997. Spatial analysis of saturated hydraulic conductivity in a soil with macropores. *Soil Technology, 10*, pg. 115-131.

Maller R., A. and Sharma, M., L., 1981. An analysis of areal infiltration considering spatial variability, Journal of Hydrology, Vol. 52., pg. 25-37, Elsevier Scientific Publishing Company, Amsterdam.

Mamba G. C., 2007. Quantifying Total Water Productivity for multi-use small reservoirs in Mzingwane Catchment, Zimbabwe, MSc Thesis, University of Zimbabwe.

Mbilinyi B. P., Tumbo S. D., Mahoo H. F., Senkondo E. M. and Hatibu N., 2005. Indigenous knowledge as decision support tool in rainwater harvesting, Physics and Chemistry of the Earth vol. 30 pg. 792–798.

McCartney M. P., Neal C, and Neal M., 1998. Use of deuterium to understand runoff generation in a headwater catchment containing a dambo, Hydrology and Earth System Sciences, Issue 2 Vol. 1, page 65-76.

McFarlane M. J., 1995. Dambo Gullying in Parts of Zimbabwe and Malawi: A Reassessment of the Causes, Conference Proceedings, Dambo farming in Zimbabwe, University of Zimbabwe Publications.

Memon S. Q., Mirza B. B. and Mari G. R., 2007. Tillage practices and effect of sowing methods on growth and yield of maize crop, Agricultura Tropica ET Subtropica, Vol. 40, Issue 3, page 89-99.

Mitchell, T. B. 1974. ‘A study of Rhodesian floods and proposed flood formulae’, The Rhodesian Engineer, Paper, 160, 199-203.

Moyo R., 2005. Impact and sustainability of drip irrigation kits, in the semi-arid lower Mzingwane Catchment, Limpopo Basin, Zimbabwe. MSc Thesis, University of Zimbabwe, Harare.

Mou L., Tian F., Hu H., and Sivapalan M., 2008. Extension of the Representative Elementary Watershed approachfor cold regions: constitutive relationships and an application, Hydrology and Earth System Sciences, Vol. 12, pg. 565–585, the European Geosciences Union.

Mufute N. L., 2007. The development of a risk-of failure evaluation tool for small dams in Mzingwane Catchment. MSc Thesis, University of Zimbabwe, Harare.

Mugabe, F. T., 2004. Evaluation of the benefits of infiltration pits on soil moisture in semi-arid Zimbabwe, Journal of Agronomy, Vol. 3, pg. 188-190.

Mugabe, F. T., 2005. Temporal and spatial variability of the hydrology of semi-arid Zimbabwe and its implications on surface water resources, unpublished PhD Thesis, University of Zimbabwe.

Munamati M., 2005. Cultivating livelihoods: An assessment of water allocation and management practices in small-scale irrigation schemes- Case study of Mzingwane Catchment. MSc Thesis, University of Zimbabwe, Harare.

Munodawafa A. and Zhou N., 2008. Improving water utilization in maize production through conservation tillage systems in semi-arid Zimbabwe, Physics and Chemistry of the Earth, Vol. 33, pg. 757-761, Elsevier Ltd.

Mupangwa W., 2008. Water and nitrogen management for risk mitigation in semi-arid cropping systems. PhD Thesis (unpublished), University of Free State, South Africa. 357pp.

Mupangwa W., Love D. and Twomlow S., 2006. Soil–water conservation and rainwater harvesting strategies in the semi-arid Mzingwane Catchment, Limpopo Basin, Zimbabwe, Physics and Chemistry of the Earth 31 (2006) pg. 893–900, Elsevier.

Mupangwa, W., Twomlow, S., Walker, S., 2011. Dead level contours and infiltration pits for risk mitigation in smallholder cropping systems of southern Zimbabwe, Physics and Chemistry of the Earth. In press.

Murty V. V. N., 1970. Percolation losses in check system of irrigation, Journal of Agricultural Engineering Resources, Vol. 15, number 4, pg. 375-378.

Mutekwa V. and Kusangaya S., 2006. Contribution of rainwater harvesting technologies to rural livelihoods in Zimbabwe: The case of Ngundu ward in Chivi District, Water SA; vol 32 No. 3; http://www.wrc.org.za.

Mutsamba and Nyagumbo, 2010. Linkages between crop residues, termite prevalence, crop lodging and subsequent crop yield under conservation agriculture in Zimbabwe, Second RUFORUM Biennial Meeting 20-24 September 2010, Entebbe, Uganda.

Mwendera E. J. and Feyen J., 1997. Tillage and evaporativity effects on the drying characteristics of silty loam: evaporation prediction models, Soil and Tillage Research, Vol. 41, pg. 127-140, Elsevier, Ltd.

Mwenge Kahinda J., Lillie E.S.B., Taigbenu A.E., Taute M., Boroto R.J., 2008. Developing suitability maps for rainwater harvesting in South Africa, Physics and Chemistry of the Earth, 33, pg. 788–799.

Mwenge Kahinda J., Rockstrom J., Taigbenu A. E. and Dimes J., 2007. Rainwater harvesting to enhance water productivity of rainfed agriculture in the semi-arid Zimbabwe, Physics and Chemistry of the Earth, Volume 32 page 1068-1073.

Nasri S., Lamachere M. and Albergel J., 2004. The impact of contour ridges on runoff from a small catchment, Rev. Sci. Eau 17 (2) pg. 265-289.

Ncube B., Magombeyi M., Munguambe P., Mupangwa W. and Love D., 2008. Methodologies and case studies for investigating upstream-downstream interactions of rainwater water harvesting in the Limpopo Basin, Proceedings of the Workshop on Increasing the Productivity and Sustainability of Rainfed Cropping Systems of Poor, Smallholder Farmers, Tamale, Ghana.

Ndiritu J. G., 2009. Automatic calibration of the pitman model using the shuffled complex evolution method, WRC Report Number: KV 229/09, ISBN 978-1-77005-897-2.

Ngwenya P. T., 2006. Effect of grazing management on the hydrological processes of rangeland in Inziza District of Zimbabwe, MSc Thesis, University of Zimbabwe.

Nyagumbo I., 2002. The effect of three tillage systems on seasonal water budgets and drainage of two Zimbabwean soils under maize, PhD Thesis, University of Zimbabwe.

Pachepsky Y., Timlin D. and Rawls W., 2003. Generalized Richards' equation to simulate water transport in unsaturated soils, Journal of Hydrology, Vol. 272, pg. 3-13, Elsevier Science.

Pandey D. N., Gupta A. K. and. Anderson D. M, 2003. Rainwater harvesting as an adaptation to climate change, CURRENT SCIENCE, VOL. 85, NO. 1, pg 46-59.

Pinder G. F. and Celia M. A., 2006. Subsurface hydrology, Book series, John Wiley & Sons, Inc., Hoboken, New Jersey, ISBN-13: 978-0-471-74243-2.

Parsons A. J. and Stone P.M., 2006. Effects of intra-storm variations in rainfall intensity on interrill runoff and erosion, Catena Vol. 67 pg. 68– 78.

Popławski T., 2008. The short-term fuzzy load prediction model, Acta Electrotechnica et Informatica Vol. 8, No. 1, pg. 39–43.

Prinz and Malik, 2002. Runoff Farming, Article prepared for WCA infoNET, Institute of Water Resources Management, Dept. Hydraulic and Rural Engineering, University of Karlsruhe, Germany, www.wca-infonet.org/id/81755.

Queensland design manual, 2004. Design Manual for Queensland, Soil Conservation Measures, www.nrw.qld.gov.au/land/management/pdf/c6scdm.pdf.

Ramos M.C., Martı´nez-Casasnovas J. A, 2006. Impact of land levelling on soil moisture and runoff variability in vineyards under different rainfall distributions in a Mediterranean climate and its influence on crop productivity, Journal of Hydrology Vol., page 131–146. Elsevier B.V.

Reason C. J. C., Hachigonta S. and Phaladi R. F., 2005. Interannual variability in rainy season characteristics over the Limpopo Region of Southern Africa, International Journal of Climatology, Vol. 25, pg. 1835-1853, Wiley InterScience.

Reggiani P., Hassanizadeh S. M., Sivapalan M. and Gray W. G., 1999. A unifying framework for watershed thermodynamics: constitutive relationships, Advances in Water Resources, Vol. 23, pg. 15-39, Elsevier, Science, Ltd.

Reggiani P. and Schellekens J., 2003. Modelling of hydrological responses: the representative elementary watershed approach as an alternative blueprint for watershed modelling: INVITED COMMENTARY, Hydrological Processes, Vol. 17, pg. 3785–3789.

Reggiani P., Sivapalan M. and Hassanizadeh S. M., 1998. A unifying framework for watershed thermodynamics: balance equations for mass, momentum, energy and entropy, and the second law of thermodynamics, Advances in Water Resources, Vol. 22, Number 4, pg. 367-398, Elsevier Science, Ltd.

Rezzoug A., Schumann A., Chifflard P., Zepp H., 2005. Field measurement of soil moisture dynamics and numerical simulation using the kinematic wave approximation, Advances in Water Resources 28 pg. 917–926, Elsevier.

Richard, G. C., Cousin I., Sillon J. F., Bruand A. and Guerif J., 2001. Effect of compaction on the porosity of a silty soil: influence on unsaturated hydraulic properties. *European Journal of Soil Science, 52*, 49-58.

Rockström J., 2000. Water Resources Management In Smallholder Farms In Eastern And Southern Africa : An Overview, Phys. Chem. Earth (B), Vol 25(3), pg. 275 – 283, Elsevier Ltd.

Ruidischa M., Ketteringb J., Arnholda S. and Huwea B., 2013. Modeling water flow in a plastic mulched ridge cultivation system on hillslopes affected by South Korean summer monsoon, Agricultural Water Management Vol. 116 pg. 204– 217.

Rukuni S., 2006. Modelling the response of small multi-purpose reservoirs to hydrology for improved rural livelihoods in the Mzingwane Catchment, Limpopo Basin.

Sadras V. O. and Calvino P. A., 2001. Quantification of Grain Yield Response to Soil Depth in Soyabean, Maize, Sunflower and Wheat, Agro climatology, Vol. 93, pg. 577-583.

Sawunyama T., 2005. Estimation of small reservoir storage capacities in Limpopo River Basin using Geographical Information Systems (GIS) and remotely sensed surface areas: A case of Mzingwane Catchment, MScThesis, University of Zimbabwe.

Savenije H. H. G., 2001. Equifinality, a blessing in disguise?, Hydrological Processes, Vol. 15, pg 2835–2838.

Sbeih M. Y., undated. The role of supplementary irrigation for food production in a semi-arid country - Palestine, www.ipcri.org/watconf/papers/mohammed.pdf.

Schaap M. G. and Leij J., 1998. Using neural networks to predict soil water retention and soil hydraulic conductivity, Soil and Tillage Rsearch, Vol 47, pg. 37-42, Elsevier Ltd.

Sen Z. and Altunkaynak A., 2005. A comparative fuzzy logic approach to runoff coefficientand runoff estimation, Hydrol. Process.Vol. 20, pag.1993–2009, Wiley InterScience.

Simunek, J., K. Huang, M. Šejna, and M. Th. van Genuchten. 1998. The HYDRUS-1D Software Package for Simulating the One-Dimensional Movement of Water, Heat and Multiple Solutes in Variably-Saturated Media, Version 1.0. IGWMC-TPS-70, Int. Ground Water Modeling Center, Colorado School of Mines, Golden, CO., 186 p.

Simunek, J., K. Huang, M. Šejna, and M. Th. van Genuchten. 1999. The HYDRUS-2D Software Package for Simulating Two-Dimensional Movement of Water, Heat and Multiple Solutes in Variably-Saturated Media. Version2.0. IGWMC-TPS-53, Int. Ground Water Modeling Center, Colorado School of Mines, Golden, CO, 251 p.

Simunek, J., van Genuchten, M. Th., Šejna, M., 2006. The HYDRUS software package for simulating two- and three-dimensional movement of water, heat, andmultiple solutes in variably saturated media. Technical manual, version 1.0, PC Progress, Prague, Czech Republic.

Singh V. P. and Xu C. Y., 1997. Sensitivity of mass transfer-based evaporation equations to errors in daily and monthly input data, Hydrological Processes, vol. 11, pg. 1465-1473, John Wiley and Sons, Ltd.

Sivandran, G., 2002. Effect of Rising Water Tables and Climate Change on Annual and Monthly Flood Frequencies. B. Eng. Thesis, Centre for Water Resourses, University of Western Australia, Crawley, Australia.

Sivapragasam, C. M., 2008. Genetic programming approach for flood routing in natural channels. *HYDROLOGICAL PROCESSES, 22*, pg. 623–628.

Skaggs T.H., Suarez D.L., and Corwin D.L., 2014. Global Sensitivity Analysis for UNSATCHEM Simulations of Crop Production with Degraded Waters, Vadose Zone J. doi:10.2136/vzj2013.09.0171.pg 1-13.

Sobieraj J.A., Elsenbeer H, Coelho R.M and Newton B., 2002. Spatial variability of soil hydraulic conductivity along a tropical rainforest catena, Geoderma Vol. 108 page 79–90, Elsevier Science.

Tan S. B. K., Shuy B. and Chua L. H. C., 2007. Modelling hourly and daily open-water evaporation rates in areas with an equatorial climate, Hydrological processes, vol 21 pg. 486-499, Wiley InterScience.

Tennant W. J. and Hewitson B. C., 2002. Intra-seasonal rainfall characteristics and their importance to the seasonal prediction problem, International Journal of Climatology, vol. 22, pg. 1033-1048, Wiley InterScience.

Tian F., Hu H., LeiZ. and Sivapalan M., 2006. Extension of the Representative Elementary Watershed approach for cold regions via explicit treatment of energy related processes, Hydrology and Earth System Sciences, Vol. 10, pg.619–644, the European Geosciences Union.

Tsakiris G., 1991. Micro-Catchment Water Harvesting in Semi-Arid Regions: Basic Design Considerations, Water Resources Management Vol. 5, pg. 85-95, Kluwer Academic Publishers, Netherlands.

Ursu I., Ursu F. and Iorga L., 2001. Neuro-fuzzy synthesis of flight control electrohydraulic servo, Aircraft Engineering and Aerospace Technology, Vol. 73, No. 5, pg. 465-471.

Ursu I. and Ursu F., 2003. An intelligent abs control based on fuzzy logic. Aircraft application, Proceedings of the International Conference on Theory and Applications of Mathematics and Informatics – ICTAMI 2003, Alba Iulia.

Usman M. T. and Reason C. J. C., 2004. Dry spell frequencies and their variability over Southern Africa, Climate Research, vol. 26, pg. 199-211, Inter-Research.

van de Giesen, N. C., 2000. Scale efects of Hortonian overland flow and rainfall-runonff dynamics in a West African catena landscape. *HYDROLOGICAL PROCESSES, 14*, pg. 165-175.

van Dijk A., I., J., M. and Bruijnzeel, L. A., 2001. Modelling rainfall interception by vegetation of variable density using an adapted analytical model.Part 1. Model description, Journal of Hydrology, Vol. 247, pg. 230-238, Elsevier Science B. V.

van Griensven A., Meixner T., Grunwald S., Bishop T., Diluzio M., Srinivasan R., 2006. A global sensitivity analysis tool for the parameters of multi-variable catchment models, Journal of Hydrology Vol. 324 pg. 10–23.

Verma S. C., 1982. Short Communications, Modified Horton's Infiltration Equation, Journal of Hydrology, Vol. 58, pg. 383-388, Elsevier Scientific Publishing Company, Amsterdam.

Vogel T., van Genuchten M. Th. and Cislerova M., 2001. Effect of the shape of the soil hydraulic functions near saturation on variably-saturated flow predictions, Advances in Water Resources, vol. 24, pg. 133-144, Elsevier Science Ltd.

Vossen P., 1990. Algorithm for the simulation of bare sandy soil evaporation and its application for the assessment of planted areas in Botswana, Agricultural and Forest Meteorology, Vol. 50, pg. 173-188, Elsevier Science Publishers B. V., Amsterdam.

Walker, S. Ogindo, H. O., 2003. The water budget of rainfed maize and bean intercrop, Physics and Chemistry of the Earth, Vol. 28, page 919 to 926, Pergamon, Elsevier Ltd.

Walker, S., Tsubo, M., 2003a. PutuRun: A simulator for rainfall-runoff-yield processes with in-field water harvesting, WRC Report No. K8/486, Water Research Commission Pretoria.

Walker, S.,Tsubo W, 2003b. Estimation of rainfall intensity for potential crop production on clay soil with in-field water harvesting practices in a semi-arid area, WRC Report No. 1049/1/02, Water Research Commission, Pretoria, ISBN No. 1-86845-986-1.

Wallace J.S., 2000. Increasing agricultural water use efficiency to meet future food production, Agriculture, Ecosystems and Environment vol. 82 pg. 105–119.

Wallace, J.S., Jackson, N.A., Ong, C.K., 1999. Modelling soil evaporation in an agroforestry system in Kenya. Agric. For. Meteorol. 94, 189–202.

Willems P., 2000. Statistical Methods in Water Resources Engineering, Lecture Notes, Katholieke Universiteit Leuven, Faculty of Engineering, Leuven, Belgium.

Willems P., 2001. Stochastic description of the rainfall input errors in lumped hydrological models, Stochastic Environmental Research and Risk Assessment, Vol. 15, pg. 132-152.

Willis T. W., Black A. S. and Meyer W. S., 1997. Estimates of deep percolation beneath cotton in the Macquarie Valley. *Irrigation Science, 17*, 141-15.

Woyessa Y. E., Hensley M., and van Rensburg L. D., 2006. Catchment management in semi-arid area of central South Africa: Strategy for improving water productivity, Water SA Vol. 32 No. 5.

Ying H., Ding Y., Li S. and Shao S., 1999. Comparison of Necessary Conditions for Typical Takagi–Sugeno and Mamdani Fuzzy Systems as Universal Approximators, IEEE Transactions on systems, manWi, and cybernetics—part a: systems and humans, VOL. 29, NO. 5, Pg. 508-514.

Zadeh, L. A., 1965. Fuzzy Sets, Information and control, Vol. 8, page 338-353.

Zehe, E. and Sivapalan, M., 2007. Towards a new generation of hydrological process models for the meso-scale: an introduction, Hydrology and Earth System Sciences, www.hydrol-earth-syst-sci.net, European Geophysical Society.

Zhang a G.P., Fenicia F., Rientjes T.H.M., Reggiani P. and Savenije H.H.G., 2005. Modelling runoff generation in the Geer river basinwith improved model parameterizations to the REW approach, Physics and Chemistry of the Earth Vol. 30pg. 285–296, Elsevier Ltd.

Zougmoréa R., Mandoc A. and Stroosnijder L., 2004. Effect of soil and water conservation and nutrientmanagement on the soil–plant water balance insemi-arid Burkina Faso, Agricultural Water Management vol. 65 pg.103–120.

A. *Appendix A: Estimation of hydraulic diffusivity from observed soil moisture data*

This appendix presents a description of the development of an empirical relationship between hydraulic conductivity of a soil at a given soil moisture in relation to the soil moisture of an adjacent profile where soil moisture flux takes place which was used as parameter input in this study. This was done by considering that hydraulic conductivity of a soil at a given soil moisture is related to the soil moisture of the soil following the model of van Genuchten (1980). Vogel *et al* (2001) used the van Genuchten-Mualem (VGM) model and its modified version to show that relative hydraulic conductivity depend on the pressure head as shown in Figure A 1.

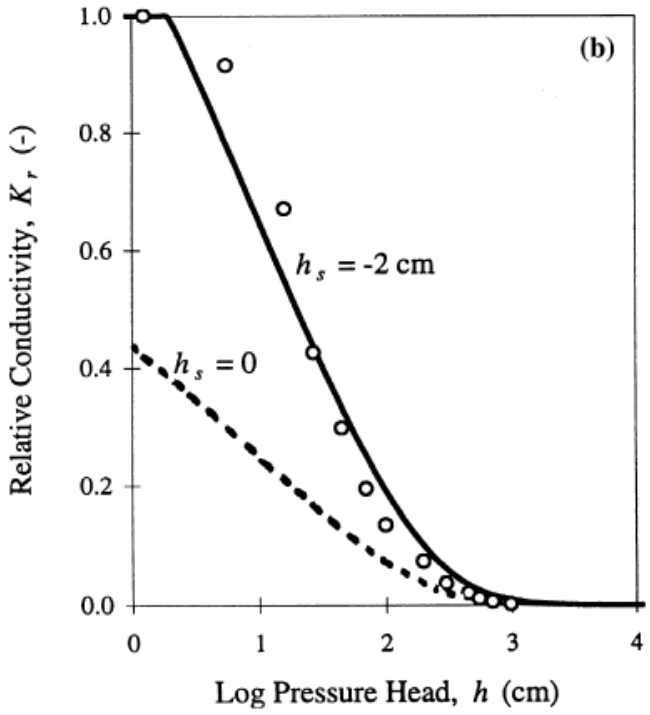

Figure A 1: variation of relative hydraulic conductivity with pressure head (dotted line is original VGM model, continuos line is modified VGM model and small cycles are observations)
(Source: Vogel et al., 2001)

According to the VGM model pressure head h is related to soil moisture by Equation A 1 (van Genuchten, 1980). By making h subject of the formula Equation A 1 changes to

Equation A 2. Relative hydraulic conductivity is also related to the pressure head by Equation A 3 according the VGM model. In Equation A 2 and Equation A 3 αh is a common term which makes it possible to combine the two equations to give Equation A 4. Substitution of αh in Equation A 3 produces Equation A 5. This shows that unsaturated hydraulic conductivity depends on soil moisture as shown by Equation A 6.

$$\theta = \theta_r + \frac{(\theta_s - \theta_r)}{[1 + (\alpha h)^n]^m}$$ Equation A 1

Where

θ is the soil moisture at a location where the suction pressure is h . h is assumed to be positive. In reality if the atmospheric pressure is considered as zero then suction pressure is negative.
$\theta_r$is the residual soil moisture or that moisture that cannot be removed from the soil due to the adhesion forces of the soil.
$\theta_s$is the saturated soil moisture.
$\alpha, n \; and \; m$ are constants derived from the soil water retention curve.

$$h = \frac{1}{\alpha}\left\{\left[\frac{\theta_s - \theta_r}{\theta - \theta_r}\right]^{\frac{1}{m}}\right\}^{\frac{1}{n}} = \frac{1}{\alpha}\left\{\left[\frac{\theta_s - \theta_r}{\theta - \theta_r}\right]^{\frac{1}{mn}}\right\}$$ Equation A 2

$$K_r(h) = \frac{\{1 - (\alpha h)^{n-1}[1 + (\alpha h)^n]^{-m}\}^2}{[1 + (\alpha h)^n]^{\frac{m}{2}}}$$ Equation A 3

$$\alpha h = \alpha * \frac{1}{\alpha}\left\{\left[\frac{\theta_s - \theta_r}{\theta - \theta_r}\right]^{\frac{1}{mn}}\right\} = \left\{\left[\frac{\theta_s - \theta_r}{\theta - \theta_r}\right]^{\frac{1}{mn}}\right\}$$ Equation A 4

$$K_r(h) = \frac{\left\{1 - \left[\frac{\theta_s - \theta_r}{\theta - \theta_r}\right]^{\frac{n-1}{mn}} \left[1 + \left[\frac{\theta_s - \theta_r}{\theta - \theta_r}\right]^{\frac{1}{m}}\right]^{-m}\right\}^2}{\left[1 + \left[\frac{\theta_s - \theta_r}{\theta - \theta_r}\right]^{\frac{1}{m}}\right]^{\frac{m}{2}}}$$ Equation A 5

But $K_r(h) = \frac{K(h)}{K_s}$

Where
$K(h)$ is hydraulic conductivity at a pressure suction head of h and K_s is hydraulic conductivity at saturation.

$$K(h) = K_s K_r(h) = K_s * \frac{\left\{1 - \left[\frac{\theta_s - \theta_r}{\theta - \theta_r}\right]^{\frac{n-1}{mn}} \left[1 + \left[\frac{\theta_s - \theta_r}{\theta - \theta_r}\right]^{\frac{1}{m}}\right]^{-m}\right\}^2}{\left[1 + \left[\frac{\theta_s - \theta_r}{\theta - \theta_r}\right]^{\frac{1}{m}}\right]^{\frac{m}{2}}}$$ Equation A 6

Deriving hydraulic conductivity using observed profile soil moisture

The soil moisture profile e.g. for a subplot m_d at time t_n can be represented by Equation A 7. In terms of Darcy's law the soil moisture flux per unit area that causes the change in soil moisture content is given by Equation A 8 and the moisture gradient by Equation A 9. The soil moisture gradient is defined as the soil moisture difference between two soil profiles divided by the distance between them. This is the equivalent of hydraulic gradient in Darcy's law. If we consider the vertical direction the soil moisture gradient can be computed from observed soil moisture for different soil horizons. By considering water balance equations for different soil horizons as discussed later soil moisture fluxes from one horizon to the next can be estimated. The hydraulic conductivity at a given soil moisture gradient was therefore computed using this approach and the results used to plot a graph from which an empirical relation that define the variation of hydraulic conductivity with soil moisture gradient was obtained.

$$\theta_{m_d t_n} = \theta_{m_d t_{n-1}} + \Delta\theta_{m_d t_{n-(n-1)}}$$ Equation A 7

Where:

$\Delta\theta_{m_d t_{n-(n-1)}} = Sum\ of\ moisture\ fluxes, Q_{m_d t_n}, into\ the\ subplot\ during\ the\ period.$

$Q_{m_d t_n} = K_s K_r(h) \frac{\partial\theta}{\partial x}$, in the x direction Equation A 8

where

$$\frac{\partial\theta}{\partial x} = \frac{\theta_{m_{d-1} t_n} - \theta_{m_{d+1} t_n}}{\Delta x}$$ Equation A 9

The moisture observations that were used were obtained during the period when runoff was observed so as to enable carrying out mass balance analysis for different soil horizons with infiltration as the external forcing. The soil moisture measured immediately after a rainfall event producing runoff was considered as t_{n-1} while soil moisture measured next to it was considered as t_n.

Three vertical soil profiles namely top layer, middle layer and the bottom layer shown in Figure A 2 were used to estimate water fluxes from the mass balance analysis of each layer. The top layer was taken as the top 200mm of the soil. This was the layer where infiltration took place. The middle layer was taken as the layer between depths of 200mm to 400mm. The bottom layer was below the 400 mm horizon to a depth below 600mm. The mass water balance equations developed for each of the layers are shown in Equation A 10 to Equation A 12. These mass balance analysis are carried out to establish a relation between unsaturated hydraulic conductivity and soil moisture. This means that the soil is in unsaturated conditions and therefore the porosity of the soil is not included in the mass balance equations.

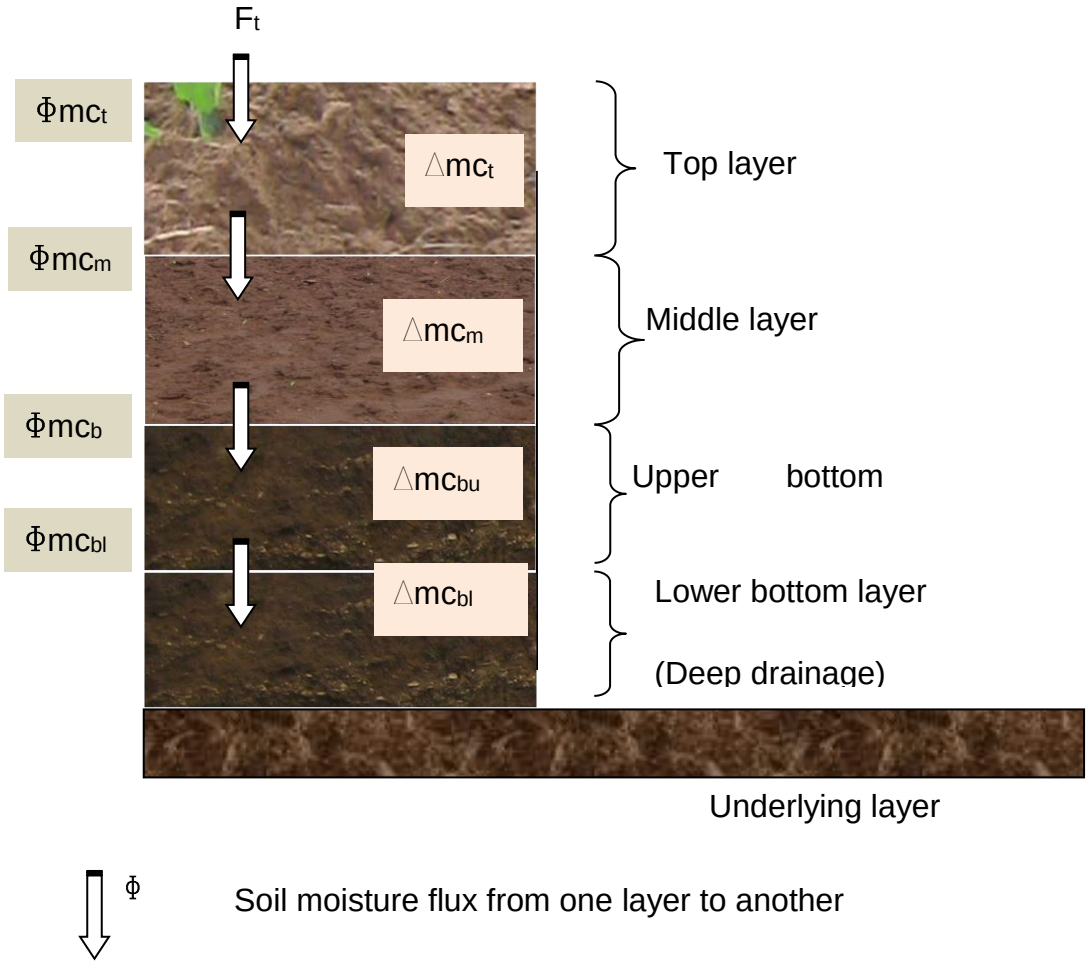

Figure A 2: Soil moisture fluxes across vertical soil aprofiles

Mass balance of top layer

$$F_t - ET_t - \Phi_m \Delta t = \Delta S_t = \Delta z \theta_{u,t} - \Delta z \theta_{u,t-1}$$ Equation A 10

Where:

F_t is the infiltration into the top layer (mm over period of observation);
ET_t is the evapotranspiration from the top layer (mm over period of observation);
Φ_m is the moisture flux into the middle layer from the top layer (mm/day);
ΔS_t is change in moisture storage of the top layer (mm/m over period of observation);
$\theta_{u,t}$ is the moisture in the upper layer at end of period of observation (mm/m);
$\theta_{u,t-1}$ is the moisture in the upper layer at beggining of period of observation (mm/m);
Δt is the period of observation equal from time t to time t-1 (days);
Δz is thickness of layer (m) which was taken as equal to 0.2m for all the horizons.

Mass balance of the middle layer

$$\Phi_m \Delta t - \Phi_b \Delta t - ET_m = \Delta S_m = \Delta z \theta_{m,t} - \Delta z \theta_{m,t-1}$$ Equation A 11

Where

Φ_b is the moisture flux from the middle layer into the bottom layer (mm/m/days);
ΔS_m is change in moisture storage of the middle layer mm/m over period of observation;
$\theta_{m,t}$ is the moisture in the middle layer at end of period of observation (mm/m);
$\theta_{m,t-1}$ is the moisture in the middle layer at beggining of period of observation (mm/m);
ET_m is the evapotranspiration from the middle layer (mm over period of observation).

Mass balance of the bottom layer

$$\Phi_b \Delta t - \Phi_d \Delta t - ET_b = \Delta S_b = \Delta z \theta_{b,t} - \Delta z \theta_{b,t-1}$$ Equation A 12

Where

Φ_d is the moistre flux from the bottom layer into deep percolation
ΔS_b is change in moisture storage of the bottom layer mm/m over period of observation
$\theta_{b,t}$ is the moisture in the bottom layer at end of period of observation (mm/m)
$\theta_{b,t-1}$ is the moisture in the bottom layer at beggining of period of observation (mm/m)
ET_b is the evapotranspiration from the bottom layer (mm over period of observation).

Φ_m in Equation A 10 and Equation A 11 can be made the subject of the formulae to produce Equation A 13 and Equation A 14. Adding and neglecting difference in ET between layers by assuming the difference in ET from two adjacent layers is small and

can be neglected gives Equation A 15. Similarly making Φ_b the subject of the formulae yields Equation A 16 and Equation A 17. Adding and neglecting difference in ET between layers then solving provide Equation A 18.

$$\Phi_m = F_t - ET_t - (\theta_{u,t} - \theta_{u,t-1})$$ Equation A 13

$$\Phi_m = \theta_{m,t} - \theta_{m,t-1} + \Phi_b + ET_m$$ Equation A 14

Assuming difference in evapotranspiration between the top layer and the middle layer is small then $ET_t = ET_m$.

$$2\Phi_m = \theta_{m,t} - \theta_{m,t-1} - (\theta_{u,t} - \theta_{u,t-1}) + \Phi_b + F_t$$ Equation A 15

$$\Phi_b = \Phi_m - ET_m - (\theta_{m,t} - \theta_{m,t-1})$$ Equation A 16

$$\Phi_b = \theta_{b,t} - \theta_{b,t-1} + \Phi_d + ET_b$$ Equation A 17

Assuming difference in evapotranspiration between the middle layer and the bottom layer is small then $ET_m = ET_b$.

$$2\Phi_b = \theta_{b,t} - \theta_{b,t-1} - (\theta_{m,t} - \theta_{m,t-1}) + \Phi_m + \Phi_d$$ Equation A 18

If the flux into the bottom layer and out of the bottom layer is neglected Φ_d will be taken as equal to Φ_b.

Substituting Φ_d in Equation A 18 with Φ_b provides Equation A 19.

$$\Phi_b = \theta_{b,t} - \theta_{b,t-1} - (\theta_{m,t} - \theta_{m,t-1}) + \Phi_m \qquad \text{Equation A 19}$$

Substituting Φ_b in Equation A 15 provides Equation A 20.

$$2\Phi_m = (\theta_{m,t} - \theta_{m,t-1}) - (\theta_{u,t} - \theta_{u,t-1}) + (\theta_{b,t} - \theta_{b,t-1}) - (\theta_{m,t} - \theta_{m,t-1}) + \Phi_m + F_t$$

Reducing to

$$\Phi_m = (\theta_{b,t} - \theta_{b,t-1}) - (\theta_{u,t} - \theta_{u,t-1}) + F_t \qquad \text{Equation A 20}$$

Similarly Equation A 19 becomes Equation A 21.

$$\Phi_b = F_t - (\theta_{u,t} - \theta_{u,t-1}) - (\theta_{m,t} - \theta_{m,t-1}) \qquad \text{Equation A 21}$$

All the fluxes could be expressed in terms of the soil moisture and infiltration into the top layer. The infiltration into the top layer was computed from the water balance of the surface layer (Equation A 22).

$$F_t = P - I - R \qquad \text{Equation A 22}$$

Where

P is the precipitation
I is the interception
R is the runoff

With the soilmoisture computed at various soil moisture values of the different layers and the soil moisture gradient known the corresponding unsaturated hydraulic conductivity was also estimated which was then ploted in a graph against its corresponding soim moisture gradient and the results are shown in Figure A 3.

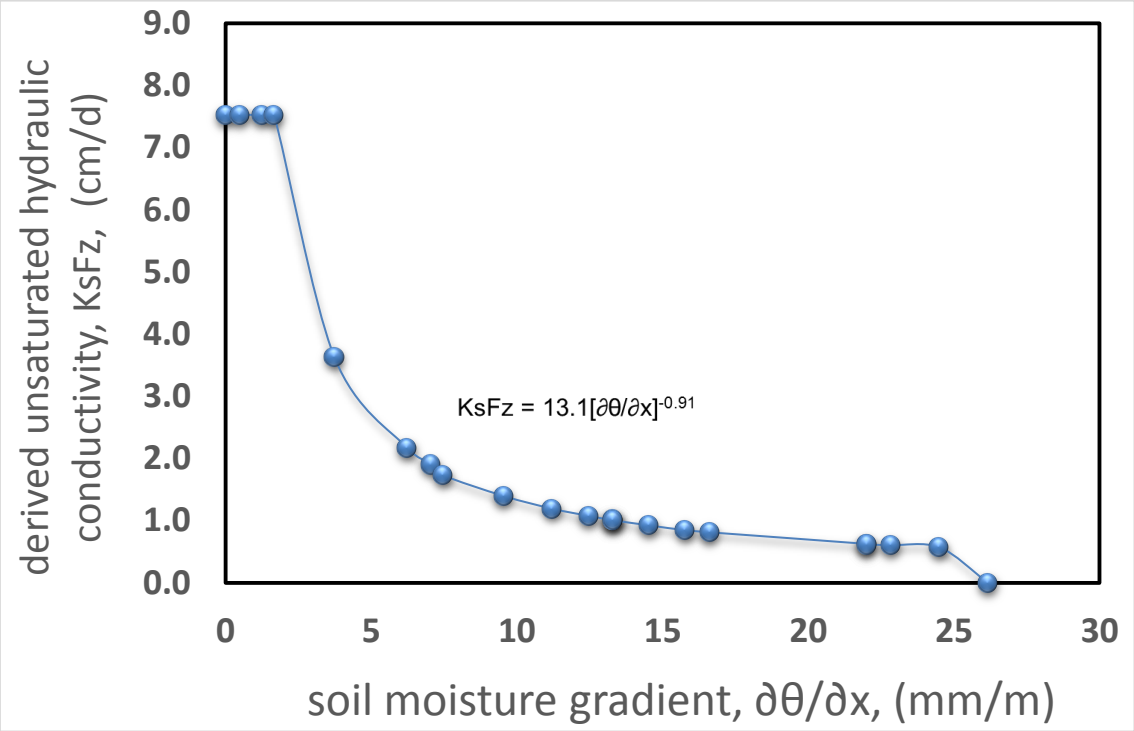

Figure A 3: The derived unsaturated hydraulic conductivity ploted against soil moisture gradient

A. *Appendix B: The estimation of macro pore flows*

Faeh (1997) in Scherrer and Naff (2003) suggested that during rainfall of low intensity infiltration is predominantly through soil matrix flow and that macro pores becomes active during higher rainfall intensities. This is because the low rainfall intensity provides sufficient time for the infiltrating water to soak into the soil matrix. Macro pore spaces are therefore occupied by excess water after the soil matrix rate of soaking is satisfied. This leads to the following assumed sequence of processes that lead to macro pore flow:

i. When a soil horizon receives soil moisture through infiltration or downward flux the water that temporally occupies macro pore spaces is eventually absorbed by the soil matrix when soil moisture is below field capacity.
ii. As soil moisture in the soil matrix increases above the field capacity macro pore spaces begin to hold water that is not shared with the soil matrix and which can eventually drain to lower soil horizons. This means that influx from infiltration or downward flux will be shared by soil matrix and macro pores.
iii. The occupation of macro pore spaces by water continues until soil moisture in the soil matrix has reached saturation level. At this stage the soil no longer has spaces to contain more water and macro pores begin to facilitate downward flux of any excess water to the underlying horizon.

The amount of water that enters the macropore spaces and that which is drained through the macropore spaces depends on the macropore storage space available at any given time.

Estimation of macro pore storage and drainage

The soil water flow into macro pores is then estimated by Equation A 23.

$$\phi_{ps} = \frac{\theta_{ps\phi}}{\theta_T} * \phi_{in} \qquad \text{Equation A 23}$$

Where

ϕ_{ps} is soil water fow into macro pore spaces
ϕ_{in} is the soil moisture flow into the soil horizon
θ_T is the total soil moisture deficit in the soil horizon given by

$$\theta_T = \theta_{id} + \theta_{ps\phi}$$

And

θ_{id} is the soil moisture deficit at previous time step

$$\theta_{id} = \theta_s - \theta_i$$

$\theta_{ps\phi}$ is the available soil water space in macro pores which is obtained from Equation A 24

$$\theta_{ps\phi} = \theta_{ps} * \left[1 - \frac{\theta_{fc} - \theta_i}{\theta_s - \theta_{fc}}\right]^{-1} \qquad \text{Equation A 24}$$

Where

θ_{ps} is the total macro pore space per horizon depth
θ_s, is soil moisture at saturation
θ_{fc} is soil moisture at field capacity and;
θ_i is the available soil moisture.

In this study plots, the macro pore space were found to be made up of cracks due to shrinkage, loose spaces around rocks in the soil horizon and holes made by burrowing animals. The average macro pore space data obtained from the field was as follows:

crack width ≈3mm
crack length≈2m/m^2
rock circumference≈0.24 m
loose space close to rock≈1mm

number of rocks$\approx 5/m^2$
burrowing animals hole diameter$\approx$6mm
number of holes$\approx 5/m^2$

This gives an average macro pore storage space of 1.46 mm per square metre area and an effective storage of 1460 $(mm)^3$ for a metre depth. If this volume is stored in one macropore of depth 1 m the macro pore would have an effective diameter equivalent to $1460 = \frac{\pi d^2}{4}$. The macro pores can be treated as circular conduits with an effective diameter of 43mm whose conductivity is estimated using Equation A 25 found in Kaufmann (2003).

$$K_m = \frac{g}{32\upsilon} * d^2$$ Equation A 25

Substituting with field data gives:

$$K_m = \frac{9.81}{32*1.14*10^{-6}} * 0.0043^2 = 5m/s.$$

This is a large conductivity which suggests that any water content above the saturation level is transported by macro pores to underlying soil horizons.

A. Appendix C: Modelled rainfall intensity using an empirical approach

Rainfall Date	Rainfall amount (mm/day)	Dry day period (days)	I_e (mm/hour)	I_t (mm/hour)	modelled intensity (mm/hour)	Rainfall Duration (hours)
2-Nov-10	4	142	3.46	-0.50	3.0	1.4
3-Nov-10	5	0	3.44	-1.00	2.4	2.0
6-Nov-10	5	3	3.44	0.00	3.4	1.5
10-Nov-10	1	5	3.50	0.87	4.4	0.2
11-Nov-10	1	0	3.50	-1.00	2.5	0.4
13-Nov-10	1	2	3.50	-0.50	3.0	0.3
15-Nov-10	75	2	2.60	1.00	3.6	20.8
19-Nov-10	3	4	3.47	0.50	4.0	0.8
28-Nov-10	4	8	3.46	0.50	4.0	1.0
30-Nov-10	5	2	3.44	-0.50	2.9	1.7
5-Dec-10	10	5	3.37	0.87	4.2	2.4
6-Dec-10	28	0	3.14	-1.00	2.1	13.1
7-Dec-10	3	0	3.47	-1.00	2.5	1.2
14-Dec-10	20	6	3.24	1.00	4.2	4.7
15-Dec-10	22	0	3.22	-1.00	2.2	9.9
16-Dec-10	3	0	3.47	-1.00	2.5	1.2
17-Dec-10	4	0	3.46	-1.00	2.5	1.6
18-Dec-10	20	0	3.24	-1.00	2.2	8.9
26-Dec-10	1	8	3.50	0.50	4.0	0.3
1-Jan-11	10	6	3.37	1.00	4.4	2.3
2-Jan-11	24	0	3.19	-1.00	2.2	11.0
7-Jan-11	12	6	3.35	1.00	4.3	2.8
8-Jan-11	8	0	3.40	-1.00	2.4	3.3
10-Jan-11	4	2	3.46	-0.50	3.0	1.4
12-Jan-11	4	2	3.46	-0.50	3.0	1.4
13-Jan-11	3	0	3.47	-1.00	2.5	1.2
14-Jan-11	8	0	3.40	-1.00	2.4	3.3
16-Jan-11	5	2	3.44	-0.50	2.9	1.7
17-Jan-11	38	0	3.02	2.00	5.0	7.6
18-Jan-11	15	0	3.31	-1.00	2.3	6.5
20-Jan-11	20	2	3.24	-0.50	2.7	7.3
22-Jan-11	2	2	3.48	-0.50	3.0	0.7
23-Jan-11	2	0	3.48	-1.00	2.5	0.8
24-Jan-11	32	0	3.09	-1.00	2.1	15.3
29-Jan-11	5	5	3.44	0.87	4.3	1.2
30-Jan-11	3	0	3.47	-1.00	2.5	1.2
31-Jan-11	1	0	3.50	-1.00	2.5	0.4

A. Appendix D: Model time series input data

	Input data		Observed soil moisture in loam soil (Field A) (mm/d)				Observed soil moisture in sandy soil (Field B) (mm/d)			
Date	Observed rainfall (mm/d)	Observed pan evaporation (mm/d)	Subplot 1	Subplot 2	Subplot 3	Subplot 4	Subplot 1	Subplot 2	Subplot 3	Subplot 4
5-Nov-08	0.0	2.4								
6-Nov-08	0.0	6.3								
7-Nov-08	0.0	3.4								
8-Nov-08	0.0	5.5								
9-Nov-08	0.0	2.8								
10-Nov-08	0.0	6.9								
11-Nov-08	0.0	3.5								
12-Nov-08	12.0	6.2								
13-Nov-08	12.0	2.4								
14-Nov-08	20.0	1.4								
15-Nov-08	5.0	5.3								
16-Nov-08	0.0	3.0								
17-Nov-08	0.0	1.9								
18-Nov-08	3.0	4.7								
19-Nov-08	12.0	3.4								
20-Nov-08	24.0	4.0								
21-Nov-08	0.0	1.2								
22-Nov-08	0.0	0.4								
23-Nov-08	20.0	9.7								
24-Nov-08	6.0	10.5								
25-Nov-08	0.0	13.0								
26-Nov-08	0.0	3.0								
27-Nov-08	0.0	7.3								
28-Nov-08	0.0	4.3								
29-Nov-08	0.0	12.1								
30-Nov-08	0.0	12.3								
1-Dec-08	0.0	1.6								
2-Dec-08	0.0	2.0								
3-Dec-08	0.0	1.5								
4-Dec-08	0.0	1.1								

	Input data		Observed soil moisture in loam soil (Field A) (mm/d)				Observed soil moisture in sandy soil (Field B) (mm/d)			
Date	Observed rainfall (mm/d)	Observed pan evaporation (mm/d)	Subplot 1	Subplot 2	Subplot 3	Subplot 4	Subplot 1	Subplot 2	Subplot 3	Subplot 4
5-Dec-08	0.0	7.1								
6-Dec-08	0.0	6.6								
7-Dec-08	1.0	5.8								
8-Dec-08	0.0	-0.9								
9-Dec-08	0.0	6.4								
10-Dec-08	0.0	10.9								
11-Dec-08	0.0	0.7								
12-Dec-08	0.0	3.9								
13-Dec-08	0.0	6.0								
14-Dec-08	0.0	3.8								
15-Dec-08	0.0	1.6								
16-Dec-08	2.0	1.8								
17-Dec-08	1.0	7.4								
18-Dec-08	1.0	0.5								
19-Dec-08	0.0	3.3								
20-Dec-08	0.0	3.5								
21-Dec-08	0.0	0.2								
22-Dec-08	0.0	4.7								
23-Dec-08	0.0	1.5								
24-Dec-08	6.0	1.2								
25-Dec-08	40.0	1.7								
26-Dec-08	12.0	3.6								
27-Dec-08	0.0	5.5								
28-Dec-08	7.0	6.4								
29-Dec-08	0.0	1.2								
30-Dec-08	30.0	2.5								
31-Dec-08	16.0	7.6								
1-Jan-09	0.0	4.9								
2-Jan-09	0.0	7.2								
3-Jan-09	0.0	4.3								
4-Jan-09	0.0	3.4								
5-Jan-09	0.0	8.2								

	Input data		Observed soil moisture in loam soil (Field A) (mm/d)				Observed soil moisture in sandy soil (Field B) (mm/d)			
Date	Observed rainfall (mm/d)	Observed pan evaporation (mm/d)	Subplot 1	Subplot 2	Subplot 3	Subplot 4	Subplot 1	Subplot 2	Subplot 3	Subplot 4
6-Jan-09	0.0	4.4								
7-Jan-09	0.0	7.5								
8-Jan-09	10.0	3.3								
9-Jan-09	2.0	4.6								
10-Jan-09	4.0	4.1								
11-Jan-09	0.0	4.1								
12-Jan-09	4.0	4.2								
13-Jan-09	0.0	2.5								
14-Jan-09	70.0	8.8								
15-Jan-09	20.0	1.6								
16-Jan-09	30.0	3.2								
17-Jan-09	3.0	5.8								
18-Jan-09	10.0	8.1								
19-Jan-09	6.0	3.4								
20-Jan-09	0.0	2.3								
21-Jan-09	0.0	2.3								
22-Jan-09	0.0	2.7								
23-Jan-09	0.0	2.2								
24-Jan-09	0.0	4.6								
25-Jan-09	0.0	4.5								
26-Jan-09	0.0	4.0								
27-Jan-09	22.0	3.9								
28-Jan-09	0.0	5.7								
29-Jan-09	2.0	5.5								
30-Jan-09	4.0	4.7								
31-Jan-09	0.0	6.2								
1-Feb-09	2.0	0.6								
2-Feb-09	1.0	5.3								
3-Feb-09	5.0	5.6								
4-Feb-09	12.0	6.1								
5-Feb-09	2.0	3.1								
6-Feb-09	16.0	8.2								

	Input data		Observed soil moisture in loam soil (Field A) (mm/d)				Observed soil moisture in sandy soil (Field B) (mm/d)			
Date	Observed rainfall (mm/d)	Observed pan evaporation (mm/d)	Subplot 1	Subplot 2	Subplot 3	Subplot 4	Subplot 1	Subplot 2	Subplot 3	Subplot 4
7-Feb-09	2.0	4.2								
8-Feb-09	0.0	5.2								
9-Feb-09	0.0	4.7								
10-Feb-09	0.0	4.6								
11-Feb-09	0.0	4.2								
12-Feb-09	0.0	3.7								
13-Feb-09	1.0	11.2								
14-Feb-09	0.0	0.8								
15-Feb-09	0.0	3.8								
16-Feb-09	0.0	5.6								
17-Feb-09	24.0	3.2								
18-Feb-09	38.0	8.9								
19-Feb-09	0.0	3.2								
20-Feb-09	0.0	5.1								
21-Feb-09	0.0	7.3								
22-Feb-09	0.0	8.4								
23-Feb-09	0.0	4.6								
24-Feb-09	30.0	3.8								
25-Feb-09	8.0	1.7								
26-Feb-09	0.0	6.6								
27-Feb-09	0.0	2.5								
28-Feb-09	0.0	3.9								
1-Mar-09	0.0	2.4								
2-Mar-09	0.0	2.5								
3-Mar-09	0.0	5.1								
4-Mar-09	0.0	4.3								
5-Mar-09	0.0	7.6								
6-Mar-09	4.0	3.2								
7-Mar-09	0.0	6.0								
8-Mar-09	0.0	9.0								
9-Mar-09	0.0	4.3								
10-Mar-09	0.0	8.0								

	Input data		Observed soil moisture in loam soil (Field A) (mm/d)				Observed soil moisture in sandy soil (Field B) (mm/d)			
Date	Observed rainfall (mm/d)	Observed pan evaporation (mm/d)	Subplot 1	Subplot 2	Subplot 3	Subplot 4	Subplot 1	Subplot 2	Subplot 3	Subplot 4
11-Mar-09	0.0	5.9								
12-Mar-09	7.0	5.7								
13-Mar-09	16.0	-2.0								
14-Mar-09	0.0	5.3								
15-Mar-09	0.0	3.4								
16-Mar-09	0.0	1.0								
17-Mar-09	0.0	0.3								
18-Mar-09	0.0	9.6								
19-Mar-09	10.0	1.1								
20-Mar-09	0.0	7.4								
21-Mar-09	0.0	1.1								
22-Mar-09	0.0	0.5								
23-Mar-09	0.0	0.6								
24-Mar-09	0.0	1.7								
25-Mar-09	0.0	4.6								
26-Mar-09	0.0	3.2								
27-Mar-09	0.0	4.3								
28-Mar-09	0.0	2.2								
29-Mar-09	0.0	2.6								
30-Mar-09	6.0	2.1								
31-Mar-09	7.0	3.6								
1-Apr-09	0.0	1.7								
2-Apr-09	0.0	1.4								
3-Apr-09	0.0	6.1								
4-Apr-09	0.0	1.4								
5-Apr-09	0.0	2.4								
6-Apr-09	0.0	6.3								
7-Apr-09	0.0	3.4								
8-Apr-09	0.0	5.5								
9-Apr-09	0.0	2.8								
10-Apr-09	0.0	6.9								
11-Apr-09	0.0	3.5								

	Input data		Observed soil moisture in loam soil (Field A) (mm/d)				Observed soil moisture in sandy soil (Field B) (mm/d)			
Date	Observed rainfall (mm/d)	Observed pan evaporation (mm/d)	Subplot 1	Subplot 2	Subplot 3	Subplot 4	Subplot 1	Subplot 2	Subplot 3	Subplot 4
12-Apr-09	0.0	6.2								
13-Apr-09	0.0	2.4								
14-Apr-09	0.0	1.4								
15-Apr-09	0.0	5.3								
16-Apr-09	0.0	3.0								
17-Apr-09	0.0	1.9								
18-Apr-09	0.0	4.7								
19-Apr-09	0.0	3.4								
20-Apr-09	0.0	4.0								
21-Apr-09	0.0	1.2								
22-Apr-09	0.0	0.4								
23-Apr-09	0.0	9.7								
24-Apr-09	0.0	10.5								
25-Apr-09	0.0	13.0								
26-Apr-09	0.0	3.0								
27-Apr-09	0.0	7.3								
28-Apr-09	0.0	4.3								
29-Apr-09	0.0	12.1								
30-Apr-09	0.0	12.3								
1-May-09	0.0	1.6								
2-May-09	0.0	2.0								
3-May-09	1.0	1.5								
4-May-09	10.0	1.1								
5-May-09	0.0	7.1								
6-May-09	0.0	6.6								
7-May-09	0.0	5.8								
8-May-09	0.0	-0.9								
9-May-09	0.0	6.4								
10-May-09	0.0	10.9								
11-May-09	0.0	0.7								
12-May-09	0.0	3.9								
13-May-09	0.0	6.0								

	Input data		Observed soil moisture in loam soil (Field A) (mm/d)				Observed soil moisture in sandy soil (Field B) (mm/d)			
Date	Observed rainfall (mm/d)	Observed pan evaporation (mm/d)	Subplot 1	Subplot 2	Subplot 3	Subplot 4	Subplot 1	Subplot 2	Subplot 3	Subplot 4
14-May-09	0.0	3.8								
15-May-09	0.0	1.6								
16-May-09	0.0	1.8								
17-May-09	0.0	7.4								
18-May-09	0.0	0.5								
19-May-09	0.0	3.3								
20-May-09	0.0	3.5								
21-May-09	0.0	0.2								
22-May-09	0.0	4.7								
23-May-09	0.0	1.5								
24-May-09	0.0	1.2								
25-May-09	0.0	1.7	12.5	10.5	8.8	10.6	8.2	8.5	9.0	8.2
26-May-09	0.0	3.6								
27-May-09	0.0	5.5								
28-May-09	0.0	6.4								
29-May-09	0.0	1.2								
30-May-09	0.0	2.5								
31-May-09	0.0	7.6								
1-Jun-09	0.0	4.9								
2-Jun-09	0.0	7.2								
3-Jun-09	0.0	4.3								
4-Jun-09	0.0	3.4								
5-Jun-09	0.0	8.2								
6-Jun-09	0.0	4.4								
7-Jun-09	0.0	7.5					6.3	7.0	7.5	6.6
8-Jun-09	0.0	3.3								
9-Jun-09	0.0	4.6								
10-Jun-09	4.0	4.1								
11-Jun-09	0.0	4.1								
12-Jun-09	0.0	4.2								
13-Jun-09	0.0	2.5								
14-Jun-09	0.0	8.8								

	Input data		Observed soil moisture in loam soil (Field A) (mm/d)				Observed soil moisture in sandy soil (Field B) (mm/d)			
Date	Observed rainfall (mm/d)	Observed pan evaporation (mm/d)	Subplot 1	Subplot 2	Subplot 3	Subplot 4	Subplot 1	Subplot 2	Subplot 3	Subplot 4
15-Jun-09	0.0	1.6								
16-Jun-09	0.0	3.2								
17-Jun-09	0.0	5.8								
18-Jun-09	0.0	8.1								
19-Jun-09	0.0	3.4								
20-Jun-09	0.0	2.3								
21-Jun-09	0.0	2.3								
22-Jun-09	0.0	2.7	10.2	9.6	8.0	9.7				
23-Jun-09	0.0	2.2								
24-Jun-09	0.0	4.6								
25-Jun-09	0.0	4.5								
26-Jun-09	0.0	4.0								
27-Jun-09	0.0	3.9								
28-Jun-09	0.0	5.7								
29-Jun-09	0.0	5.5								
30-Jun-09	0.0	4.7								
1-Jul-09	0.0	6.2								
2-Jul-09	0.0	0.6								
3-Jul-09	0.0	5.3								
4-Jul-09	0.0	5.6								
5-Jul-09	2.0	6.1								
6-Jul-09	0.0	3.1	9.9	9.0	7.5	9.4				
7-Jul-09	0.0	8.2								
8-Jul-09	0.0	4.2								
9-Jul-09	0.0	5.2								
10-Jul-09	0.0	4.7								
11-Jul-09	0.0	4.6								
12-Jul-09	0.0	4.2								
13-Jul-09	0.0	3.7								
14-Jul-09	0.0	11.2								
15-Jul-09	0.0	0.8								
16-Jul-09	0.0	3.8								

	Input data		Observed soil moisture in loam soil (Field A) (mm/d)				Observed soil moisture in sandy soil (Field B) (mm/d)			
Date	Observed rainfall (mm/d)	Observed pan evaporation (mm/d)	Subplot 1	Subplot 2	Subplot 3	Subplot 4	Subplot 1	Subplot 2	Subplot 3	Subplot 4
17-Jul-09	0.0	5.6								
18-Jul-09	0.0	3.2								
19-Jul-09	0.0	8.9								
20-Jul-09	0.0	3.2								
21-Jul-09	0.0	5.1								
22-Jul-09	0.0	7.3								
23-Jul-09	0.0	8.4								
24-Jul-09	0.0	4.6								
25-Jul-09	0.0	3.8								
26-Jul-09	0.0	1.7								
27-Jul-09	0.0	6.6								
28-Jul-09	0.0	2.5								
29-Jul-09	0.0	3.9								
30-Jul-09	0.0	2.4								
31-Jul-09	0.0	2.5								
1-Aug-09	0.0	5.1								
2-Aug-09	0.0	4.3								
3-Aug-09	0.0	7.6								
4-Aug-09	0.0	3.2								
5-Aug-09	0.0	6.0								
6-Aug-09	0.0	9.0								
7-Aug-09	0.0	4.3								
8-Aug-09	0.0	8.0								
9-Aug-09	0.0	5.9								
10-Aug-09	0.0	5.7								
11-Aug-09	0.0	-2.0								
12-Aug-09	0.0	5.3								
13-Aug-09	0.0	3.4								
14-Aug-09	0.0	1.0								
15-Aug-09	0.0	0.3								
16-Aug-09	0.0	9.6								
17-Aug-09	0.0	1.1	9.5	8.3	7.1	8.6				

	Input data		Observed soil moisture in loam soil (Field A) (mm/d)				Observed soil moisture in sandy soil (Field B) (mm/d)			
Date	Observed rainfall (mm/d)	Observed pan evaporation (mm/d)	Subplot 1	Subplot 2	Subplot 3	Subplot 4	Subplot 1	Subplot 2	Subplot 3	Subplot 4
18-Aug-09	0.0	7.4								
19-Aug-09	0.0	1.1								
20-Aug-09	0.0	0.5					5.4	6.4	6.3	5.5
21-Aug-09	0.0	0.6								
22-Aug-09	0.0	1.7								
23-Aug-09	0.0	4.6								
24-Aug-09	0.0	3.2								
25-Aug-09	0.0	4.3	9.6	8.2	7.2	8.9				
26-Aug-09	0.0	2.2								
27-Aug-09	0.0	2.6					5.9	6.5	6.4	5.9
28-Aug-09	0.0	2.1								
29-Aug-09	0.0	3.6								
30-Aug-09	0.0	1.7								
31-Aug-09	0.0	1.4								
1-Sep-09	0.0	6.1								
2-Sep-09	0.0	1.4								
3-Sep-09	0.0	2.4								
4-Sep-09	0.0	6.3								
5-Sep-09	0.0	3.4								
6-Sep-09	0.0	5.5								
7-Sep-09	0.0	2.8								
8-Sep-09	0.0	6.9	8.7	7.4	6.19	7.9				
9-Sep-09	0.0	3.5								
10-Sep-09	0.0	6.2								
11-Sep-09	0.0	2.4								
12-Sep-09	0.0	1.4								
13-Sep-09	0.0	5.3								
14-Sep-09	0.0	3.0								
15-Sep-09	0.0	1.9								
16-Sep-09	0.0	4.7								
17-Sep-09	0.0	3.4								
18-Sep-09	0.0	4.0								

	Input data		Observed soil moisture in loam soil (Field A) (mm/d)				Observed soil moisture in sandy soil (Field B) (mm/d)			
Date	Observed rainfall (mm/d)	Observed pan evaporation (mm/d)	Subplot 1	Subplot 2	Subplot 3	Subplot 4	Subplot 1	Subplot 2	Subplot 3	Subplot 4
19-Sep-09	0.0	1.2								
20-Sep-09	0.0	0.4								
21-Sep-09	0.0	9.7								
22-Sep-09	0.0	10.5								
23-Sep-09	0.0	13.0								
24-Sep-09	0.0	3.0	8.8	7.3	6.65	8.0				
25-Sep-09	0.0	7.3								
26-Sep-09	0.0	4.3					3.7	4.6	5.3	4.2
27-Sep-09	0.0	12.1								
28-Sep-09	0.0	12.3								
29-Sep-09	0.0	1.6								
30-Sep-09	0.0	2.0								
1-Oct-09	0.0	1.5								
2-Oct-09	0.0	1.1								
3-Oct-09	0.0	7.1	8.1	6.8	5.90	7.4	4.0	4.7	5.6	4.4
4-Oct-09	0.0	6.6								
5-Oct-09	0.0	5.8								
6-Oct-09	0.0	-0.9								
7-Oct-09	0.0	6.4								
8-Oct-09	0.0	10.9								
9-Oct-09	0.0	0.7	9.1	7.8	7.20	8.2				
10-Oct-09	0.0	3.9								
11-Oct-09	0.0	6.0								
12-Oct-09	0.0	3.8								
13-Oct-09	0.0	1.6								
14-Oct-09	0.0	1.8								
15-Oct-09	0.0	7.4								
16-Oct-09	0.0	0.5	8.5	6.0	6.20	7.4				
17-Oct-09	0.0	3.3					4.5	5.3	5.5	4.7
18-Oct-09	0.0	3.5								
19-Oct-09	0.0	0.2								
20-Oct-09	0.0	4.7								

	Input data		Observed soil moisture in loam soil (Field A) (mm/d)				Observed soil moisture in sandy soil (Field B) (mm/d)			
Date	Observed rainfall (mm/d)	Observed pan evaporation (mm/d)	Subplot 1	Subplot 2	Subplot 3	Subplot 4	Subplot 1	Subplot 2	Subplot 3	Subplot 4
21-Oct-09	0.0	1.5								
22-Oct-09	0.0	1.2								
23-Oct-09	0.0	1.7								
24-Oct-09	0.0	3.6								
25-Oct-09	0.0	5.5								
26-Oct-09	0.0	6.4								
27-Oct-09	0.0	1.2								
28-Oct-09	0.0	2.5								
29-Oct-09	0.0	7.6								
30-Oct-09	0.0	4.9								
31-Oct-09	14.0	7.2								
1-Nov-09	0.0	4.3								
2-Nov-09	0.0	3.4								
3-Nov-09	0.0	8.2								
4-Nov-09	0.0	4.4								
5-Nov-09	0.0	7.5	14.0	8.4	9.50	9.8	5.1	5.1	5.9	4.5
6-Nov-09	0.0	3.3								
7-Nov-09	0.0	4.6								
8-Nov-09	0.0	4.1								
9-Nov-09	0.0	4.1								
10-Nov-09	0.0	4.2								
11-Nov-09	0.0	2.5								
12-Nov-09	0.0	8.8								
13-Nov-09	2.0	1.6								
14-Nov-09	0.0	3.2								
15-Nov-09	0.0	5.8								
16-Nov-09	2.0	8.1								
17-Nov-09	0.0	3.4	10.7	7.8	7.66	8.7				
18-Nov-09	0.0	2.3								
19-Nov-09	0.0	2.3								
20-Nov-09	10.0	2.7								
21-Nov-09	24.0	2.2								

	Input data		Observed soil moisture in loam soil (Field A) (mm/d)				Observed soil moisture in sandy soil (Field B) (mm/d)			
Date	Observed rainfall (mm/d)	Observed pan evaporation (mm/d)	Subplot 1	Subplot 2	Subplot 3	Subplot 4	Subplot 1	Subplot 2	Subplot 3	Subplot 4
22-Nov-09	0.0	4.6								
23-Nov-09	0.0	4.5								
24-Nov-09	0.0	4.0	12.9	12.2	11.63	12.3				
25-Nov-09	0.0	3.9								
26-Nov-09	0.0	5.7	10.5	11.7	10.91	12.9				
27-Nov-09	0.0	5.5					10.6	8.6	10.4	8.9
28-Nov-09	0.0	4.7					10.2	8.6	9.6	9.0
29-Nov-09	0.0	6.2								
30-Nov-09	0.0	0.6								
1-Dec-09	2.0	5.3								
2-Dec-09	16.0	5.6								
3-Dec-09	0.0	6.1								
4-Dec-09	24.0	3.1								
5-Dec-09	0.0	8.2								
6-Dec-09	0.0	4.2								
7-Dec-09	0.0	5.2	14.6	13.7	11.42	15.0				
8-Dec-09	3.0	4.7					16.4	13.2	14.4	13.6
9-Dec-09	0.0	4.6								
10-Dec-09	0.0	4.2	14.4	13.3	12.59	14.4				
11-Dec-09	3.0	3.7								
12-Dec-09	80.0	11.2								
13-Dec-09	0.0	0.8								
14-Dec-09	0.0	3.8	17.2	15.6	14.48	17.9	21.9	18.7	19.0	18.9
15-Dec-09	0.0	5.6								
16-Dec-09	0.0	3.2								
17-Dec-09	0.0	8.9	17.0	13.9	14.98	16.1				
18-Dec-09	3.0	3.2								
19-Dec-09	0.0	5.1								
20-Dec-09	0.0	7.3								
21-Dec-09	0.0	8.4								
22-Dec-09	0.0	4.6								
23-Dec-09	0.0	3.8								

	Input data		Observed soil moisture in loam soil (Field A) (mm/d)				Observed soil moisture in sandy soil (Field B) (mm/d)			
Date	Observed rainfall (mm/d)	Observed pan evaporation (mm/d)	Subplot 1	Subplot 2	Subplot 3	Subplot 4	Subplot 1	Subplot 2	Subplot 3	Subplot 4
24-Dec-09	0.0	1.7								
25-Dec-09	0.0	6.6								
26-Dec-09	0.0	2.5								
27-Dec-09	0.0	3.9								
28-Dec-09	0.0	2.4								
29-Dec-09	0.0	2.5								
30-Dec-09	0.0	5.1								
31-Dec-09	0.0	4.3								
1-Jan-10	0.0	7.6								
2-Jan-10	0.0	3.2								
3-Jan-10	0.0	6.0								
4-Jan-10	0.0	9.0								
5-Jan-10	56.0	4.3	20.0	17.0	18.35	19.2	24.1	20.7	23.1	20.9
6-Jan-10	1.0	8.0								
7-Jan-10	0.0	5.9								
8-Jan-10	0.0	5.7	17.6	14.5	14.88	17.1	23.2	20.8	21.1	20.6
9-Jan-10	0.0	-2.0	17.3	14.6	15.26	16.8	21.8	19.3	20.4	19.6
10-Jan-10	0.0	5.3								
11-Jan-10	0.0	3.4	16.1	13.2	13.21	16.0	19.6	19.3	19.6	18.4
12-Jan-10	0.0	1.0								
13-Jan-10	0.0	0.3								
14-Jan-10	0.0	9.6								
15-Jan-10	0.0	1.1					18.7	17.7	19.3	16.4
16-Jan-10	0.0	7.4					18.7	17.4	18.5	16.5
17-Jan-10	0.0	1.1								
18-Jan-10	0.0	0.5								
19-Jan-10	0.0	0.6					15.9	15.5	17.2	15.3
20-Jan-10	0.0	1.7								
21-Jan-10	4.0	4.6					16.1	15.4	15.9	14.2
22-Jan-10	4.0	3.2								
23-Jan-10	0.0	4.3					15.5	14.2	15.7	13.7
24-Jan-10	0.0	2.2								

	Input data		Observed soil moisture in loam soil (Field A) (mm/d)				Observed soil moisture in sandy soil (Field B) (mm/d)			
Date	Observed rainfall (mm/d)	Observed pan evaporation (mm/d)	Subplot 1	Subplot 2	Subplot 3	Subplot 4	Subplot 1	Subplot 2	Subplot 3	Subplot 4
25-Jan-10	0.0	2.6	13.0	11.5	8.70	12.2	14.7	13.5	15.7	13.9
26-Jan-10	0.0	2.1								
27-Jan-10	6.0	3.6								
28-Jan-10	8.0	1.7	15.0	13.3	13.54	14.1	16.8	14.5	16.2	15.0
29-Jan-10	0.0	1.4								
30-Jan-10	5.0	6.1	15.4	13.8	14.83	15.5	16.6	14.8	15.9	15.1
31-Jan-10	0.0	1.4	15.0	12.9	13.90	14.3				
1-Feb-10	2.0	2.4								
2-Feb-10	0.0	6.3					16.9	15.1	16.3	15.1
3-Feb-10	0.0	3.4								
4-Feb-10	0.0	5.5	14.7	12.9	12.74	14.0	17.3	15.7	16.4	14.9
5-Feb-10	0.0	2.8								
6-Feb-10	0.0	6.9	13.5	11.8	11.96	13.4	14.8	14.5	15.9	14.0
7-Feb-10	0.0	3.5								
8-Feb-10	0.0	6.2								
9-Feb-10	0.0	2.4	12.1	10.3	10.20	11.7	12.7	12.2	14.3	12.7
10-Feb-10	0.0	1.4								
11-Feb-10	5.0	5.3	12.3	10.3	9.96	11.6	14.4	13.4	15.6	13.4
12-Feb-10	0.0	3.0								
13-Feb-10	0.0	1.9	12.2	10.1	8.90	11.5	13.6	13.4	14.2	12.2
14-Feb-10	0.0	4.7								
15-Feb-10	0.0	3.4	11.1	9.6	9.11	10.6	12.4	12.9	13.6	11.5
16-Feb-10	0.0	4.0								
17-Feb-10	0.0	1.2								
18-Feb-10	0.0	0.4								
19-Feb-10	20.0	9.7								
20-Feb-10	12.0	10.5	16.8	16.8	16.09	17.6	17.3	15.6	18.3	15.8
21-Feb-10	6.0	13.0								
22-Feb-10	2.0	3.0	17.1	16.9	16.68	17.7	19.1	18.4	19.8	18.4
23-Feb-10	0.0	7.3								
24-Feb-10	2.0	4.3								
25-Feb-10	4.0	12.1	18.0	17.7	17.56	18.3				

	Input data		Observed soil moisture in loam soil (Field A) (mm/d)				Observed soil moisture in sandy soil (Field B) (mm/d)			
Date	Observed rainfall (mm/d)	Observed pan evaporation (mm/d)	Subplot 1	Subplot 2	Subplot 3	Subplot 4	Subplot 1	Subplot 2	Subplot 3	Subplot 4
26-Feb-10	0.0	12.3					20.5	19.9	20.8	20.4
27-Feb-10	10.0	1.6								
28-Feb-10	3.0	2.0								
1-Mar-10	3.0	1.5								
2-Mar-10	0.0	1.1								
3-Mar-10	32.0	7.1								
4-Mar-10	16.0	6.6	19.3	20.4	19.81	20.2				
5-Mar-10	6.0	5.8								
6-Mar-10	0.0	-0.9								
7-Mar-10	0.0	6.4								
8-Mar-10	0.0	10.9								
9-Mar-10	3.0	0.7								
10-Mar-10	0.0	3.9								
11-Mar-10	0.0	6.0								
12-Mar-10	0.0	3.8								
13-Mar-10	0.0	1.6								
14-Mar-10	6.0	1.8								
15-Mar-10	0.0	7.4								
16-Mar-10	0.0	0.5	16.4	16.9	14.80	17.9				
17-Mar-10	0.0	3.3								
18-Mar-10	0.0	3.5	14.8	14.9	13.76	15.1	21.5	20.5	20.3	22.1
19-Mar-10	0.0	0.2					19.2	18.6	19.2	19.0
20-Mar-10	0.0	4.7	14.4	14.6	13.85	15.1	18.5	19.0	19.5	18.9
21-Mar-10	0.0	1.5					14.3	14.4	15.4	16.0
22-Mar-10	0.0	1.2								
23-Mar-10	0.0	1.7								
24-Mar-10	0.0	3.6								
25-Mar-10	0.0	5.5								
26-Mar-10	6.0	6.4								
27-Mar-10	0.0	1.2								
28-Mar-10	0.0	2.5								
29-Mar-10	0.0	7.6								

	Input data		Observed soil moisture in loam soil (Field A) (mm/d)				Observed soil moisture in sandy soil (Field B) (mm/d)			
Date	Observed rainfall (mm/d)	Observed pan evaporation (mm/d)	Subplot 1	Subplot 2	Subplot 3	Subplot 4	Subplot 1	Subplot 2	Subplot 3	Subplot 4
30-Mar-10	0.0	4.9								
31-Mar-10	0.0	7.2								
1-Apr-10	0.0	4.3								
2-Apr-10	0.0	3.4	11.9	12.8	11.55	13.2				
3-Apr-10	0.0	8.2								
4-Apr-10	0.0	4.4								
5-Apr-10	0.0	7.5								
6-Apr-10	10.0	3.3								
7-Apr-10	26.0	4.6								
8-Apr-10	0.0	4.1								
9-Apr-10	32.0	4.1	13.5	12.2	9.35	13.1				
10-Apr-10	20.0	4.2					11.6	13.2	13.6	12.3
11-Apr-10	0.0	2.5								
12-Apr-10	0.0	8.8								
13-Apr-10	0.0	1.6								
14-Apr-10	0.0	3.2								
15-Apr-10	0.0	5.8								
16-Apr-10	0.0	8.1								
17-Apr-10	0.0	3.4								
18-Apr-10	0.0	2.3								
19-Apr-10	0.0	2.3								
20-Apr-10	0.0	2.7								
21-Apr-10	0.0	2.2								
22-Apr-10	0.0	4.6								
23-Apr-10	10.0	4.5								
24-Apr-10	0.0	4.0								
25-Apr-10	0.0	3.9								
26-Apr-10	6.0	5.7								
27-Apr-10	0.0	5.5								
28-Apr-10	0.0	4.7								
29-Apr-10	0.0	6.2								
30-Apr-10	0.0	0.6								

	Input data		Observed soil moisture in loam soil (Field A) (mm/d)				Observed soil moisture in sandy soil (Field B) (mm/d)			
Date	Observed rainfall (mm/d)	Observed pan evaporation (mm/d)	Subplot 1	Subplot 2	Subplot 3	Subplot 4	Subplot 1	Subplot 2	Subplot 3	Subplot 4
1-May-10	0.0	5.3								
2-May-10	0.0	5.6								
3-May-10	0.0	6.1								
4-May-10	0.0	3.1								
5-May-10	0.0	8.2								
6-May-10	0.0	4.2								
7-May-10	0.0	5.2	9.5	10.2	9.22	10.5	11.3	9.7	10.4	10.4
8-May-10	0.0	4.7								
9-May-10	0.0	4.6								
10-May-10	0.0	4.2								
11-May-10	0.0	3.7								
12-May-10	0.0	11.2								
13-May-10	0.0	0.8								
14-May-10	0.0	3.8	9.6	7.8	8.02	9.9	8.7	6.9	7.7	7.0
15-May-10	0.0	5.6								
16-May-10	0.0	3.2								
17-May-10	0.0	8.9								
18-May-10	0.0	3.2								
19-May-10	0.0	5.1								
20-May-10	0.0	7.3	10.8	8.5	9.15	9.9	10.5	8.7	9.1	9.4
21-May-10	0.0	8.4								
22-May-10	0.0	4.6								
23-May-10	44.0	3.8								
24-May-10	0.0	1.7								
25-May-10	0.0	6.6								
26-May-10	0.0	2.5								
27-May-10	0.0	3.9								
28-May-10	0.0	2.4								
29-May-10	0.0	2.5								
30-May-10	0.0	5.1								
31-May-10	10.0	4.3	15.4	13.7	14.88	15.1				
1-Jun-10	0.0	7.6								

	Input data		Observed soil moisture in loam soil (Field A) (mm/d)				Observed soil moisture in sandy soil (Field B) (mm/d)			
Date	Observed rainfall (mm/d)	Observed pan evaporation (mm/d)	Subplot 1	Subplot 2	Subplot 3	Subplot 4	Subplot 1	Subplot 2	Subplot 3	Subplot 4
2-Jun-10	0.0	3.2								
3-Jun-10	0.0	6.0	16.1	14.3	14.47	13.9	18.5	16.4	15.9	18.1
4-Jun-10	0.0	9.0	14.8	14.4	14.47	14.1				
5-Jun-10	0.0	4.3					18.1	16.7	16.2	18.0
6-Jun-10	0.0	8.0								
7-Jun-10	0.0	5.9	13.6	13.3	13.42	11.7	16.8	15.4	14.7	16.7
8-Jun-10	0.0	5.7								
9-Jun-10	0.0	-2.0								
10-Jun-10	0.0	5.3								
11-Jun-10	0.0	3.4								
12-Jun-10	0.0	1.0								
13-Jun-10	0.0	0.3								
14-Jun-10	0.0	9.6								
15-Jun-10	0.0	1.1								
16-Jun-10	0.0	7.4								
17-Jun-10	0.0	1.1								
18-Jun-10	0.0	0.5								
19-Jun-10	0.0	0.6								
20-Jun-10	0.0	1.7								
21-Jun-10	0.0	4.6	12.2	9.9	10.20	12.5	13.3	12.6	12.4	14.1
22-Jun-10	0.0	3.2								
23-Jun-10	0.0	4.3					17.1	14.8	14.6	16.1
24-Jun-10	0.0	2.2								
25-Jun-10	0.0	2.6	11.6	10.2	11.12	11.4	13.5	13.2	12.7	13.5
26-Jun-10	0.0	2.1	12.4	10.7	11.63	11.5	13.8	13.2	12.6	13.8
27-Jun-10	0.0	3.6								
28-Jun-10	0.0	1.7								
29-Jun-10	0.0	1.4								
30-Jun-10	0.0	6.1								
1-Jul-10	0.0	1.4								
2-Jul-10	0.0	2.4	12.2	10.1	10.62	9.6	12.2	11.6	12.2	12.1
3-Jul-10	0.0	6.3	10.8	11.3	10.48	11.2	13.8	13.4	12.9	14.4

	Input data		Observed soil moisture in loam soil (Field A) (mm/d)				Observed soil moisture in sandy soil (Field B) (mm/d)			
Date	Observed rainfall (mm/d)	Observed pan evaporation (mm/d)	Subplot 1	Subplot 2	Subplot 3	Subplot 4	Subplot 1	Subplot 2	Subplot 3	Subplot 4
4-Jul-10	0.0	3.4								
5-Jul-10	0.0	5.5								
6-Jul-10	0.0	2.8								
7-Jul-10	0.0	6.9								
8-Jul-10	0.0	3.5								
9-Jul-10	0.0	6.2								
10-Jul-10	0.0	2.4								
11-Jul-10	0.0	1.4	11.1	10.9	9.73	10.8				
12-Jul-10	0.0	5.3								
13-Jul-10	0.0	3.0								
14-Jul-10	0.0	1.9								
15-Jul-10	0.0	4.7					12.5	12.0	11.6	12.2
16-Jul-10	0.0	3.4	10.6	10.1	10.29	10.8	12.4	12.8	12.4	13.0
17-Jul-10	0.0	4.0								
18-Jul-10	0.0	1.2								
19-Jul-10	0.0	0.4								
20-Jul-10	0.0	9.7								
21-Jul-10	0.0	10.5					12.5	12.6	11.9	12.8
22-Jul-10	0.0	13.0					12.6	13.1	12.8	13.1
23-Jul-10	0.0	3.0								
24-Jul-10	0.0	7.3	11.4	9.7	9.94	10.8	12.6	12.8	12.5	13.1
25-Jul-10	0.0	4.3	11.4	8.9	10.27	11.2				
26-Jul-10	0.0	12.1	11.8	11.1	9.37	11.3				
27-Jul-10	0.0	12.3								
28-Jul-10	0.0	1.6								
29-Jul-10	0.0	2.0								
30-Jul-10	0.0	1.5								
31-Jul-10	0.0	1.1								
1-Aug-10	0.0	7.1	11.7	9.0	9.46	10.8	11.7	12.0	11.9	12.1
2-Aug-10	0.0	6.6								
3-Aug-10	0.0	5.8	10.8	11.5	11.48	10.5				
4-Aug-10	0.0	-0.9								

	Input data		Observed soil moisture in loam soil (Field A) (mm/d)				Observed soil moisture in sandy soil (Field B) (mm/d)			
Date	Observed rainfall (mm/d)	Observed pan evaporation (mm/d)	Subplot 1	Subplot 2	Subplot 3	Subplot 4	Subplot 1	Subplot 2	Subplot 3	Subplot 4
5-Aug-10	0.0	6.4								
6-Aug-10	0.0	10.9					11.8	11.8	12.0	12.0
7-Aug-10	0.0	0.7	12.5	8.5	10.02	10.8	12.5	12.4	12.6	12.7
8-Aug-10	0.0	3.9								
9-Aug-10	0.0	6.0								
10-Aug-10	0.0	3.8								
11-Aug-10	0.0	1.6								
12-Aug-10	0.0	1.8	11.1	9.2	8.85	10.2	10.5	10.5	12.1	10.9
13-Aug-10	0.0	7.4	11.6	9.5	9.30	10.7	12.2	12.4	12.7	12.3
14-Aug-10	0.0	0.5								
15-Aug-10	0.0	3.3								
16-Aug-10	0.0	3.5								
17-Aug-10	0.0	0.2								
18-Aug-10	0.0	4.7								
19-Aug-10	0.0	1.5								
20-Aug-10	0.0	1.2								
21-Aug-10	0.0	1.7								
22-Aug-10	0.0	3.6								
23-Aug-10	0.0	5.5								
24-Aug-10	0.0	6.4								
25-Aug-10	0.0	1.2					11.6	12.1	12.0	11.6
26-Aug-10	0.0	2.5	10.4	10.4	8.74	10.3				
27-Aug-10	0.0	7.6	12.7	10.7	9.34	9.6				
28-Aug-10	0.0	4.9								
29-Aug-10	0.0	7.2								
30-Aug-10	0.0	4.3								
31-Aug-10	0.0	3.4								
1-Sep-10	0.0	8.2								
2-Sep-10	0.0	4.4	12.4	9.6	9.94	8.9				
3-Sep-10	0.0	7.5	10.9	7.9	7.62	10.0	11.1	11.3	11.9	10.8
4-Sep-10	0.0	3.3								
5-Sep-10	0.0	4.6								

	Input data		Observed soil moisture in loam soil (Field A) (mm/d)				Observed soil moisture in sandy soil (Field B) (mm/d)			
Date	Observed rainfall (mm/d)	Observed pan evaporation (mm/d)	Subplot 1	Subplot 2	Subplot 3	Subplot 4	Subplot 1	Subplot 2	Subplot 3	Subplot 4
6-Sep-10	0.0	4.1								
7-Sep-10	0.0	4.1	11.6	8.3	7.84	10.1	10.8	11.2	11.8	10.7
8-Sep-10	0.0	4.2								
9-Sep-10	0.0	2.5	10.9	7.8	7.59	9.8	10.5	11.3	11.6	10.3
10-Sep-10	0.0	8.8	10.9	9.8	7.88	10.0	10.5	11.3	11.6	10.3
11-Sep-10	0.0	1.6								
12-Sep-10	0.0	3.2								
13-Sep-10	0.0	5.8								
14-Sep-10	0.0	8.1								
15-Sep-10	0.0	3.4								
16-Sep-10	0.0	2.3								
17-Sep-10	0.0	2.3								
18-Sep-10	0.0	2.7								
19-Sep-10	0.0	2.2								
20-Sep-10	0.0	4.6								
21-Sep-10	0.0	4.5								
22-Sep-10	0.0	4.0								
23-Sep-10	0.0	3.9								
24-Sep-10	0.0	5.7								
25-Sep-10	0.0	5.5								
26-Sep-10	0.0	4.7								
27-Sep-10	0.0	6.2								
28-Sep-10	0.0	0.6								
29-Sep-10	0.0	5.3								
30-Sep-10	0.0	5.6								
1-Oct-10	0.0	6.1								
2-Oct-10	0.0	3.1								
3-Oct-10	0.0	8.2								
4-Oct-10	0.0	4.2								
5-Oct-10	0.0	5.2								
6-Oct-10	0.0	4.7								
7-Oct-10	0.0	4.6								

	Input data		Observed soil moisture in loam soil (Field A) (mm/d)				Observed soil moisture in sandy soil (Field B) (mm/d)			
Date	Observed rainfall (mm/d)	Observed pan evaporation (mm/d)	Subplot 1	Subplot 2	Subplot 3	Subplot 4	Subplot 1	Subplot 2	Subplot 3	Subplot 4
8-Oct-10	0.0	4.2								
9-Oct-10	0.0	3.7								
10-Oct-10	0.0	11.2								
11-Oct-10	0.0	0.8								
12-Oct-10	0.0	3.8								
13-Oct-10	0.0	5.6								
14-Oct-10	0.0	3.2								
15-Oct-10	0.0	8.9								
16-Oct-10	0.0	3.2								
17-Oct-10	0.0	5.1								
18-Oct-10	0.0	7.3								
19-Oct-10	0.0	8.4								
20-Oct-10	0.0	4.6								
21-Oct-10	0.0	3.8								
22-Oct-10	0.0	1.7								
23-Oct-10	0.0	6.6								
24-Oct-10	0.0	2.5								
25-Oct-10	0.0	3.9								
26-Oct-10	0.0	2.4								
27-Oct-10	0.0	2.5								
28-Oct-10	0.0	5.1								
29-Oct-10	0.0	4.3								
30-Oct-10	0.0	7.6								
31-Oct-10	0.0	3.2								
1-Nov-10	0.0	6.0								
2-Nov-10	4.0	9.0								
3-Nov-10	5.0	4.3								
4-Nov-10	0.0	8.0					6.2	5.9	4.8	4.9
5-Nov-10	0.0	5.9					7.0	5.3	6.0	5.3
6-Nov-10	5.0	5.7								
7-Nov-10	0.0	-2.0								
8-Nov-10	0.0	5.3								

	Input data		Observed soil moisture in loam soil (Field A) (mm/d)				Observed soil moisture in sandy soil (Field B) (mm/d)			
Date	Observed rainfall (mm/d)	Observed pan evaporation (mm/d)	Subplot 1	Subplot 2	Subplot 3	Subplot 4	Subplot 1	Subplot 2	Subplot 3	Subplot 4
9-Nov-10	0.0	3.4					5.7	5.3	5.4	5.6
10-Nov-10	1.0	1.0								
11-Nov-10	1.0	0.3								
12-Nov-10	0.0	9.6								
13-Nov-10	1.0	1.1	14.2	10.7	11.53	13.6	7.0	5.6	5.5	5.8
14-Nov-10	0.0	7.4								
15-Nov-10	75.0	1.1								
16-Nov-10	0.0	0.5								
17-Nov-10	0.0	0.6								
18-Nov-10	0.0	1.7	14.2	11.0	11.48	13.8	12.0	10.9	5.6	9.2
19-Nov-10	3.0	4.6								
20-Nov-10	0.0	3.2					10.7	10.7	12.7	8.9
21-Nov-10	0.0	4.3								
22-Nov-10	0.0	2.2								
23-Nov-10	0.0	2.6								
24-Nov-10	0.0	2.1								
25-Nov-10	0.0	3.6								
26-Nov-10	0.0	1.7	14.4	10.8	10.44	11.0	12.1	13.2	14.1	11.8
27-Nov-10	0.0	1.4								
28-Nov-10	4.0	6.1								
29-Nov-10	0.0	1.4	18.2	15.2	15.73	14.5				
30-Nov-10	5.0	2.4					15.9	15.1	16.4	15.3
1-Dec-10	0.0	6.3								
2-Dec-10	0.0	3.4	18.5	15.7	15.11	15.0				
3-Dec-10	0.0	5.5	19.1	16.0	16.12	16.8	20.3	19.3	19.4	18.8
4-Dec-10	0.0	2.8								
5-Dec-10	10.0	6.9								
6-Dec-10	28.0	3.5								
7-Dec-10	3.0	6.2								
8-Dec-10	0.0	2.4								
9-Dec-10	0.0	1.4								
10-Dec-10	0.0	5.3								

	Input data		Observed soil moisture in loam soil (Field A) (mm/d)				Observed soil moisture in sandy soil (Field B) (mm/d)			
Date	Observed rainfall (mm/d)	Observed pan evaporation (mm/d)	Subplot 1	Subplot 2	Subplot 3	Subplot 4	Subplot 1	Subplot 2	Subplot 3	Subplot 4
11-Dec-10	0.0	3.0								
12-Dec-10	0.0	1.9	19.3	13.9	13.97	14.0	22.6	21.2	20.4	19.7
13-Dec-10	0.0	4.7								
14-Dec-10	20.0	3.4								
15-Dec-10	22.0	4.0								
16-Dec-10	3.0	1.2								
17-Dec-10	4.0	0.4								
18-Dec-10	20.0	9.7								
19-Dec-10	0.0	10.5								
20-Dec-10	0.0	13.0								
21-Dec-10	0.0	3.0								
22-Dec-10	0.0	7.3								
23-Dec-10	0.0	4.3	16.9	15.0	15.87	17.5	25.3	23.3	21.3	21.5
24-Dec-10	0.0	12.1	18.9	13.6	15.73	14.9				
25-Dec-10	0.0	12.3								
26-Dec-10	1.0	1.6								
27-Dec-10	0.0	2.0								
28-Dec-10	0.0	1.5								
29-Dec-10	0.0	1.1								
30-Dec-10	0.0	7.1								
31-Dec-10	0.0	6.6								
1-Jan-11	10.0	5.8								
2-Jan-11	24.0	-0.9								
3-Jan-11	0.0	6.4								
4-Jan-11	0.0	10.9								
5-Jan-11	0.0	0.7								
6-Jan-11	0.0	3.9								
7-Jan-11	12.0	6.0								
8-Jan-11	8.0	3.8	20.6	18.0	19.54	17.9	21.8	21.4	15.9	19.7
9-Jan-11	0.0	1.6								
10-Jan-11	4.0	1.8					23.4	23.4	15.8	22.2
11-Jan-11	0.0	7.4								

	Input data		Observed soil moisture in loam soil (Field A) (mm/d)				Observed soil moisture in sandy soil (Field B) (mm/d)			
Date	Observed rainfall (mm/d)	Observed pan evaporation (mm/d)	Subplot 1	Subplot 2	Subplot 3	Subplot 4	Subplot 1	Subplot 2	Subplot 3	Subplot 4
12-Jan-11	4.0	0.5								
13-Jan-11	3.0	3.3								
14-Jan-11	8.0	3.5								
15-Jan-11	0.0	0.2								
16-Jan-11	5.0	4.7								
17-Jan-11	38.0	1.5								
18-Jan-11	15.0	1.2								
19-Jan-11	0.0	1.7								
20-Jan-11	20.0	3.6								
21-Jan-11	0.0	5.5								
22-Jan-11	2.0	6.4								
23-Jan-11	2.0	1.2								
24-Jan-11	32.0	2.5								
25-Jan-11	0.0	7.6								
26-Jan-11	0.0	4.9								
27-Jan-11	0.0	7.2	19.0	16.0	16.78	16.3				
28-Jan-11	0.0	4.3								
29-Jan-11	5.0	3.4								
30-Jan-11	3.0	8.2								
31-Jan-11	1.0	4.4								
1-Feb-11	0.0	7.5								
2-Feb-11	2.0	3.3								
3-Feb-11	3.0	4.6								
4-Feb-11	0.0	4.1								
5-Feb-11	0.0	4.1								
6-Feb-11	0.0	4.2								
7-Feb-11	0.0	2.5								
8-Feb-11	0.0	8.8								
9-Feb-11	0.0	1.6								
10-Feb-11	0.0	3.2								
11-Feb-11	0.0	5.8								
12-Feb-11	0.0	8.1								

	Input data		Observed soil moisture in loam soil (Field A) (mm/d)				Observed soil moisture in sandy soil (Field B) (mm/d)			
Date	Observed rainfall (mm/d)	Observed pan evaporation (mm/d)	Subplot 1	Subplot 2	Subplot 3	Subplot 4	Subplot 1	Subplot 2	Subplot 3	Subplot 4
13-Feb-11	0.0	3.4								
14-Feb-11	0.0	2.3								
15-Feb-11	0.0	2.3								
16-Feb-11	0.0	2.7								
17-Feb-11	0.0	2.2								
18-Feb-11	0.0	4.6								
19-Feb-11	0.0	4.5								
20-Feb-11	0.0	4.0	9.4	7.3	6.56	7.7				
21-Feb-11	5.0	3.9								
22-Feb-11	0.0	5.7								
23-Feb-11	0.0	5.5								
24-Feb-11	0.0	4.7								
25-Feb-11	36.0	6.2								
26-Feb-11	0.0	0.6	13.6	9.6	10.58	9.4				
27-Feb-11	2.0	5.3								
28-Feb-11	1.0	5.6								
1-Mar-11	0.0	6.1								
2-Mar-11	0.0	3.1								
3-Mar-11	0.0	8.2								
4-Mar-11	0.0	4.2								
5-Mar-11	0.0	5.2	11.7	8.1	9.18	8.8	12.6	11.3	9.8	12.6
6-Mar-11	0.0	4.7								
7-Mar-11	0.0	4.6								
8-Mar-11	0.0	4.2								
9-Mar-11	0.0	3.7								
10-Mar-11	0.0	11.2								
11-Mar-11	0.0	0.8								
12-Mar-11	0.0	3.8								
13-Mar-11	0.0	5.6								
14-Mar-11	0.0	3.2								
15-Mar-11	0.0	8.9								
16-Mar-11	0.0	3.2								

	Input data		Observed soil moisture in loam soil (Field A) (mm/d)				Observed soil moisture in sandy soil (Field B) (mm/d)			
Date	Observed rainfall (mm/d)	Observed pan evaporation (mm/d)	Subplot 1	Subplot 2	Subplot 3	Subplot 4	Subplot 1	Subplot 2	Subplot 3	Subplot 4
17-Mar-11	0.0	5.1								
18-Mar-11	0.0	7.3								
19-Mar-11	0.0	8.4								
20-Mar-11	0.0	4.6								
21-Mar-11	0.0	3.8								
22-Mar-11	0.0	1.7								
23-Mar-11	14.0	6.6								
24-Mar-11	0.0	2.5								
25-Mar-11	0.0	3.9								
26-Mar-11	0.0	2.4	11.0	8.1	9.28	9.1	11.6	9.4	6.8	11.2
27-Mar-11	11.0	2.5								
28-Mar-11	0.0	5.1								
29-Mar-11	0.0	4.3								
30-Mar-11	0.0	7.6								
31-Mar-11	0.0	3.2								
1-Apr-11	0.0	6.0								
2-Apr-11	0.0	9.0								
3-Apr-11	0.0	4.3								
4-Apr-11	0.0	8.0								
5-Apr-11	0.0	5.9								
6-Apr-11	0.0	5.7								
7-Apr-11	0.0	-2.0								
8-Apr-11	0.0	5.3	9.9	7.6	8.50	7.5	10.0	8.0	6.1	9.2
9-Apr-11	0.0	3.4								
10-Apr-11	0.0	1.0								
11-Apr-11	0.0	0.3								
12-Apr-11	0.0	9.6								
13-Apr-11	0.0	1.1								
14-Apr-11	0.0	7.4								
15-Apr-11	0.0	1.1								
16-Apr-11	0.0	0.5					10.2	8.2	6.3	9.1
17-Apr-11	0.0	0.6								

	Input data		Observed soil moisture in loam soil (Field A) (mm/d)				Observed soil moisture in sandy soil (Field B) (mm/d)			
Date	Observed rainfall (mm/d)	Observed pan evaporation (mm/d)	Subplot 1	Subplot 2	Subplot 3	Subplot 4	Subplot 1	Subplot 2	Subplot 3	Subplot 4
18-Apr-11	0.0	1.7								
19-Apr-11	0.0	4.6								
20-Apr-11	0.0	3.2								
21-Apr-11	7.0	4.3								
22-Apr-11	2.0	2.2								
23-Apr-11	0.0	2.6								
24-Apr-11	0.0	2.1								
25-Apr-11	5.0	3.6								
26-Apr-11	0.0	1.7								
27-Apr-11	6.0	1.4								
28-Apr-11	0.0	6.1								
29-Apr-11	0.0	1.4								
30-Apr-11	0.0	2.4								
1-May-11	0.0	6.3								
2-May-11	5.0	3.4					12.0	9.3	7.8	9.9
3-May-11	0.0	5.5								
4-May-11	0.0	2.8								
5-May-11	0.0	6.9								
6-May-11	0.0	3.5								
7-May-11	0.0	6.2								
8-May-11	0.0	2.4								
9-May-11	0.0	1.4								
10-May-11	0.0	5.3								
11-May-11	0.0	3.0								
12-May-11	0.0	1.9								
13-May-11	0.0	4.7								
14-May-11	0.0	3.4								
15-May-11	0.0	4.0								
16-May-11	0.0	1.2								
17-May-11	0.0	0.4								
18-May-11	0.0	9.7								
19-May-11	0.0	10.5								

	Input data		Observed soil moisture in loam soil (Field A) (mm/d)				Observed soil moisture in sandy soil (Field B) (mm/d)			
Date	Observed rainfall (mm/d)	Observed pan evaporation (mm/d)	Subplot 1	Subplot 2	Subplot 3	Subplot 4	Subplot 1	Subplot 2	Subplot 3	Subplot 4
20-May-11	0.0	13.0								
21-May-11	0.0	3.0								
22-May-11	0.0	7.3								
23-May-11	0.0	4.3								
24-May-11	0.0	12.1								
25-May-11	0.0	12.3								
26-May-11	0.0	1.6								
27-May-11	0.0	2.0								
28-May-11	0.0	1.5								
29-May-11	0.0	1.1								
30-May-11	0.0	7.1								
31-May-11	0.0	6.6								